AUTOMATED SYNTHESIS AND EVALUATION OF POTENTIAL NEW ANTI-MICROBIAL AGENTS

KATY JANE TIMS

Doctor of Philosophy

ASTON UNIVERSITY

September 2002

ASTON UNIVERSITY

Automated Synthesis And Evaluation Of Potential New Anti-Microbial Agents

A thesis submitted by Katy Jane Tims B.Sc. (Hons) for the degree of Doctor of Philosophy

September 2002

Abstract

A series of N^1-benzylideneheteroarylcarboxamidrazones was prepared in an automated fashion, and tested against *Mycobacterium fortuitum* in a rapid screen for antimycobacterial activity. Many of the compounds from this series were also tested against *Mycobacterium tuberculosis*, and the usefulness as *M.fortuitum* as a rapid, initial screen for anti-tubercular activity evaluated. Various deletions were made to the N^1-benzylideneheteroarylcarboxamidrazone structure in order to establish the minimum structural requirements for activity. The N^1-benzylideneheteroarylcarbox-amidrazones were then subjected to molecular Modelling studies and their activities against *M.fortuitum* and *M.tuberculosis* were analysed using quantitative structure-analysis relationship (QSAR) techniques in the computational package TSAR (Oxford Molecular Ltd.). A set of equations predictive of antimycobacterial activity was hereby obtained. The series of N^1-benzylideneheteroarylcarboxamidrazones was also tested against a multidrug-resistant strain of *Staphylococcus aureus* (MRSA), followed by a panel of Gram-positive and Gram-negative bacteria, if activity was observed for MRSA. A set of antimycobacterial N^1-benzylideneheteroarylcarboxamidrazones was hereby discovered, the best of which had MICs against *M.fortuitum* in the range 4-8μgml^{-1} and displayed 94% inhibition of *M.tuberculosis* at a concentration of 6.25μgml^{-1}. The antimycobacterial activity of these compounds appeared to be specific, since the same compounds were shown to be inactive against other classes of organisms. Compounds which were found to be sufficiently active in any screen were also tested for their toxicity against human mononuclear leucocytes.

Polyethylene glycol (PEG) was used as a soluble polymeric support for the synthesis of some fatty acid derivatives, containing an isoxazoline group, which may inhibit mycolic acid synthesis in mycobacteria. Both the PEG-bound products and the cleaved, isolated products themselves were tested against *M.fortuitum* and some low levels of antimycobacterial activity were observed, which may serve as lead compounds for further studies.

Keywords

Amidrazones, *Mycobacterium tuberculosis*, MRSA, Molecular Modelling, Soluble Polymer

ACKNOWLEDGMENTS

I would like to thank Dr. Dan Rathbone and Prof. David Billington for their constant support and guidance throughout the course of this work. I would especially like to thank Dr. Rathbone for all his encouragement, patience and understanding.

Many thanks to Dr. Peter Lambert for his guidance with the antibacterial screening, to Dr. Mike Coleman for his guidance in the cytotoxicity screen and to Dr. Carl Schwalbe for all the crystallographic work.

I would like to express my gratitude for the help, technical assistance and advice from Mike Davis and Karen Farrow.

Thankyou to everybody in the medicinal chemistry labs who kept me going when things went pear-shaped, Julie Simpson, Chris Langley, Fiona Salvage, Nafisa Rafiq, Aisha Ali and Karen Farrow. Thankyou also to Dr. Bill Fraser, for advice and chats on chemistry and life in general. I would also like to thank Annette Phipps for all her support and encouragement.

Finally, I would like to thank my Mum and Dad for their support and encouragement throughout my time at university, and last but by no means least, Andy, whose patience and understanding went beyond the call of duty.

GIFTS

Thankyou to Dr. P.A. Griffiths, Hospital Research Laboratory, City Hospital, NHS Trust, Birmingham, for the kind donation of *Mycobacterium fortuitum* (NCTC 10394). I would also like to thank Dr. Griffiths for generously carrying out the MIC of compound **2PYbn** against *Mycobacterium tuberculosis* (H37Rv) under Category 3 conditions.

Thankyou also to Prof. T.S.J. Elliot, Department of Clinical Microbiology, University Hospital, NHS Trust, Birmingham, for the kind donation of clinical MRSA and VRE strains.

PUBLICATIONS

Billington D.C., Coleman M.D., Ibiabuo J., Lambert P.A., Rathbone D.L., Tims K.J. (1998). Synthesis and Antimycobacterial Activity of Some Heteroarylcarboxamidrazone Derivatives. *Drug Design Discov.*, 15, 269-275.

Billington D.C., Tims K.J., Rathbone D.L. (1998). Automated Synthesis and Antimycobacterial Activity of a Series of 2-Heteroarylcarboxamidrazones and Related Compounds. *J. Pharm. Pharmacol.* 50 (Supplement), 262.

Billington D.C., Coleman M.D., Lambert P.A., Rathbone D.L., Schwalbe C.H., Tims K.J. (1998). 2-Heteroarylcarboxamidrazones as Potential Therapeutic Agents for Multi-Drug Resistant TB. *J. Pharm. Pharmacol.* 50 (Supplement), 245.

Schwalbe C.H., Gallagher C., Lowe P.R., Billington D.C., Rathbone D.L., Tims K.J. (1999). Comparison of structural features and antimycobacterial activity in isomeric pyridyl-carboxamidrazones. *J. Pharm. Pharmacol.* 51 (Supplement), 262.

Coleman M.D., Endersby C., Hovey M.C., Tims K.J., Rathbone D.L., Billington D.C., (1999). In-vitro toxicity evaluation of two novel anti-tubercular 2-pyridylheteroarylcarboxamidrazone derivatives. *J. Pharm. Pharmacol.* 51 (Supplement), 243.

Coleman M.D., Rathbone D.L., Endersby C.R., Hovey M.C., Tims K.J., Lambert P.A., Billington D.C. (2000). Preliminary in vitro toxicological evaluation of a series of 2-pyridylcarboxamidrazone candidate anti-tuberculosis compounds: II. *Environ. Toxicol. Pharmacol.* 8, 167-172.

Billington D.C., Rathbone D.L., Tims K.J., Attkins N., Cann S.W., Billington D.C. (2000). QSAR Studies On a Large Set of Antimycobacterial *N*^{1}-Benzylideneheteroarylcarboxamidrazones. *J. Pharm. Pharmacol.* 52 (Supplement), 97.

Schwalbe C.H., Rathbone D.L., Tims K.J., Billington D.C., Sandbhor U., Padhye S. (2000). Effects of functional group deletion on structural features and antimycobacterial activity in pyridyl-carboxamidrazones. *J. Pharm. Pharmacol.* 52 (Supplement), 105.

Tims K.J., Rathbone D.L., Lambert P.A., Attkins N., Cann S.W., Billington D.C. (2000). *Mycobacterium fortuitum* as a screening model for *Mycobacterium tuberculosis*. *J. Pharm. Pharmacol.* 52 (Supplement), 135.

LIST OF CONTENTS

LIST OF TABLES

LIST OF FIGURES

LIST OF SCHEMES

ABBREVIATIONS

ACP	Acyl carrier protein
AIDS	Acquired immunodeficiency disease
APCI-MS	Atmospheric pressure chemical ionisation mass spectrometry
Ar	Aromatic
bs	Broad singlet
BTS	British thoracic Society
CPZ	Chlorpromazine
d	Doublet
DBU	1,8-Diazabicycloundec-7-ene
DCC	1,3-Dicyclohexylcarbodiimide
DCE	Dichloroethane
DCM	Dichloromethane
DEPT	Distortionless enhancement by polarisation transfer
DMAP	4-Dimethylaminopyridine
DMF	Dimethylformamide
DNA	Deoxyribonucleic acid
DOTS	Directly observed therapy short course
EMB	Ethambutol
ETH	Ethionamide
eq	Equivalents
Eqn	Equation
FDA	Federal Drugs Aministration
FTIR	Fourier transform infra red
FQ	Fluoroquinolones
GISA	Glycopeptide-intermediate *Staphlococcus aureus*
HCl	Hydrochloric acid
hex	Hextet
HPLC	High performance liquid chromotography
HTS	High throughput screening
INH	Isoniazid (isonicotinylhydrazide)
inh.	inhibition
m	Multiplet
MDR	Multi-drug resistant
MIC	Minimum inhibitory concentration
MNL	Mononuclear leucocytes

mp	Melting point
MRSA	Methicillin resistant *Staphylococcus aureus*
MS	Mass spectrometry
MW	Molecular weight
NAD	Nicotinamide adenine dinucleotide
NAP	Nitroimidazopyran
NCS	N-chlorosuccinamide
NFQ	Non-fluorinated quinolones
NMR	Nuclear magnetic resonance
ov.m	Overlapping multiplet
PAS	*para*-Aminosalicylic acid
Pd-C	Palladium on charcoal
PE	Petroleum ether
PEG	Polyethylene glycol
Pyraz	Pyrazinyl
Pyr	Pyridyl
PZA	Pyrazinamide
q	Quartet
QSAR	Quantitative structure-activity relationship
Quin	Quinolyl
quint	Quintet
RIF	Rifampicin
R.f.	Retention factor
ROS	Reactive oxygen species
RT	Room temperature
s	Singlet
SAR	Structure-activity relationships
sat.	Saturated
sept	Septet
SM	Streptomycin
subst.	Substituted
t	Triplet
TAACF	Tuberculosis Antimicrobial Acquisition and Coordinating Facility
TB	Tuberculosis
TEA	Triethylamine
THF	Tetrahydrofuran
TLC	Thin layer chromatography
VRE	Vancomycin resistant enterococci
VRSA	Vancomycin resistant *Staphylococcus aureus*
WHO	World Health Organisation

CHAPTER 1
DRUG DISCOVERY

1.1 THE PROCESS

In rational drug design, a suitable biological target is identified and potential inhibitors designed. Test compounds are synthesised, which may be screened either against an appropriate isolated cellular target, or against the whole cell *in vitro*. If a compound is a 'hit', i.e. displays biological activity, then derivatives of this structure are synthesised, in order to try and improve the activity. The chemically optimised or 'lead' compounds are then put forward as potential drug candidates, and so subjected to extensive studies in a development phase, including toxicology and studies of the metabolism of the molecule within the body and excretion from it. If a compound passes these tests, it can then enter clinical trials.

In 1996, for every approved drug in the United States an average of 6,200 compounds were synthesised. Of these, 6.5 were tested in humans and only 2.5 made it to phase III clinical trials (the final stage before approval). Up to this stage the process cost about $350 million and took about 12.8 years[1].

The overall research and development spend in the US pharmaceutical industry rose from $6 billion dollars in 1988 to approximately $21 billion in 1998[1]. To maintain the increasing cost of research and development, pharmaceutical companies have had to re-evaluate the drug discovery process. The goal has been to make the process faster and more efficient and so hopefully to introduce new drugs to the market at a greater rate.

1.2 ADVANCES IN BIOLOGICAL SCREENING

During the late 1980's, rapid progress in molecular biology and gene technology meant that the biological methods needed to identify and prepare the proteins (e.g. drug receptors, enzymes, ion-channels) directly associated with medical symptoms of disease were discovered. Very efficient drug test systems were designed, often using target proteins to reliably ascertain *in vitro* activity. Only tiny amounts of test substances were needed, and, more importantly, the process was automated. This so-called 'high throughput screening' (HTS) allowed thousands of compounds to be tested in the time which would previously have been required to hand screen perhaps only a few dozen compounds. This massive increase in screening capacity lead to the rate-determining step in drug discovery becoming the synthesis of new compounds for biological testing[2,3].

1.3 A NEW APPROACH TO CHEMICAL SYNTHESIS

Medicinal chemists have always aimed to synthesise, purify, characterise and test compounds for biological activity. Once an active molecule has been identified, its structure is then varied slightly in an attempt to optimise the activity. A new active substance is obtained using a mixture of intuitive chemical variation and trial and error. It is possible that many thousands of molecular variations could be synthesised before a marketable product is found[2]. A medicinal chemist, synthesising one compound at a time by hand, could make around 50 to 100 compounds a year, at a cost of thousands of dollars per compound[4]. Not only was this not particularly cost-effective, but the numbers of compounds being produced in this manner were simply not enough to match the capabilities of the new HTS programmes. In the early 1990's, in order to meet the increased demand for compounds, chemists started to synthesise large 'libraries' of structurally similar molecules en-masse. This new approach often involved making all possible combinations of a series of reactants and was therefore termed 'combinatorial chemistry', a process which resulted in a large number of products[2]. It was estimated that a medicinal chemist employing these combinatorial techniques would produce around 3,300 compounds per month, at a cost of only $12 each[5].

Since the advent of combinatorial chemistry, many more compounds are synthesised annually than the 6,200 per approved drug in the US mentioned in Section 1.1. It is however, *libraries* of compounds that tend to be produced by combinatorial chemistry, so although there are many more compounds to test, the *different types* of molecules available may not be as diverse as those synthesised previously.

1.4 COMBINATORIAL CHEMISTRY

Combinatorial chemistry is based on the premise that the probability of finding a 'hit' in a random screening process is proportional to the number of places one looks for it. If one simultaneously generates numerous molecules then there are obviously numerous places to look and therefore a higher chance of finding a biologically active molecule. The principle of combinatorial chemistry is to synthesise all possible combinations (or a structurally diverse representative sample) of a set of reagents or 'building blocks'. The number of products attainable from a given set of components increases exponentially, while the number of components required increases only arithmetically. The result is a fundamental shift away from traditional stepwise organic synthesis to reaction and process design strategies that allow for the simultaneous production of large sets of related molecules[6].

To give a general example of combinatorial chemistry; if coupling monomer A with monomer B gives the product AB, then combinatorial synthesis can take a range of building blocks A_1-A_n and react those with building blocks B_1-B_n to make any product combination (Figure 1.1)[7].

Conventional Synthesis

$A + B \longrightarrow AB$

Combinatorial Synthesis

$A_1 + B_{(1\text{-}n)} \longrightarrow A_1B_1, A_1B_2, A_1B_3 \ldots\ldots A_1B_n$

$A_2 + B_{(1\text{-}n)} \longrightarrow A_2B_1, A_2B_2, A_2B_3 \ldots\ldots A_2B_n$

.
.
.

$A_n + B_{(1\text{-}n)} \longrightarrow A_nB_1, A_nB_2, A_nB_3 \ldots\ldots A_nB_n$

Figure 1.1 Comparison of conventional and combinatorial synthesis

Combinatorial libraries are created by one of two methods. 'Split and mix' synthesis creates a mixture of compounds simultaneously in one vessel, this has the benefit of further increasing the numbers of compounds which can be screened in one go, but if the mixture is found to demonstrate biological activity, then the mixture must be deconvoluted in order to discover which component is the active one. Secondly, 'parallel synthesis' can be used to give spatially discrete compounds, i.e. one compound per vessel, so of course the products are far easier to analyse and test.

1.4.1 Synthesising Compounds as Mixtures

Initially the field of combinatorial chemistry focused on the synthesis of peptide and oligonucleotide libraries, based on the solid-phase peptide synthesis according to Merrifield[2]. The synthesis of peptides lent itself to this solid-phase synthesis, due to the limited range of synthetic transformations required, and high yielding, reproducible chemistry[7]. Solid-phase synthesis of peptides or oligonucleotides were often made as mixtures as described below.

1.4.1.1 Split and Mix Synthesis

Split and mix chemistry is a way of producing mixtures of compounds. The screening of mixtures is not a new idea; pharmaceutical companies have always tested natural product extracts from micro-organisms and plants for biological activity, and these often contain many hundreds of different molecules[3].

The split and mix technique was first used in the generation of peptides[2,6-9]. In split and mix combinatorial synthesis, compounds are assembled on the surface of a resin support, either microparticles or beads (Figure 1.2). The beads are divided into a number of equal portions (x), each of these are then separately reacted with a single different reagent or building block (A, B, C etc.). After the reaction is completed, the excess reagents are washed away using an appropriate solvent and the individual reacted beads are recombined and mixed well. Then they are divided into x equal portions again, reacted with a further set of reagents and washed, to give mixtures containing all the possible dimers. The process may be repeated n times to give a total of x^n products. Each bead in the library will carry multiple copies of a single library member, due to the beads having many reactive sites. The compounds may be screened whilst still attached to the resin, or as a mixture of the cleaved products off the resin[6,7,9].

In this way, biologically active peptides were discovered, isolated and identified using various deconvolution and sorting strategies, but their use as drugs was severely limited. Peptides have low bioavailability and are susceptible to proteolytic degradation. It is also extremely difficult to translate them into non-peptidic drug candidates[2,6].

Split and mix synthesis has since been adapted to produce large numbers of small organic molecules (MW< 600-700), which are inherently better potential drug candidates, due to their more favorable pharmokinetic properties[6,9]. Once again though, the testing of mixtures presented the same problem; when a mixture displayed biological activity, then the active constituent had to be determined. This was often achieved by multiple, systematic, iterative resyntheses and rescreening of specific mixtures and compounds. It is a lengthy and laborious process, so encoding strategies were developed in which molecular tags were attached to either the solid-phase beads themselves or the linker groups, in order to identify the active molecules after screening[2,7-9].

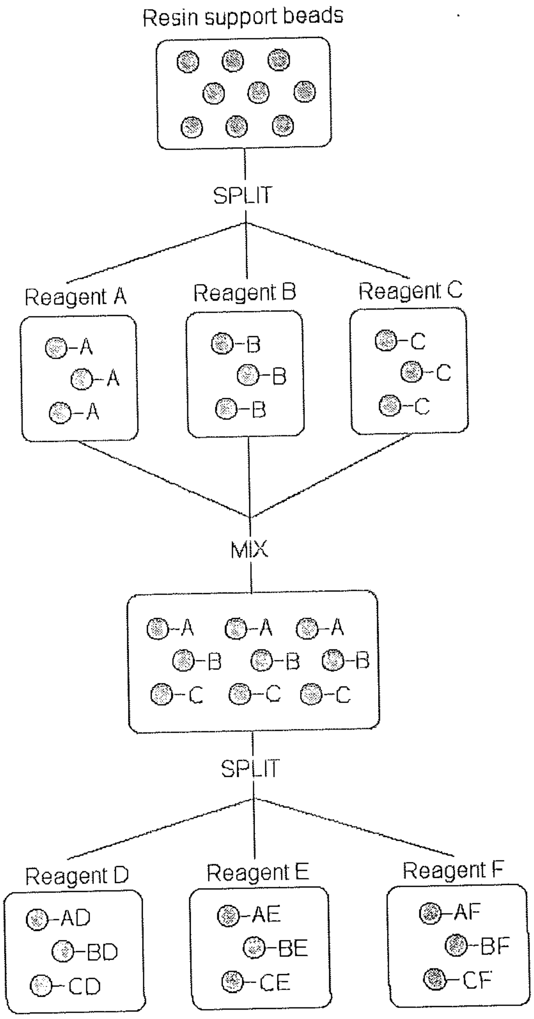

Figure 1.2 Split and mix synthesis

Combinatorial synthesis of solution-phase mixtures is possible[10], but there is a lack of control over reaction completion and purification at each step. This means that the possible number of reaction steps is quite limited. The abundance of each component within the mixture may differ widely[2] and solution-phase mixtures have a large potential for the production of unwanted by-products.

The use of mixtures significantly increases the number of compounds that can be synthesised and tested per time unit. In order for the biological testing to be fair, however, the synthesis must deliver all compounds in approximately equimolar amounts. There are also potential problems with actually testing compounds as mixtures; this can frequently produce equivocal or false results, false positives arising due to the synergistic activities of different molecules with the target[6,9]. A common view is that one can afford to miss some active compounds during screening because a sufficient number of interesting molecules will still be detected, due to the large numbers of test compounds prepared. This can be justified as long as any attempt to determine structure-activity relationships takes into account the fact that negative results may be unreliable[9].

1.4.2 Synthesising Single Compounds - Parallel Synthesis

Increasingly, synthesis has moved away from making complex mixtures of compounds for biological screening, and towards the production of single compounds in spatially discrete reaction vessels[11]. This method has been termed 'parallel synthesis' and allows individual compounds to be prepared simultaneously, in greater quantities and with relatively high purity. Since only one compound is produced per reaction vessel, smaller numbers of compounds are usually produced by this method as opposed to mixture synthesis. Biological testing may also be a slower process when testing individual compounds, but equally it can often be very advantageous too; the problems of false results which can be encountered when testing mixtures (described above) are avoided.

1.4.3 Solution-phase Synthesis versus Solid-phase Synthesis

In principle, combinatorial synthesis can be performed both in solution and on solid-phase; each method has its own advantages and disadvantages.

1.4.3.1 Solution-phase

Solution-phase chemistry is often used for high yielding single step reactions. It can be used for chemistry involving two or maybe three sequential synthetic steps, but anything more complicated results in problematic parallel purification[3]. A huge number of organic transformations have been carried out in solution, and so solution-phase chemistry provides access to many classes of compounds. The number of reaction steps required are reduced for solution-phase syntheses as there is no need to either attach the starting material onto, or cleave the final product from, a support. Product purification may often be conveniently achieved for reactions in solution by liquid-liquid or solid-liquid partitioning or by the use of scavengers to remove undesired material[12,13]. Compounds may be prepared in larger quantities than with solid-phase chemistry and may be scaled-up easily in the traditional manner should an active compound be found.

1.4.3.2 Solid-phase

Solid-phase synthesis is often preferred when more than two steps are required, mainly due to the ease of purification by washing away any non-resin bound by-products and excess reagents. This is achieved by using an appropriate solvent and facilitates multistep reactions. Another advantage of synthesis on the solid-phase is that it can be readily automated and a range of substrates with varying reactivities can easily be accommodated by the use of excess reagent to drive every reaction to completion. Small organic molecule synthesis on solid supports however, is nowhere near as well optimised as the established synthesis of peptides and nucleotides. This means that the extra labour and time required for the development of such syntheses can be considerable. The range of available supports and linkers may limit possible chemistry and methods for the analytical monitoring of reactions and identifying intermediates are not well developed[2]. Problems may arise in solid phase syntheses due to the heterogeneous reaction conditions. This can lead to nonlinear kinetic behavior, unequal distribution of reagents and/or access to the chemical reaction if the reaction sites are in 'pockets'. These limitations have prompted research into a methodology which employs a soluble polymer support (See Section 9.1), which is called liquid-phase synthesis and avoids the difficulties of solid-phase synthesis, whilst preserving its positive aspects[14]. Solid-phase synthesis also requires the extra steps to link to, and cleave from, the support and the amounts of final product obtained are often small due to the limited loading capacity of the solid-phase supports.

1.4.4 Compound Libraries

Compound libraries can be divided into two types in terms of their diversity; random primary libraries and focused libraries. The diversity of a library can be measured by various parameters such as molecular shape, volume, molecular weight (MW), polarity, solubility and pharmacophore that the compounds within the library exhibit.

1.4.4.1 Random Primary Libraries

Random primary libraries tend to be prepared when there is little or no information about the target of interest; such as receptor or enzyme structure, or structure-activity relationships[6,15]. When this is the case, the chance of finding active compounds in a library increases with the diversity of the compounds within it. An infinite diversity, or as many different shapes and sizes of compounds as possible is needed to find maximum activity[2,6]. Therefore, random primary libraries tend to be numerically large, containing either many types of different compounds, or similar compounds but with a wide variety of functional group substitutions.

1.4.4.2 Directed or Focused Libraries

Directed or focused libraries are prepared when there is some structural information about the substrate, inhibitor or ligand that interacts with a specific target[13]. It may be that the molecular structure of a biomolecule is known, or that the 3D x-ray structure has been solved. Any information about the structure-activity relationship reduces the need for chemical diversity and can direct the process to produce analogues of an active structure, optimising the original 'lead'. It may be that the lead structure or structures were discovered through the screening of a random library, which a focused library can then attempt to optimise[15,16]. By its very nature, members of a focused or directed library will all contain a common pharmacophore, beyond this, maximum chemical diversity can be generated in a way that is believed to be compatible with retention of the pharmacophores activity[1]. Focused libraries are therefore much smaller than random libraries.

1.4.5 Current Directions

One indication of the maturity of the field of combinatorial chemistry is the upsurge of academic journals dedicated to the subject; *Combinatorial Chemistry* started in 1998 and *Journal of Combinatorial Chemistry* followed in 1999[5]. Combinatorial chemistry is definitely here to stay. Considerable efforts have been devoted to new technologies for the analysis of combinatorial libraries, equipment to miniaturise libraries is being produced and computer technologies continue to be developed, all to aid the efficiency of combinatorial chemistry.

1.4.5.1 Analysis and Purification

Chemical analysis and quality control are of paramount importance for all libraries. Large libraries of single compounds can be problematic to analyse as not all reactions work, so for screening it is a great advantage to be able to characterise these libraries for structure and purity. One of the most exciting developments in the area of analysis of libraries is high-throughput NMR. It is now possible to autosample plates of compounds, pass them through an NMR probe an get the NMR spectrum on the compounds in three minutes per sample[5]. Other analytical instruments such as mass spectrometers are also being customised for combinatorial applications.

Where mixtures of compounds are produced, the difficulty of adequate chemical analysis increases with the number of components. In these cases mass spectrometry (MS) and high performance liquid chromatography (HPLC) analysis in combination have emerged as the most suitable techniques to be utilised[10]. HPLC systems are also in use for library purification[5].

Solid-phase organic synthesis offers many practical advantages over solution-phase chemistry (see Section 1.4.3.2), but effective monitoring of reactions on resin remains problematic. High-throughput NMR is not widely available and although mass spectroscopic techniques can offer high-throughput, too many molecules do not have the appropriate ionisation properties for this to be universally applicable. In an attempt to address this problem, the concept of analytical constructs has been introduced, in which the solid supported substrate and linker are attached to the support via a MS sensitiser (which also acts as a peak splitter) and a second orthogonal linker (Figure 1.3)[17].

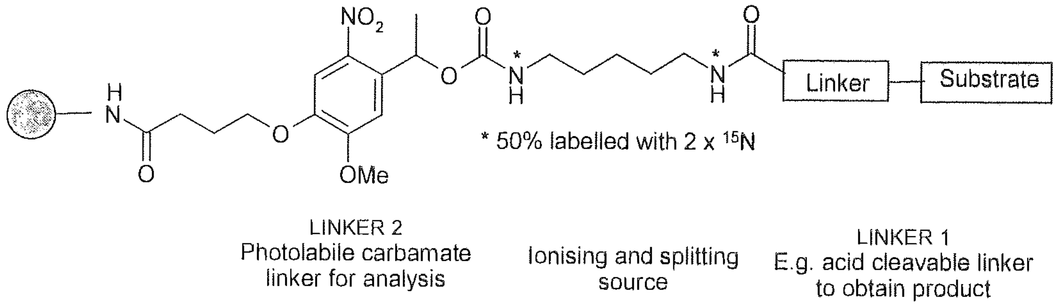

Figure 1.3 Alternative cleavages of the photolabile analytical construct

The construct can be cleaved in either the classical (e.g. with acid) manner to afford the substrate alone, or can be cleaved photochemically to give the analytical fragment, containing the substrate, classical linker and a free amine. The amine, revealed by photocleavage, sensitises the entire fragment to electrospray MS, now guaranteeing that all substrates are readily visible by high throughput MS when cleaved in this fashion. The diamine sensitiser portion contains isotopically labelled atoms, a 1:1 mixture of $^{14}N_2$-diamine and doubly labelled $^{15}N_2$. This hallmarks all MS signals derived from the construct resin as characteristic doublets, distinguishing them from extraneous signals and background noise. The sensitiser enables samples from just one bead to be resolved by MS[17,18]. There are however, a few drawbacks to this elegant approach; the reaction and its products cannot be quantified and producing a construct such as this will increase the cost of synthesis considerably.

Also for syntheses on solid support, Novartis Pharmaceuticals has developed infrared spectrometry (IR) techniques to identify quantitative reaction products (as a percentage conversion) directly on a single bead. This method is greatly advantageous as prior to this, the compound had to be cleaved off the bead before analysis. The analysis can be carried out without interrupting the reaction, which makes reaction optimisation on the solid-phase much easier, especially for multistep synthesis[5].

1.4.5.2 Miniaturisation

As applications of combinatorial chemistry proliferate, the ability to keep equipment size and so reagent quantities and therefore cost to a minimum is of growing importance[5]. There have been a number of "labs on chips" made available for miniaturisation. These chips contain cavities with wettable surfaces to be contacted and filled with liquid reagents, one example is Orchid Biocomputers' 2 inch square chips which can be used to carry out chemical reactions in submicrolitre volumes in 144-well arrays[5,19]. Miniaturisation in the chemistry and biology arena is highly interdisciplinary and the never-ending demand for high-throughput will drive forward the miniaturisation of HTS too[19], saving costs in the testing stages as well as synthesis, since less protein or reagent will be required for the biological assays.

1.4.5.3 Artificial Intelligence

A major question that is now being addressed is "just because it is possible to synthesise and screen thousands of compounds per month is this an effective use of resources?". The enormous amount of data that this process generates and the work involved in processing and interpreting the information gained, presents a major challenge for information management, especially if the structural information obtained from biological screening is to be optimised. Chemists in the pharmaceutical industry have recently begun to apply techniques of neural networks and artificial intelligence to try and predict which molecules within a given library are most likely to display the required biological profile for a given drug discovery programme. The aim is to intelligently use the data produced by HTS and molecular modelling to filter and identify the best candidates for combinatorial synthesis[3].

Compound libraries, whether physical or virtual (not physically prepared, but stored in computer memory), are often subjected to diversity analysis in order to identify the minimum acceptable set required for synthesis and testing. This set should cover all the chemical properties (molecular shape, volume, MW, polarity, solubility, etc.) of the entire library, whilst minimising the number of compounds to be prepared and screened, thus decreasing costs. The objective is therefore changing from synthesis and screening of a maximum number of compounds, to the synthesis and screening of the minimum number of compounds required to achieve the required profile of a compound set against a given biological target. In this way artificial intelligence and automation are continually improving the effectiveness of the drug discovery process.

CHAPTER 2
THE STAPHYLOCOCCI AND ENTEROCOCCI

It is the discovery of penicillin which truly marks the advent of the antibiotic era. In 1928 Alexander Flemming, a pathologist at St.Mary's Hospital in London noticed that when *Penicillium notatum* moulds contaminated his culture plates, it killed the staphylococci growing there. He later isolated the inhibiting substance and named it penicillin. Penicillin was not developed for clinical use, however, until over a decade later.

It is therefore the development of the sulfonamide drugs by Gerhard Domagk in the 1930's, which really initiated the use of antibacterial agents in therapy. Shortly after the clinical success of the sulfonamides, Howard Florey and Ernst Chain at Oxford University developed practical methods for the production of Flemming's penicillin and clinical trials of the drug started in the early 1940's. Over the next forty years many structurally diverse, highly effective antibacterial agents were discovered through natural product screens and subsequently developed into effective drugs. Since the early 1980's however, the introduction of new agents for clinical use has declined; a result of both the challenge of identifying new drug classes, and a decline in research and development in this area by pharmaceutical companies. This lack of interest in antibacterials by companies was probably due to the belief that plenty of effective drugs were available, that the financial returns would not justify the efforts required to develop new agents (it currently costs around $300 million to bring a drug to market), and the opinion that bacterial infections had, to all intents and purposes, been conquered[20].

Alarmingly, we now appreciate that, at the same time in which development of new antibacterial agents has been much reduced, there has been a rapid increase in bacterial resistance to existing agents. This presents a new and very serious threat to global public health[21]. Although many different bacteria show some resistance to some drugs currently available, this report will focus on resistance in *Staphylococcus aureus*, the Entercocci and *Mycobacterium tuberculosis.*

2.1 *STAPHYLOCOCCUS AUREUS* AND ENTEROCOCCI

Staphylococcus aureus is a Gram-positive, coagulase positive bacterium which is responsible for many severe infections, such as sepsis of wounds and burns, endocarditis (destruction of the heart valves, leading to heart failure) and pneumonia[22]. Initially this type of infection was treated with β-lactam drugs (such as penicillin), but resistance soon became a problem. Methicillin was developed to combat these resistant strains, as it did not appear to be cleaved by the β-lactamase enzyme responsible for penicillin resistance. Unfortunately, methicillin resistant *S.aureus* (MRSA) strains also emerged quickly after the introduction of the drug into therapy. The first outbreaks occurred in European hospitals in the early 1960's, and MRSA has since spread world-wide[23]. The escalation of incidences of MRSA is presently causing serious concern, as MRSA are very adaptable and seem to respond rapidly to antibiotic selection, to the extent that some strains are now resistant to all clinically used antibiotics except vancomycin. Vancomycin is the only drug approved for use against MRSA in the USA, but in Europe, another glycopeptide, teicoplanin is also available.

Enterococci (such as *E.faecalis* and *E.faecium*), are also Gram-positive bacteria, which commonly live in the gut, but can cause urinary tract infections, abdominal abscesses, endocarditis[22] and infections associated with catheters and other medical devices. Glycopeptide resistance has emerged in these organisms, and vancomycin-resistant enterococci (VRE), such as *Enterococcus faecium,* first reported in 1988, are becoming an increasing problem in hospitals. Fortunately, enterococci are not particularly virulent pathogens, and predominantly only affect patients who have a serious underlying disease.

The major concern now is that vancomycin resistance could be transferred from enterococci to *S.aureus*. Resistance to glycopeptides has already been observed in some coagulase negative staphylococci, such as *S.haemolyticus* and *S.epidermidis* which have developed resistance to teicoplanin, and some species show intermediate resistance to vancomycin[24]. Coagulase negative staphylococci are the species that do not produce the enzyme protein, coagulase. *S.aureus* on the other hand is coagulase positive, that is, it does produce coagulase, which works in conjunction with blood serum factors to coagulate plasma. Coagulase also contributes to fibrin production around staphylococcal lesions which helps them persist in tissues. Fibrin is also deposited on the surface of individual staphylococci, which may help prevent ingestion by phagocytes. The production of coagulase is considered synonymous with invasive pathogenic potential and bacteria which do this are therefore generally thought of as more problematic[22].

Until fairly recently, there had been no clinical reports of vancomycin resistant MRSA, although vancomycin resistant *S.aureus* had been obtained *in vitro* by plasmid transfer from enterococci[25]. In 1997, however, a clinical strain of MRSA with reduced vancomycin susceptibility was isolated in Japan[26]. The potential of reduced susceptibility strains such as this, and others reported in America, to spread around the globe, is a major concern at this time[27].

The threat of high-level vancomycin resistant *S.aureus* has, unfortunately now been realised. Two cases of vancomycin resistant *S.aureus* (VRSA) have recently been reported, one in Michigan[28] and the other in Pennsylvania[29]. Since *S.aureus* is a much more aggressive pathogen than the enterococci, the worry is, that without any new drug alternatives, we could be faced with a "superbug" for which there is no cure.

2.2 THE EMERGENCE OF RESISTANCE

Poor patient compliance with drug regimens can bring about drug resistance. Patients often fail to complete the full course of prescribed antibiotics, because they feel better after a few days. This means that only the most susceptible bacteria are killed, allowing the more resistant bacteria to survive. This process is known as selective pressure; with less competition, the more resistant bacteria find it easier to thrive. The occurrence of drug resistance may also be closely linked to doctors prescribing antibiotics unnecessarily, often due to patient demand rather than medical need, perhaps for a viral infection which is unaffected by antibiotics[30].

Resistant bacteria can transfer their resistance through mating. A male cell joins a female cell via an F pilus (sex pilus) and transfer of plasmids, such as a drug resistance plasmid, can occur from one cell to the other. This confers the donor characteristics upon the recipient cell and so the number of resistant cells at the infection site can increase rapidly. The next person to be infected by this bacterial strain will also show resistance to that particular drug.

Antibiotics are also used widely in animal husbandry, not only to treat or prevent infections, but also as growth promoters. Antibiotics in feed promote growth of farm animals by killing the bacteria which occur naturally in the gut, thus improving nutrient uptake and therefore growth rate. It is thought that the extensive use of drugs for this purpose may encourage the spread of antibiotic resistance, although whether multidrug resistant bacteria can spread from animals to humans is still under debate.

2.3 BACTERIAL RESISTANCE MECHANISMS

There are a number of mechanisms by which bacteria can become resistant to antibiotics. The antibacterial agent may be chemically modified and inactivated by an enzyme, or there may be alteration of the drug target site within the cell. Sometimes an organism may bypass the effect of an antimicrobial, by using an alternative pathway or enzyme. Efflux mechanisms may actively pump the antibacterial out of the cell before it can have any effect, or the agent may be sequestered by cellular proteins, such that any antimicrobial action is blocked[31]. Resistance to a wide range of antibacterial agents has been reported in *S.aureus* and *E.faecium*, some of which will be discussed in greater detail below.

2.3.1 Resistance to β-lactam Antibiotics

2.3.1.1 β-lactamase Mediated Resistance

Penicillin and its analogues, also known collectively as the β-lactam antibiotics, have been used extensively in treatment of bacterial infections since penicillin was first used therapeutically in 1941. The first report that extracts from bacteria could destroy penicillin was published in 1940 and strains of *S.aureus* resistant to penicillin soon emerged[32]. The resistance was a result of the bacteria's ability to produce the enzyme β-lactamase, which hydrolyses the β-lactam ring, rendering the molecule inactive (see Figure 2.1). This type of resistance is now very common, with reports that up to 93% of hospital strains are resistant to β-lactamase labile penicillins.

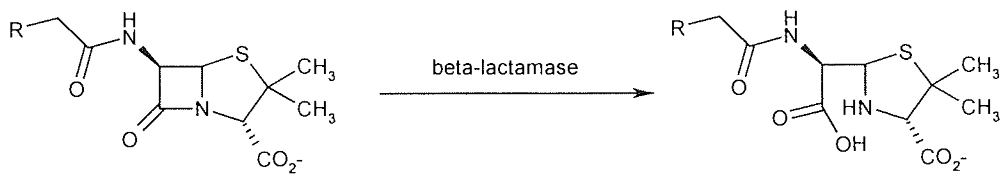

Figure 2.1 Cleavage of a penicillin by β-lactamase, to give the inactive penicillinoic acid

β-lactam antibiotics act at the staphylococcal membrane to inhibit peptidoglycan synthesis. Therefore, β-lactamase is either produced at the membrane or released into the surrounding medium, rather than being located in the cytoplasm, as the drug does not pass beyond the cell wall. β-lactamase formation is normally induced by the β-lactams themselves, although the detailed mechanism of this induction is unknown.

To overcome the failure of β-lactam therapy, investigations were initiated to find β-lactams that are not hydrolysed by β-lactamase. It was discovered that benzyl penicillin **1** could be enzymatically deacylated to produce 6-aminopenicillanic acid (6-APA) **2**. The 6-APA was then treated with a number of acyl halides to give semisynthetic penicillins. One of these was methicillin **3**, with a bulky 2,6-dimethoxybenzyl substituent. This was only very slowly hydrolysed by staphylococcal β-lactamase.

Other β-lactams produced were the carbapenems, which have a carbon atom in place of the sulfur atom, and the cephalosporins in which the β-lactam ring is fused to a 6-membered dihydrothiazine ring. Some cephalosporins, such as cephalothin **4**, are effective against β-lactamase producing *S.aureus*, as they are not substrates for the enzyme[30].

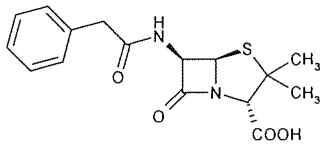

1

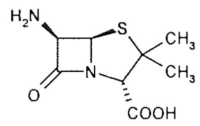

2

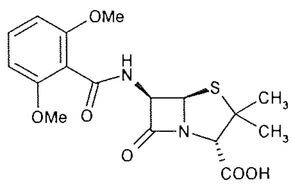

3

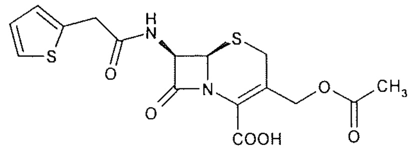

4

Figure 2.2 Some β-lactam antibiotics. Benzylpenicillin **1**, 6-aminopenicillanic acid (6-APA) **2**, Methicillin **3**, Cephalothin **4**

Another approach to overcome the problem of β-lactamase mediated resistance, was the search for an inhibitor of this enzyme that could act in synergy with a β-lactam antibiotic, that would otherwise be destroyed. It was discovered that such a compound was produced by a *Streptomyces* species, and this was called Clavulanic acid **5**. Clavulanic acid only displayed very weak antibacterial activity, but was found to be a potent β-lactamase inhibitor. Therefore it could be used to protect lactamase-sensitive, but otherwise potent antibiotics, such as ampicillin, from deactivation by the enzyme[33]. Other β-lactamase inhibitors have since been synthesised[33], such as tazobactam **6**.

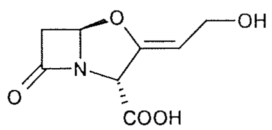

5

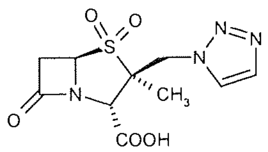

6

Figure 2.3 Clavulanic acid **5** and tazobactam **6**, are inhibitors of β-lactamase

2.3.1.2 Methicillin Resistance

Methicillin was introduced into therapy as a β-lactamase stable β-lactam. It was only very slowly hydrolysed by the enzyme, so could still be used effectively against β-lactamase producing bacteria. Bacterial resistance to methicillin, however, rapidly developed just two years after the drug was put into wide use.

Staphylococci can become resistant to methicillin either by mutation, or by acquisition of a foreign DNA element coding for methicillin resistance. The latter is more efficient and clinically more important. The methicillin resistance genetic determinant *mecA* confers resistance against all β-lactams, including cephalosporins and carbapenems.

2.3.1.3 *mecA*

Penicillin binding proteins (PBPs) are membrane bound peptidases that catalyse the transpeptidation reaction which cross links the peptidoglycan of the bacterial cell walls. β-lactam antibiotics are substrate analogues that covalently bind to the serine residue of the PBP active site, thus inactivating the enzyme.

PBPs 1, 2 and 3 are essential for cell growth and for the survival of methicillin susceptible strains. These PBPs have a high affinity for most β-lactam drugs, and the binding of these antibiotics is lethal.

Methicillin resistant staphylococci possess additional chromosomal DNA, known as *mec*, which is not found in susceptible strains. *mec* Contains *mecA*, the structural gene for PBP 2a (also termed PBP 2') and it is this which, when induced, confers methicillin resistance to the cell. PBP 2a has a low affinity for β-lactam antibiotics, and can compensate for the loss of essential functions of the high affinity PBPs, at concentrations of antibiotic which would otherwise be lethal. The structural basis for this low affinity is not understood[23].

Under normal growth conditions, in the absence of β-lactams, PBP 2a does not seem to contribute to cell wall composition or function. The mechanism and components of the cascade which lead from extra-cellular β-lactam, to signal transduction and the final induction of PBP 2a is not known[31].

2.3.2 Resistance to Other Antibacterial Agents

2.3.2.1 *Drug Inactivation Mechanisms*

Bacterial resistance to β-lactam antibiotics due to the production and action of the enzyme β-lactamase is an example of a drug inactivation mechanism. As previously mentioned, β-lactamase cleaves the β-lactam ring, rendering the drug inactive.

Aminoglycoside antibiotics, such as streptomycin, kanamycin and gentomycin inhibit protein synthesis by binding to the 30S ribosomal unit. This group of drugs have been widely used to treat staphylococcal infections and resistance has been observed[31].

The major mechanism of aminoglycoside resistance is drug inactivation by cellular enzymes produced by plasmids within the bacteria. Enzymes such as adenyltransferases or phospho-transferases (which both modify the hydroxyl group of the drug) and acetyltransferases (which acetylate the amino group), alter the three dimensional structure of the compounds. All of these modified products lose the ability to bind ribosomes, so do not inhibit protein synthesis and thus are rendered inactive[35].

2.3.2.2 Target Site Alteration

Macrolides such as erythromycin have a bacteriostatic effect by binding to the 50S ribosomal subunit, preventing protein synthesis. Resistance to macrolides is prevalent among staphylococci and this is due to target site alteration of the ribosome such that there is reduced affinity for the macrolide antibiotic[31].

The fluoroquinolone antibiotics, such as ciprofloxacin **10**, were introduced in the mid 1980's and were proven to be effective against MRSA in the clinic. It was assumed that the problem of MRSA was then under control, but a study by the Centres for Disease Control showed that ciprofloxacin resistance of MRSA went from less than 5% to more than 80% within one year[35].

Fluoroquinolones exert their antibacterial effect by interfering with the enzyme, DNA gyrase. This is an essential enzyme involved in DNA replication and repair. Target alterations in DNA gyrase, more specifically amino acid substitutions, decrease the fluoroquinolone sensitivity of the enzyme. A fluoroquinolone efflux system has also been described.

2.3.2.3 Efflux Mechanisms

Tetracycline inhibits protein synthesis by binding to the 30S ribosomal subunit. These antibiotics have not been widely used to treat staphylococcal infections, but resistance due to active efflux mechanisms have been noted. Drug efflux is driven by the proton motive force of the transmembrane electrochemical gradient, and it is a divalent metal ion (e.g.Co^{2+})/tetracycline complex which is transported out of the cell[31].

2.3.2.4 Sequestration

Bleomycin is a glycopeptide that induces multiple double strand breaks in DNA, which lead to cell death. Although bleomycin has not been used as an antibacterial agent (it has been used as an antitumor agent), resistance to bleomycin has been found in many *S.aureus* isolates. Resistance is conferred by so called Ble proteins which sequester the drug, i.e. bind bleomycin and inactivate it without modification of the drug[31].

2.3.3 Vancomycin Resistance

Vancomycin, and its analogue teicoplanin, are glycopeptide antibiotics which act by forming complexes with the peptidoglycan precursors at the outer surface of the cytoplasmic membrane. This prevents the precursors from being added to the growing cell wall polymer, thus disrupting cell wall synthesis.

The emergence of resistance to vancomycin was first documented in *E.faecium* and *E.faecalis* in 1988. Two major forms occur: *vanA* isolates are resistant to both vancomycin and teicoplanin and *vanB* isolates are normally only resistant to vancomycin, both of which have similar mechanisms of resistance[36] [See Section 2.3.3.2].

Enterococci strains have been able to transfer their resistance to *S.aureus* in the laboratory and the initial fear that this could also happen in nature is being realised. The first strain of glycopeptide-intermediate *S.aureus* (GISA, sometimes called vancomycin-intermediate *S.aureus*), with reduced susceptibility to vancomycin, was reported in 1996 in Japan, and several cases have since been reported in the US[30] . These bacterial strains did not contain either the *vanA* or *vanB* determinants, instead it is thought that resistance in these cases may be due to an intrinsic mechanism of augmented cell wall synthesis. The cell wall of these GISA strains appeared to be twice as thick as normal, by electron microscopy and an increase in cell wall murein precursors was also observed[26]. So far, GISA strains have been susceptible to other antibiotics. The emergence of high-level vancomycin resistant *S.aureus* (VRSA), in the clinic, which was completely resistant to vancomycin has recently been reported. These *S.aureus* strains had actually acquired the *vanA* vancomycin resistance gene from the enterococci[28,29].

The following discussion focuses on the known glycopeptide resistance mechanism of the enterococci, which could now be incorporated into the cells of *Staphylococcus aureus*.

2.3.3.1 *The Target of Glycopeptides*

Glycopeptides do not interact with cell wall enzymes, but form complexes with the peptidoglycan precursors at the outer surface of the cytoplasmic membrane. The glycopeptide antibiotics cannot penetrate into the cytoplasm, and interaction with the target can only take place after translocation of the precursors, bound to the surface of the undecaprenol carrier, to the outside of the membrane. Figure 2.4 shows the normal synthesis of glycopeptide where a pentapeptide precursor is incorporated into the nascent peptidoglycan via a transglycosylase enzyme. Glycopeptides, such as vancomycin, form a complex with the D-ala-D-ala terminus of the peptidoglycan precursor. Once this complex has been formed, the pentapeptide subunit can no longer be incorporated into the nascent peptidoglycan which leads to accumulation of precursors within the cytoplasm.

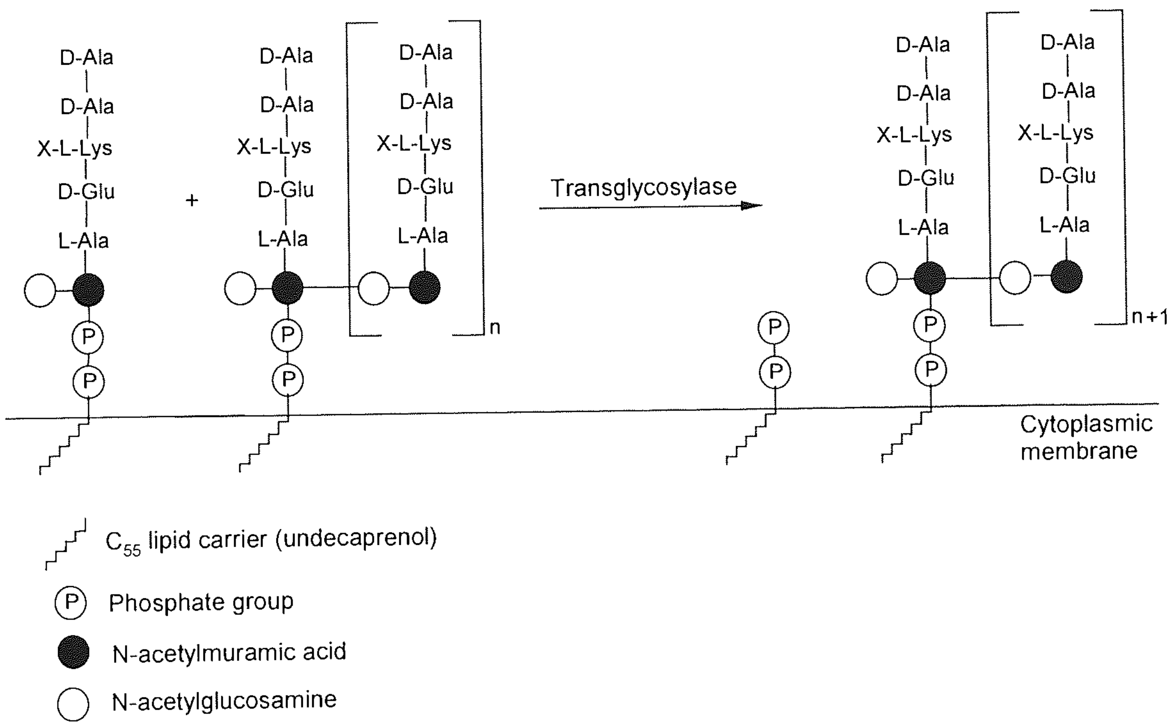

Figure 2.4 Reaction catalysed by the transglycosylases at the outer surface of the cytoplasmic membrane[37]

2.3.3.2 Molecular Basis for Glycopeptide Resistance

It is the D-ala-D-ala residue of the peptidoglycan precursors which interacts with the glycopeptides, such as vancomycin, preventing cell wall synthesis and causing cell death. Resistant bacteria containing the Van determinants, effectively re-engineer their cell wall, replacing the terminal D-ala with D-lac. This substitution results in an ester linkage, rather than an amide linkage of the terminal moiety and results in the loss of one vital hydrogen bond in complex formation with vancomycin. The resultant drug binding is at least one thousand-fold weaker and results in bacterial resistance[35].

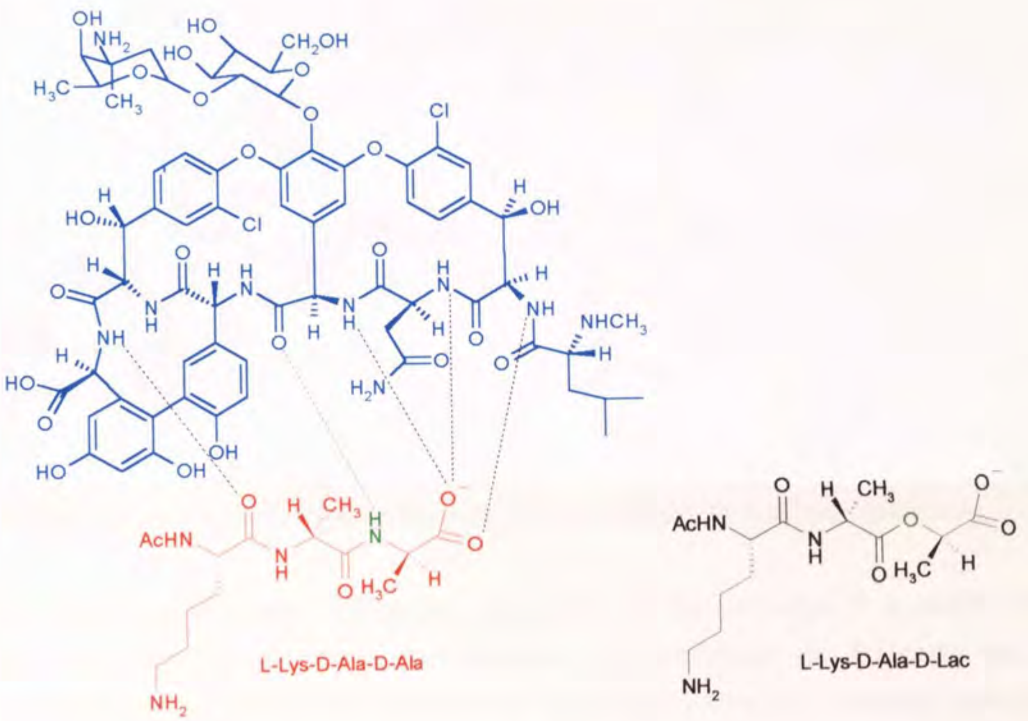

Figure 2.5 Binding model of cell wall precursor fragments to vancomycin. The dotted lines indicate hydrogen bonding. Note that the change from the amide linked D-Ala-D-Ala, to the ester linked D-Ala-D-lac, results in the loss of a key hydrogen bond[35]

2.4 NEW DRUGS TO TREAT DRUG RESISTANT BACTERIA

2.4.1 Quinupristin-dalfopristin

Quinupristin-dalfopristin, known as Synercid, is a combination streptogramin antibiotic treatment for parenteral administration. Quinupristin **7** and dalfopristin **8** are analogues of streptogramin B and streptogramin A respectively, which bind on two different sites on the ribosome. The streptogramin A component binds to the 50S ribosomal subunit, the streptogramin B component binds to the 70S subunit and these act synergistically to inhibit protein synthesis[36].

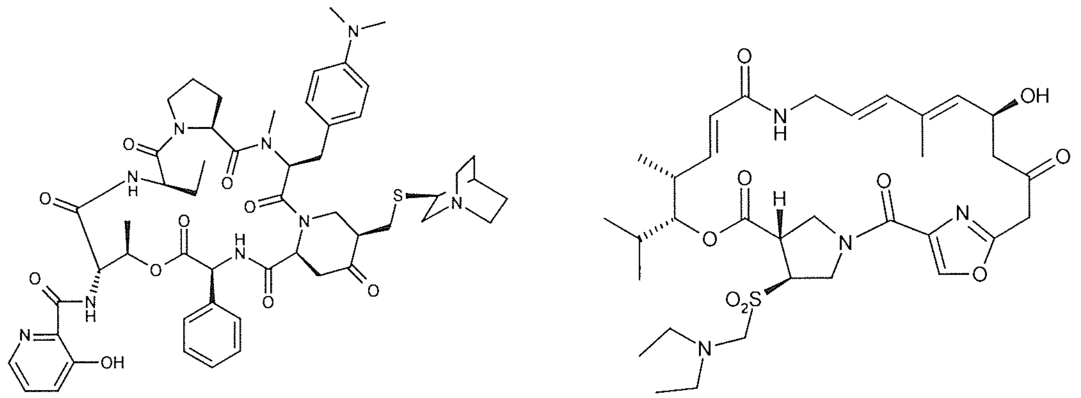

7 **8**

Figure 2.6 Quinupristin **7** (Streptogramin B) and Dalfopristin **8** (Streptogramin A)

One of the main problems with quinupristin-dalfopristin is that although it is active against *E.faecium*, it has only limited activity against *E.faecalis*. Superinfection with *E.faecalis* has been reported during quinupristin-dalfopristin treatment of vancomycin resistant *E.faecium*, and as the majority of nosocomial isolates of enterococci are *E.faecalis*, this may prove to be a limitation to its use.

Even in clinical trials, resistance to quinupristin-dalfopristin has been a problem. Isolates may be resistant to quinupristin as a result of the usual streptogramin B resistance mechanism (methylation of the target's binding site) and although this does not confer resistance to the drug combination, it may result in diminished efficacy. During clinical trials in 1996, 3 out of 24 patients (12.5%) had isolates of *E.faecium* which were resistant to quinupristin-dalfopristin[36].

Virginiamycin is another streptogramin A and B combination drug, which has been used in animal husbandry as a growth promoter for many years[38,39]. Studies in Europe have shown that the use of this drug selects for virginiamycin resistant strains of *E.faecium*, which are cross resistant to quinupristin-dalfopristin[39]. Clinical isolates of *E.faecium* resistant to quinupristin-dalfopristin have been identified in countries where the drug has never been used[38]. It therefore seems likely that the exchange of resistant strains or resistant genes may occur between *E.faecium* isolates from nonhuman and human sources. This is thought to pose a potential risk to public health, although the extent of the problem has not been quantified. As a consequence, the use of virginiamycin has already been banned in the European Union[38].

2.4.2 Semisynthetic Glycopeptides

Semisynthetic glycopeptides have been produced, by scientists at Lilly, which are active against clinical VRE isolates. Although due to the phenomenon of cross resistance, this activity may seem surprising, most of the naturally occurring glycopeptides and semisynthetic analogues that were tested did prove to be inactive against vancomycin resistant enterococci. One set of compounds did show activity though, and these were the N-alkyl vancomycins. Modifications of this type have also been carried out on other glycopeptides, where the side chain is varied, to yield compounds with high potency against MRSA's and VRE's (0.5-1μgml^{-1}) one of which, LY333328 **20**, has entered clinical trials in the USA[34].

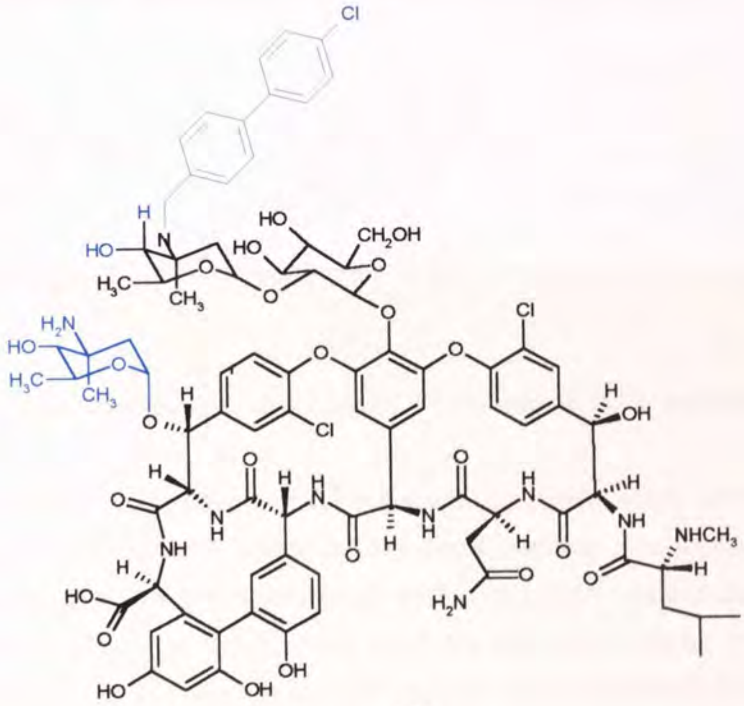

20

Figure 2.7 Semisynthetic glycopeptide LY333328 **20**. The vancomycin backbone is shown in black.

Unfortunately, the glycopeptide structure is not particularly amenable to modifications and the N-alkylation mentioned above is the only one to date which has any real positive effect on activity[34]. Therefore the structure may be somewhat limited as far as future development is concerned.

2.4.3 Fluoroquinolones

Ciprofloxacin **10**, introduced in the late 1980's, was one of the first fluoroquinolones introduced and it was hoped that these relatively new drugs would solve the increasing problem of multidrug resistant Gram-positive bacteria. Regretably, extensive use of these drugs selected rapidly for quinolone resistant MRSA[40].

Despite this, substantial research into this area has continued and a large number of fluoroquinolones with enhanced activity against VRE are undergoing development. Agents such as trovafloxacin **11** (Pfizer) which demonstrate improved potency against Gram-positive bacteria have been undergoing clinical trials[36,41]. Some of these new fluoroquinolones show activity against low-level ciprofloxacin resistant staphylococci, but almost all of these fail against high level ciprofloxacin resistant staphylococci[42]. It is therefore likely that ciprofloxacin resistant staphylococci could quickly become resistant to any similar fluoroquinolones which are introduced into chemotherapy.

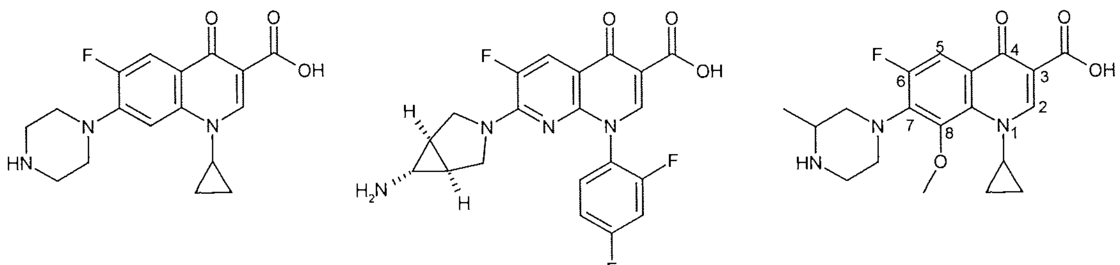

10 **11** **12**

Figure 2.8 Fluoroquinolones, ciprofloxacin **10**, trovafloxacin **11**, gatifloxacin **12**

8-Methoxy quinolones, such as gatifloxacin **12**[43], are novel quinolones which demonstrate improved activity against Gram-positive bacteria, compared with non-8-methoxy compounds. It has also been shown that the introduction of the 8-methoxy group on the quinolone nucleus actually reduces the selection of resistant strains of bacteria[44]. This could be particularly useful in the clinic, where resistance to fluoroquinolones is commonplace and cross-resistance between fluoroquinolones is a genuine problem.

2.4.4 2-Pyridones

The 2-pyridones are a novel class of compounds, which are analogues of the fluoroquinolones, and also act by inhibiting DNA gyrase. The 2-pyridones are structurally different to the fluoroquinolones, as the N1 nitrogen of the fluoroquinolone has been transposed to the ring junction next to the C4 position.

The orally active lead compound ABT-719 **13** has potent activity against various quinolone resistant Gram-positive bacteria, including MRSA and VRE. The *in vitro* activities are superior to existing fluoroquinolones, and this may prove to be an interesting class of compounds[41].

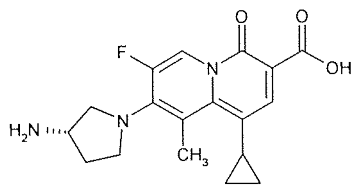

Figure 2.9 ABT-719 **13**, possesses activity against quinolone resistant Gram-positive bacteria

2.4.5 Non-Fluorinated Quinolones (NFQs)

A generation of quinolone derivatives that lack fluorine at the C6 position of the quinolone nucleus have been reported; these are known as non-fluorinated quinolones or NFQs of which T-3811 **14** is an example. In one study, T-3811 was either equally or more active (i.e. reduced MIC values) against Gram-positive pathogens than all other quinolones tested. NFQs generally display similar *in vitro* antibacterial activities to their fluorinated counterparts, whilst being less toxic. The use of these molecules appears to select for unique resistance-mutations. Furthermore, cross-resistance between the NFQs and fluoroquinolones has not yet been observed[44].

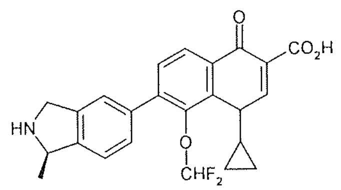

Figure 2.10 Quinolone T-3811 **14**; a non-fluorinated quinolone, due to lack of fluorine at C6

2.4.6 Glycylcyclines

These are semisynthetic analogues of the tetracyclines. The major modification is at the C9 position; for example, substitution with a t-butylglycylamido (TBG) group on minocycline gives (TBG-MINO) **15**. Such compounds show improved activity against isolates resistant to tetracycline and minocycline. The glycylcyclines seem to evade efflux from the cells, and maintain their activity through resistant mechanisms involving target modification of mRNA[41].

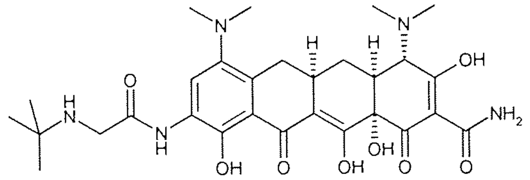

Figure 2.11 TBG-MINO **15**

2.4.7 Novel β-lactam Antibiotics

As already discussed in Section 2.3.1.3, it is a penicillin binding protein, PBP2a, which accounts for the β-lactam resistance in MRSA. Efforts have been made to develop β-lactams capable of inhibiting PBP2a activity in order to achieve activity against MRSA.

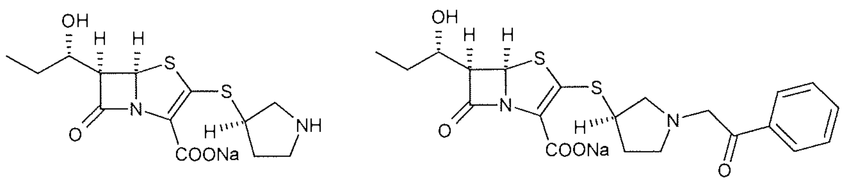

Figure 2.12 Novel β-lactam antibiotics active against MRSA strains.

Ishiguro and co-workers have produced a series of 5,6-cis-penem derivatives, designed to have affinity for PBP2a of MRSA. Of these, the two compounds **16** and **17** not only bound to PBP2a, but were also able to form stable acyl intermediates with β-lactamases by blocking the deacylating water molecule. This conferred potent activity against both MRSA and a wide variety of β-lactamase producing microorganisms[45].

2.4.8 Oxazolidinones

In vitro studies of oxazolidinones have shown that this novel class of compounds is active against mycobacteria and Gram-positive bacteria, including some antibiotic resistant strains[46,47]. Pharmacia and Upjohn have done much research in this area and both eperezolid **18** and linezolid **19** demonstrated similar potency to vancomycin against staphylococci, including MRSA, and enterococci. There was no evidence of cross resistance to any known antibiotic in the strains tested. As a result of this, these compounds were put forward to start clinical trials in 1996[48]. Preclinical testing failed to demonstrate significant differences between the two oxazolidinones, eperezolid and linezolid; the latter was selected only after Phase I clinical trials, based on a superior pharmokinetic profile.

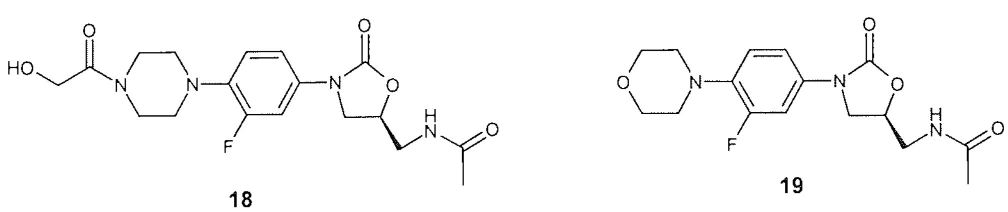

Figure 2.13 Oxazolidinones eperezolid **18** and clinically available linezolid **19**

Early studies of MRSA active oxazolidinones by DuPont showed that these compounds act by inhibiting protein synthesis[40]. Detailed studies of the mechanism of action of linezolid have shown that it binds to the 50S ribosomal subunit where it blocks the formation of the initiation complex. Without this critical initiation complex, protein synthesis cannot occur, so the bacterial cell cannot carry out essential functions and dies. Most other antibiotics which inhibit protein synthesis, do so at the later chain elongation step. This explains why cross resistance has not been observed between linezolid and other protein synthesis inhibitors. Indeed at present, it appears that none of the existing bacterial resistant mechanisms affect either linezolid itself or binding of linezolid to the 50S ribosomal subunit[48].

Linezolid has been shown to be active against all multidrug resistant Gram-positive bacteria, including glycopeptide and quinupristin-dalfopristin resistant isolates. This drug therefore has a massive clinical potential, although some have questioned its clinical efficacy due to its lack of *in vitro* bactericidal activity[38]. Linezolid was, however, approved by the US FDA for sale in April 2000 and is now marketed in the UK as Zyvox, having been approved at the start of 2001[49].

2.5 NOVEL APPROACHES TO COMBAT RESISTANCE

2.5.1 'Self-Regenerating' Antibiotics

Bacteria often become resistant to drugs by structural modification of the molecule to render an inactive form. Research is being carried out to produce antibiotics which actually regenerate themselves after the resistance enzymes have altered the structure. For example, a wide spread aminoglycoside (e.g. kanamycin) inactivation mechanism is phosphorylation, which interferes with the interaction of the drug and its target. A self-regenerating aminoglycoside, that is a substrate for the resistance enzyme, has been developed which yields a chemically unstable molecule upon phosphorylation. The phosphate group is eliminated spontaneously and the original antibiotic is regenerated (Figure 2.14)[50].

The effectiveness of both kanamycin and the modified aminoglycoside in killing susceptible and resistant *E.coli* was analysed. When resistant *E.coli* is treated with kanamycin, the MIC increases 500-1,000 fold compared to that for susceptible bacteria. For the regenerating aminoglycoside, the MIC increases only 4 fold, but the MIC for susceptible bacteria was higher for the regenerating aminoglycoside than for kanamycin, so it is unlikely to be a replacement for kanamycin. This is still, however, an interesting and viable strategy to counter the cases of resistance when a group is transferred to the drug itself, as it lowers the MIC for resistant bacteria[30].

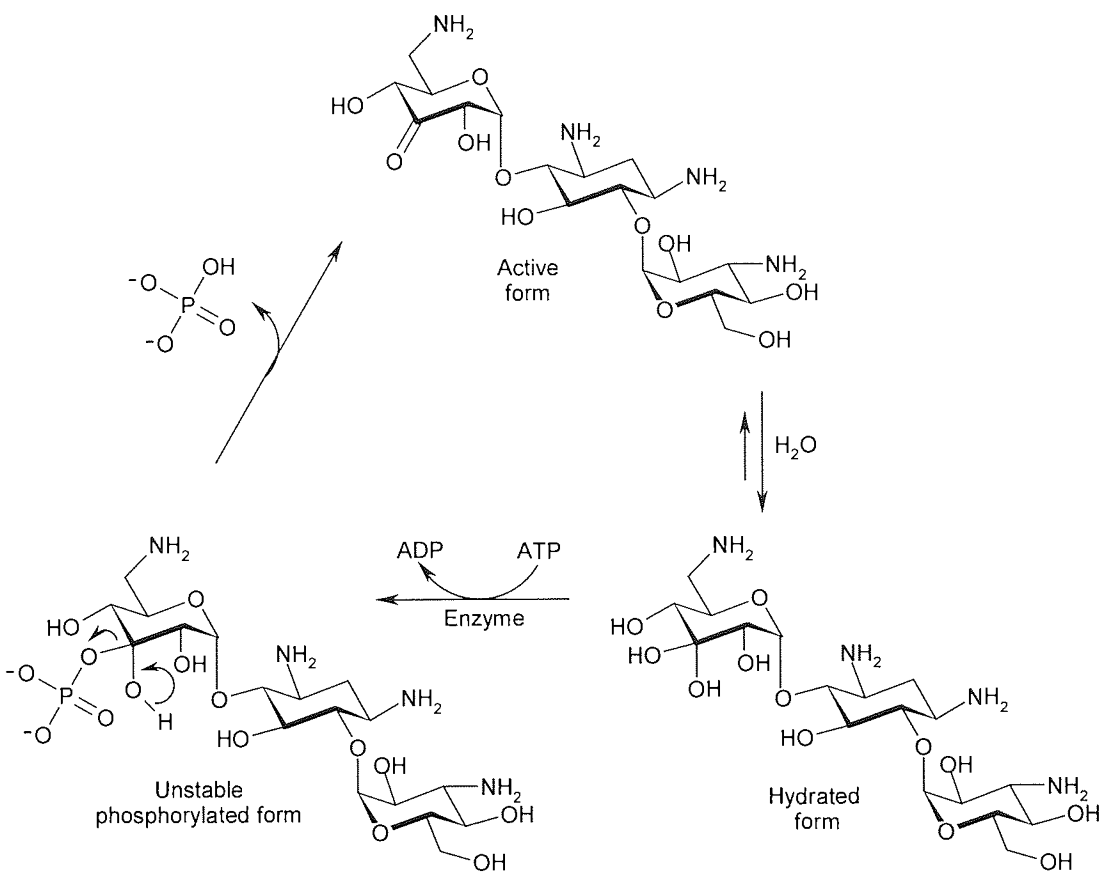

Figure 2.14 Antibiotic regenerates itself after being phosphorylated by resistance enzyme

2.5.2 'Self-Destructing' Antibiotics

Many antibiotics are not readily metabolised in the bodies of animals or humans, so are excreted in the fully active form. Approximately 22,500,000 kg of antibiotics are pumped into the environment annually, and it has been suggested that these can apply selective evolutionary pressure on bacteria, allowing them to develop resistance[51].

An analogue of cephalosporanic acid has been synthesised, which is modified at the C7 position with a protected hydrazine function. The protecting group is removed on exposure to UV-visible light for several hours, as it has been hypothesised it might be in the environment. The unprotected hydrazine then reacts intramolecularly with the lactam carbonyl group, destroying the lactam ring and eliminating antibacterial activity (Figure 2.15)[30].

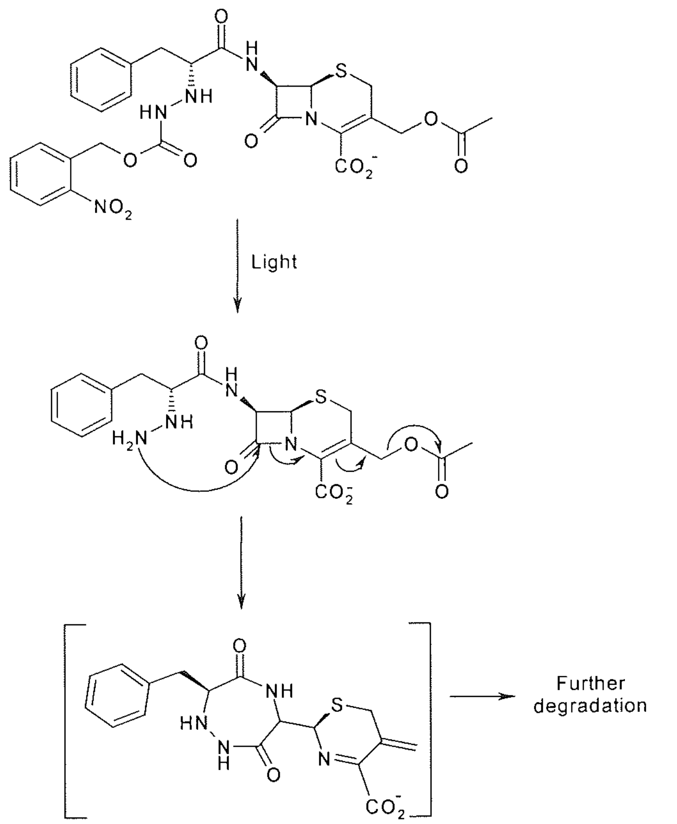

Figure 2.15 Light triggers the self destruction of this cephalosporin antibiotic

The authors of this work suggest that this cephalosporin represents the prototype molecule of this kind[51]. Obviously this particular approach would not be of use in destroying antibiotics in sewers, where there is an absence of light, but it is possible that molecules which are sensitive to aqueous pH could be produced[30]. The general concept could also be used for other classes of antibiotics, providing suitable intramolecular reactions could be identified which would destroy the antibiotic nucleus, rendering it inactive and incapable of selection of resistant organisms in nature[51].

CHAPTER 3
MYCOBACTERIUM TUBERCULOSIS

Tuberculosis (TB), caused by the pathogen *Mycobacterium tuberculosis*, is the leading cause of death in Europe and the US in recorded history. Paleopathologic studies have shown evidence of spinal tuberculosis in neolithic and early Egyptian remains. Estimates suggest that 20% of deaths in London in 1651 were due to TB, and that in the early 19th century, TB may well have accounted for one third of all deaths in Paris at that time[52].

Mycobacterium bovis causes TB in cattle, usually infecting the lungs, but it can be transmitted to other organs. If it is transmitted to the cow's udder, the animal's milk can become infected. *M.bovis* can also cause TB in humans and in the 1930's, before milk was regularly pasteurised, there were 50,000 cases of TB due to *M.bovis* infection every year in the UK and over 2,500 deaths. Today, less than 1% of all human TB cases are caused by *M.bovis*, with only those working in close contact with cattle being at risk[53].

Pulmonary TB initially manifests itself as nodules in the lungs called tubercles which later evolve into ulcers. The most obvious symptom is a cough, accompanied by fatigue, chest pain, weight loss and fever. In the latter stages, sputum becomes red, as blood vessels rupture and lung tissue is destroyed[54]. TB infection can also spread from the lungs, via the bloodstream, to all body organs, such as the bones, intestines, urinary tract and the skin.

During the mid 19th century, treatment of TB consisted of prolonged rest in the open air which led to the introduction of specialised sanatoria. In the early 1900's, Albert Calmette and Camille Guerin developed a live attenuated strain of *Mycobacterium bovis*, and in 1921 used it to immunise a child whose mother had died of TB. Nowadays, approximately 100 million people around the world are vaccinated with BCG (bacille Calmette-Guerin) per year. At the time of writing, there has been an alarming resurgence of TB in schools, the worst hit place being Crown Hills School in Leicester. One child fell ill with a persistent cough, went to a GP and was diagnosed with asthma. It was about one year, after a chest x-ray, before this cough was actually diagnosed as a symptom of tuberculosis. Following this, people at the school with whom the child had close contact were given a tuberculin skin test, and of these people, 164 had active TB. 90% of this group had been given the BCG vaccine[55].

In 1947, streptomycin was introduced as the first anti-tuberculous drug and this was the beginning of the chemotherapeutic era for TB, which dramatically reduced mortality resulting from the disease[52].

The incidences of TB steadily declined from 1885 to 1985, but in 1985 this trend reversed and the number of TB cases started to increase once more. In 1993, the World Health Organisation (WHO) designated TB a global health emergency[56]. There are now over 8 million new cases a year, with a death toll of 3 million, over 95% of which occur in the developing world[54]. Research by the Public Health Laboratory Service in January 2001, showed that the number of people with TB in the UK has now hit an 18 year high and that London has more cases of respiratory tuberculosis than any other European city, with over 4,000 diagnoses a year[57]. Tuberculosis is currently the world's number one killer among infectious diseases[58].

The re-emergence of TB is largely attributed to the human immunodeficiency virus (HIV) pandemic which occurred at around the same time. HIV impairs the immune system, and so increases susceptibility to any infection, including TB. HIV may also reactivate latent *M.tuberculosis* infections so that the patient develops clinical tuberculosis, which can then be transmitted to other patients and health care workers[52]. The chances of an HIV-negative individual with latent *M.tuberculosis* actually developing TB is 10% over a lifetime. For HIV-positive individuals with latent *M.tuberculosis*, the likelihood of developing TB increases to 8% per year. Similarly, active TB hastens progression to AIDS in the HIV-positive individual. The synergy between HIV and TB has a devastating effect worldwide, with about a third of acquired immunodeficiency disease (AIDS) sufferers actually dying from TB[54]. The problem of HIV-TB co-infection is not only an issue for AIDS sufferers; indeed, AIDS sufferers are more susceptible to acquiring TB infection in the first instance, but this acts as a reservoir of the disease, which has the potential to infect other patients, health care workers and the community as a whole[52].

It is known that the travel and migration of people, helps to spread all communicable diseases[59]. This is particularly true of TB, which is spread in the aerosol when an infected person coughs and can be caught by simply breathing the contaminated air. In Buenos Aires, for example, it is thought that bus travel could account for up to 30% of the new infections diagnosed there[58]. Tuberculosis is widely viewed as a disease of either the developing countries or the poor and homeless. However, with the ease of transmission of TB, and the huge increase in tourism, international travel and migration, TB infection can occur anywhere. The Times newspaper, in April 2001, described tuberculosis as the "world traveler that does not need a visa"[60]. The British Thoracic Society (BTS) reported that in the UK in 1998, 56% of all reported TB cases were from people not born in the UK. The BTS goes on to suggest that "all immigrants and longstay visitors to the UK from Asia, Africa and South America should be screened for TB"[60].

The emergence of drug resistant tuberculosis has compounded the problem[52]. The growing number of cases of multidrug-resistant (MDR) TB worldwide is of utmost concern. (An MDR strain is one which is resistant to at least isoniazid and rifampicin.) As even more strains evolve that are not susceptible to the currently available drugs, our capability of controlling this disease is under threat[58].

3.1 GENERAL CHARACTERISTICS OF TB

The mycobacterial cell wall differs from other bacterial cell walls as it has a thick waxy coat composed of complex lipids and carbohydrates, which makes it impermeable to many drugs. The matrix of the cell wall is made up of peptidoglycan, arabinogalactan and the characteristic molecules of mycobacteria, mycolic acids (Figure 3.1). The mycolic acids are large (C70-C90) α-alkyl branched, β-hydroxylated fatty acids which are covalently linked perpendicular to the cell wall to provide a matrix in which glycolipids may intercalate, forming a 'pseudo' lipid bilayer[61]. It is this structure which accounts for the unusual hydrophobicity of mycobacterial cells, the low permeability of the cell wall and their intrinsic resistance to many antibiotics.

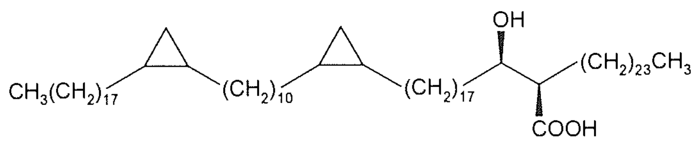

20

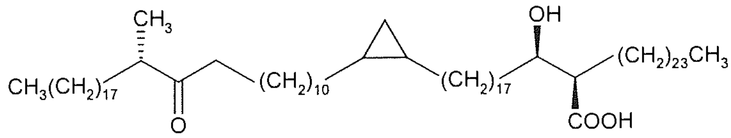

21

Figure 3.1 Mycolic acids in *M.tuberculosis* are cyclopropanated. α-mycolate **20**, ketomycolate **21**

M.tuberculosis is also unusual in that it is able to survive inside macrophages; in fact, it predominantly grows inside them, rather than extracellularly[62]. As the mycobacteria multiply, the numbers become so overwhelming that the macrophage dies, releasing the bacilli to be taken up by more macrophages[58]. Macrophages contain an oxidative cytocidal system which is activated upon ingestion of a particle or microbe, but *M.tuberculosis* is resistant to these reactive oxygen intermediates. The molecular basis for this intracellular survival is not completely understood[52], although it is thought to be a result of the action of an enzyme known as KatG. This is a catalase-peroxidase enzyme within the *M.tuberculosis* cell which detoxifies the reactive oxygen intermediates that the macrophage produces[62]. The *M.tuberculosis* cell also contains superoxide dismutase, an enzyme common to many organisms, which catalyses the conversion of highly reactive and destructive superoxide anions into hydrogen peroxide and molecular oxygen[63].

M.tuberculosis grows very slowly, with each cell only dividing about once every 24 hours (*E.coli* reproduces once every 20-30 minutes). It also has an unexplained ability to enter phases of very slow growth (known as semi-dormancy) and even total dormancy. The individual bacilli clump together and as a result there are organisms in a patients body, in an anaerobic environment, that hardly 'see' the immune system or the drugs used to treat the disease. They have a tendency to persist, so if someone has dormant bacilli in their lungs, they could end up with the active form of the disease in later life, perhaps as a result of an immune disorder, or old age[64].

3.2 RESISTANCE

As discussed in Section 2.2, poor patient compliance with drug regimens can bring about drug resistance in any bacteria. The current treatment for TB is complex and long, lasting up to six months, and often the course is not followed precisely or not completed. It may be, particularly in developing countries, that there is a lack of good practice in TB treatment and monitoring due to poor health care systems, or simply the absence of the necessary drug supplies to treat the condition. Whatever the situation, if the correct drug regimen is not received and maintained, replicating mycobacteria at the infection site can develop into a drug resistant strain[65].

Mycobacterium tuberculosis does not appear to acquire drug resistance through exchange of plasmids, which is often the case with drug resistant bacteria. Instead, normal error rates of DNA replication in *M.tuberculosis* ensure that spontaneous mutations arise that confer resistance in the absence of antibiotic exposure. Spontaneous mutation to confer resistance to isoniazid, for example, occurs in about 1 in 10^6 bacteria; resistance rates for ethambutol and streptomycin are similar. Rifampicin resistance occurs in about 1 in 10^8 bacteria. If the bacterial load is great enough, the effect of treating a patient with a single drug will be the suppression of susceptible bacteria and the selection for growth of a drug resistant strain. Avoidance of selection for resistance is one of the reasons for treating TB with multiple drugs. For example, the probability of resistance arising when rifampicin and isoniazid are used in combination is only 1 in 10^{14} (10^6x10^8), low enough to prevent selection for resistance to either drug[64].

3.3 DRUGS CURRENTLY AVAILABLE TO TREAT *M.TUBERCULOSIS*

Streptomycin, introduced in 1947, was the first effective anti-tuberculous drug. In 1952, isoniazid (INH) was found to be a more effective treatment, and is still one of the first line drugs used in treatment today.

Although several drugs have been introduced and used in the past to combat TB (See Figure 3.2), these are now rarely used individually. The most effective therapy for TB is a combination of drugs; an initial intensive two month regime of isoniazid (INH) **22**, pyrazinamide (PZA) **25,** rifampicin (RIF) **26**, and ethambutol (EMB) **27** or streptomycin to ensure that mutants resistant to a single drug do not emerge. Isoniazid and rifampicin are then taken for a further four months to sterilise the tissues completely[65,66]. Due to the length and complexity of this course of treatment along with its associated side effects, patient compliance is often poor and this ultimately leads to drug resistance within strains of bacteria[54]. Combination therapy is also the current treatment for MDRTB, but with resistance becoming an ever-increasing problem, it is clear that there is an urgent need for new drugs to combat TB.

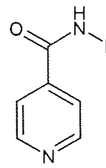

22

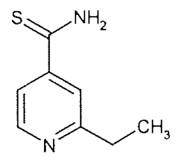

23

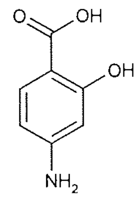

24

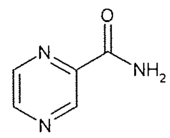

25

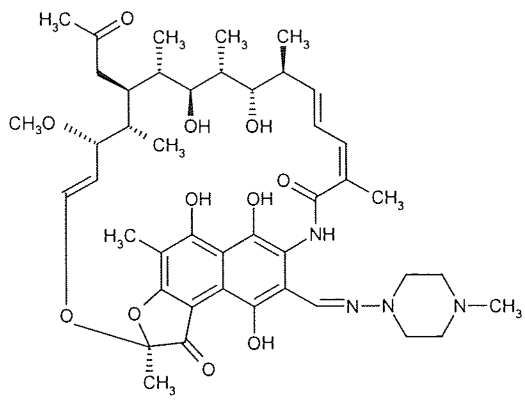

26

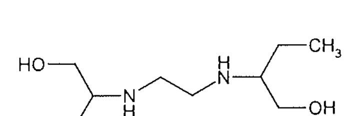

27

Figure 3.2 Antitubercular agents, isoniazid **22**, ethionamide **23**, *p*-aminosalicylic acid **24**, pyrazinamide **25**, rifampicin **26**, ethambutol **27**

Our understanding of the molecular mechanisms for resistance of *M.tuberculosis* to anti-mycobacterial agents has increased significantly over the last few years. For each of the first line drugs at least one gene has been identified in which specific mutations lead to a resistant phenotype. However, there is still much to be understood before the full picture can be defined[65].

3.3.1 Isoniazid

Although isoniazid has proved to be very useful in therapy, it is toxic and has shown to be carcinogenic in some assays[34].

3.3.1.1 The Activation of Isoniazid

Isoniazid (isonicotinic acid hydrazide, isonicotinylhydrazide, INH) **22** is actually a prodrug that requires cellular activation into a poorly understood active form. This activation requires the KatG catalase-peroxidase enzyme of the mycobacterium, although the actual function of this enzyme is unclear[67].

In 1994, Johnsson and Schultz published a mechanism of INH activation *in vitro*, where KatG serves to oxidise INH to a number of species, including a highly reactive acyldiimide **28** or acyldiazonium ion **29**, the latter of which may react with water to produce isonicotinic acid **30**, which was the major product identified. The acyldiimide could decompose via a diazenyl radical to afford the corresponding acyl radical **31**. The acyl radical could then either gain a proton to give pyridine-4-carboxaldehyde **32**, or react with molecular oxygen to give the peracid **33** (Figure 3.3)[68]. Other studies have shown that 4-pyridylmethanol is produced upon activation of the drug[69,70]. Any of the free radical species formed in this activation process may be toxic to the organism in a nonspecific fashion, whilst the other activated species are reactive and so are capable of interacting with cellular nucleophiles, possibly inactivating a specific target. Despite these findings, the actual mechanism of INH activation *in vivo*, is still under debate.

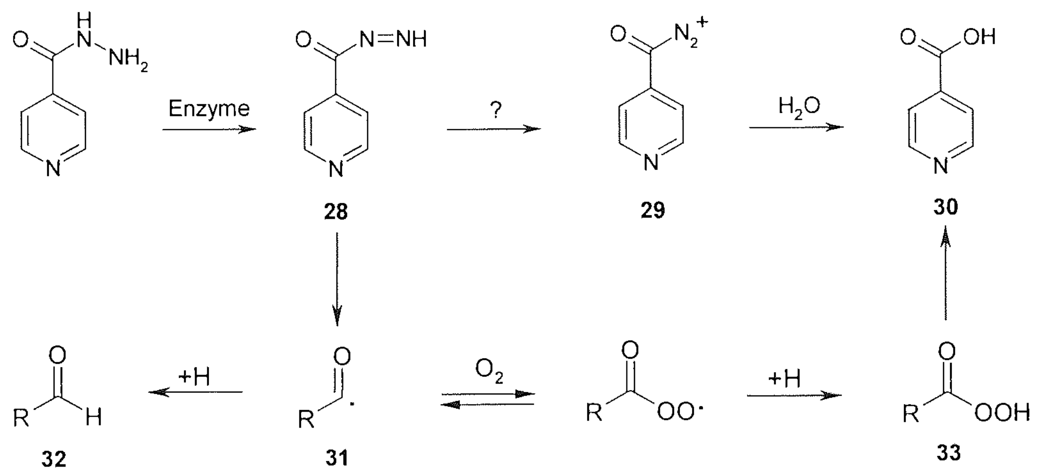

Figure 3.3 Proposed activation of isoniazid (R=4-pyridyl)[68]

It has been suggested that there may not actually be a specific mechanism of INH activation. Macrophages produce hydrogen peroxide and this demonstrates a synergistic toxic effect with INH, so it was thought that this alone could be capable of oxidising INH[67]. It has since been shown, however, that the enzyme KatG will catalyse INH oxidation in the absence of peroxide and that oxidation bizarrely requires a reducing agent such as hydrazine (a spontaneous decomposition product appearing in INH solutions), but only under aerobic conditions (Figure 3.4). The hydrazine serves to reduce the ferric (Fe^{III}) "resting" form of the heme enzyme to produce a ferrous (Fe^{II}) enzyme (Figure 3.4, step a). This ferrous enzyme then reacts with molecular oxygen to produce an active oxyferrous enzyme (Figure 3.4, step b)[70,71]. Whether such a reaction occurs *in vivo* is not known. It has also been suggested that superoxide should stimulate INH activity in mycobacteria. The oxyferrous enzyme is a resonance equivalent of the superoxyferric enzyme, consequently a direct reaction between the ferric resting enzyme and the endogenous superoxide anion could also activate the enzyme (Figure 3.4, pathway c). This has been shown to be true *in vitro* for the mycobacterium *M.smegmatis*. This finding by Wang *et al*, led them to suggest that it should be possible to improve INH therapy for mycobacterial diseases by supplementing INH treatments with a superoxide-producing agent such as clofazimine **34**[72] (Figure 3.5). This is a drug sometimes used in the treatment of leprosy and also shows some activity against *M.tuberculosis* itself[71-73].

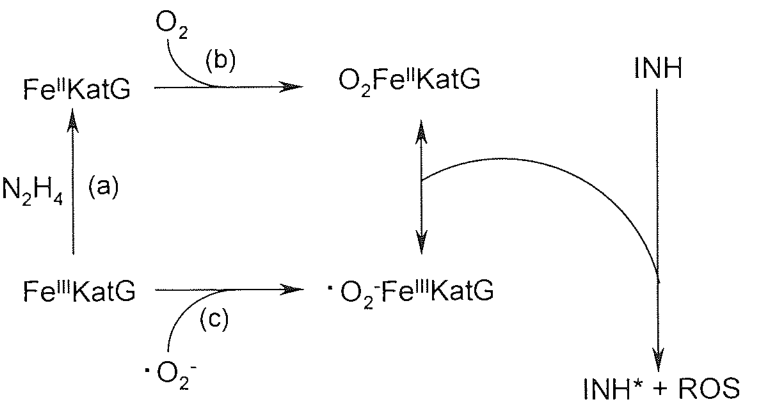

Figure 3.4 (a) Formation of the ferrous KatG enzyme from the ferric resting enzyme by hydrazine followed by (b) reaction with O_2 to give the oxyferrous enzyme (c) reaction of superoxide with the ferric enzyme form to give the superoxyferric enzyme. Either of these oxygenated enzyme forms can activate INH. INH* is the activated INH and ROS refers to the reactive oxygen species formed[71].

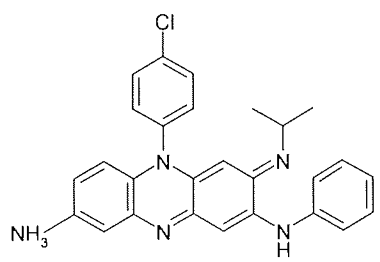

Figure 3.5 Clofazimine **34**

In summary, the active form of isoniazid remains elusive. The definition of the actual active form of isoniazid seems unlikely due to the highly reactive nature of the intermediates and the extremely complex chemistry of the acylpyridine nucleus[67]. It is possible that the oxidation process is as complex *in vivo* as the *in vitro* studies suggest and that multiple activation pathways operate with discrete outcomes for different cellular targets[70].

3.3.1.2 The Mechanism of Action of Isoniazid

Several lines of evidence suggest that a specific pathway is activated upon INH treatment, but the relative structural simplicity of isoniazid and the numerous possibilities of its activated forms has led to the proposal that INH acts indiscriminately upon multiple targets. The actual mechanism of killing by INH therefore remains controversial[70].

Although the reactive species formed upon INH activation is unclear, the molecular target of this activated species has been shown to lie in the biosynthetic pathway for the unique mycobacterial cell wall lipids, the cyclopropanated mycolic acids[62,74,75]. It is postulated that these mycolic acids play a central role in both the cell envelope architecture and its permeability. Thus, when cells are treated with INH and mycolic acid synthesis is inhibited, the integrity of the cell wall is compromised. Electron microscopy of *M.tuberculosis* cells treated with INH at the MIC shows that the cells become deformed, the changes starting at the bacterial poles, which probably represent the weaker regions of the growing cell. It was also observed that there was loss of cellular material into the medium, indicating that INH induces a change in the permeability of the mycobacterial cell envelope. These observations correlate with the hypothesis that INH treatment results in defective cell wall synthesis[75]. Since the cell wall integrity is essential for the survival of the mycobacterium in the infected host, this inhibition is fatal.

A genetic approach to isolating the factors involved in INH resistance in *M.smegmatis* resulted in the identification of an enoyl-acyl carrier protein (enoyl-ACP) reductase named InhA that conferred resistance to INH and ethionamide, an analogue of INH. *In vitro* assays showed that InhA catalysed the reduction of unsaturated fatty acids, namely 2-*trans*-octenoyl-ACP, as well as corresponding short chain enoyl-CoA esters up to 16 carbon atoms in length. It was suggested that InhA was a component enzyme of a fatty acid synthase system, capable of catalyzing mycolic acid synthesis from short chain precursors. Recombinant InhA from *M.tuberculosis* was also shown to be sufficient to confer INH resistance to *M.smegmatis*. However, when overexpression of InhA was performed in *M.tuberculosis* rather than *M.smegmatis*, INH resistance was either only slightly increased or remained unchanged. Since *M.smegmatis* is significantly less sensitive to INH than *M.tuberculosis*, the biological relevance of the these studies have been questioned. InhA also appears to catalyse the wrong reaction to account for the observed biological consequences of INH treatment in *M.tuberculosis*. The drug induces the accumulation of saturated hexacosanoic acid (C_{26}) and inhibits the production of acids longer than this. It is predicted, however, that inhibition of InhA activity would actually result in the accumulation of an unsaturated population of fatty acids[70,74,76]. There is some connection between INH resistance and inhibition of InhA, but the story is not complete[70].

An alternative study to investigate the target of activated INH, based on the presumption that accumulation of a lipid precursor to mycolic acids would occur on a small discrete ACP, came to a different conclusion[70,76]. Differential protein analysis of INH-treated and control cells revealed that a small ACP, dubbed AcpM, was upregulated on INH treatment. Also upregulated was a second larger protein which was shown to be a complex, containing AcpM and a ketoacyl synthase (KasA). This protein complex was also shown to contain INH, both by mass spectrometry and radio-labelling studies. Unlike InhA, AcpM and KasA are dramatically upregulated by INH treatment, and studies of the acyl-AcpM population showed an accumulation of saturated hexacosanoic acid. An untreated population of acyl-AcpM displayed a broader range of fatty acids consisting of an abundant species with over fifty carbon atoms. It was therefore thought that accumulation of hexacosanyl-AcpM may be the metabolic consequence of KasA inhibition by activated INH. Overexpression of AcpM is toxic in mycobacteria, suggesting that careful regulation of AcpM levels is an important determinant of cell wall control. Hyperexpression of KasA on the other hand, leads to a two- to fourfold increase in resistance to INH[69].

The biosynthesis of fatty acids requires two multienzyme complexes, FAS I and FAS II. FAS I is the primary means of *de novo* synthesis, producing the C_{14-26} fatty acyl-CoA derivatives and FAS II then functions as an elongation system to give mycolic acids[61]. Several of the protein components of the FAS II multienzyme complex have been identified. KasA is thought to extend the short chain acyl precursors to approximately forty carbons in length and a second ketoacyl synthase, KasB, then continues extension to full length mycolates. Completion of each elongation cycle initiated by KasA and KasB involves other enzymes, including InhA. Thus KasA and InhA have another connection in addition to their role in INH sensitivity. Under normal intracellular conditions these proteins are component parts of a multifunctional enzyme complex, so changes outside the active sites of both these proteins may lead to more profound changes in the association of the protein complex. It is possible that changes in KasA could lead to changes in InhA, and vice-versa, altering the interaction with activated INH or its metabolites[69].

Unfortunately, despite these target studies, the actual mechanism of INH toxicity and the mechanism of cell death in *M.tuberculosis* remains largely unknown and is still an active topic of research[69].

3.3.1.3 Resistance to Isoniazid

Resistance to isoniazid is most commonly a result of inactivation of the enzyme KatG, which is required to activate the INH prodrug, usually resulting from a point mutation in the *katG* gene. Since the active form of INH is not produced, it cannot exert its toxic effect. If KatG is inactivated however, one might expect that the tubercle bacilli lose their main defence mechanism against the toxic peroxidases produced by the macrophage, but the cells survive[62]. This is because loss of KatG function is accompanied by an increased expression of an alkylhydroperoxidase reductase, AhpC, a protein that is also capable of detoxifying the potentially damaging organic species[66,69,77].

3.3.2 Ethionamide

Ethionamide (ETH) **23**, a structural analogue of INH is a useful second line antituberculosis drug. Both ETH and INH inhibit mycolic acid synthesis, but there is no cross resistance between the two drugs, indicating that they have different modes of action.

Since INH requires activation via KatG, it was thought that an activation process may also be required for ETH. It has since been shown that a monooxygenase homolog, termed EthA, activates ETH to give electrophilic S-oxides which are then free to react with cellular nucleophiles. Alternatively, when administered to humans, ETH could be activated by eukaryotic oxidative processes, such as the cytochrome P-450 monooxygenases. Rat liver microsomes, for example, generate a highly reactive S-oxide from ETH (See Figure 3.6), which exhibits greater activity against *M.tuberculosis in vivo* than ETH itself[78].

EthA activation of ETH is the equivalent to the KatG activation of INH. Inactivation of one drug specific process would account for resistance to only that particular drug, and no cross resistance between the structural analogues of isoniazid and ethionamide would be observed. Indeed, as previously mentioned, this has found to be the case in *vivo*.

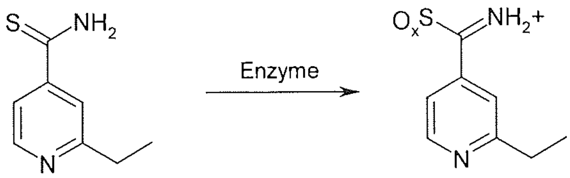

Figure 3.6 Proposed activation of ETH **23** to an ETH S-oxide

3.3.3 *para*-Aminosalicylic acid

p-Aminosalicylic acid (PAS) **24** is an intravenous drug which is rarely used today[65]. It may be added to tuberculosis chemotherapy regimens. It is particularly useful used in conjunction with INH, to prevent the emergence of isoniazid-resistant organisms[79].

3.3.4 Pyrazinamide

Pyrazinamide (PZA) **25** is the only drug shown to have activity against semi-dormant tubercle bacilli. Its action is also synergistic with INH and RIF, so it is an important part of chemotherapy, shortening the course from 9 or 12 months to 6 months. It is interesting to note that even at high MICs, PZA has no significant bactericidal effect and is primarily considered a 'sterilising drug', i.e. prevents further reproduction of the bacilli.

It is thought that PZA, like INH, is transported into the cell as a neutral species, where it is then converted into its active form; pyrazinoic acid. This hypothesis arose from the fact that *M.bovis*, which is intrinsically resistant to PZA, lacks the enzyme Pzase which brings about this conversion.

This notion was strengthened by *in vitro* studies which demonstrated that PZA-resistant *M.tuberculosis* was actually susceptible to pyrazinoic acid.

The cellular target for PZA however, has not been identified, although the similarity of PZA to nicotinamide suggests that enzymes involved in pyrimidine nucleotide biosynthesis are possible targets[66].

3.3.5 Ethambutol

Ethambutol (EMB) **27** is known to inhibit cell wall biogenesis, having been shown to inhibit the polymerisation step of arabinan synthesis. Arabinan is an essential component of the mycobacterial cell wall which, when linked to the peptidoglycan via galactan, provides the support for the relatively impermeable mycolyl layer[61]. The primary cellular target of EMB is thought to be the enzyme arabinosyl transferase[66].

3.3.6 Rifampicin

Rifampicin (RIF) **26** has a high bactericidal action and so, along with INH, forms the backbone of short-course chemotherapy. RIF has long been believed to target mycobacterial RNA polymerase and thereby kill the organism by interfering with the transcription process. It has since been shown that RIF specifically inhibits the elongation of full length transcripts of RNA, having no effect on the initiation of transcription[66]. RIF specifically inhibits bacterial RNA polymerase and does not affect mammalian cells in this way[33].

In *M.tuberculosis*, RIF resistance is usually due to mutation of the *rpoB* gene, which confers conformational changes in the β subunit of RNA polymerase, leading to defective binding of the drug and consequently resistance[66].

3.3.7 Streptomycin

Streptomycin (SM) disrupts the encoding of tRNA and so inhibits or disrupts mRNA translation. As previously mentioned in Section *2.3.2.1*, the most common mechanism of resistance to SM in bacteria is acetylation of the drug by aminoglycoside modifying enzymes. This does not happen however in *M.tuberculosis*. Instead, SM resistance stems from alteration of the drug target rather than drug modification. It is thought that this resistance may be partially attributed to mutations in ribosomal proteins and rRNA, although it has also been suggested that SM resistance could be due to alterations in the permeability of the mycobacterial cell wall[66].

3.4 DIRECTLY OBSERVED THERAPY SHORT COURSE (DOTS)

The length and complexity of the antituberculosis treatment regimen tempts many patients to stop taking medication soon after they feel better. To circumnavigate this problem, Directly Observed Therapy Short Course, known as DOTS was introduced. DOTS is a public health strategy advocated by WHO. With this strategy, when an infectious case is detected, health and community workers are mobilised to oversee the patient swallowing the correct dosage of drugs on a daily basis and to document that the patient has indeed been cured[58,64]. In some areas the patients receive money for participating. Transferring DOTS to every part of the world with a tuberculosis epidemic is not economically feasible, especially when the cost of treatment is taken into consideration. WHO estimates that the treatment of drug susceptible tuberculosis costs about $2,000 per patient, which increases to as much as $250,000 for drug resistant cases cured. Obviously there are many communities in developing countries that cannot afford the drugs, let alone set up a program and employ people to oversee the drugs being taken.

Still, many healthcare officials believe that if DOTS programs are targeted to specific locales, such as New York City and Russian jails, where overcrowding and poor sanitary conditions create conditions ripe for the spread of any form of TB, many drug resistant forms could be cut off at the source[64].

3.5 NEW DRUGS TO TREAT *M.TUBERCULOSIS*

3.5.1 Rifamycin Derivatives

Rifamycin was first isolated in 1957, and over a hundred semisynthetic derivatives have since been prepared[34]. Rifampicin **26**, discovered in 1965, is currently used in the treatment of TB including MDRTB. Rifabutin, a spiropiperidyl derivative of rifampicin, is more active than rifampicin against sensitive strains of *M.tuberculosis* and also has improved pharmokinetic properties. Rifabutin has lower oral bioavailability and a longer half-life than rifampicin, which allows it to be given less frequently[80]. Unfortunately, rifabutin is not effective against MDRTB[41]. In 1998, rifapentine, a cyclopentyl derivative of rifampicin[80], was introduced into therapy. This was the first antituberculosis drug to be approved by the FDA in 25 years, but like the existing drugs, it must be taken over a period of 6 months in combination with other drugs. Rifapentine has the advantage over rifampicin that it only needs to be taken once weekly in the last 4 months of treatment, rather than twice weekly for rifampicin[65]. PathoGenesis currently have a rifampicin derivative in Phase II clinical trials, called rifalazil. *In vitro* studies show the molecule to be up to 100 times more potent than rifampicin and more importantly, has a longer half-life. This would allow physicians to shorten the treatment period and lower both the dose and the frequency of doses, thus reducing the overall cost of therapy[64].

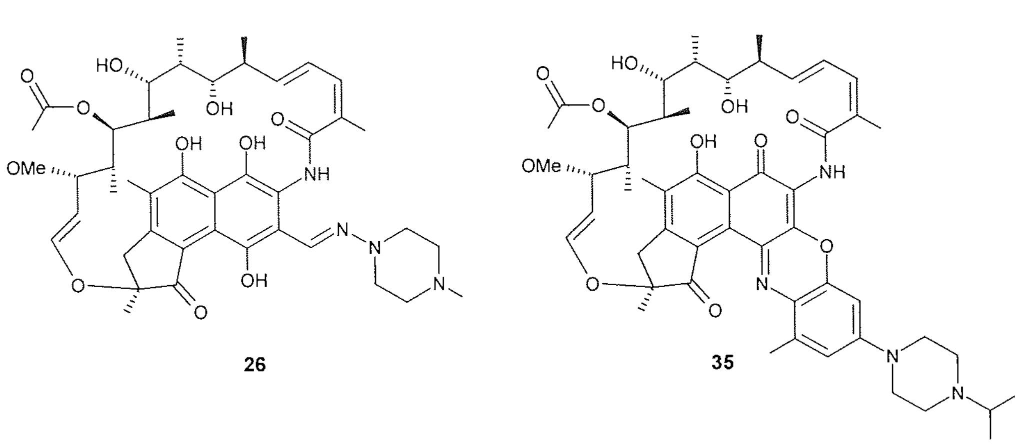

26 35

Figure 3.7 Rifampicin **26** and KRM-1648 **35**

A new group of rifampicin derivatives, the benzoxazino-rifampicins, has been synthesised and of these KRM-1648 **35**, is the lead compound (Figure 3.7)[81]. KRM-1648 is more potent, both *in vitro* and *in vivo* against *M.tuberculosis* than rifampicin[62] and rifabutin, and has also been shown to have activity against some, but not all, strains of drug resistant *M.tuberculosis*[67].

3.5.2 Isoniazid Derivatives

Isonicotinylhydrazones (Figure 3.8) have been synthesised from isoniazid **22** (isonicotinylhydrazine, INH), and have been found to be significantly more active than isoniazid itself *in vitro*, against isoniazid-susceptible *M.tuberculosis*. The compounds were not, however, effective in inhibiting the growth of isoniazid-resistant *M.tuberculosis*. This is not surprising due to the obvious chemical similarity to isoniazid. It is interesting to note that the lipophilicity of these isonicotinylhydrazones was not critical to affecting their potency, which is unusual for anti-tubercular compounds, for which increased lipophilicity tends to improve their penetration of the hydrophobic mycobacterial cell wall.

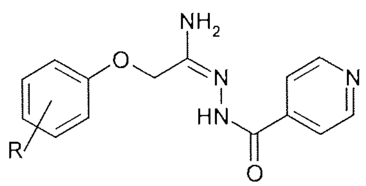

Figure 3.8 Isonicotinylhydrazone

Sub-inhibitory concentrations of isonicotinylhydrazones were also shown to enhance the activity of current first-line drugs against TB, such as ethambutol and rifampicin, resulting in a four-fold decrease in the MIC. The synergic effects between the isonicotinylhydrazones and ethambutol were also observed against isoniazid-resistant strains of *M.tuberculosis*[82].

3.5.3 Fluoroquinolones

The fluoroquinolones (FQs) were initially developed for broad spectrum antibacterial use, but some have been shown to possess promising antimycobacterial activities. Temafloxacin, for example, is an analogue of ciprofloxacin **10** which demonstrated good activity against mycobacteria. Temafloxacin has a phenyl substituent in place of the cyclopropyl group on ciprofloxacin.

Due to the highly lipophillic cell wall of mycobacteria, research into the effect of lipophilicity at the N-1 position of fluoroquinolones was investigated. From this study, it was concluded that increasing the lipophilicity at the N1 site did not actually correlate to improved activity and suggested that increasing the lipophilicity of the side chain at C7 may be more important[83].

Levofloxacin **36** is a fluoroquinolone which displays activity comparable to ethambutol and pyrazinamide, but lower than that of isoniazid and rifampicin[84].

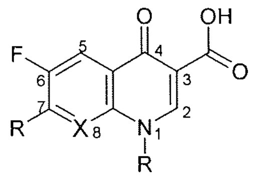

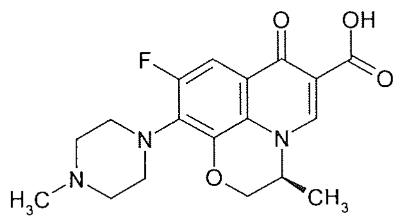

36

Figure 3.9 General structure and numbering system of the fluoroquinolones and levofloxacin **36**

3.5.4 4-Quinolylhydrazones

The 4-quinolylhydrazones (Figure 3.10), derivatives of quinolone, have been shown to possess some interesting activity against *M.tuberculosis*[85]. Savini *et al* synthesised a set of thirty-nine 4-quinolylhydrazones, the majority of which displayed an inhibitory activity of between 95 and 100% against isoniazid-sensitive *M.tuberculosis*.

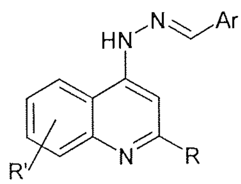

Figure 3.10 General structure of the 4-quinolylhydrazones

The activity of these compounds is significantly affected by substituents both on the quinoline nucleus (R') and the hydrazonic moiety (Ar). On the quinoline nucleus the most effective substituents were 6-cyclohexyl, 7-alkoxy and 7-chloro. For the hydrazonic moiety, greater activity was observed for *para-* and *ortho*-methoxynaphthyl substituents. The MIC of these compounds ranged from 0.78-3.13μg/ml. Chlorodisubstitution led to inactive derivatives. A methyl group appeared to be the most favourable substitution at the 2- position of the quinoline nucleus[85].

3.5.5 Oxazolidinones

These drugs have already been discussed in Section 2.4.8, but during their investigations, the Upjohn group also identified a subclass of oxazolidinones with potent *in vitro* activity against mycobacteria.

U-100480 **37** exhibited activities of 0.5-4μgml^{-1} in clinical isolates of *M.tuberculosis* resistant to conventional drugs. The initial pharmokinetic and toxicity profiles in rats were favourable, suggesting that the oxazolidinones may be promising antimycobacterial agents too[46].

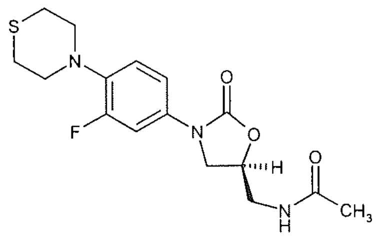

Figure 3.11 Oxazolidinone U-100480 **37** is active against MDRTB

3.5.6 Nitroimidazopyrans

The 3-nitroimidazopyrans (NAPs) are a new class of antitubercular agents. 328 NAPs have been tested by PathoGenesis, of which PA-824 **38** is the lead compound. PA-824 was not the most potent NAP against cultured *M.tuberculosis* isolates, but it was the most active when orally administered to infected mice. This suggests that PA-824 might possess a more desirable pharmokinetic profile than the more active compounds tested. The stereochemistry at C3 was important for activity, the *S* enantiomers being at least 10-fold more active than the *R* enantiomers. PA-824 showed activity against MDR strains of tuberculosis that were comparable to those against susceptible strains, indicating that there is no cross-resistance with current antitubercular drugs. This lead compound also displays activity against static, non-replicating bacilli.

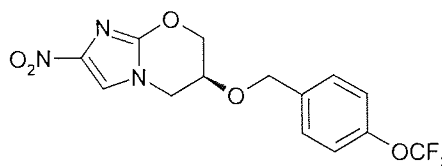

Figure 3.12 Nitroimidazopyran PA-824 **38**

The NAPs are actually pro-drugs, which require activation by nitro-reduction, dependent on a *M.tuberculosis* cofactor. The activity of PA-824 against MDR-TB and non-replicating mycobacteria suggested that NAPs act via a new mechanism. Studies have shown that PA-824 inhibits both protein and cell wall lipid synthesis. The compound inhibits the oxidation of cell wall hydroxymycolates to ketomycolates, the latter being essential for the normal growth and survival of *M.tuberculosis* in macrophages. It is not known though, whether NAP lethality lies in this action, or the concurrent effect on protein synthesis[86].

PA-824 is a promising drug candidate demonstrating potent activity against all known forms of tuberculosis[87].

3.5.7 Phenothiazines

Chlorpromazine **39** and thioridazine **40** are phenothiazines which are currently used in the management of psychosis. These agents have, however, been shown to inhibit the respiration of clinical isolates of *M.tuberculosis* that are resistant to all the first-line antituberculosis drugs[88].

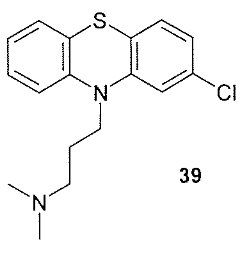

39

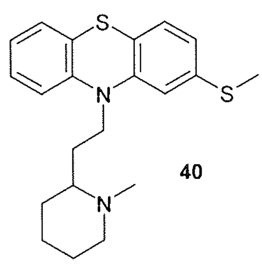

40

Figure 3.13 Phenothiazines, chlorpromazine **39** and thioridazine **40**

It has long been known that chlorpromazine (CPZ) displayed a wide range of activity against viruses, bacteria and mycobacteria. The amount of CPZ required for *in vitro* antimicrobial activity (around 25mg/l) was however, beyond that clinically achievable (around 0.5mg/l of plasma at best). Pulmonary macrophages though, concentrate CPZ 100-fold above the concentration found in plasma, so the internal macrophage concentration is actually sufficient for activity against the mycobacteria therein[89].

Long term treatment with CPZ leads to unwanted side effects, so the antimycobacterial effect of thioridazine has been studied. Thioridazine is the mildest of the phenothiazines, the most common side effect being drowsiness, and this displayed antitubercular activities comparable to those of CPZ, against both sensitive and MDRTB strains. It is anticipated, but not yet proven, that thioridazine is also concentrated by macrophages. Researchers have suggested the possibility of using thioridazine in therapy for patients with newly diagnosed TB and an undetermined drug susceptibility profile.

When a patient has MDRTB it is important that the antibiotic susceptibility profile of the strain is identified, so that the correct treatment can be given. There can be a long interim period between diagnosis of TB and conformation of drug susceptibility, and inappropriate treatment during this time could worsen the problem. It is argued that the use of thioridazine, which inhibits all encountered strains of MDRTB, may be helpful in restraining the disease, until the antibiotic susceptibility is fully known. Since the longest time period required for susceptibility results to be known is 6-7 weeks, no significant side effects other than mild drowsiness are anticipated to develop during this time[88-90].

3.6 THE SEARCH FOR A NEW VACCINE AND DIAGNOSTIC TOOLS

The effectiveness of the current BCG vaccine has been brought into question; from clinical trials it seems that although the vaccine does usually work well in children, it is not effective in adults[58]. The protective efficacy of this vaccine is variable, ranging from 0-80%, so there is a clear need for a new, rationally designed vaccine[91]. One group in the US is investigating the effect of the secreted proteins of *M.tuberculosis* in mice and guinea pigs. The research has shown that these proteins protect the animal models from TB to different degrees. They are hoping that by sifting through a pool of about 200 proteins they can identify the most effective 20 candidates, which could be the basis of a vaccine. Other approaches include the use of surface exposed proteins, plasmid DNA vector based vaccines and recombinant and mutant BCG vaccines[58,92].

The proteins of *M.tuberculosis* are also being investigated with regards to the development of a new, on the spot diagnosis of TB. The ideal proteins for such a test would be those that distinguish TB from other lung infections and detect it at an early stage. Current diagnostic tools include the tuberculosis skin test, but this is not an indicator of active disease. A positive skin test would also be given by those who have had TB and been cured, those who have been infected but do not have the active disease, and those who have been vaccinated with BCG. Other diagnostics include chest x-rays, smear tests and bacterial cultures, but these only detect the disease in its later stage of progression. A test that only detects the active disease, can detect it in the early stages, and could be performed and evaluated on the spot by a technician, would be a very useful tool[58].

3.7 THE GENOME SEQUENCE OF *M.TUBERCULOSIS*

The complete genome sequence of the best characterised strain of *M.tuberculosis*, H37Rv, was published in 1998; a result of a multi-institutional effort, supported by the Wellcome Trust. This strain has been used extensively in biomedical research as it has retained full virulence in animal models (unlike some clinical isolates), it is susceptible to drugs and is amenable to genetic manipulation[91]. There is some doubt, however, of whether it actually causes disease in humans. It is of interest therefore, that the genome sequence of a second, particularly virulent strain of *M.tuberculosis*, CDC1551, which does cause classical TB in humans is also soon to be published (although it is already available in electronic form on The Institute for Genomic Research (TIGR) Website: www.tigr.org.)[58,64]. It was hoped that it would be possible to detect either genetic differences or differences in gene expression which could be responsible for human infectivity. This is going to take further research however, as a large number of the genetic differences between the two strains are in portions of the genome that code for proteins with no known biological function, according to Claire Fraser, president of TIGR. She went on to say that for the genes whose function is understood, there is no immediately obvious difference between the two strains[64].

The genome of *M.tuberculosis* strain H37Rv contains around 4,000 genes and it has revealed some interesting facts about the organism and its survival. Several proteins are encoded for by the genome that are normally associated with anaerobic metabolism. In standard microbiology textbooks, *M.tuberculosis* is generally considered to be a strict aerobe. The organism is, however, believed to be capable of remaining dormant in a host for many years, forming clumps of bacilli, a portion of which must be in a relatively anaerobic environment. The fact that *M.tuberculosis* has the genes for anaerobic metabolism suggests that indeed the organism can survive microaerophilically and may even do so more than we realise[58,91]. Perhaps one of the most remarkable revelations was the mycobacteria's preponderance of enzymes for lipid metabolism. *M.tuberculosis* produces about 250 distinct enzymes involved in fatty acid metabolism, compared with only about 50 for *E.coli*. As a result of this finding, it is now thought that *M.tuberculosis* probably lives primarily on lipids in its host; the host cell membranes providing fatty acid precursors of the mycobacterial cell wall constituents. This means that in terms of drug design, lipid degradative enzymes should be targeted, rather than lipid biosynthetic enzymes, as it is the degraded lipids on which they survive[58,92].

The availability of *M.tuberculosis* genome sequences should improve our understanding of the biology of the organism and, hopefully, stimulate more focused, rational approaches to the design of new drugs, vaccines and diagnostic tools[92].

CHAPTER 4
N^1-BENZYLIDENEHETEROARYLCARBOXAMIDRAZONES: LIBRARY SYNTHESIS AND RELATED CHEMISTRY

The aim of this work was, firstly, to produce a large library of chemically diverse N^1-benzylidene-heteroarylcarboxamidrazones, for which there is literary precedent of antimycobacterial activity, and to test them against *Mycobacterium fortuitum*, as a screen for antitubercular activity; secondly, to assess *M.fortuitum* as a screen for *M.tuberculosis* by screening compounds against *M.tuberculosis* itself, where possible; thirdly, to test these novel compounds against *Staphylococcus aureus* and MRSA, and fourthly, to assess any compound displaying antibacterial or antimycobacterial activity, for its general toxicity against human white blood cells.

4.1 WHY SYNTHESISE N^1-BENZYLIDENEHETEROARYLCARBOXAMIDRAZONES?

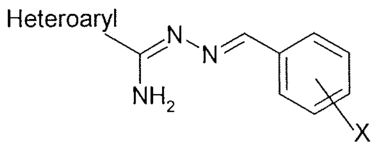

Figure 4.1 The general structure of the N^1-benzylideneheteroarylcarboxamidrazones

The general structure of the N^1-benzylideneheteroarylcarboxamidrazones is shown in Figure 4.1. These compounds have proven to be of interest in the field of TB research; the antimycobacterial activities of a set of 2-pyridyl, 4-pyridyl and some 2-quinolylcarboxamidrazones have been examined and presented in a series of papers by Mamalo *et al*[93-96]. From these works, the Mamalo group assimilated some qualitative structure-activity relationships. For their 2-pyridyl set of nineteen compounds, they found that there was a rough correlation between increased lipophilicity and improved mycobacterial inhibition. They found that compounds in which the arylmethylidene group possessed more polar substituents, such as methoxy, cyano or nitro groups, activity was either diminished or lost[93]. Further work demonstrated that when the pyridine-based group was altered to 4-pyridyl, the activity approximately mirrored that of the 2-pyridyl compounds[93,94]. The only 2-quinolylcarboxamidrazones for which the results are available are a small selection of 1-benzyl-1H-indol-3-ylidene derivatives (e.g. **43**, Figure 4.2). From these results, it was observed that the substitution of 2-pyridyl by 2-quinolyl resulted in a reduction of activity against mycobacteria[95]. The most active compounds discovered by Mamalo *et al* are shown in Figure 4.2 and included 2-chlorophenyl or 2-bromophenyl moieties, with both 2-pyridyl **41**, **42** and 4-pyridyl-heteroaryl substituents, and some 1-benzyl-1H-indol-3-ylidene derivatives of 2-pyridylcarboxamidrazone **54** (all with MIC 8μgml^{-1} against TB strain H37Rv).

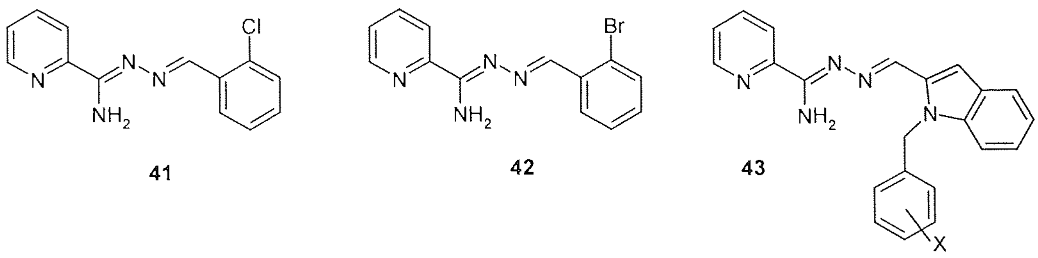

Figure 4.2 The most active compounds discovered by Mamalo *et al*

The work described above produced some interesting results, however, only a limited number of compounds was made (twenty-eight pyridine-2-, nineteen pyridine-4-, and nine quinoline-2- compounds). This report aims to build upon the foundations laid by Mamalo *et al* and to probe further the structure-activity relationships of these heteroarylcarboxamidrazone derivatives, using a combination of automated synthesis and rapid primary screening[97].

4.2 THE N^1-BENZYLIDENEHETEROARYLCARBOXAMIDRAZONE LIBRARY

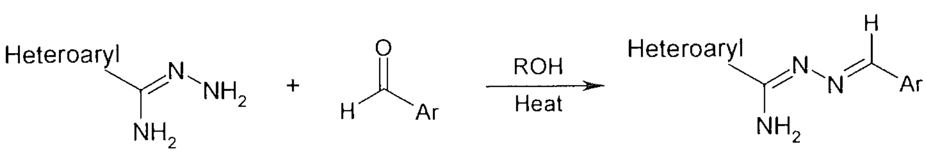

Scheme 4.1 Preparation of N^1-benzylideneheteroarylcarboxamidrazones

4.2.1 Varying The Aldehyde

The preparation of the N^1-benzylideneheteroarylcarboxamidrazones is shown in Scheme 4.1. As previously mentioned, the Mamalo group investigated and drew conclusions from a small data set of amidrazones which were synthesised in this manner. The aldehydes used by Mamalo *et al*, however, only displayed a limited variety of aryl-substituents; methyl or methoxy groups, halogens, one compound with a cyano group and two with nitro groups. These are also all very small substituents.

A large variety of aldehydes were incorporated into this study and will be referred to by a lower-case two letter code, throughout. The structures can be viewed in Table 4.1.

In this work, a large library of compounds was to be produced robotically. Before this process could be started though, it was necessary to probe the versatility of the reaction, to see if it could cope with aldehydes possessing different electronic and steric properties.

Initially, some 4-substituted benzaldehydes with differing electronic natures were chosen to investigate the reaction. For example, 4-isopropylbenzaldehyde **ad** and 4-hydroxybenzaldehyde **by**, were used to represent aldehydes with electron-donating groups, whilst 4-chlorobenzaldehyde[93,94] **dh** and 4-cyanobenzaldehyde[93,94,96] **dp** represented electron-withdrawing substituents. The 4-position was favoured at this developmental stage due to the ease of analysis in ^{1}H NMR.

Steric factors were then taken into consideration. For example, would bulky substituents in either one or both of the ortho positions of the benzaldehyde hinder the reaction? For this, 2-ethylbenzaldehyde **ai**, the 2-alkyloxybenzaldehydes **ay-bc**, 2-benzyloxybenzaldehyde **be**, and the disubstituted 2,6-dichlorobenzaldehyde **dj**, were used to investigate. 2-Trifluoromethylbenzaldehyde **dm** was used to test a bulky electron-withdrawing substituent, and bulky silyl-ether **eg**, was used to test a very steric, strongly electron-donating one.

Pyridine-2-carboxamidrazone **2PY** was reacted with all these 'test' aldehydes and the products analysed by ^{1}H NMR, which showed that all the reactions proceeded to give the desired products. From this, it was established that the reaction was very versatile, and that almost any aromatic aldehyde could be used.

Most of the aldehydes used in this work were commercially available, some were prepared in the laboratory (**bi**, **bj**, **bk**, **bl**, **bp**, **bq**, **br**, **cp**, **da**) and a few were prepared by a previous worker using standard literature procedures (**az**, **ba**, **bb**, **bc**, **bo**).

Table 4.1 The aldehyde-derived residues used in library synthesis

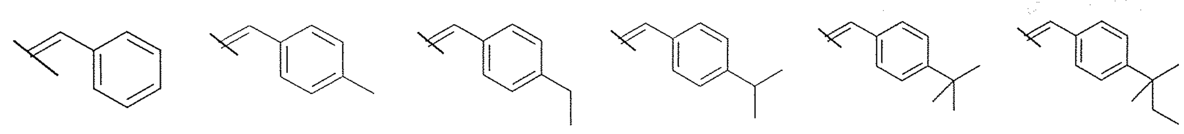

aa ab ac ad ae af

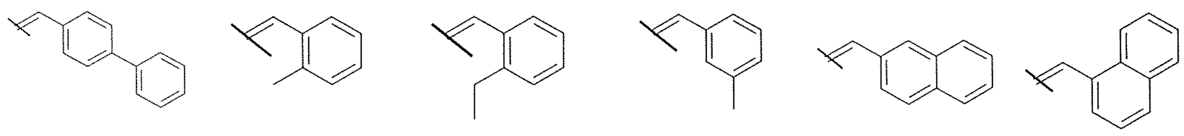

ag ah ai aj ak al

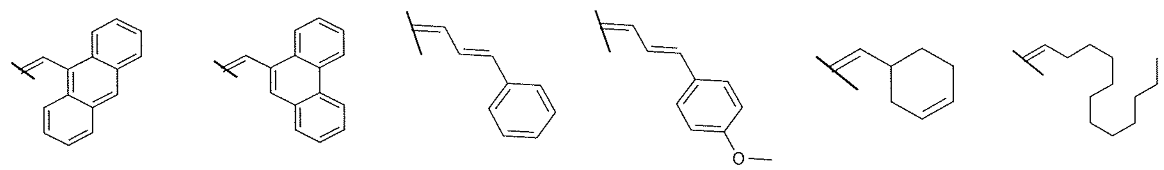

am an ao ap aq ar

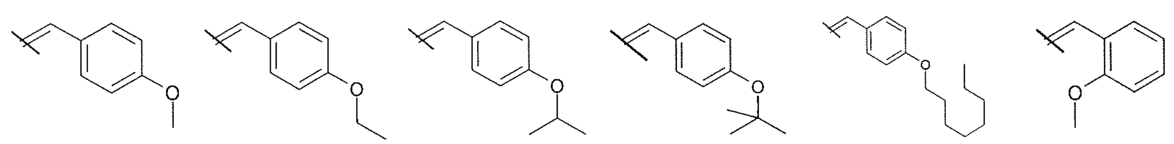

as at au av aw ax

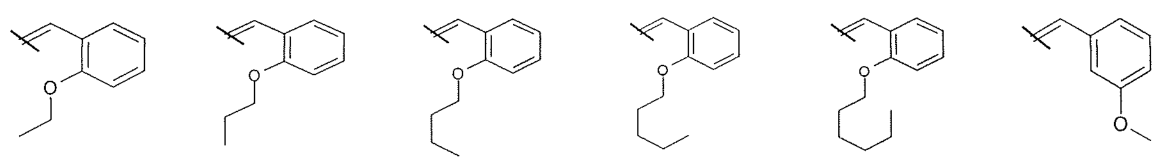

ay az ba bb bc bd

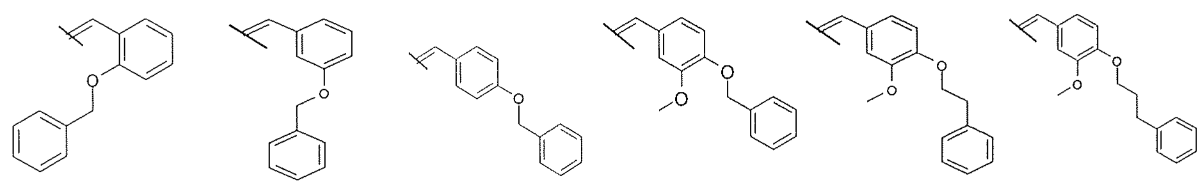

be bf bg bh bi bj

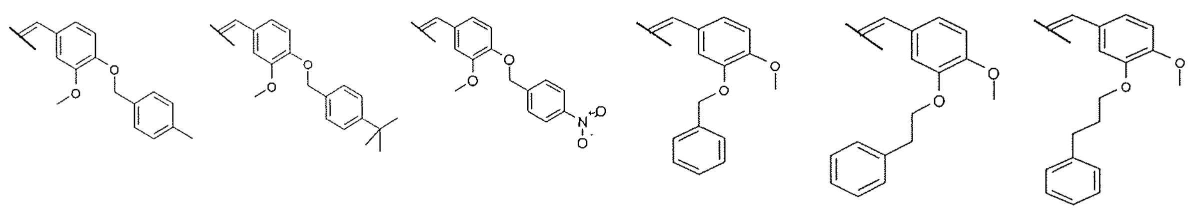

bk bl bm bn bo bp

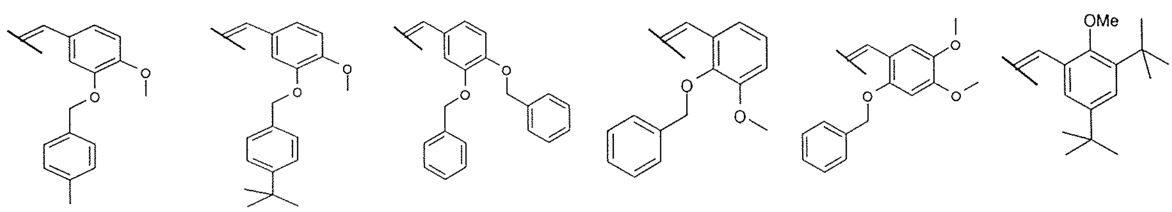

bq br bs bt bu bv

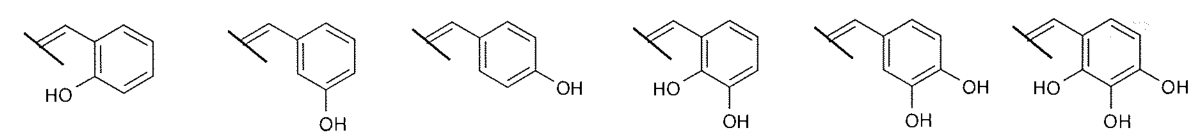

bw bx by bz ca cb

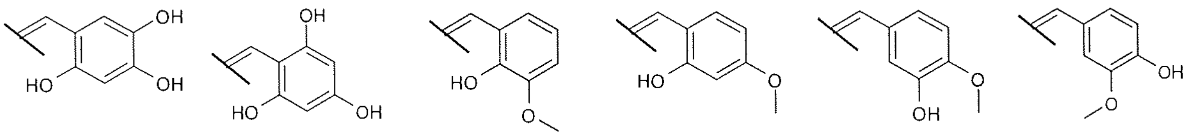

cc cd ce cf cg ch

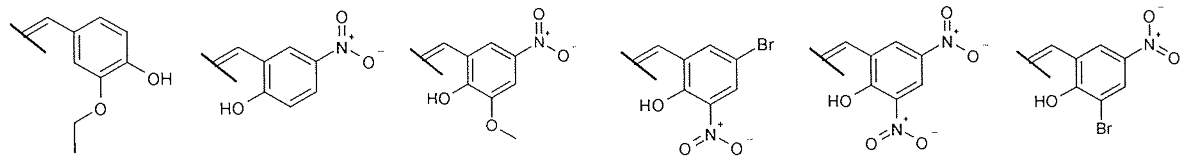

ci cj ck cl cm cn

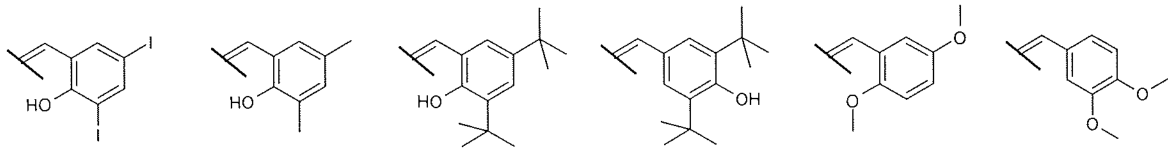

co cp cq cr cs ct

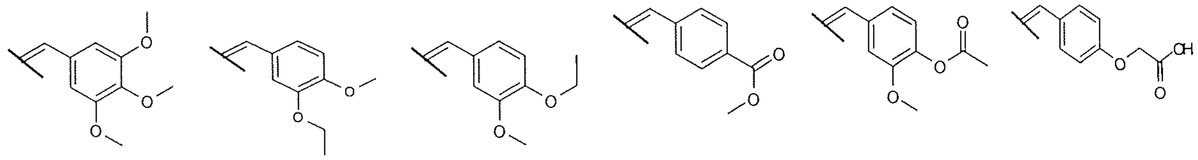

cu cv cw cw cy cz

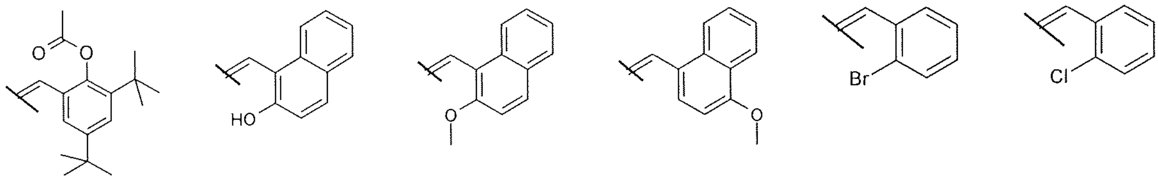

da db dc dd de df

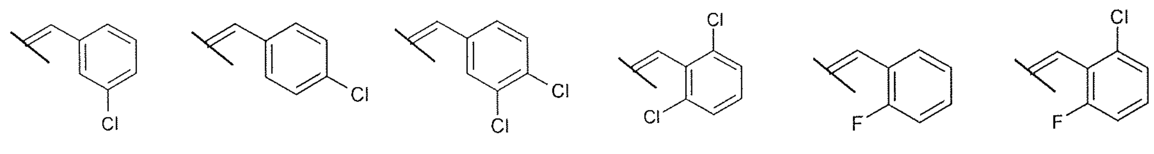

dg dh di dj dk dl

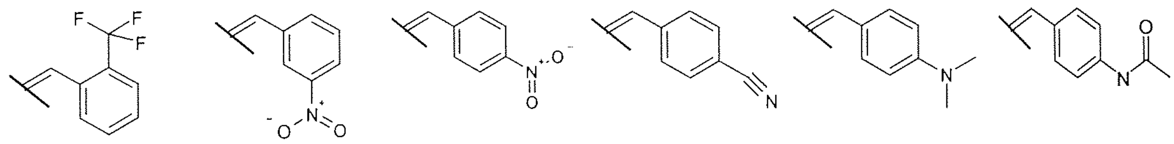

dm dn do dp dq dr

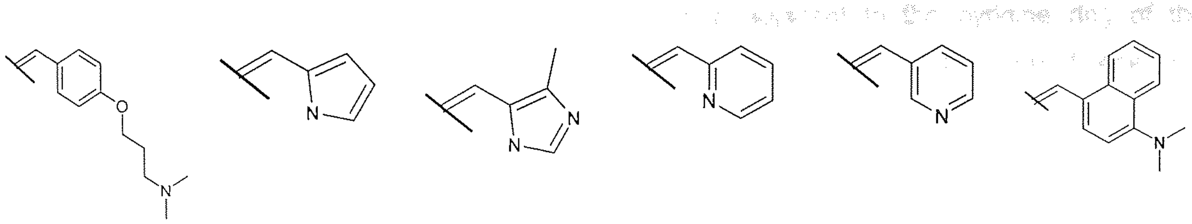

ds **dt** **du** **dv** **dw** **dx**

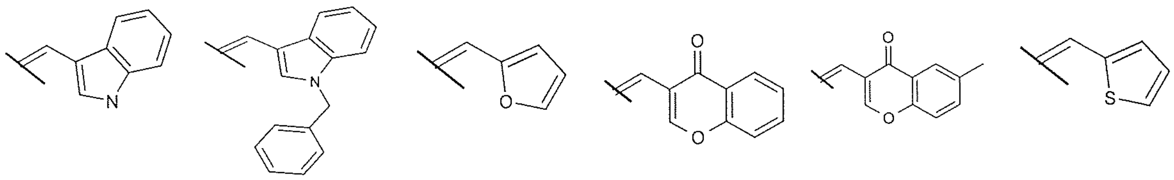

dy **dz** **ea** **eb** **ec** **ed**

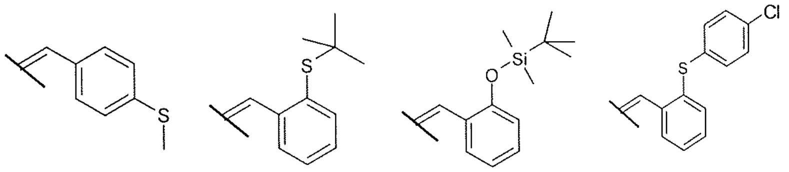

ee **ef** **eg** **eh**

4.2.2 Varying The Amidrazone Moiety

The heteroarylcarboxamidrazones building blocks **2PY**, **3PY**, **4PY**, **PZ**, **QN** (see Figure 4.3) were prepared by the action of hydrazine (hydrazine hydrate for **2PY**[93], **PZ**, **QN**[95] and 80% hydrazine for **3PY** and **4PY**[98]) upon the corresponding cyano compounds.

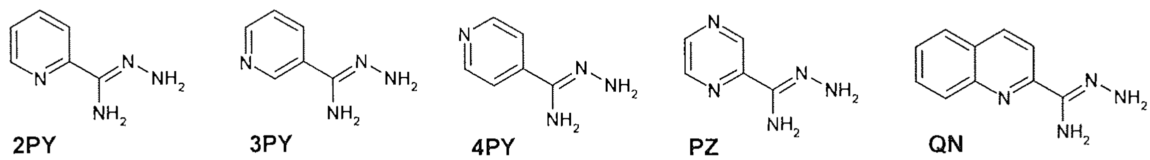

2PY 3PY 4PY PZ QN

Figure 4.3 The carboxamidrazones used

Pyridine-2- and quinoline-2-carboxamidrazones were synthesised due to the known antimycobacterial activity of their aldehyde derivatives[93,94,96] and pyrazine-2-carboxamidrazone was used on account of its structural similarity to these compounds, as well as its relationship to the antitubercular agent pyrazinamide **25**[97]. On the basis of any observed biological activity, further focused libraries of pyridine-3- **3PY** and pyridine-4-carboxamidrazones **4PY**, and 2-pyridylhydrazones (prepared from 2-pyridylhydrazine **HD**, Scheme 4.2), were also to be synthesised and screened. The pyridine-3- and pyridine-4-carboxamidrazones were synthesised in order to investigate the biological effect of changing the position of the nitrogen atom in the pyridine ring. The 2-pyridylhydrazones were synthesised to investigate the importance of the original amidrazone linker. The hydrazone compounds lack the CNH_2 group adjacent to the pyridine ring of the heteroarylcarboxamidrazones, which shortens the linker group between the benzylidene and heteroaryl moieties, and results in a very different molecular shape: it was of interest how this would affect biological activity.

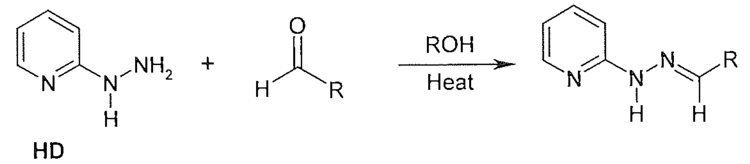

Scheme 4.2 Preparation of N^1-benzylidene-2-pyridylhydrazones

4.2.2.1 Stability of The Carboxamidrazone Starting Materials

Pyridine-2-, pyrazine-2- and quinoline-2-carboxamidrazones all appeared to be stable. Pyridine-3-carboxamidrazone was very unstable and pyridine-4-caboxamidrazone was unstable after prolonged storage. Both samples appeared to liquefy and darken in colour, as the compound changed. A route of decomposition for substituted pyrazinamidrazones was proposed by Foks *et al*[99] (Scheme 4.3). In order to postulate the same mechanism for the pyridine-3- and pyridine-4- compounds, there would have to be hydrazine present in the sample. From ^{1}H NMR analysis, it was known that there was no hydrazine remaining in the samples, after the synthesis and work-up of these compounds.

It was later observed, during its reaction with aldehydes, that pyridine-3-carboxamidrazone could decompose and generate its own hydrazine (see Section 4.3 and Scheme 4.5). If this decomposition is happening continuously, then it is possible that the Foks mechanism of decomposition, does occur for the pyridine-3- compound. There have been no similar observations for pyridine-4-carboxamidrazone, but this compound was much more stable than the pyridine-3- version, lasting for months, rather than weeks. Perhaps the self-decomposition to produce hydrazine does also occur for pyridine-4-carboxamidrazone, but on a much slower time-scale.

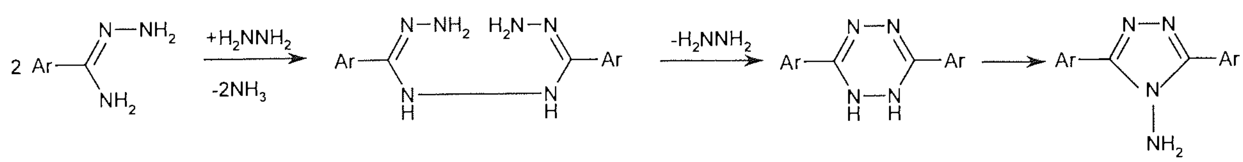

Scheme 4.3 Possible decomposition of pyridine-3- and pyridine-4-carboxamidrazones[99]

It was observed, however, that if the pyridine-3- and pyridine-4-carboxamidrazones were kept in a dessicator under vacuum, then decomposition did not occur.

4.2.3 N^1-Benzylideneheteroarylcarboxamidrazone Library Synthesis

An initial library of the condensation products of heteroarylcarboxamidrazones and aldehydes was prepared using automated parallel solution phase synthesis. A robotic pipetting station was used to transfer stock solutions of previously synthesised heteroarylcarboxamidrazones in methanol, and stock solutions of aldehydes in ethanol, into a matrix of 90 empty 4ml vials. A heating block was used to heat the matrix of reactions at reflux for an appropriate period. Upon cooling, most of the products precipitated out of solution, and a crude work-up was effected by automation to remove the soluble excess starting materials and by-products. Ethanol was transferred by pipette, into the product vials, allowed to stand, and then removed: a process known as trituration, which was repeated twice more. For the more soluble products which dissolved in ethanol, either ether or petroleum ether was used to wash the compounds instead, in order to increase the product recovery. Within each matrix of 90 vials, the separate vials contained only one heteroarylcarboxamidrazone and only one aldehyde building block, to give one product per vial.

The product compound codes are such that if pyridine-2-carboxamidrazone **2PY**, is reacted with benzaldehyde **aa**, then the product is called **2PYaa**. The capital letters refer to the amidrazone or hydrazone moiety and the two lower-case letters refer to the aldehyde-derived substituent.

The compounds **2PYaa**, **2PYab**, **2PYax**, **2PYde**, **2PYdf**, **2PYdh**, **2PYdi**, **2PYdo**, **2PYdp** and **4PYaa**, **4PYab**, **4PYax**, **4PYde**, **4PYdf**, **4PYdh**, **4PYdi**, **4PYdo**, **4PYdp** have been reported previously by Mamalo *et al*[93,94,96].

All compounds were characterised by positive atmospheric pressure ionisation mass spectrometry (APCI-MS) and all exhibited a dominant $(M+H)^+$ peak. Prior to biological testing, at least 10% of the compounds were analysed by ^1H NMR, which confirmed the structures, with purity generally greater than 85%, and often greater than 95%. The only impurities generally detected in the NMR spectra were excess aldehyde, except in the case of the pyridine-3-carboxamidrazones, where a side reaction occurred (discussed in Section 4.3). Thin layer chromatography of all the compounds also showed the same trend, where only one spot was usually seen, unless some unreacted aldehyde remained, or, for pyridine-3-carboxamidrazones, a by-product was produced.

The high purity of these products may be somewhat surprising since it has been reported that amidrazones can self-condense at elevated temperatures[99,100]. This potential side reaction, however, was not observed, except perhaps in the case of pyridine-3-carboxamidrazones, where bis-hydrazones (Figure 4.4) were isolated. The fact that this side reaction was not generally observed may be due to the fact that an excess of aldehyde was used, and that the reaction components were assembled at ambient temperature before being heated up, relatively slowly, to the boiling point of methanol. It is likely that this operation, combined with precipitation of the benzylidene products, favoured benzylidene formation over the competing self-condensation reaction pathway[97].

4.3 THE PYRIDINE-3-CARBOXAMIDRAZONE SIDE REACTION

When reactions with pyridine-3-carboxamidrazones were carried out, a bis-hydrazone by-product (Figure 4.4) was always observed. By-product formation was specific for pyridine-3-carboxamidrazone and was never observed during the synthesis of pyridine-2-, pyridine-4-, pyrazine-2-, or quinoline-2-carboxamidrazones.

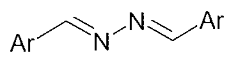

Figure 4.4 The general structure of the bis-hydrazone by-product, where Ar is derived from the reactant aldehyde

The bis-hydrazone could be formed if there was residual hydrazine in the carboxamidrazone starting material, which could react with the aldehyde, as in Scheme 4.4.

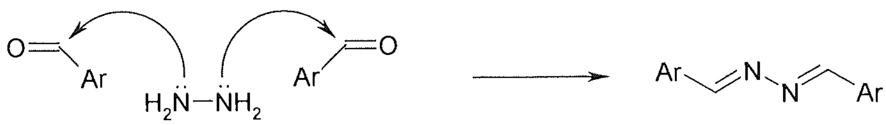

Scheme 4.4 Potential reaction of hydrazine with two molecules of aldehyde

This is unlikely, however, since steps were taken to remove excess hydrazine: either extracting the reaction mixture with water or washing the solid product with ether. ^{1}H NMR analysis showed that there was no remaining hydrazine in the samples.

If there is an absence of hydrazine itself in the samples used, then the alternative is that hydrazine is formed *in situ*, by decomposition of the carboxamidrazone. This hypothesis is supported by the observation of a molecular ion peak at 105 in the APCI-MS, for almost all of the pyridine-3-carboxamidrazone reactions. This peak indicates the presence of pyridine-3-carbonitrile (MW=104), which is a decomposition product of pyridine-3-carboxamidrazone; the other product of decomposition being free hydrazine (Scheme 4.5). This is the reverse of the reaction used to synthesise the compound.

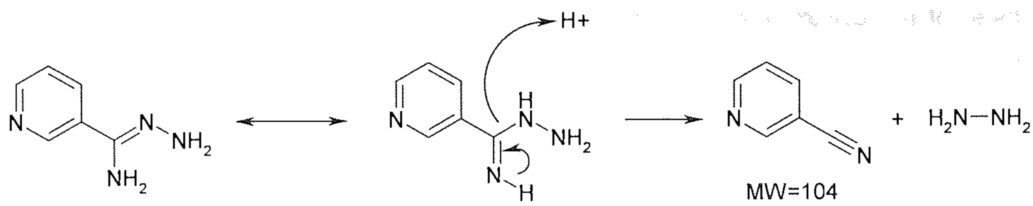

Scheme 4.5 Decomposition of pyridine-3-carboxamidrazone

4.3.1 The Effect of Temperature on Pyridine-3-carboxamidrazone Reactions

Investigation into how this reaction proceeds at different temperatures, showed that at room temperature, the only product was the bis-hydrazone, formed from hydrazine and the reactant aldehyde. At 40°C, this was also the main product, but a trace of the desired pyridine-3-carboxamidrazone product was observed. At 80°C, more of the pyridine-3-carboxamidrazone product was formed, but the reaction was not seen to go to completion without the formation of some amount of the bis-hydrazone by-product. Heat was therefore necessary to produce the required benzylidenepyridine-3-carboxamidrazone.

These data can be summarised in Scheme 4.6. In solution, together with an aldehyde, the pyridine-3-carboxamidrazone can act in one of two ways: it can either decompose to give the pyridine-3-carbonitrile **3-CNPY** and hydrazine, or react with the aldehyde to give a benzylidenepyridine-3-carboxamidrazone product **3PYprod**. At lower temperatures, the rate of decomposition (k^1) is greater than the rate of condensation with the aldehyde (k^2), and it is decomposition of the pyridine-3-carboxamidrazone that dominates.

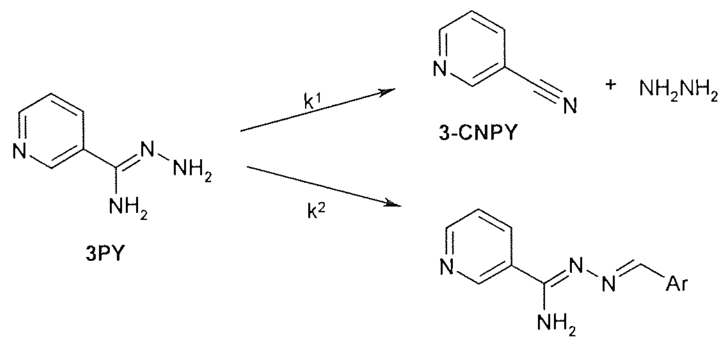

Scheme 4.6 Two reaction routes for the pyridine-3-carboxamidrazone: decomposition with reaction rate k^1 or reaction with an aldehyde, with reaction rate k^2

Heat was, therefore, required to obtain the desired benzylidenepyridine-3-carboxamidrazones. This suggests that the activation energy (E_A) needed for pyridine-3-carboxamidrazone to react with an aldehyde is greater than that required for decomposition, as shown in Figure 4.5. Increasing the temperature also increases reaction rate k^2, relative to k^1, such that the aldehyde condensation product is formed, although decomposition still continues to some extent.

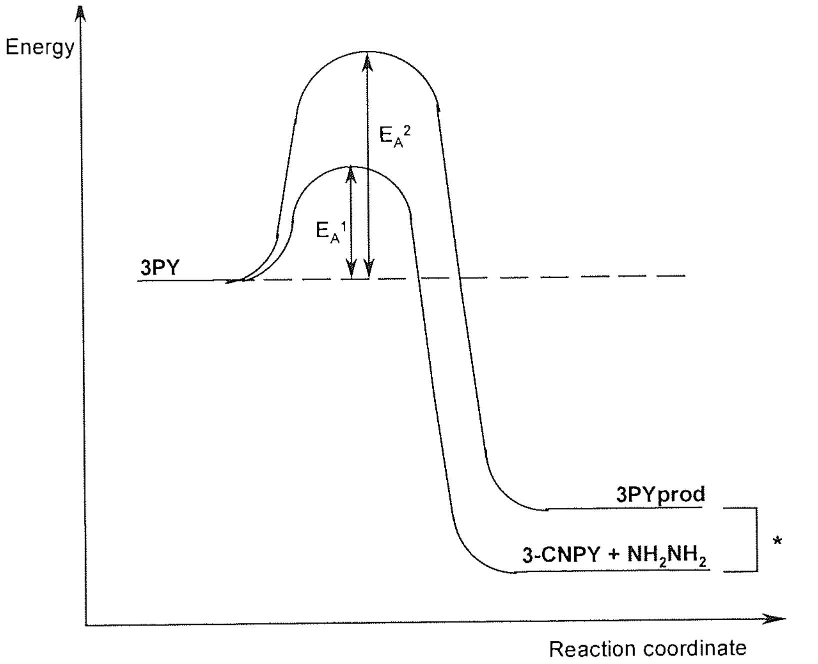

Figure 4.5 The energetics of the two possible pyridine-3-carboxamidrazone reactions are such that the activation energy (E_A) required for decomposition to occur is smaller than that needed for reaction with the aldehyde to form **3PYprod**.
(*) Figure not to scale.

4.3.2 Why is this Side-Reaction Specific For Pyridine-3-carboxamidrazones?

As mentioned earlier, the bis-hydrazone side-reaction was not observed for any of the other carboxamidrazones used. This is probably due to the positioning of the nitrogen atom in the heteroaryl rings, and the resulting electronic natures. Pyridine-3-carboxamidrazone is the only compound to have the nitrogen group at the 3-position. All of the other carboxamidrazones possess nitrogen in either the 2-, or 4-position; and so are electronically different. As shown in Scheme 4.7, a resonance-stabilised form of pyridine-4-carboxamidrazone can be drawn, locating the negative charge on the ring-nitrogen atom. This can also be done for pyridine-2-carboxamidrazone. A similar resonance structure cannot, however, be drawn for pyridine-3-carboxamidrazone and perhaps it is this lack of stabilisation that makes the 3-pyridyl compound more susceptible to decomposition.

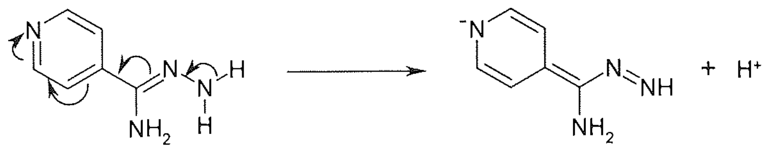

Scheme 4.7 A resonance-stabilised form of pyridine-4-carboxamidrazone

4.4 ATTEMPTED OPTIMISATION OF LEAD COMPOUNDS

Several compounds exhibited promising activity against the organisms tested (Chapters 5 and 7). Against *M.fortuitum*, **2PYbh**, **2PYbn**[101] and **4PYbn** were the most promising compounds. **4PYcq** was the lead compound with the most interesting activity against *S.aureus*, *E.faecium* and MRSA (Figure 4.6). It was thought that further investigation into the structure-activity relationships of these compounds could prove interesting. In order to vary further the benzylidene substituents on these lead compounds, some commercially unavailable aldehydes were synthesised (Section 4.4.1).

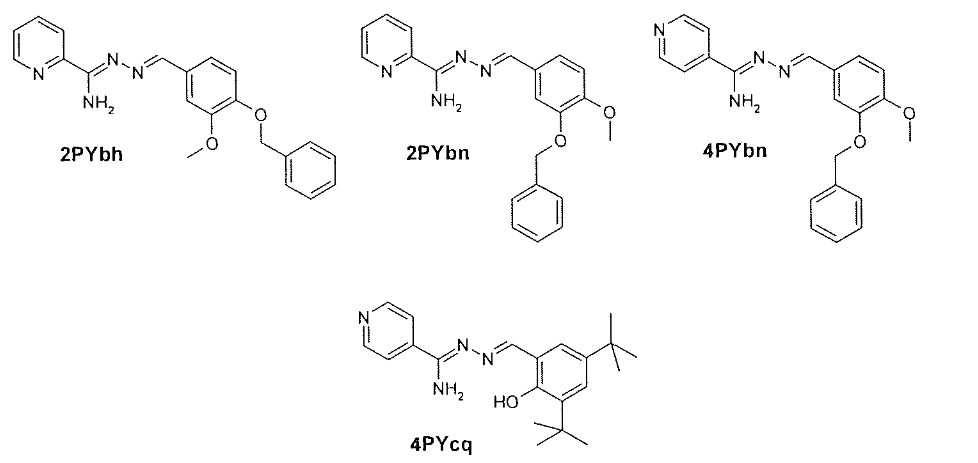

Figure 4.6 The lead structures for *M.fortuitum* (**2Ybh**, **2PYbn**, **4PYbn**) and MRSA (**4PYcq**)

4.4.1 Aldehydes Synthesised to Explore Activity Against *M.fortuitum*

Aldehydes **bh** and **bn** afforded antimycobacterial activity for some pyridine-2- and pyridine-4-carboxamidrazones. The aldehydes, whose substituents are shown in Table 4.2, were synthesised as analogues of **bh** and **bn**, where the methoxy group remains in either the 3- or 4- position, but the original benzyloxy substituents are replaced by phenylalkoxy groups (e.g. **bi**, **bj**, **bo**, **bp**), or by substituted-benzyloxy groups (e.g. **bk**, **bl**, **bq**, **br**). The purpose of selecting these particular aldehydes for synthesis, was to investigate the effect on biological activity of lengthening the molecules and increasing their lipophilicity (for results see Section 6.3).

Table 4.2 Substituents derived from the aldehydes synthesised to further investigate compound activities against *M.fortuitum*

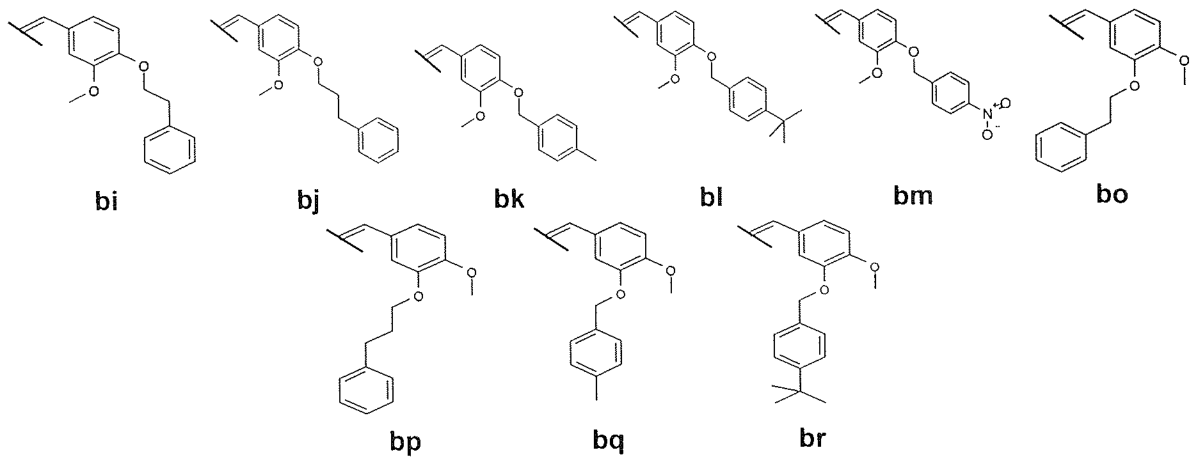

These aldehydes were all prepared in the same way (See Scheme 4.8), using a variation of the Williamson Synthesis[101] for the preparation of ethers.

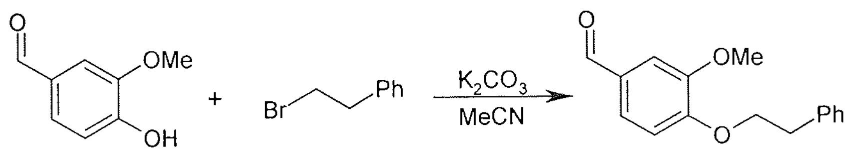

Scheme 4.8 Synthesis of the aldehyde **bi**

In this reaction, the reactant is an aldehyde. The Williamson Synthesis usually utilises sodium hydroxide as the base, however, if sodium hydroxide was used in the above case, it is likely that side products involving reaction of the aldehyde group could occur, as shown in Scheme 4.9. This reaction is known as the Cannizzaro Reaction, where one molecule of aldehyde oxidizes another to the acid and is itself reduced to the primary alcohol[102]. To prevent this from happening, potassium carbonate was used instead of a hydroxide.

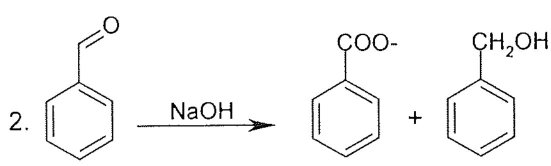

Scheme 4.9 The Cannizzaro Reaction: reaction of an aromatic aldehyde with aqueous or alcoholic hydroxide

4.4.2 Aldehydes Synthesised to Explore Activity Against Bacteria

The compound **4PYcq** demonstrated the best antibacterial activity of all the compounds tested. Some analogues of aldehyde **cq** were synthesised (See Table 4.3) to investigate the effect of various molecular alterations (See Section 7.3.2.2 for biological results).

Table 4.3 Substituents derived from the aldehydes synthesised to further investigate the antibacterial activity of **4PYcq**

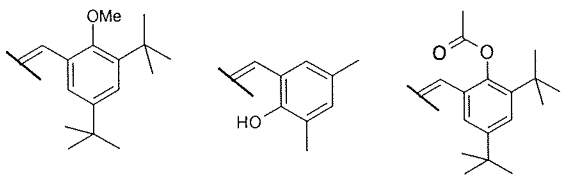

bv **cp** **da**

Aldehydes **bv** and **da** were both derived from aldehyde **cq**. Alkylation of the hydroxyl group of **cq**, by methyl iodide gave **bv**, and acetylation of the same hydroxyl group using acetic anhydride gave **da**. **bv** was synthesised to investigate the importance of the hydroxyl group of **cq**, and **da** was prepared for much the same reason, although it is possible that hydrolysis of the acetyl group of this molecule could occur *in vivo*, to give the original compound.

Aldehyde **cp** was prepared from 2,4-dimethylphenol and paraformaldehyde according to the method proposed by Casiraghi *et al* [103].In this aldehyde, the *t*-butyl groups of **cq** are replaced by less lipophilic methyl groups; it was of interest how this would affect activity.

4.5 SUBSTITUTING ALDEHYDES FOR KETONES

The synthesis of some cycloalkylidenecarboxamidrazones has previously been reported[97]. These compounds were formed by the condensation of some cyclic ketones **em**, **en**, **eo** (displayed in Table 4.4) with amidrazones (**2PY**, **PZ**, **QN**), using the same conditions as for the reaction with aldehydes. None of the resulting cycloalkylidenecarboxamidrazones displayed any biological activity.

Table 4.4 Cyclic ketones

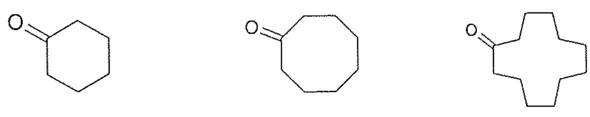

em **en** **eo**

It was of interest to expand this ketone chemistry further, to include some close analogues of aldehydes which had already proven to afford activity to the pyridinecarboxamidrazones. For this, three ketones were utilised, all of which were analogues of aldehyde **ae**, these are shown in Table 4.5. Aldehyde **ae** was chosen to study further using structurally similar ketones, as its amidrazone condensation products had been shown to be amongst the most active, even providing some activity to pyridine-3-carboxamidrazone, the reaction products of which were generally inactive. These were also attractive compounds to use due to their para-substitution which eases ^{1}H NMR analysis.

Table 4.5 The ketone derived substituents used

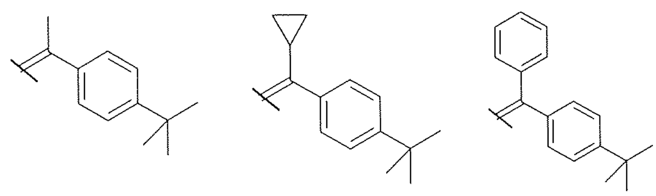

ep K4 **eq K5** **er K6**

A small library of the condensation products of pyridinecarboxamidrazones, 2-pyridylhydrazine and the ketones **ep-er** was prepared using automated parallel solution phase synthesis as described in Section 4.2.3. TLC and APCI-MS analysis showed that only the reactions involving ketone **ep** were successful under the conditions described in Section 4.2.3, i.e. heated at 65°C for one hour, then 75°C for two hours. Ketones **eq** and **er** proved to be inactive under the same conditions, no reaction having taken place. The experiment was repeated for ketones **eq** and **er**, using *iso*-propanol as a solvent and the mixture was heated at 100°C for 16 hours. TLC analysis again proved that no reaction had occurred.

Ketones are generally less susceptible to nucleophilic addition than aldehydes, due to a combination of steric and electronic factors. A ketone contains a second alkyl or aryl group where an aldehydes contains a hydrogen atom. Obviously a second group will hinder the approach of a nucleophile more than the small hydrogen atom of the aldehyde. Also, alkyl groups release electrons, which will reduce the electrophilic nature of the carbonyl-carbon atom, making it less reactive.

This experiment showed that when the second group was a methyl group, as in **ep**, the chemistry proceeded normally. In ketone **eq**, the alkyl group was increased in size to an cyclopropyl group and as a result, no reaction took place. Equally, when the second group was changed to a benzene ring in **er**, steric phenomena again prevented any reaction from occurring, even at elevated temperature.

4.6 DIMERISATION OF PYRIDINE-2-CARBOXAMIDRAZONE

It has been reported that amidrazones can self condense at elevated temperatures[99,100]. To investigate this, the reaction shown in Scheme 4.10 was set up and heated under reflux for approximately two and a half days. The isolated product of the reaction was the amidrazone dimer as shown in Scheme 4.10. This aminotriazole is the same compound that was proposed as a potential by-product in amidrazone synthesis by Nielson *et al* [100] and Foks *et al* [99]. There is not, however, any published physical data available with which to compare.

This experiment was carried out as it was thought that the ^{1}H NMR spectrum of the dimer would prove useful as a reference, in order to identify this potential side-product should it occur during the reactions of aldehydes with the heteroarylcarboxamidrazones. This reaction and its product, however, was not observed in any of the ^{1}H NMR spectra of the library products.

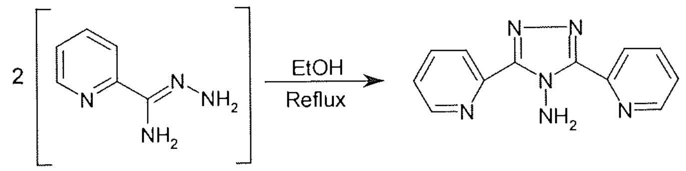

Scheme 4.10 Dimerisation of pyridine-2-carboxamidrazone

4.7 ATTEMPTED ALDEHYDE BIS-ADDITION OF THE CARBOXAMIDRAZONE

During the synthesis of the benzylideneheteroarylcarboxamidrazones, addition was only observed on the terminal *N*[1]-amine. Addition onto the alternative free amine, or a mixture of the aldehyde adding onto both of these sites was never observed; neither has it been reported in the literature. Attempts were made to react aldehydes on this second site, as shown in Scheme 4.11: two different methods were tried.

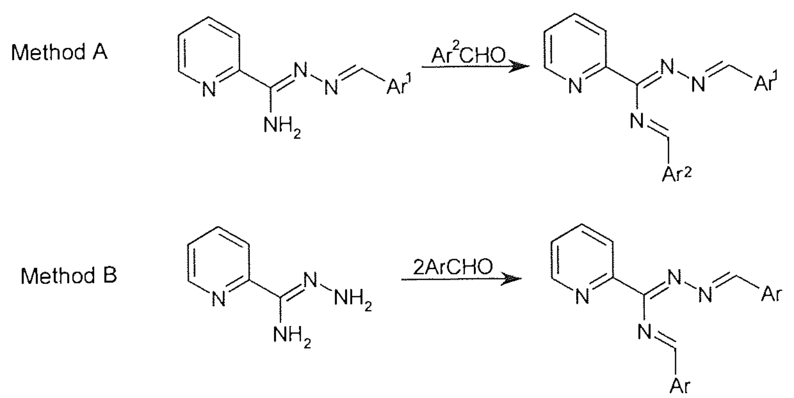

Scheme 4.11 Two methods of attempted synthesis of bis-addition of aldehyde

Addition onto the second, pendant amine did not occur, even after prolonged heating. This is probably a result of the fact that the carboxamidrazone moiety can exist in two tautomeric forms as shown in Figure 4.7. Although ^1H NMR studies show that in solution, these products tend to assume form **A**, the fact that the molecule is capable of this resonance stabilisation means that the pendant amine is much less reactive.

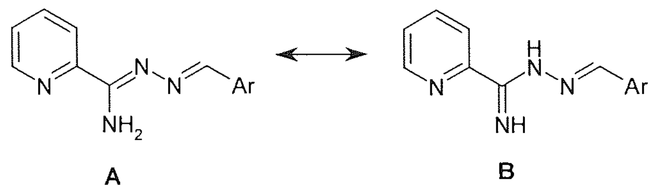

Figure 4.7 Tautomeric forms of a benzylidenepyridine-2-carboxamidrazone

4.8 ALTERNATIVES TO PYRIDINE

The chemistry has so far been dominated by heteroarylcarboxamidrazones. For biological activity, it appeared that the pyridine-2- or pyridine-4- group was essential for activity. It was of interest to see if altering this group, to a non-nitrogen containing ring would negate activity. It was desirable to maintain an electron-withdrawing functionality at the 2- or 4- position, to ensure the least deviation from the original compounds. For this reason, the candidates 2-nitrobenzonitrile and 2-chlorobenzonitrile were chosen. Using the same method that was used to prepare the heteroarylcarboxamidrazones, the benzonitriles were mixed with hydrazine (Scheme 4.12) and left for ten days. Only the synthesis of 2-nitrobenzenecarboxamidrazone **2NO₂BZ** was successful; no reaction occurred using 2-chlorobenzonitrile, maybe because the chloro-group did not have the necessary electron-withdrawing capacity.

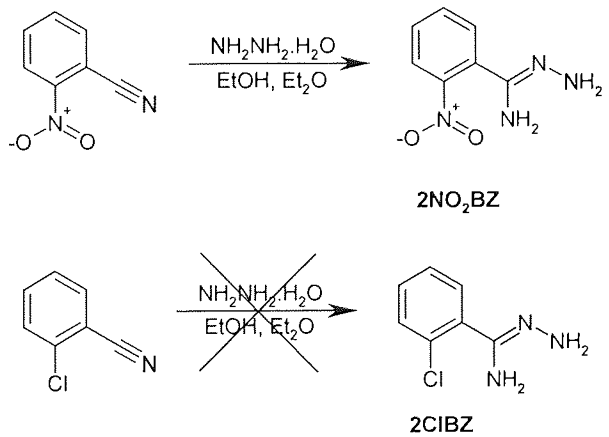

Scheme 4.12 2-Nitro- and 2-chloro-benzonitrile with hydrazine

$2NO_2BZ$ was then reacted with a few of the aldehydes which had previously afforded activity to the pyridine-2-carboxamidrazones (**ae**, **af**, **bh**, **bn**, **dx**, **eh**). By testing the resulting compounds against

M.fortuitum, and comparing the results with those of the equivalent pyridine-2-carboxamidrazones, it could be ascertained whether or not the pyridine functionality was necessary for antimycobacterial activity.

4.8.1 Analysis of The 2-Nitrobenzenecarboxamidrazones $2NO_2BZ$ by Mass Spectroscopy

The ^1H NMR spectra of the products from the reaction of the 2-nitrobenzenecarboxamidrazone **$2NO_2BZ$** with aldehydes, were consistent with the benzylidene-2-nitrobenzenecarboxamidrazones and indicated a purity of greater than 95%. The mass spectrometry data, however, was not so straightforward. The $(M+H)^+$ peak for the product was not observed for compound **$2NO_2BZ$** or any of its aldehyde adducts. Instead, peaks were consistently observed at $[(M+H)^+]-43$, $[(M+H)^+]-44$, $[(M+H)^+]-46$ and $[(M+H)^+]-61$. It is known that nitrobenzenes typically to lose their nitro groups during mass spectroscopy[103] and this would account for the $[(M+H)^+]-46$ signal. It is not really understood how the other peaks in the spectra arise, but they seem to be a fingerprint for these 2-nitrobenzenecarboxamidrazone compounds.

4.9 ATTEMPTED REDUCTION OF THE CARBOXAMIDRAZONE IMINE BOND

The investigation into the N^1-benzylidenepyridinecarboxamidrazones compounds so far has included;

- excision of the C-NH_2 bond adjacent to the ring, by using 2-pyridylhydrazone in place of pyridine-2-carboxamidrazone
- replacing the hydrogen of the imine bond with a larger group by reacting the amidrazones with ketones instead of aldehydes
- replacing the heteroaryl ring for a nitrobenzene ring

All these changes resulted in a loss of activity for the carboxamidrazones. The pendent amine of the carboxamidrazones had proved to be inactive (Section 4.7). The last remaining site for possible alteration of these benzylideneheteroarylcarboxamidrazones was the imine bond. Here, the attempted reduction of that imine bond (as shown in Figure 4.8) is discussed.

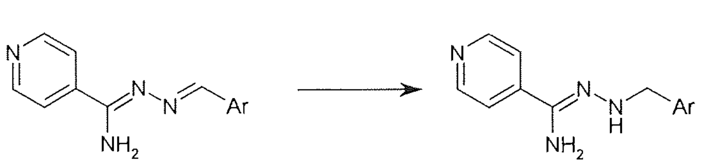

Figure 4.8 Proposed reduction of the benzylidine-pyridine-4-carboxamidrazone imine bond

4.9.1 Attempted Reduction With Lithium Aluminum Hydride

The addition of *N'*-[3,5-di-(tert-butyl)-2-hydroxybenzylidene]-pyridine-4-carboxamidrazone **4PYcq**, to lithium aluminum hydride, at room temperature, under dry conditions, failed to give the desired product. Although a new spot was observed by TLC, with a lower R.f. than the starting material, this was found to be protonated starting material **4PYcq**. This was proven by extraction of the compound, with potassium carbonate, which resulted in **4PYcq** itself. The protonation must have occurred during the work-up of the reaction, when the reaction is quenched using ammonium chloride which is slighhtly acidic at pH4.

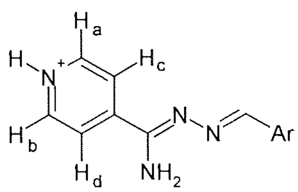

Figure 4.9 Protonated pyridine-4-carboxamidrazone

It was the pyridyl nitrogen which was protonated, as shown in Figure 4.9. The proton on the pyridyl nitrogen atom is exchangeable, and is not seen in the ^1H NMR. Protons H_a and H_b, being adjacent to this exchangeable proton, are affected greatly by it, and were not actually observed in the spectrum, as the signal is broadened out completely. H_c and H_d being further away from the site of protonation, are still seen, but the doublet which would be expected is observed as a broad singlet.

4.9.2 Attempted Catalytic Hydrogenation Using Palladium-on-Charcoal

N'-[3,5-Di-(tert-butyl)-2-hydroxybenzylidene]-pyridine-4-carboxamidrazone **4PYcq**, shaken with palladium on charcoal (Pd-C) under positive hydrogen pressure (120Psi) for 72 hours failed to give the desired product. Despite the high pressure, and the long reaction time, the recovered residue consisted only of starting material.

4.9.3 Attempted Catalytic Hydrogenation Using Raney Nickel and Cyclohexadiene

N'-[3,5-Di-(tert-butyl)-2-hydroxybenzylidene]-pyridine-4-carboxamidrazone **4PYcq**, heated at 80°C with Raney nickel, and cyclohexadiene as a supply of hydrogen[105] failed to give the desired product. When the same reaction was attempted, but under positive hydrogen pressure and not heated, no reaction was observed either. Ideally, a reaction would have been carried out under conditions of both heat and pressure, but equipment for such an experiment was not available at Aston University, during the period of this study.

4.9.4 Conclusion

All attempts to reduce the carboxamidrazone imine bond were unsuccessful. Furthermore, in all cases the only compound isolated at the end of each reaction was the starting material itself. This demonstrates that the imine bond is very stable, probably due to the conjugation through the molecule.

CHAPTER 5
ANTIMYCOBACTERIAL TESTING RESULTS

5.1 WHY USE *M.FORTUITUM* AS A SCREEN FOR *M.TUBERCULOSIS?*

Mycobacterium tuberculosis itself is a virulent human pathogen, and as such, is a Hazard Category 3 organism, requiring specialised handling facilities. It is also a slow growing mycobacterium, requiring 12-25 days incubation at 37°C[106]. The facilities to handle *M.tuberculosis* were not available at Aston University, but more importantly, a *rapid* primary screen was required for this work, due to the large numbers of compounds that were expected to be generated.

Mycobacterium fortuitum (reference strain NCTC 10394) was chosen as a model for *M.tuberculosis*, as it is a fast growing mycobacterium (3-4 days at 37°C). It could also be used on a laboratory bench, as it is not usually a human pathogen, only displaying pathogenicity in immunosuppressed individuals[106]. *M.fortuitum* therefore, provided a safe and rapid initial screen.

A selection of compounds was chosen for testing against *M.tuberculosis* (H37Rv) by the Tuberculosis Antimicrobial Acquisition and Coordinating Facility (TAACF) in the U.S., and the results used to assess the validity of using *M.fortuitum* as a model for *M.tuberculosis* (Section 5.4).

5.2 THE ANTIMYCOBACTERIAL TESTING

Each compound was tested once for a zone of inhibition on agar, against *M.fortuitum* (reference strain NCTC 10394), with 20μl of a 5mgml^{-1} test solution being placed in each well. It was noted that a compound which produced a larger zone of inhibition did not necessarily give a higher MIC reading. This suggested that different compounds permeated the agar to different extents. Since compounds of high lipophilicity may not permeate through the hydrophilic agar, 'gate-testing', i.e. testing of substances in broth at a single concentration of 32μgml^{-1} was also carried out[107].

If a zone of inhibition, or activity at 32μgml^{-1} was observed, then the compound was purified, where necessary, and the MIC for that compound was measured in broth. Some compounds were sent to the TAACF in the U.S. to be tested for inhibition of *M.tuberculosis* and percentages of inhibition are given where appropriate. The full results table is given below, and the interesting activities are discussed in Section 5.3.

Table 5.1 Antimycobacterial testing results versus *M.fortuitum* (*M.fort*) and *M.tuberculosis* (*M.tuber*) * denotes that the compound was taken from the library of Dr. D.L. Rathbone † highlights that the compound was found inactive via the zone method, but active via the gate method †† indicates that the end-point of the MIC reading could not be found due to limited compound solubility ** Results against *M.tuberculosis* strain H37Rv as provided by TAACF

Code	*M. fort* Zone	*M. fort* Gate[107]	*M. fort* MIC (μgml^{-1})	*M. tuber* %Inh.**
2PYaa	x	x		24
2PYab†	x	✓	16-32	40
2PYac		✓	16-32	
2PYad†	x	✓	8-16	69
2PYae	✓		8-16	80
2PYaf	✓		4-8	94
2PYag	x	x		66
2PYah	✓		>128	0
2PYai	✓		64-128	50
2PYaj	✓		>128	0
2PYak*	x	x		
2PYal*	✓		18-21	20
2PYam	x	x		90
2PYan	x	x		82
2PYao	x	x		
2PYaq*	x	x		
2PYar	x	x		
2PYas†	x	✓	16-32	0
2PYat		x		
2PYau		x		
2PYav		x		
2PYaw		x		
2PYax		✓	16-32	
2PYay†	x	✓	16-32	10
2PYaz		✓	16-32	
2PYba		x		
2PYbb		x		
2PYbc		x		
2PYbe	✓		25-30	59
2PYbf	✓		32-64	
2PYbg		✓	16-32	60
2PYbh	✓		4-8	42
2PYbi†	x	✓	8-16	
2PYbj	x	x		
2PYbk	x	x		
2PYbl	x	x		
2PYbm	x	x		
2PYbn	✓		4-8	72
2PYbo†	x	✓	8-16	
2PYbp	x	x		
2PYbq†	x	✓	16-32	
2PYbr	x	x		
2PYbs	x	x		0
2PYbt	✓		16-32	
2PYbu	x	x		68
2PYbw	x	x		38
2PYbx*	x	x		0
2PYby*	x	x		0
2PYbz	x	x		0
2PYca	x	x		1
2PYcb	x	x		

Code	*M. fort* Zone	*M. fort* Gate[107]	*M. fort* MIC (μgml^{-1})	*M. tuber* %Inh.**
2PYcc	x	x		7
2PYcd	x	x		
2PYce	x	x		43
2PYcf	x	x		33
2PYcg	x	x		2
2PYch	x	x		
2PYci	x	x		0
2PYcj	x	x		16
2PYck	x	x		19
2PYcl	x	x		10
2PYcm	x	x		14
2PYcq	x	x		
2PYcr	x	x		
2PYcs	x	x		18
2PYct	x	x		3
2PYcu*	x	x		0
2PYcv	x	x		10
2PYcw	x	x		0
2PYcx*	x	x		0
2PYcy	x	x		1
2PYcz	x	x		15
2PYdb	x	x		35
2PYdc	x	x		67
2PYdd	✓		16-32	
2PYde*	x	x		
2PYdf*	x	x		
2PYdg	✓		64-128	51
2PYdh*	x	x		
2PYdi*	x	x	>128	60
2PYdj*	x	x		21
2PYdk*	x	x		11
2PYdl*	x	x		10
2PYdm†	x	✓	16-32	46
2PYdn†	x	✓	16-32	0
2PYdo	x	x		16
2PYdp*	x	x		
2PYdq*	x	x		2
2PYdr	x	x		0
2PYds	x	x		0
2PYdt*	✓		>50	
2PYdu	x	x		
2PYdv*	✓		>50	
2PYdw*	x	x		
2PYdx	✓		8-16	
2PYdy*	x	x		0
2PYdz*	x	x		
2PYea*	x	x		0
2PYeb	✓		>128	
2PYec	x	x		
2PYed†	x	✓	16-32	0
2PYee	x	x	>128	42

Code	*M. fort* Zone	*M. fort* Gate[107]	*M. fort* MIC (μgml^{-1})	*M. tuber* %Inh.**
2PYef*	x	x	>128	72
2PYeg*	x	x		47
2PYeh*	✓		12.5-25	51
3PYab	x	x		
3PYac		x		
3PYad		x		
3PYae	✓		32-64	
3PYaf	✓		32-64	
3PYag	x	x		
3PYah	x	x		
3PYai	x	x		
3PYaj	x	x		
3PYak	x	x		
3PYal	x	x		
3PYam	x	x		
3PYan	x	x		
3PYas	x	x		
3PYat	x	x		
3PYau	x	x		
3PYav	x	x		
3PYaw	x	x		
3PYax	x	x		
3PYay	✓		>128	
3PYaz		x		
3PYba		x		
3PYbb		x		
3PYbc		x		
3PYbe	x	x		
3PYbf	✓		>64††	
3PYbg	x	x		
3PYbh	x	x		
3PYbm	x	x		
3PYbn	x	x		
3PYbs	x	x		
3PYbt	x	x		
3PYbu	x	x		
3PYca	x	x		
3PYcb	x	x		
3PYcc	x	x		
3PYcd	x	x		
3PYcf	x	x		
3PYcj	x	x		
3PYcl	x	x		
3PYcm	x	x		
3PYcq	x	x		
3PYcr	x	x		
3PYdb	x	x		
3PYdc	x	x		
3PYdd	x	x		
3PYdg	x	x		
3PYdq	x	x		
3PYds	x	x		
3PYdt	x	x		
3PYdv	x	x		
3PYdw	x	x		
3PYdx	x	x		
3PYeg	x	x		

Code	*M. fort* Zone	*M. fort* Gate[107]	*M. fort* MIC (μgml^{-1})	*M. tuber* %Inh.**
3PYeh	x	x		
4PYaa	x	x		
4PYab	x	x		
4PYac	x	x		
4PYad	x	x		
4PYae	✓		8-16	79
4PYaf	✓		8-16	73
4PYag	x	x		
4PYah	x	x		
4PYai	x	x		
4PYaj	x	x		
4PYak	x	x		
4PYal	✓		16-32	
4PYam†	x	✓	16-32	
4PYan	x	x		
4PYao	x	x		
4PYar	x	x		
4PYas	x	x		
4PYat		x		
4PYau		x		
4PYav		x		
4PYaw		x		
4PYax	x	x		
4PYay	x	x		
4PYaz		x		
4PYba		x		
4PYbb		x		
4PYbc		x		
4PYbe	x	x		
4PYbf	x	x		
4PYbg	x	x		
4PYbh	x	x		
4PYbi	x	x		
4PYbj	x	x		
4PYbk	x	x		
4PYbl	x	x		
4PYbm	x	x		
4PYbn	✓		5-10	
4PYbo	x	x		
4PYbp	x	x		
4PYbq	x	x		
4PYbr	x	x		
4PYbs	x	x		
4PYbt	x	x		
4PYbu	x	x		
4PYbw	x	x		
4PYbz	x	x		
4PYca	x	x		
4PYcb	x	x		
4PYcc	x	x		
4PYcd	x	x		
4PYce	x	x		
4PYcf	x	x		
4PYcg	x	x		
4PYch	x	x		
4PYci	x	x		
4PYcj	x	x		

Code	*M. fort* Zone	*M. fort* Gate[107]	*M. fort* MIC (μgml^{-1})	*M. tuber* %Inh.**
4PYck	x	x		
4PYcl	x	x		
4PYcm	x	x		
4PYcq	✓		>32[++]	
4PYcr	✓		>32[++]	
4PYcs	x	x		
4PYct	x	x		
4PYcw	x	x		
4PYcy	x	x		
4PYcz	x	x		
4PYdb	x	x		
4PYdc	x	x		
4PYdd	x	x		
4PYdg	x	x		
4PYdm	x	x		
4PYdn	x	x		
4PYdo	x	x		
4PYdq	x	x		
4PYdr	x	x		
4PYds	x	x		
4PYdt	x	x		
4PYdv	x	x		
4PYdw	x	x		
4PYdx	✓		16-32	
4PYed	x	x		
4PYee	x	x		
4PYef	x	x		
4PYeg	x	x		
4PYeh	✓	x	16-32	
PZaa	x	x		0
PZab*	x	x		0
PZad*	x	x		0
PZae	✓		>32[++]	48
PZaf[†]	x	✓	8-16	22
PZag	x	x		74
PZah	x	x		0
PZai	x	x		0
PZaj*	x	x		
PZak*	x	x		
PZal*	x	x		0
PZam	x	x		
PZan	x	x		18
PZao*	x	x		0
PZaq*	x	x		0
PZar	x	x		
PZas	x	x		
PZaw		x		
PZax	x	x		0
PZay*	x	x		0
PZaz		x		
PZba		x		
PZbb		x		
PZbc		x		
PZbe*	x	x		0
PZbf	✓		>64	
PZbg	x	x		48
PZbh	✓		>32[++]	

Code	*M. fort* Zone	*M. fort* Gate[107]	*M. fort* MIC (μgml^{-1})	*M. tuber* %Inh.**
PZbm	x	x		
PZbn	✓		>32[++]	
PZbs	x	x		7
PZbt	x	x		14
PZbu	x	x		6
PZbw	x	x		0
PZbx*	x	x		
PZby*	x	x		0
PZbz	x	x		o
PZca	x	x		
PZcb	x	x		12
PZcc	x	x		19
PZcd	x	x		0
PZce	x	x		0
PZcf	x	x		47
PZcg	x	x		0
PZch	x	x		0
PZci	x	x		0
PZcj	x	x		35
PZck	x	x		
PZcl	x	x		
PZcm	x	x		31
PZcq	x	x		
PZcr	x	x		43
PZcs	x	x		0
PZct	x	x		0
PZcu*	x	x		
PZcv	x	x		0
PZcw	x	x		0
PZcx*	x	x		2
PZcy	x	x		0
PZcz	x	x		0
PZdb	x	x		42
PZdc	x	x		
PZdd	x	x		29
PZde*	x	x		0
PZdf*	x	x		6
PZdg	x	x		0
PZdh*	x	x		0
PZdi*	x	x		
PZdj*	x	x		
PZdk*	x	x		
PZdl*	x	x		
PZdm*	x	x		
PZdn	x	x		0
PZdo	x	x		0
PZdp*	x	x		
PZdq	x	x		
PZdr	x	x		0
PZds	x	x		17
PZdt*	x	x		
PZdu	x	x		0
PZdv	x	x		0
PZdw*	x	x		
PZdx	x	x		17
PZdy*	x	x		0
PZdz*	x	x		

Code	*M. fort* Zone	*M. fort* Gate[107]	*M. fort* MIC (μgml^{-1})	*M. tuber* %Inh.**
PZea*	x	x		0
PZeb	x	x		4
PZec	x	x		0
PZed*	x	x		
PZee*	x	x		0
PZef*	x	x		
PZeg*	x	x		0
PZeh	x	x		
QNaa	x	x		0
QNab*	x	x		0
QNad*	x	x		0
QNae	x	x		0
QNaf	x	x	>128	79
QNag	x	x		0
QNah	x	x		0
QNai*	x	x		0
QNaj*	x	x		0
QNak*	x	x		0
QNal*	x	x		0
QNam	x	x		0
QNan	x	x		0
QNao*	x	x		0
QNaq*	x	x		6
QNar	x	x		0
QNas*	x	x		0
QNaw		x		
QNax	x	x		0
QNay*	x	x		0
QNaz		x		
QNba		x		
QNbb		x		
QNbc		x		
QNbe*	x	x		18
QNbf	✓		>64[++]	28
QNbg	x	x		0
QNbh	✓		>32[++]	0
QNbm	x	x		
QNbn	✓		>32[++]	0
QNbs	x	x		0
QNbt	x	x		
QNbu	x	x		12
QNbw	x	x		0
QNbx	x	x		0
QNby*	x	x		6
QNbz	x	x		0
QNca	x	x		0
QNcb	x	x		
QNcc	x	x		0
QNcd	x	x		0
QNce	x	x		0
QNcf	x	x		0
QNcg*	x	x		0
QNch*	x	x		0
QNci	x	x		0
QNcj	x	x		0
QNck	x	x		0
QNcl	x	x		0

Code	*M. fort* Zone	*M. fort* Gate[107]	*M. fort* MIC (μgml^{-1})	*M. tuber* %Inh.**
QNcm	x	x		0
QNcq	x	x		0
QNcr	x	x		0
QNcs	x	x		0
QNct	x	x		0
QNcu*	x	x		0
QNcv	x	x		0
QNcw	x	x		0
QNcx*	x	x		0
QNcy	x	x		0
QNcz	x	x		0
QNdb	x	x		0
QNdc	x	x		0
QNdd	x	x		0
QNde*	x	x		0
QNdf*	x	x		0
QNdg*	x	x		0
QNdh*	x	x		0
QNdi*	x	x		0
QNdj*	x	x		0
QNdk*	x	x		0
QNdl*	x	x		0
QNdm*	x	x		0
QNdn	x	x		0
QNdo	x	x		
QNdp*	x	x		0
QNdq*	x	x		0
QNdr	x	x		0
QNds	✓		64-128	0
QNdt*	x	x		0
QNdu*	x	x		10
QNdv*	x	x		
QNdwv	x	x		12
QNdx	x	x		0
QNdy	x	x		27
QNdz*	x	x		
QNea*	x	x		0
QNeb*	x	x		2
QNec	x	x		0
QNed*	x	x		0
QNee	x	x		0
QNef*	x	x		0
QNeg*	x	x		13
QNeh*	x	x		0
HDaa	x	x		
HDab	x	x		
HDac	x	x		
HDad	x	x		
HDae	x	x		
HDaf	x	x		
HDag	x	x		
HDah	x	x		
HDai	x	x		
HDaj	x	x		
HDak	x	x		
HDal	x	x		
HDam	x	x		27

Code	*M. fort* Zone	*M. fort* Gate[105]	*M. fort* MIC (μgml^{-1})	*M. tuber* %Inh.**
HDan	x	x		
HDas	x	x		
HDaw	x	x		
HDax	✓		>128	
HDay	x	x		
HDaz	x	x		
HDba	x	x		
HDbb	x	x		
HDbc	x	x		
HDbe	x	x		
HDbf	x	x		
HDbg	x	x		
HDbh	x	x		
HDbm	x	x		
HDbn	x	x		
HDbo	x	x		
HDbq	x	x		
HDbs	x	x		
HDbt	x	x		
HDbu	x	x		
HDbz	✓		30-40	
HDca	✓		>128	
HDcb	x	x		
HDcc	x	x		
HDcd	x	x		
HDce	✓		20-30	
HDcf	✓		30-40	

Code	*M. fort* Zone	*M. fort* Gate[105]	*M. fort* MIC (μgml^{-1})	*M. tuber* %Inh.**
HDan	x	x		
HDcj	x	x		
HDck	x	✓	16-32	
HDcl	x	x		25
HDcm	x	x		
HDcn	x	x		
HDco	x	x		
HDcq	x	x		
HDcr	x	x		
HDdb	✓		>128	
HDdc	x	x		
HDdd	x	x		
HDdg	x	x		
HDdm	x	x		
HDdn	x	x		
HDdq	x	x		
HDds	x	x		
HDdt	x	x		
HDdv	✓		>128	
HDdw	x	x		
HDdx	x	x		
HDeb	x	x		
HDed	x	x		
HDeg	x	x		
HDeh	x	x		

5.3 DISCUSSION OF *MYCOBACTERIUM FORTUITUM* TESTING RESULTS

As mentioned previously, Mamalo *et al* have reported the antimycobacterial activity of a series of benzylideneheteroarylcarboxamidrazones[93-96]. It is important to point out that the biological testing procedures of Mamalo *et al* were different to the ones used here. The Mamalo group report MIC data for *Mycobacterium tuberculosis* (H37Rv) itself, and a panel of other strains of mycobacteria, including *M.fortuitum*. The strain of *M.fortuitum* used by the group was an isoniazid resistant strain, which was, in general, unaffected by the carboxamidrazones. The *M.fortuitum* strain used in this study was isoniazid sensitive (1-2μgml^{-1}).

5.3.1 Antimycobacterial Testing of The Starting Materials

The amidrazone starting materials themselves **2PY**, **3PY**, **4PY**, **PZ** and **QN**, displayed no activity against *M.fortuitum* in their unsubstituted form.

All the aldehyde reactants were tested against *M.fortuitum*. Some displayed antimycobacterial activity; namely; **ac**, **am**, **be**, **bf**, **bg**, **bh**, **bn**, **bo**, **dd**, **dn**, **dx**, **eh**. The antimycobacterial activity of the amidrazone-aldehyde adducts were, however, far superior to that of the aldehyde precursors alone, being two- to four-fold more potent. Table 5.2 displays the activities of the 'active' aldehydes and compares them to the activities of their amidrazone adducts.

Table 5.2 The MIC values of the aldehydes active against *M.fortuitum* and their pyridine-2-carbox-amidrazone adducts. ++ indicates that the end-point of the MIC reading could not be found due to limited compound solubility, * denotes the MIC of the 4PY adduct, as 2PY adduct was inactive.

Aldehyde Code	Aldehyde Structure	MIC aldehyde ($\mu g ml^{-1}$)	MIC 2PY adduct ($\mu g ml^{-1}$)
ac	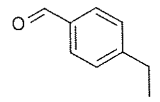	>128	16-32
am	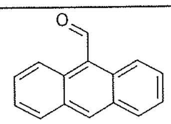	>32++	16-32*
be	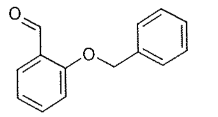	64-128	25-30
bf	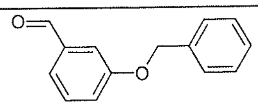	64-128	32-64
bg	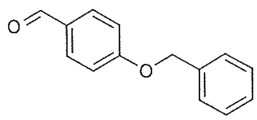	64-128	16-32
bh	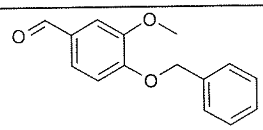	32-64	4-8
bn	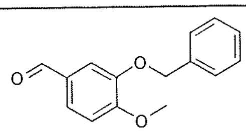	16-32	4-8
bo	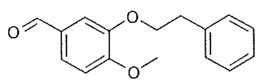	>128	8-16
dd	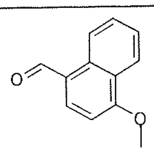	64-128	16-32
dn	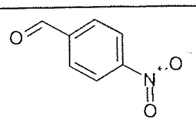	64-128	16-32
dx	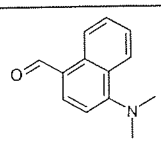	64-128	8-16
eh	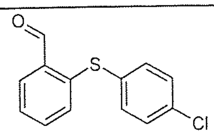	>128	12.5-25

5.3.2 The Benzylideneheteroarylcarboxamidrazone Results

This section aims to give a broad overview of the antimycobacterial results obtained in this study. The data will later be subjected to molecular modelling and quantitative structure-activity relationship (QSAR) studies in order to try to develop hypotheses about how the activity of these compounds arises.

The compounds **2PYaa**, **2PYab**, **2PYax**, **2PYde**, **2PYdf**, **2PYdh**, **2PYdi**, **2PYdo**, **2PYdp** and **4PYaa**, **4PYab**, **4PYax**, **4PYde**, **4PYdf**, **4PYdh**, **4PYdi**, **4PYdo**, **4PYdp** have been reported previously by Mamalo *et al*[91,92,94]. The results of this study cannot be directly compared to those of Mamalo *et al*, as the group tested their compounds directly on *M.tuberculosis*, to generate MIC values. The Mamalo group also tested their compounds against a strain of *M.fortuitum*, but whereas the strain of *M.fortuitum* used in this study was isoniazid sensitive, Mamalo's strain was resistant to isoniazid. The *M.tuberculosis* results that were obtained in this study from the TAACF utilised the same reference strain (H37Rv) as the Mamalo group, but rather than MIC values, the results are given as percentage inhibition of growth.

The Mamalo group only investigated a limited variety of functional groups mostly, halogens and methyl or methoxy groups all of which are very small substituents. In this study, much bulkier substituents are also investigated.

Only compounds with activity against *M.fortuitum* are presented in Tables 5.3-5.7. The data have been separated into sub-sets according to functional group, and the trends within these sets will be discussed.

Table 5.3 *M.fortuitum*-active alkyl-substituted benzylideneheteroarylcarboxamidrazones

Code	Structure	MIC μgml^{-1}
2PYab	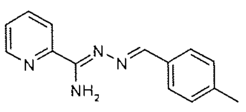	16-32
2PYac	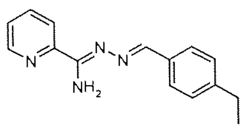	16-32
2PYad	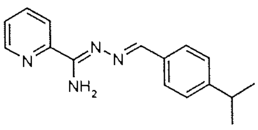	8-16
2PYae	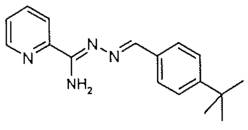	8-16
3PYae	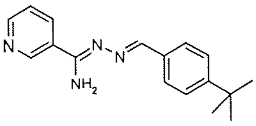	32-64
4PYae	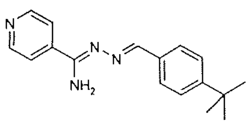	8-16
2PYaf	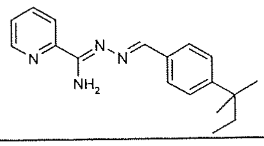	4-8
3PYaf	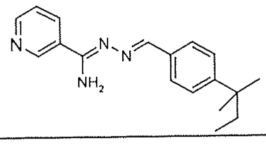	32-64
4PYaf	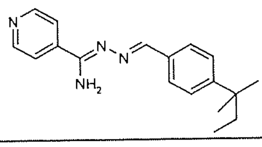	8-16
PZaf	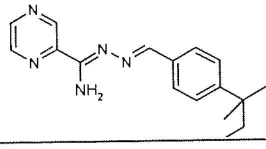	8-16
2PYai	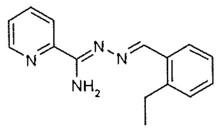	64-128

In the set of alkyl-substituted benzylideneheteroarylcarboxamidrazones, the 4-alkyl series displayed the best antimycobacterial activity. As shown in Table 5.3, 4-methylbenzylidene-pyridine-2-carboxmidrazone **2PYab**, and 4-ethylbenzylidene-pyridine-2-carboxamidrazone **2PYac**, both had MICs of 16-32μgml^{-1}. When the same substituents were placed in the 2-position, activity was lost for the compound with the 2-methyl group **2PYah**, and severely diminished for the compound with the 2-ethyl group **2PYai** (64-128μgml^{-1}). Changing the methyl group to the 3-postion **2PYaj** also resulted in a loss of activity.

Increasing the carbon chain length of the alkyl substituent, at the 4-postion, improved the activity of the compound. For example, in changing from the 4-ethyl-benzylidenepyridine-2-carboxamidrazone **2PYai**, to the 4-isopropyl **2PYad** or 4-*t*-butyl-benzylidenepyridine-2-carboxamidrazone **2PYae**, the activity increases from 16-32μgml^{-1}, to 8-16μgml^{-1}. Increasing the carbon chain further to give 4-(1,1-dimethylpropyl)benzylidene-pyridine-2-carboxamidrazone **2PYaf**, resulted in more potent activity still, MIC 4-8μgml^{-1}. This is to be expected when one considers the highly lipophilic nature of the mycobacterial cell wall. It is also consistent with the observations of Mamalo *et al*, who noted that lipophilicity was important for antimycobacterial activity and that decreasing the lipophilicity of the benzylidene nucleus resulted in reduced activity[92].

It is of interest that most of the benzylideneheteroarylcarboxamidrazones which displayed activity against *M.fortuitum* in this study were actually specific for mycobacteria and were inactive against Gram-positive bacteria (Section 7.2.1). This is true for this series of compounds, except for the 4-(1,1-dimethylpropyl)benzylidene compounds **2PYaf**, **3PYaf**, **4PYaf**, **PZaf**, which also displayed activity against some staphylococci and enterococci. It seems that the extension of the alkyl group to five carbons causes the compound to lose its specificity for mycobacteria.

The pyridine-2- **2PY** and pyridine-4-benzylidenecarboxamidrazones **4PY**, with the more lipophillic substituents in the series **ae** and **af**, approximately mirror each others activity, a trend which Mamalo *et al* have previously reported[93,94,96]. This is not true, however, for the rest of the compounds in Table 5.3 for which only the pyridine-2- compounds displayed activity. Changing the amidrazone moiety to pyridine-3- **3PY** resulted in activity either being lost, or diminished. The quinoline-2-benzylidenecarboxamidrazones **QN**, were inactive, as were most pyrazine-2-benzylidenecarboxamidrazones **PZ**, with the exception of **PZaf**, which was the only active pyrazine compound in the whole study.

Table 5.4 *M.fortuitum*-active heteroarylnaphthylidene- and heteroarylanthrylidene-carboxamidrazones

Code	Structure	MIC μgml^{-1}
2PYal	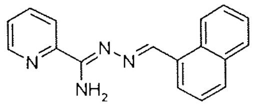	18-21
4PYal	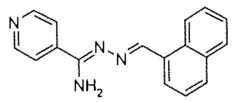	16-32
2PYdx	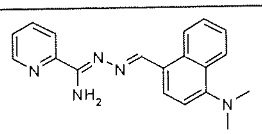	8-16

Code	Structure	MIC μgml^{-1}
4PYdx	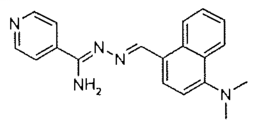	16-32
2PYdd	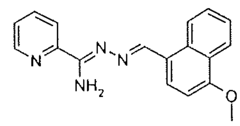	16-32
4PYam	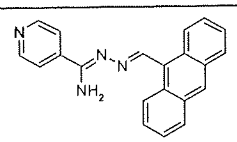	16-32

For both the pyridine-2- **2PY** and pyridine-4- **4PY** naphthylidenecarboxamidrazones, the 1-naphthyl derivative **al**, was active in the range 16-32μgml^{-1} (See Table 5.4). Interestingly, the derivatives of the 2-naphthylidene isomer **ak**, were inactive. Similarly, **4PYam**, with a 9-anthrylidene residue was active, but the same compound with the 9-phenanthrylidene isomer **an** was not. Generally, if the pyridine-4- isomer was active, so was the pyridine-2-, this was not the case for the 9-anthrylidene compound, however, where **2PYam** was inactive.

Additions to the naphthylidene ring, did not affect the biological activity very much. The addition of the mildly electron-donating methoxy group to the naphthylidene ring, keeps activity in the same range as the unsubstituted molecule for the pyridine-2-compound **2PYdd**, but causes **4PYdd** to lose activity completely. When the strongly electron-donating 4-dimethylamino group, is substituted onto the naphthylidene compound **2PYdx**, the MIC improves, but for the equivalent pyridine-4-compound **4PYdx**, the activity remains approximately the same as the unsubstituted molecule.

If we consider the pyridine-2- set of compounds in Table 5.4, the 4-dimethylamino substituted naphthylidene compound **2PYdx**, is the most active of the set. The dimethylamino group is the most electron-donating, and also the bulkiest substituent used. The resulting improved activity could be due to the steric nature of this functional group, rather than its electronic effects as indicated above. Indeed, the increased activity could be due to a combination of both these factors.

The next set of compounds to be discussed are the alkoxy- and benzyloxy-substituted benzylidene-heteroarylcarboxamidrazones, shown in Table 5.5. Mamalo *et al*, surmised that methoxy substituents, which decreased the lipophilicity of the benzylidene nucleus, were "remarkably less active" than the corresponding halogen and alkyl substituted compounds. Although this was true for a variety of di- and tri-methoxy substituted compounds which were synthesised (all MIC $\geq 256\mu g ml^{-1}$ against *M.tuberculosis*, H37Rv), Mamalo's group also synthesised 2-methoxybenzylidene-pyridine-2-carboxamidrazone **2PYax**, which, in his studies was, in fact, active at $16\mu g ml^{-1}$ and equi-active with their 4-methyl-, 2,4-dimethyl- and 4-bromo-benzylidene derivatives. Only two compounds in Mamalo's study were more active, 2-chloro- **52** and 2-bromo-benzylidene-pyridine-2-carbox-amidrazone **53** with MICs $8\mu g ml^{-1}$ [93]. The compound **2PYax** was also active in the studies for this thesis versus *M.fortuitum*, at a concentration of $16\text{-}32\mu g ml^{-1}$.

It is unlikely that the set of compounds shown in Table 5.5 would have been predicted as possessing activity, from the conclusions of Mamalo *et al.* The range of substituents here though, has been broadened from just the small methoxy group, by introducing the benzyloxy and alkylphenoxy functionalities too.

Table 5.5 *M.fortuitum*-active alkoxy- and benzyloxy-substituted benzylideneheteroaryl-carboxamidrazones

Code	Structure	MIC $\mu g ml^{-1}$
2PYas	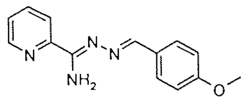	16-32
2PYax	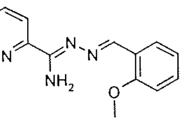	16-32
2PYay	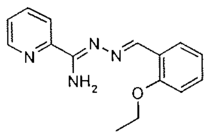	16-32
2PYaz	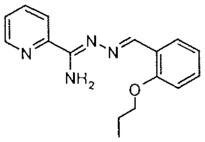	16-32
2PYbe	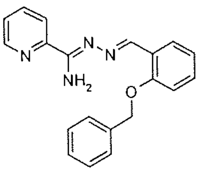	25-30
2PYbf	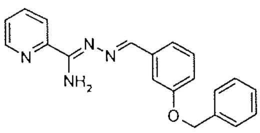	32-64
2PYbg	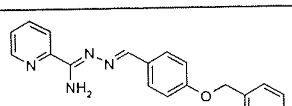	16-32
2PYbh	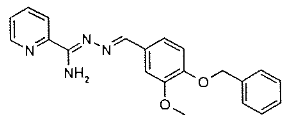	4-8
2PYbi	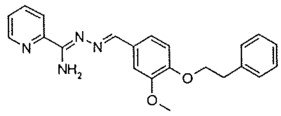	8-16
2PYbn	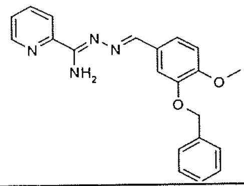	4-8
4PYbn	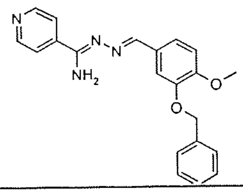	4-8
2PYbo	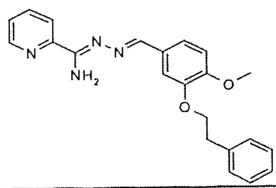	8-16
2PYbq	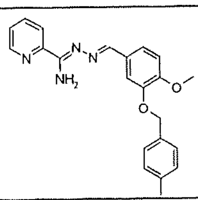	16-32
2PYbt	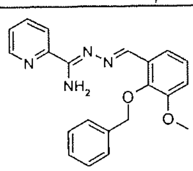	16-32

As previously mentioned, 2-methoxybenzylidene-pyridine-2-carboxamidrazone **2PYax**, was active in this study, with MIC 16-32$\mu g ml^{-1}$. Changing the methyl group to the 4-position in **2PYas**, retains the activity, however, placing the methyl group in the 3-position **2PYbd**, causes the compound to lose activity.

If we consider the 2-alkoxybenzylidene-pyridine-2-carboxamidrazones **2PYax-2PYbc**, one might predict that increasing the chain length of the alkoxy group would increase the activity of the compounds, due to the increased lipophilicity. This is not, however, the case. The 2-ethoxy **2PYay** and 2-propoxy **2PYaz** compounds are active in the same range as 2-methoxybenzylidene-pyridine-2-carboxamidrazone **2PYax**. Increasing the alkoxy carbon chain length still further to 2-butyloxy **2PYba**, 2-pentyloxy **2PYbb** or 2-hexyloxy **2PYbc**, results in a loss of antimycobacterial activity.

2-Benzyloxybenzylidene-pyridine-2-carboxamidrazone **2PYbe** was active (MIC 25-30μgml^{-1}) in the same range as 2-methoxybenzylidene-pyridine-2-carboxamidrazone **2PYax**. Changing the position of the benzyloxy group followed the same trend as changing the position of the methyl group: with the benzyloxy group in the 4-position **2PYbg** the compound retains activity, but by putting it in the 3-postion **2PYbf** activity is diminished (MIC 32-64μgml^{-1}).

Focusing on the di-substituted-benzylidene compounds; adding a 3-methoxy group to **2PYbe**, to give **2PYbt** resulted in activity in the same range as the original compound (MIC 16-32μgml^{-1}). Adding a 3-methoxy group to **2PYbg** to give **2PYbh**, however, improved the activity considerably, resulting in an MIC 4-8μgml^{-1}. 3-benxyloxy-4-methoxybenzylidene-pyridine-2-carboxamidrazone **2PYbn**, a structural isomer of **2PYbh**, was also active in the range 4-8μgml^{-1} [101].

Based on the observed activity of **2PYbh** and **2PYbn**, which were amongst the most active compounds found, a small selection of new aldehydes (**bi**-**bl** and **bp**-**br**) was prepared and reacted with the carboxamidrazones. These aldehydes were synthesised as it was of interest how elongating the molecules would affect their biological activity. **2PYbi** and **2PYbo** differ from **2PYbh** and **2PYbn** respectively, in that the benzyloxy group is exchanged for a phenethyloxy group. In both cases, the activity decreased twofold, to 8-16μgml^{-1}. Changing the phenethyloxy groups for phenpropyloxy groups, as in **2PYbj** and **2PYbp**, resulted in a loss of activity. The 3-methoxy-4-(4-methylbenzyloxy)benzylidene derivative **2PYbq** displayed an MIC of 16-32μgml^{-1}, far less active than the original compound **2PYbh** and the 3-methoxy-4-(4-t-butylbenzyloxy)benzylidene derivative **2PYbr** was completely inactive.

Contrary to Mamalo's observations, this group of compounds does not generally display the trend of pyridine-4- **4PY** compounds mirroring the activity of the pyridine-2- **2PY** compounds. It is of interest though, why, in the set of isomers, **2PYbh**, **2PYbn**, **4PYbh** and **4PYbn**, only **4PYbh** was inactive. All of the other three compounds were highly active, with MICs 4-8μgml^{-1} approaching that of isoniazid (MIC 1-2μgml^{-1}) against *M.fortuitum*. This difference in activity is discussed further in Section 6.3.

Table 5.6 *M.fortuitum*-active miscellaneous benzylideneheteroarylcarboxamidrazones

Code	Structure	MIC μgml^{-1}	Code	Structure	MIC μgml^{-1}
2PYdm	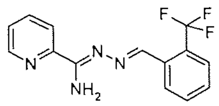	16-32	**2PYeh**	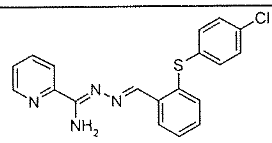	12.5-25
2PYdn	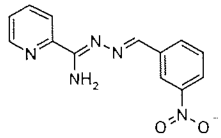	16-32	**4PYeh**	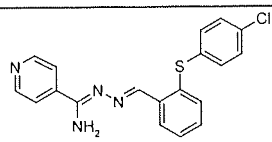	16-32
2PYed	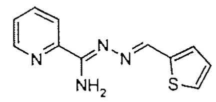	16-32	**QNds**	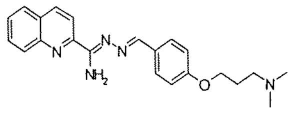	64-128

From Table 5.6, it can be seen that the pyridine-2- and pyridine-4- activities are mirrored in compounds **2PYeh** and **4PYeh**. Aldehyde **eh** was itself very mildly active against *M.fortuitum*, with an MIC greater than 128μgml^{-1}.

During this study, only one quinoline compound **QNds** was observed to have any activity, but it is rather weak at MIC 64-128 μgml^{-1}.

Substituents 2-trifluoromethylbenzylidene **dm**, 3-nitrobenzylidene **dn**, thiophenylidene **ed**, were all active at MIC 16-32μgml^{-1}, but only with pyridine-2-carboxamidrazone.

According to Mamalo *et al*, a nitro substituent should negate biological activity[93]. The compound which the Mamalo group tested in order to come up with this theory was 4-nitrobenzylidene-pyridine-2-carboxamidrazone **2PYdo**, which was also synthesised and tested in this study. Our results concurred that the 4-nitro compound was inactive, but the 3-nitro isomer **2PYdn** was active. This activity cannot be explained by general toxicity, as it was inactive against both the Gram-positive and Gram-negative bacteria tested in this study (Chapter 7, Table 7.1).

Table 5.7 *M.fortuitum*-active benzylidenepyridine-2-hydrazones

Code	Structure	MIC $\mu g ml^{-1}$
HDbz	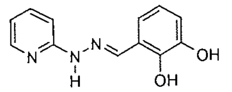	30-40
HDce	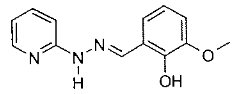	30-40
HDcf	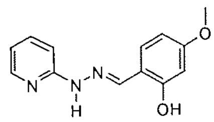	30-40
HDck	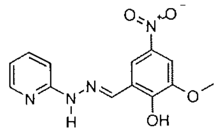	16-32

The antimycobacterial activities of the benzylidenepyridine-2-hydrazones in Table 5.7, is not really understood. The benzylidenepyridine-2-hydrazones were synthesised in order to investigate the effect of excising the CNH_2 group adjacent to the pyridine ring of the heteroarylcarboxamidrazones, which shortens the linker group between the benzylidene and heteroaryl moieties as shown in Figure 5.1. A very different molecular shape results and the deletion of the CNH_2 group is accompanied by placement of a hydrogen atom on the adjacent nitrogen atom: it was of interest how this would affect biological activity.

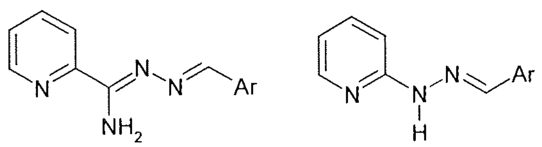

2PY-Ar **HD-Ar**

Figure 5.1 The 2-pyridylhydrazones **HD-Ar** differs from the pyridine-2-carboxamidrazones **2PY-Ar** as it lacks the CNH_2 group adjacent to the pyridine ring

Interestingly, when a benzylidene substituent which afforded activity for a pyridine-2-carboxamidrazone, was added to pyridine-2-hydrazone, no activity was observed. This shows that the amidrazone moiety is essential for the activity of the heteroarylcarboxamidrazones. Antimycobacterial activity was, however, observed for some pyridine-2-hydrazones, but only with compounds containing a 2-hydroxybenzylidene functionality. The most active compound **HDck**, also possesses a polar nitro group. This is contrary to the general trend of lipophillic molecules being useful as potential antimycobacterial agents. It is possible that all of these agents are just generally toxic; **HDcf**, for example, was also active against *E.faecium* and *S.aureus* (including an MRSA strain). Phenols are known as effective disinfectants[33]. It is quite possible that the compounds in Table 5.7 are purely protein denaturing agents, damaging bacterial membranes and thus possessing general antibacterial activity. The activity of these compounds clearly act via a different mechanism to that of the amidrazones, and since their activity appears to be non-specific, will not be discussed further.

5.3.2.1 *Substituting Pyridine-2-carboxamidrazone **2PY** With* 2-*Nitrobenzenecarboxamidrazone **$2NO_2BZ$***

For biological activity, it appeared that the pyridine-2- or pyridine-4- group was essential for activity. It was of interest to see if altering this group, to a non-nitrogen containing ring would negate activity. It was desirable to maintain an electron-withdrawing functionality at the 2- or 4- position, to ensure the least deviation from the original compounds. 2-Nitrobenzenecarboxamidrazone **$2NO_2BZ$** (see Figure 5.2) was synthesised and reacted with some of the aldehydes which had previously afforded activity to the pyridine-2-carboxamidrazones (**ae**, **af**, **bh**, **bn**, **dx**, **eh**).

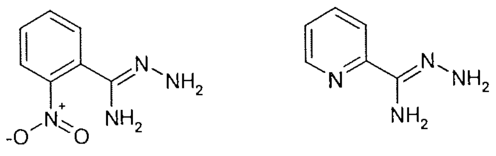

$2NO_2BZ$ **2PY**

Figure 5.2 Comparison of 2-nitrobenzenecarboxamidrazone **$2NO_2BZ$** and pyridine-2-carboxamidrazone **2PY**

None of the resulting compounds displayed any antimycobacterial against *M.fortuitum*, therefore, it can be concluded that the pyridine functionality is necessary for antimycobacterial activity.

5.3.2.2 *General Trends*

The amidrazone moiety is essential for the activity of these compounds. When a benzylidene-pyridine-2-carboxamidrazone is active, changing to the corresponding benzylidenepyridine-2-hydrazone negates activity completely. Also, when one of the aldehyde reactants was active itself, condensing it with benzylidenepyridine-2-carboxamidrazone improved the activity, whereas reacting it with pyridine-2-hydrazone resulted in a loss of activity. Although some activity was detected from the benzylidenepyridine-2-hydrazones, it was only with a set of 2-hydroxybenzylidenes, which did not display activity with carboxamidrazones anywhere else in this study. These 2-hydroxybenzylidene-pyridine-2-hydrazones cannot, therefore, be considered to act in the same way as the active benzylideneheteroarylcarboxamidrazones.

The benzylidenepyridine-2-carboxamidrazones proved to be the most active compounds in the study generally, with some of the equivalent benzylidenepyridine-4-carboxamidrazones also displaying similar activity. The benzylidenepyridine-3-carboxamidrazones tended to be either inactive, or considerably less active than the corresponding pyridine-2- and pyridine-4- compounds. The quinoline-2-compounds were inactive, as were the pyrazine-2- compounds, with the exception of **PZaf**.

When considering the benzylidene components of the active amidrazones, quite a range of substituents were found to afford antimycobacterial activity. It is again, important to note, that the antimycobacterial compounds found in this study were actually specific for mycobacteria. As the biological testing involved a whole cell system, it is not known how these compounds work inside the mycobacteria, what the molecular target is, or even if they all actually act in the same way. If the target is an enzyme, then the molecule has to reach that enzyme, by first penetrating the lipophillic cell wall. There may be a number of molecular properties which dictate whether or not the compound reaches the enzyme to provide antimycobacterial activity.

5.4 *M.FORTUITUM* AS A SCREENING MODEL FOR *M.TUBERCULOSIS*

In this study *M.fortuitum* has been used as a model for *M.tuberculosis*[108], the reasons for which are discussed in Section 5.1. This section evaluates this rapid screen model, by comparing the *M.fortuitum* results with those obtained for *M.tuberculosis* at the Tuberculosis Antimicrobial Acquisition and Coordinating Facility (TAACF). A set of 207 compounds was screened against both organisms. Figure 5.3 shows a scatter-graph which plots the activities of these compounds, on both organisms, against each other.

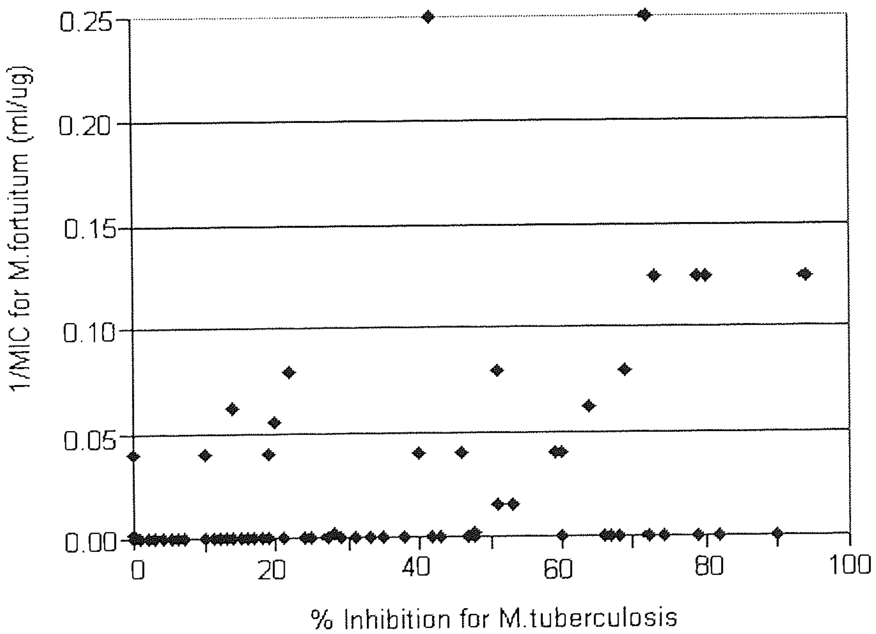

Figure 5.3 Scatter-plot of 1/MIC for M.fortuitum against % Inhibition of *M.tuberculosis*

Of the 207 compounds tested, 125 (60%) displayed zero activity against both organisms. It is also of note that the compound which displayed the greatest inhibition (94%) of *M.tuberculosis* **2PYaf** (see Figure 5.4), was also amongst the most active compounds against *M.fortuitum*, with an MIC of 8-16$\mu g ml^{-1}$ (1/MIC= 0.125$\mu g^{-1} ml$).

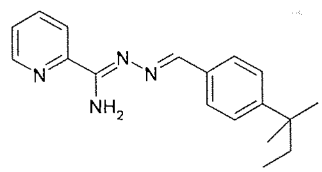

Figure 5.4 **2PYaf** was the most active compound found against *M.tuberculosis*

The *M.fortuitum* screen did not, however, predict activity for nine of the compounds which displayed an inhibition of 60% or greater, against *M.tuberculosis*. These are shown in Figure 5.5.

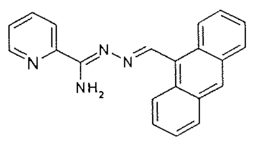

2PYam 90%Inh.

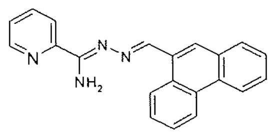

2PYan 82%Inh.

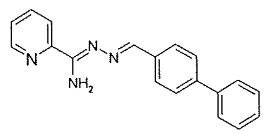

2PYag 66%Inh.

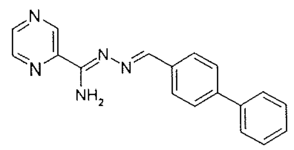

PZag 74%Inh.

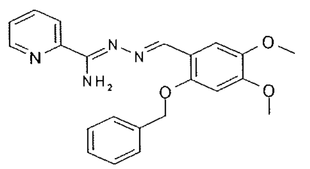

2PYbu 68%Inh.

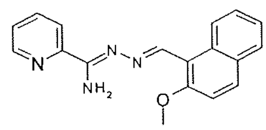

2PYdc 67%Inh.

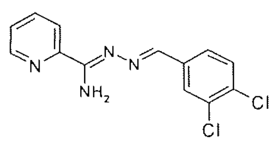

2PYdi 60%Inh.

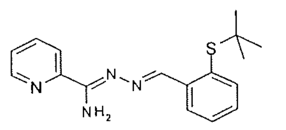

2PYef 72%Inh.

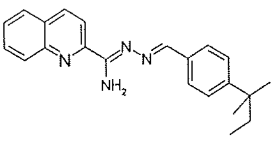

QNaf 79%Inh.

Figure 5.5 The nine antitubercular compounds which were not predicted by the *M.fortuitum* screen and their % inhibitions against *M.tuberculosis* at a concentration of 6.25μgml^{-1}.

It is unfortunate that these compounds were not predicted by this *M.fortuitum* screen, as false negatives found at this stage would not be tested further and so the activity is completely missed. False positives, however, would be easier to cope with, as the compounds will be tested again, and the inactivity noted further down the line.

Of the compounds in Figure 5.5, however, **2PYam** and **2PYan** would be highly toxic, due to their anthracene moieties. From toxicology studies by Coleman *et al*[109], it has been shown that **2PYef** is about four times more toxic than isoniazid, as is **PZag**. If **PZag** is highly toxic, then this is almost certainly due to the biphenyl group, so **2PYag** would also be very toxic. All of these five compounds would therefore, be unacceptable as potential antitubercular drugs due to excessive toxicity.

5.4.1 Using The *M.fortuitum* Screen To Reduce The Data Set For TB Screening

If there was a perfect, direct correlation between the activities of compounds against *M.fortuitum* and *M.tuberculosis*, then a straight line plot would be expected. The scatter-plot in Figure 5.3 does not form a straight line. This is not really surprising, however, since the two organisms are different. Nevertheless, the data can still be used to give an indication of where antitubercular activity may be found. For example, if only the compounds with an MIC of 16μgml^{-1} (1/MIC=0.0625μg^{-1}ml) or less are considered (see Figure 5.6), the data set is substantially reduced. The remaining eleven compounds would then be tested against *M.tuberculosis*. Of these eleven compounds, all showed some activity against *M.tuberculosis*, seven of which displayed activity of 60% inhibition or more.

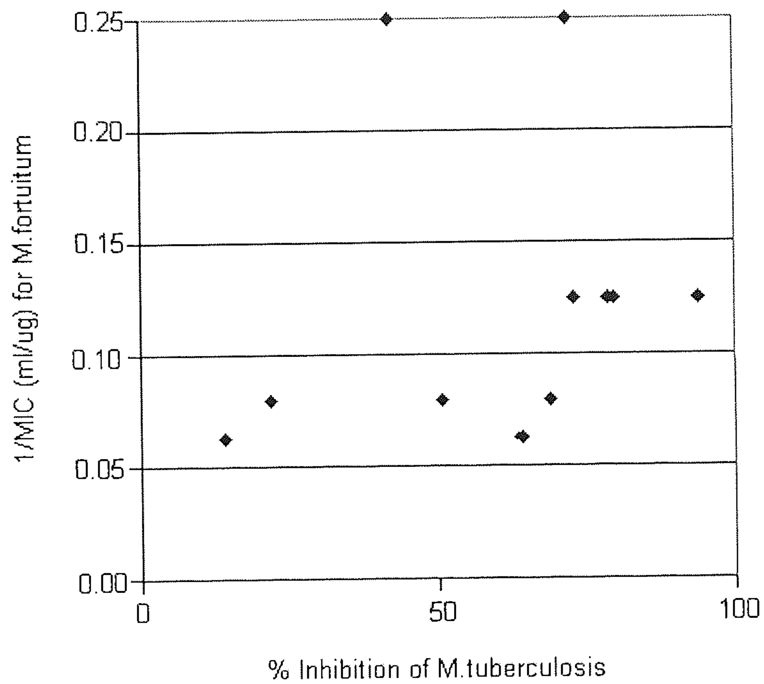

Figure 5.6 The scatter-plot data points where *M.fortuitum* activity is 16μgml^{-1} (1/MIC=0.0625μg^{-1}ml) or less

5.4.2 Evaluation of The *M.fortuitum* Screen

It is of course, difficult to compare the two sets of mycobacterial results directly, since their activity is measured in different ways, i.e. an MIC measurement for *M.fortuitum* and a percentage inhibition for *M.tuberculosis*. In order to compare an MIC value with the inhibition results for tuberculosis **2PYbn** was tested for its MIC against *M.tuberculosis* strain H37v, which is the same strain as used for inhibition testing at TAACF[109]. The results of the MIC and inhibition testing for **2PYbn** against *M.tuberculosis* and the MIC versus *M.fortuitum*, are shown in Table 5.8.

Table 5.8 Comparison of *M.fortuitum* MIC, with *M.tuberculosis* MIC and %Inhibition results for **2PYbn**

Code	Structure	*M.fortuitum* MIC (μgml^{-1})	*M.tuberculosis* MIC (μgml^{-1})	*M.tuberculosis* % Inhibition
2PYbn	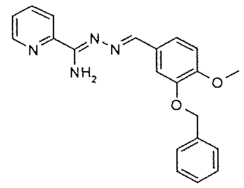	4-8	8-16	72

It can be seen that the *M.fortuitum* screen predicted this compounds activity against *M.tuberculosis* very well, with **2PYbn** showing similar activity between the two organisms. An MIC of 8-16μgml^{-1} against *M.tuberculosis* equates to a percentage inhibition of around 72%, at a concentration of 6.25μgml^{-1}, which although reasonable, is not high enough to be considered worthy of further investigation by the TAACF.

5.4.3 Conclusion

Although the *M.fortuitum* screen may have its limitations, it could be used as a valuable preliminary screen, rapidly helping to identify the compounds which are worth submitting for the more hazardous and time consuming antitubercular screen. It is a simple, inexpensive screen, which is particularly useful to help whittle down large numbers of compounds, which would otherwise require screening against *M.tuberculosis* itself. It is likely that if a compound is active against *M.fortuitum* at a concentration of 16μgml^{-1} or less, then it will also display at least some antitubercular activity.

The TAACF only consider compounds with an inhibitory activity of 90% or more, at a concentration of 6.25μgml^{-1}, worthy of further investigation into their potential as antitubercular drugs. Of the 207 compounds tested in this study, only two, **2PYaf** and **2PYam**, were worthy of further investigation. Unfortunately, **2PYam**, due to its anthracene moiety, is highly toxic. Therefore, the only potential antitubercular drug of the set is **2PYaf**, and the activity of this compound *was predicted* by the preliminary *M.fortuitum* screen.

CHAPTER 6
MOLECULAR MODELLING

A large, chemically diverse library of structurally similar compounds has been synthesised, and biological data against *M.fortuitum* (for all 495 compounds), and *M.tuberculosis* (for 207 compounds), was obtained. It was desirable therefore, to attempt to use these data sets in order to investigate the physical properties of these molecules which correlated with activity. It would then be possible to identify compounds from a virtual library (existing only in a computer database) that would be likely to possess antimycobacterial activity. In this way, the number of compounds required to be synthesised in the laboratory, and therefore, time and costs, could be reduced greatly.

Before any modelling of the benzylideneheteroarylcarboxamidrazones could begin, it was important to be familiar with the structure of these compounds. This is discussed below.

6.1 BENZYLIDENEHETEROARYLCARBOXAMIDRAZONE STRUCTURE

The structure of the benzylideneheteroarylcarboxamidrazone products allows either the *E*- or *Z*-configuration about the carbon-nitrogen imine bond. In all the proton NMR spectra studied for these compounds, only one isomer was detected. On the basis of steric considerations, it would be reasonable to assume that the reaction may favour the *E*- configuration. Single crystal x-ray analysis was performed on N^1-[4-(1,1-dimethylpropyl)benzylidene]-pyridine-2-carboxamidrazone **2PYaf**[111,112] and indeed, the expected *E*- configuration was observed. Other crystal structures have since been determined with various heteroaryl groups and benzylidene functionalities: **PZak**, **PZal**, **QNbx**[111], **2PYae**, **4PYae**, **2PYbh**, **4PYbh**[113], **3PYae** and **2PYdn**[114], all of which share the expected *E*- configuration.

X-ray crystal analysis of the benzylidenepyridine-2-carboxamidrazones has shown that intramolecular hydrogen bonding can occur between the pendant amine hydrogen atoms and the pyridine N1 amidrazone atoms. This intramolecular bonding, together with the conjugation of the structure through the amidrazone functionality, results in an almost planar molecule[111,112]. This is shown for N^1-[4-(1,1-dimethylpropyl)benzylidene]-pyridine-2-carboxamidrazone **2PYaf** in Figure 6.1. The x-ray analysis of this compound also showed that partial intermolecular hydrogen bonds between neighbouring molecules are important in the packing of the crystal structure.

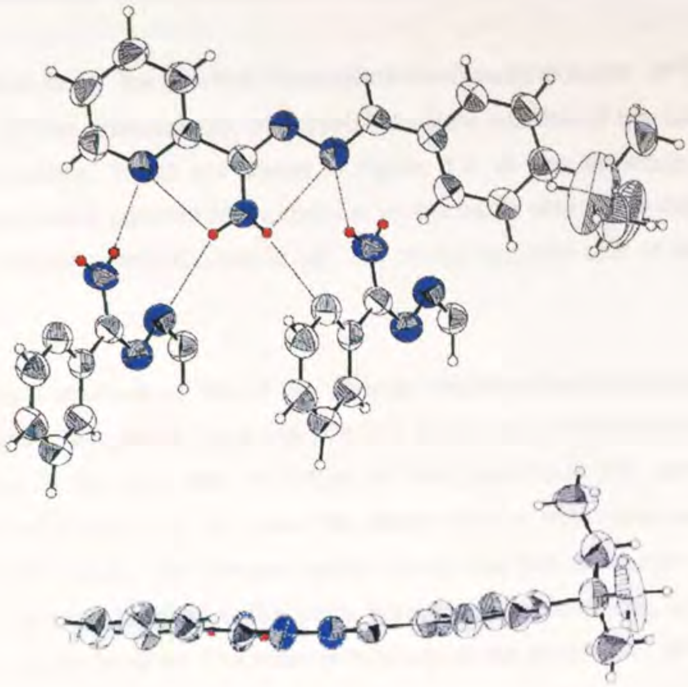

Figure 6.1 X-ray crystal structure of **2PYaf**. Nitrogen atoms are shown in blue and selected hydrogen atoms in red. The elliptical size of the atom indicates the confidence of the atom position such that a small size relates to a high level of confidence. The *t*-pentyl atoms are shown as large, as this group appears to have freedom of movement within the crystal. Top: Shows the intramolecular hydrogen bonding already explained, and partial intermolecular hydrogen bonds from neighbouring molecules. Bottom: A side profile of the crystal structure shows that the molecule is nearly planar.

The importance of the intramolecular hydrogen bonding in the crystalline structure of benzylidene-pyridine-2-carboxamidrazones is interesting, but does this play an important roll *in vivo*? For some of the compounds tested, the pyridine-4-carboxamidrazone derivatives were equi-active with the pyridine-2-carboxamidrazones. Due to the position of the nitrogen atom in the pyridine-4-compounds, it is intuitively impossible for these atoms to form intramolecular hydrogen bonds with the amine hydrogen atoms. In these cases therefore, where both pyridine-2- and pyridine-4-compounds share antimycobacterial activity, the ability to hold a coplanar conformation is clearly not biologically important.

6.1.1 The Conformations Of A Pyridine-3-carboxamidrazone Crystal Structure

Only one crystal structure of the pyridine-3-benzylidenecarboxamidrazone **3PY** series has been determined to date; **3PYae**. Interestingly, this crystal structure consists of two sets of molecules in two different conformations. These are shown in Figure 6.2. In one molecule, the heteroaryl-N atom is 'down' relative to the pendent NH_2 group i.e. on the same side of the molecule as the NH_2 group. In the other, the heteroaryl-N atom is 'up', i.e. on the opposite side of the structure as the pendent NH_2 group.

This is the only crystal structure of the all the various heteroarylbenzylidenecarboxamidrazones which have been determined, where there are different molecular conformations within the crystal. This is probably due to the fact that molecules of the pyrazine-2- **PZ,** quinoline-2- **QN** and pyridine-2- **2PY** series (Figure 6.1), all have the ability to form intramolecular hydrogen bonds between the hydrogen atoms of the pendent amine group and the heteroaryl N atom. Thus, the conformation with hydrogen bonding is the more favourable conformation, over the alternative conformation where it is impossible. The heteroaryl group of the pyridine-4- **4PY** compounds, can only have one conformation due to the symmetry of the heteroaryl group.

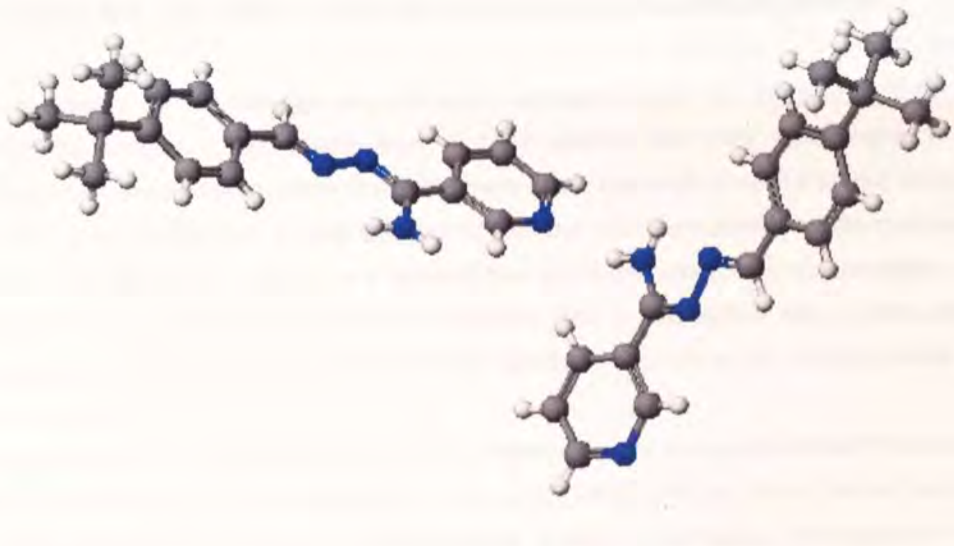

Figure 6.2 The **3PYae** crystal consists two sets of molecules with two different conformations. The spatial arrangement of the two different molecules shown is the same as within the crystal structure. Left: The heteroaryl-N atom is 'down', i.e. on the same side of the structure as the pendent NH_2 group. Right: The heteroaryl-N atom is 'up', i.e. on the opposite side of the structure as the pendent NH_2 group

When the two conformers are viewed from the side, as in Figure 6.3, it can be seen that the heteroaryl-N 'down' position is the most planar. This is also the conformer which results from the energy-minimisation calculations (Section6.2). This 'down' conformation is, therefore, the one used for the molecular property calculations to follow.

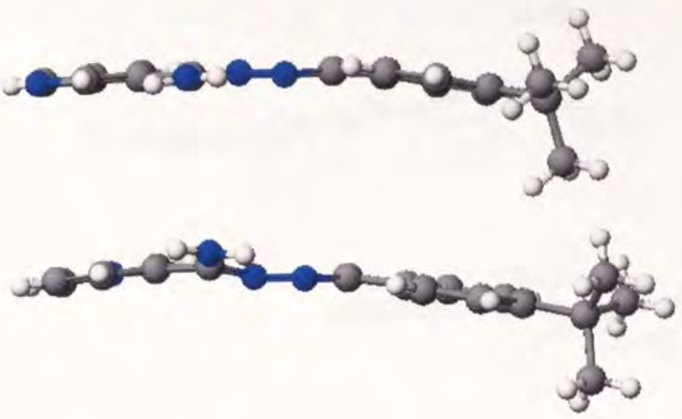

Figure 6.3 The two conformers of the crystal structure **3PYae**. Top: The 'down' structure is fairly planar. Bottom: The 'up' structure is much more bent.

6.2 MODELING THE BENZYLIDENEHETEROARYLCARBOXAMIDRAZONES

It was necessary to standardise the chemical structures prior to subjecting them to any computational analysis. It was known from ^{1}H NMR spectra and x-ray crystallography that the molecules adopt the *E*-conformation about the imine bond, but what about the spatial arrangement of the rest of the molecule? It was decided to use the minimum-energy conformations of the molecules as a standard. Whilst it was realised that the minimum-energy conformation may not necessarily be the conformation that the molecules hold in the active site, it does provide a starting point from which the molecules can be compared to each other, on an equal basis.

Over three hundred *N*^{1}-benzylideneheteroarylcarboxamidrazone energy-minimised structures were obtained; optimised first using molecular mechanics (MM2, CAChe WorkSystem Version 3.2, Oxford Molecular Ltd.), followed by semi-empirical quantum mechanical optimisation, using the AM1 basis set in MOPAC[113] using the program CAChe. This resulted in many unrealistic conformations for the pyridine-3- and pyridine-4- series, where the molecules were very 'kinked'. Figure 6.4 shows the results of the MOPAC minimisation for the *N*^{1}-[4-(1,1-dimethylpropyl)benzylidene]-pyridinecarboxamidrazone series, **2PYaf**, **3PYaf**, **4PYaf**.

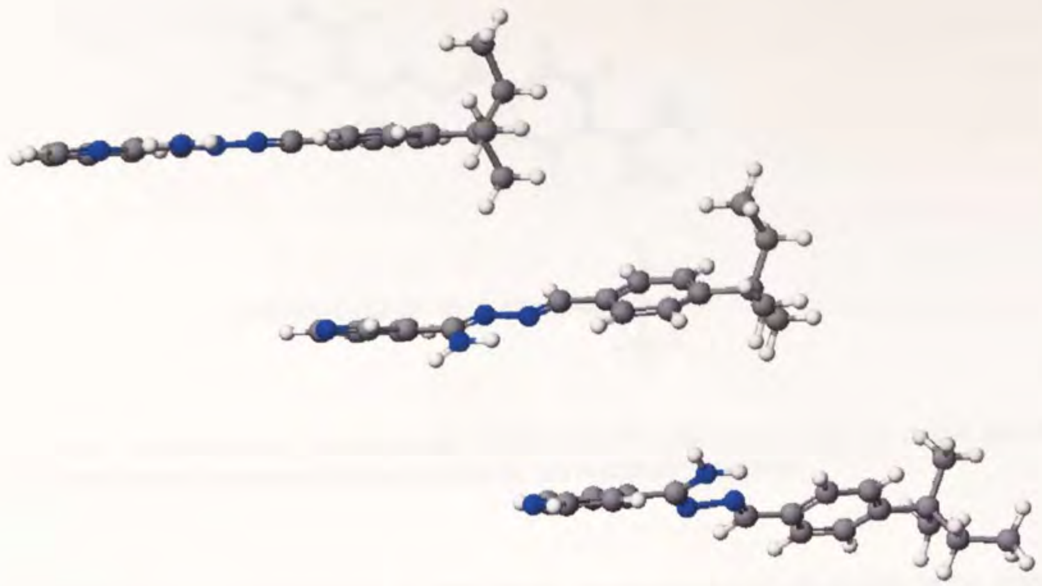

Figure 6.4 MOPAC (AM1) energy-minimised structures, viewed such that the plane of the pyridine ring is perpendicular to the page. Top: **2PYaf**, Almost planar which is agreeable with the crystal structure. Middle: **3PYaf** is kinked. Bottom **4PYaf** is kinked.

Due to these kinked conformations, it was found necessary to optimise these structures further using the PC GAMESS program, utilising *ab initio*, quantum mechanical molecular orbital calculations in the 3-21G basis[114]. An even more thorough optimisation was available, using the same program, but implementing the 6-31G basis set. The 3-21G calculation took 1-4 days to complete, depending on the complexity of the molecule. The 6-31G calculations generally took twice as long as the 3-21G calculations. When the two optimised structures are compared, however, they are practically identical, as Figure 6.5 shows. Since the two protocols produced very similar results, and the 3-21G optimisation took far less time, this was chosen as the energy-minimisation step for all the compounds.

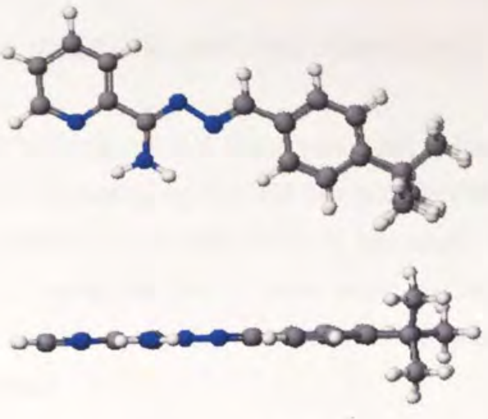

Figure 6.5 Superimposing the outcomes of both the PC GAMESS 3-21G and 6-31G for **2PYae**, shows that the two energy-minimised structures are practically identical.

The GAMESS 3-21G calculations all resulted in energy-minimised structures which were very similar in conformation to that held in the crystal structure of the compounds. Figure 6.4 compares the MOPAC and GAMESS 3-21G minimised molecules with the crystal structure of **3PYae**.

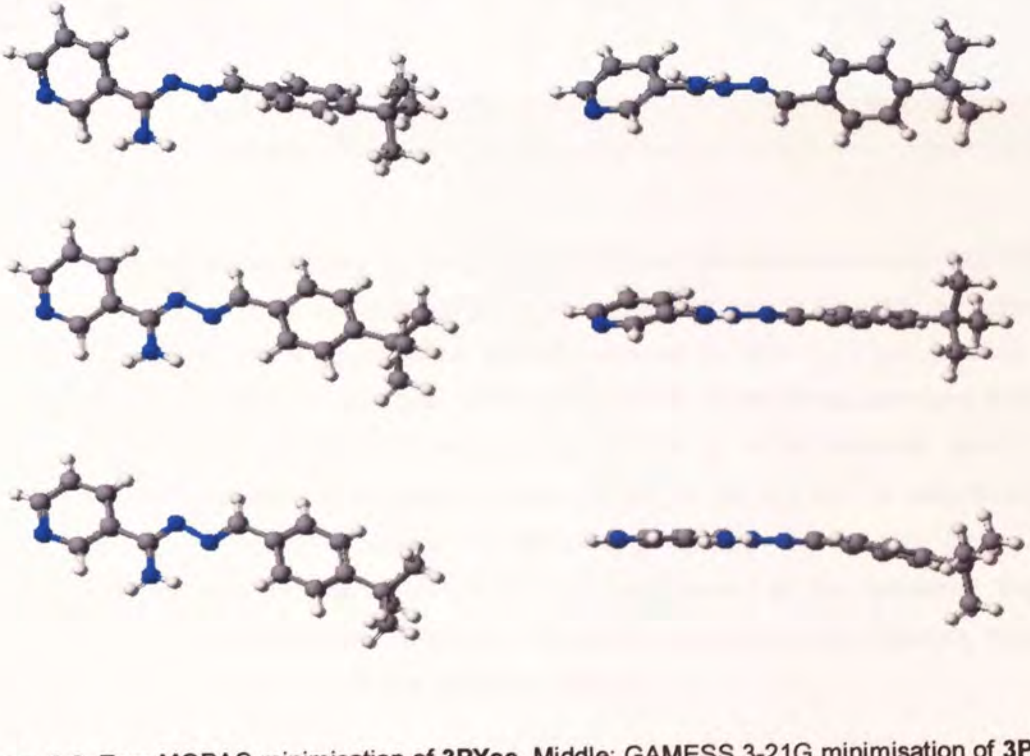

Figure 6.6 Top: MOPAC minimisation of **3PYae**. Middle: GAMESS 3-21G minimisation of **3PYae**. Bottom: Crystal structure of **3PYae**. All three molecules down the left hand side are orientated the same way, by superposition of atoms 1-3 (see Figure 6.7). The side profile views of the molecules down the right hand side are orientated such that the view is approximately down the C-NH_2 bond

6.3 FOUR ISOMERS, ONLY ONE INACTIVE COMPOUND

As previously mentioned in Section 5.3.2, there was a set of four isomers; **2PYbh**, **4PYbh**, **2PYbn** and **4PYbn**, which gave interesting results. Of this set, **2PYbh**, **2PYbn** and **4PYbn** represented three of the four most active compounds found in this study. **4PYbh**, however, was completely inactive (See Table 6.1). Being isomers of each other, all four compounds obviously share the same molecular weight and log P, so why is it that three of these compounds are highly active (4-8μgml^{-1}) and one is inactive?

Table 6.1 Four isomeric structures and their activity.

Code	Structure	MIC (μgml^{-1})	Code	Structure	MIC (μgml^{-1})
2PYbh	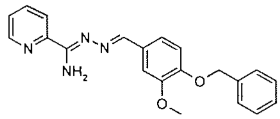	4-8	**4PYbh**	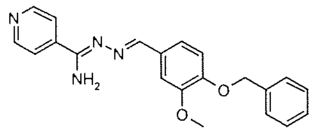	Inactive
2PYbn	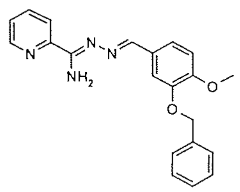	4-8	**4PYbn**	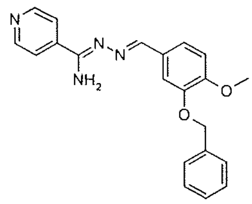	4-8

In order to investigate this conundrum, the lengths and widths of the molecules were measured, on the basis that size constraints may be important if the molecules are to fit within an active site. Based on the assumption that it would be the nitrogen atom of the heteroaryl group which would bind to the active site, perhaps by hydrogen bonding, the length of the molecules were measured from the nitrogen atom of the heteroaryl group, to the furthest tip of the molecule (as shown in Figure 6.7). This is a reasonable assumption to make, based on the fact that no quinoline-2- **QN**, compounds were active (the extra bulk of the quinoline group over the pyridine groups could prevent binding, thus explaining the inactivity) and that replacement of the heteroaryl ring by a nitrobenzene group also resulted in loss of activity. The length and width measurements, along with the biological activity of the compounds are shown in Table 6.2.

Table 6.2 The length and widths and associated activity of the **bh** and **bn** derivatives and closely related compounds. An inactive compound is denoted by (-). Het= Heteroaryl ring

Aldehyde Code	Structure	2PY			4PY		
		N-length (Å)	Aryl-width (Å)	1/MIC ($\mu g^{-1}ml$)	N-length (Å)	Aryl-width (Å)	1/MIC ($\mu g^{-1}ml$)
bn	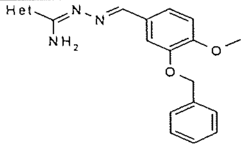	12.62	11.21	0.25	14.64	9.41	0.25
bo	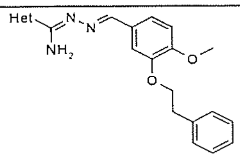	12.67	11.79	0.125	14.49	11.81	-
bp	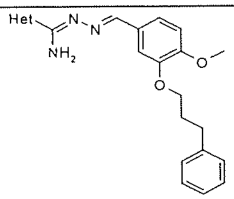	12.92	13.73	-	14.63	13.74	-
bq	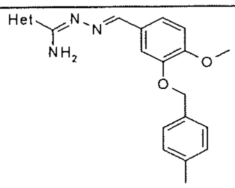	12.92	12.26	0.0625	14.64	12.25	-
bh	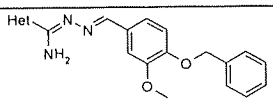	15.59	7.02	0.25	18.43	7.03	-
bi	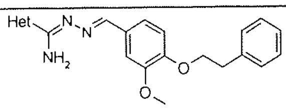	17.02	7.04	0.0625	17.86	7.01	-
bk	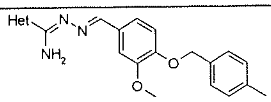	17.78	7.09	-	19.61	7.09	-
bj	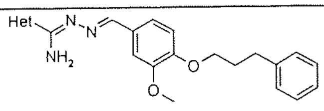	19.06	7.05	-	20.96	7.05	-

No activity was observed for pyridine-2- **2PY** compounds of length >17.02Å, or width >12.26Å. For the pyridine-4- **4PY** series, no activity was observed for compounds of length >14.64Å or width >9.41Å.

6.4 QUANTITATIVE STRUCTURE-ACTIVITY RELATIONSHIP (QSAR) ANALYSIS

The GAMESS 3-21G energy-minimised structures described in Section 6.2, were to be subjected to quantitative structure-activity relationship (QSAR) analysis. This was to be carried out using TSAR (Oxford Molecular Ltd.) which calculates the physical properties of the molecules, some of which, such as lipole and dipole moments, are vectorised. In order for these vectorised properties to be comparable with one another, all the molecules must all be aligned in the same way. This was done by common superposition of atoms 1-3, and the total set was orientated in the x,y,z frame, as shown for the pyridine-2- example in Figure 6.7[117] (The .mol file for the molecule upon which all molecules were superimposed is given in the appendix).

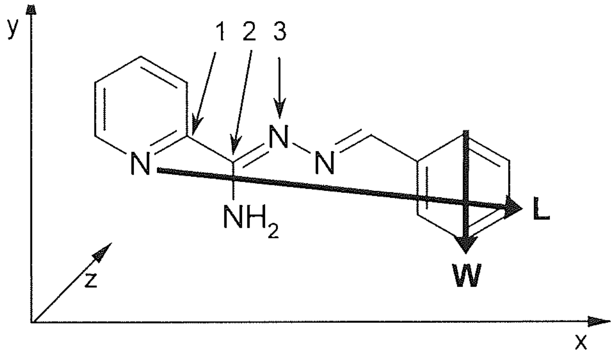

Figure 6.7 Orientation of the benzylideneheteroarylcarboxamidrazones in the x,y,z frame. All molecules were aligned by superposition of atoms 1,2 and 3.

In addition to the molecular properties to be calculated by TSAR, the distances were measured from the heteroaryl nitrogen atom to the furthest tip of the molecule (L), and the width of the arylidene substituents (W) were measured in CAChe(Oxford Molecular Ltd.) as indicated by the heavy arrows in Figure 6.7[117].

In total, sixteen parameters and the associated biological data were subjected to multiple regression analysis in TSAR. This was carried out with the available data for both *M.fortuitum* and *M. tuberculosis* separately. The calculations were set up such that the TSAR program self-predicted all rows within the project, using a 'leave one out' approach, thus validating itself. Tables of the TSAR results data can be found in the appendix.

Due to the vectorised nature of various molecular properties, some negative numbers were produced during the property calculations. During some of the initial studies, TSAR produced equations with terms such as natural logarithms and square roots of data; functions which cannot be carried out on negative numbers. Therefore, the TSAR calculations were repeated, but with the elimination of these transformations.

6.4.1 Some Basic Structure-Activity Relationships (SAR)

6.4.1.1 Correlation of Activities Against M.fortuitum With Some Key Molecular Properties

It was hypothesised in Section 6.3, that the size of the molecules, in particular, the lengths of the molecules from the heteroaryl N-atom and the width of the aryl groups, were an important factor in dictating biological activity against *M.fortuitum*. Figure 6.8 shows a plot of 1/MIC against N-length for this organism, and there is no direct correlation. Figure 6.9 shows the plot of 1/MIC against aryl width and there appears to be no correlation whatsoever here, either.

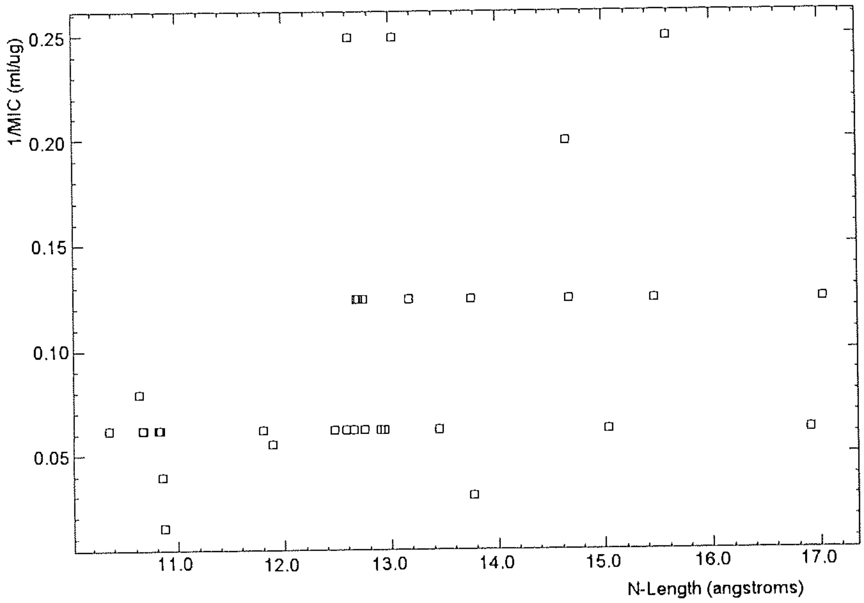

Figure 6.8 Graph to show 1/MIC against N-length for *M.fortuitum*

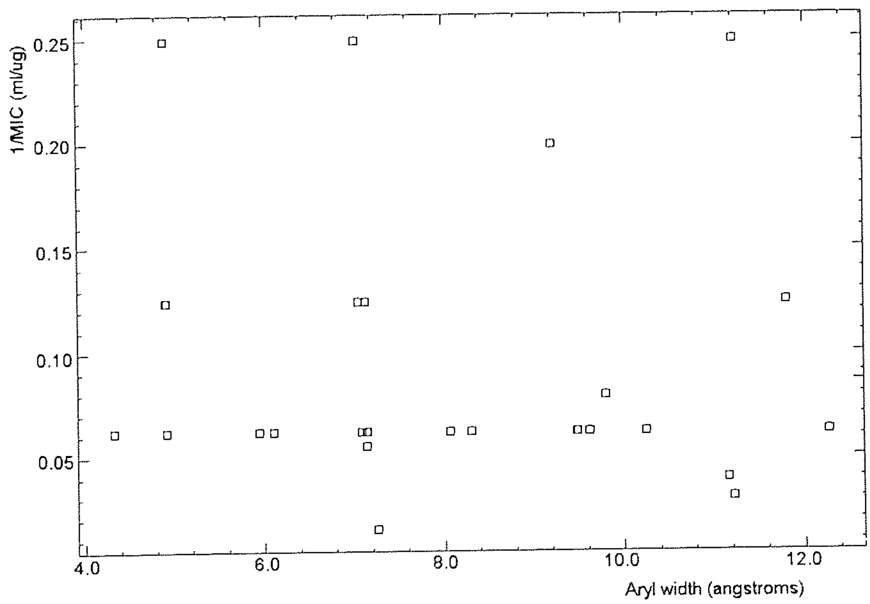

Figure 6.9 Graph to show 1/MIC against aryl width for *M.fortuitum*

It has already been mentioned that log P is known as an important factor in antimycobacterial compounds and that increasing the log P usually boosts the activity. Figure 6.10 shows a plot of 1/MIC against log P for *M.fortuitum*, and there may be a slight parabolic relationship between the two properties, but the correlation is not strong.

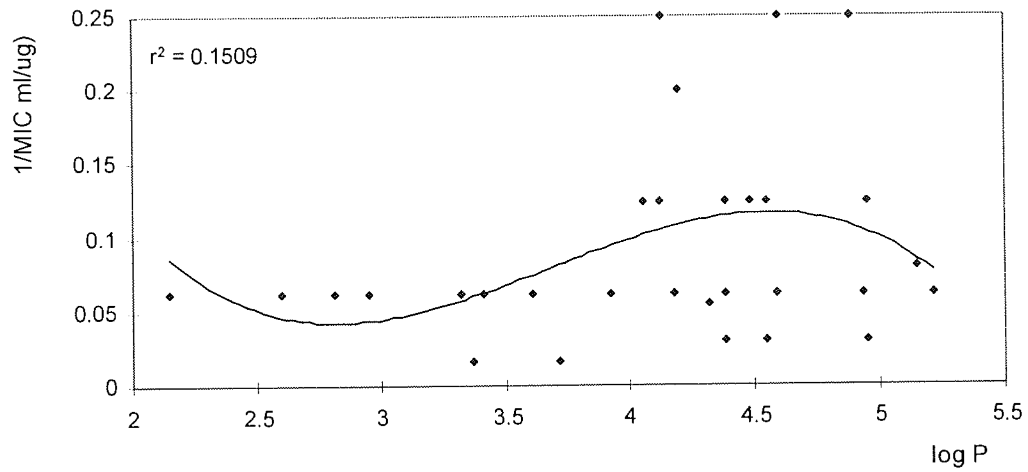

Figure 6.10 Graph to show 1/MIC against log P for *M.fortuitum*

Having briefly looked separately at the three molecular properties which were thought to contribute most to the activity of the heteroarylbenzylidenecarboxamidrazones against *M.fortuitum*, it is clear that no one property fully dominates and explains the variation in activities by themselves. It was necessary, therefore, to carry out multiple regression analysis to try and explain the activities.

6.4.1.2 Correlation of Log P Against M.tuberculosis

Figure 6.11 shows a plot of % inhibition of *M.tuberculosis* against log P for the benzylidene-heteroarylcarboxamidrazones. This data set seems to demonstrate a better correlation than in Figure 6.10, where a similar data was plotted for *M.fortuitum*. It is well documented that log P is an important factor in determining the extent of activity of antimycobacterial compounds. Increasing the log P tends to increase the activity, due to the compounds improved ability to penetrate the particularly lipophillic mycobacterial cell wall. Both organisms are mycobacteria. The *M.tuberculosis* results probably give an improved graphical correlation, as the data set is much better; being a continuous data set for activity as opposed to the discrete data obtained for *M.fortuitum*. The parabolic relationship between log P and % inhibition suggests that there is an optimum log P value, in the region of 5-5.5.

Once more, however, the spread of data in Figure 6.11 indicates that there must be other properties also involved in determining the activities of these compounds and multiple regression analysis was to be used to try and identify these.

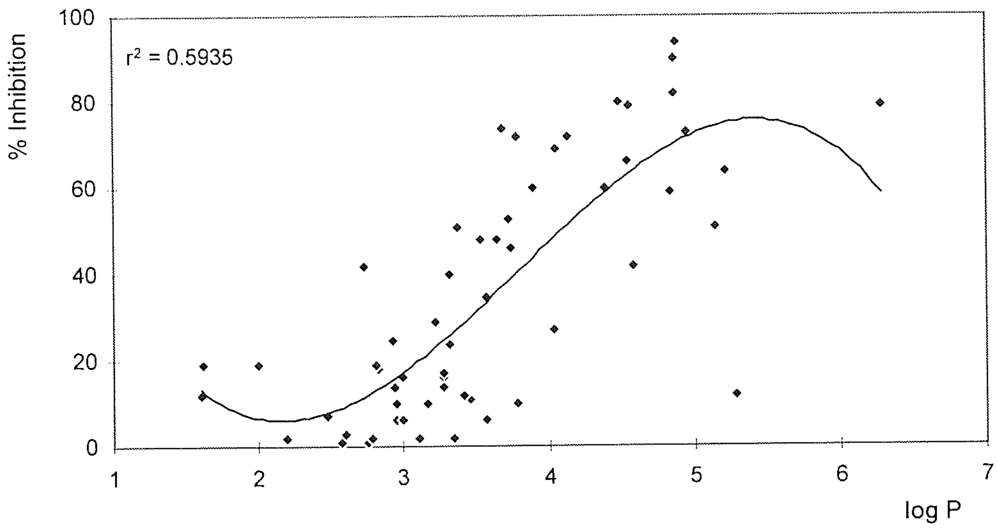

Figure 6.11 Graph to show % Inhibition against log P for *M.tuberculosis*

6.4.1 Multiple Regression Analysis

In multiple regression analysis, a number of input x variables (in this case molecular properties) are used in an equation to predict y (activity). When a model equation is reached, various test results are provided with which the validity and accuracy of the model equation can be probed.

The multiple regression coefficient, squared (r^2), indicates how well the regression equation explains the y variable: the closer the value is to 1.0, the better the equation is. An s value is also given, which is the standard error of the regression model. For a model with good predictive power, this is an estimate of how accurately the model will predict unknown y values. The F value is measure of variance and is derived from the sum of squares values and degrees of freedom[117].

As mentioned previously, the program uses cross validation as a rigorous internal check on the models derived using this regression technique. In turn, each row of data is deleted, and its y value predicted using the rest of the data. This is used to give an estimate of the true predictive power of the model, i.e., how reliable predicted values for untested compounds are likely to be. A coefficient is derived from this cross validation; it is the cross validated equivalent of r^2 and is denoted as r^2(CV).This is a measure of the predictive power of the model, the closer the value is to 1.0, the better the predictive power. It is usually a smaller value than r^2 itself, but if r^2(CV) is a much smaller value than r^2, it is likely that the regression has probably overfitted the data, and the equation would be unreliable for the prediction of untested data.

The major drawback of regression analysis is the danger of overfitting the data. This is the risk that an apparently good regression equation will be found which is based on a chance numerical relationship between the y variable and one or more of the x variables, rather than a genuine predictive relationship. When an overfitted model is used predictively, the predicted values for untested data will turn out to be very different from the true values (when these are eventually determined), even though the predicted values for the original, tested compounds used to derive the regression equation were close to the true values. The resulting regression equation, therefore, has no predictive power. The technique of cross validation reduces the risk of these chance correlations going undetected[118].

6.4.2 Using Multiple Regression Analysis To Study The *M.fortuitum* Results

6.4.2.1 All Types of Heteroarylbenzylidenecarboxamidrazones

The full set of heteroarylbenzylidenecarboxamidrazones was to be subjected to multiple regression analysis. As Figure 6.12 shows, the whole set of 240 compounds, gave very poor results. A valid regression equation could not be obtained for the entire data set. It was hypothesised that this was mainly due to the very large numbers of inactive compounds biasing the data set.

Predicted 1/MIC= 0.0040/A +0.0238/B -0.0009

n=240 s value=0.036 F value=33.113 r^2=0.224 r^2 (CV)=-0.031

A= Lipole y B= Total dipole

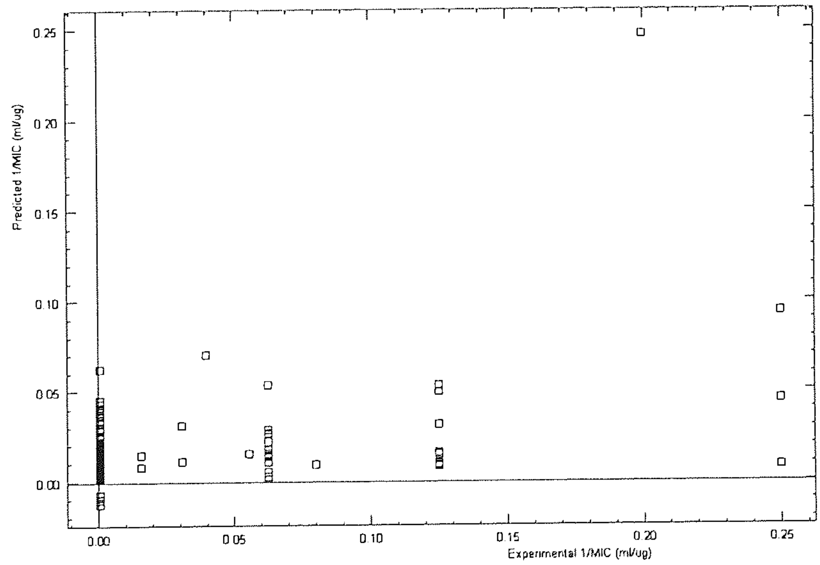

Figure 6.12 Graph of the entire set of heteroarylbenzylidenecarboxamidrazone data against *M.fortuitum*

For the above reason, the significant outliers at the low activity end of the data set were removed from the project These included the quinoline-2- **QN** compounds, and the molecules where the length and/or width were greater than it was hypothesised would fit in the active site (see Section 6.3), i.e. length >17.02Å, or width >12.26Å in the pyridine-2- **2PY** series, or length >14.64Å or width >9.41Å in the pyridine-4- **4PY** series.

Some compounds were also removed if they had little structural similarity with the active compounds, these included derivatives of the carbonyl containing aldehydes, **cx**, **cy**, **cz**, **dr**, the pyridyl aldehydes **dv**, **dw**, the indolyl aldehydes **dy**, **dz**, and aldehydes **eb**, **ec**.

For this data set it was also found necessary to remove some of the compounds which were found to be active. Although this is far from ideal, it can be understood, when it is realised that it was the 3-nitrobenzylidene-pyridine-2-carboxamidrazone **2PYdn** and the 2-trifluoromethylbenzylidene-pyridine-2-carboxamidrazone **2PYdm**, which needed to be removed; the only compounds with electron-withdrawing substituents to possess any biological activity. The 4-alkylbenzylidene-pyrazinylcarboxamidrazones **PZae** and **PZaf** also had to be removed in order to obtain the following equation:

Predicted 1/MIC= $1.839\times10^{-5}A^3 - 1.436\times10^{-5}B^3 + 5.683\times10^{-4}C^3 + 0.1934/D + 2.957\times10^{-3}E + 3.433\times10^{-3}/E + 0.0572/F + 7.979G - 0.1228$

n=115	s value=0.027	F value=34.419	r^2=0.722	r^2 (CV)=0.398

A= N-length	C= Log P	E= Lipole y	G= Dipole x
B= Aryl width	D= Total lipole	F= Total dipole	

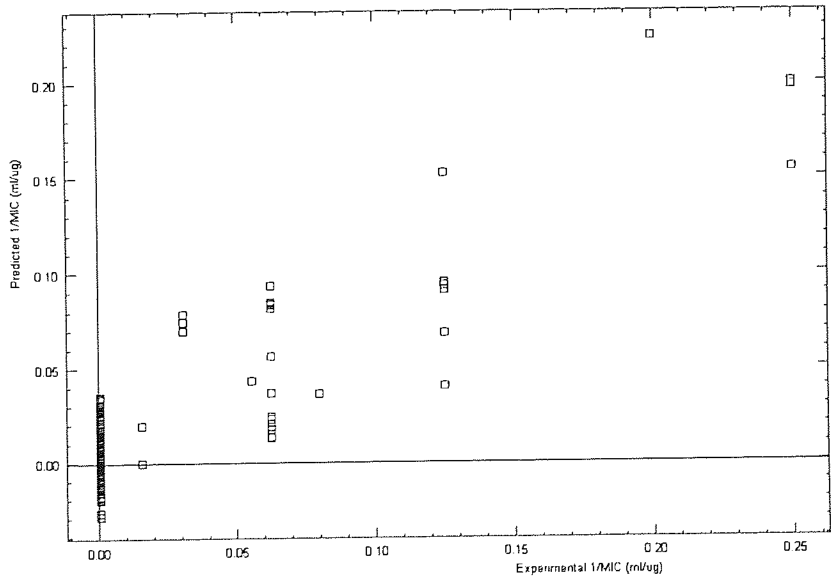

Figure 6.13 Graph of the reduced set of all types of heteroarylbenzylidenecarboxamidrazones against *M.fortuitum*

6.4.2.2 The Pyridine-2-benzylidenecarboxamidrazone Set

In light of the preceding equations, it was thought that a better equation might be obtained if the compounds were subdivided according to the heteroaryl group. Since the most data was available for the pyridine-2-benzylidenecarboxamidrazones **2PY** compounds, these were subjected to multiple regression analysis. Again, the significant outliers with length >17.02Å, or width >12.26Å were removed from the calculation, as were compounds with little structural similarity with the active compounds, as mentioned in the last section. **2PYdm**, **2PYdn** had to be removed as in Section 6.4.2.1, and so did the sulfur containing compound 2-(4-chlorothiophenyl)-benzylidene-pyridine-2-carboxamidrazone **2PYeh**, in order to obtain the following equation:

Predicted 1/MIC= $8.885 \times 10^{-5} A^3 - 5.560 \times 10^{-4} B^2 + 0.01143/C + 0.04798/D - 0.1220$

n=55 s value=0.0300 F value=48.605 r^2=0.795 r^2 (CV)=0.671

A= N-length B= Aryl width C= Lipole y D= Total dipole

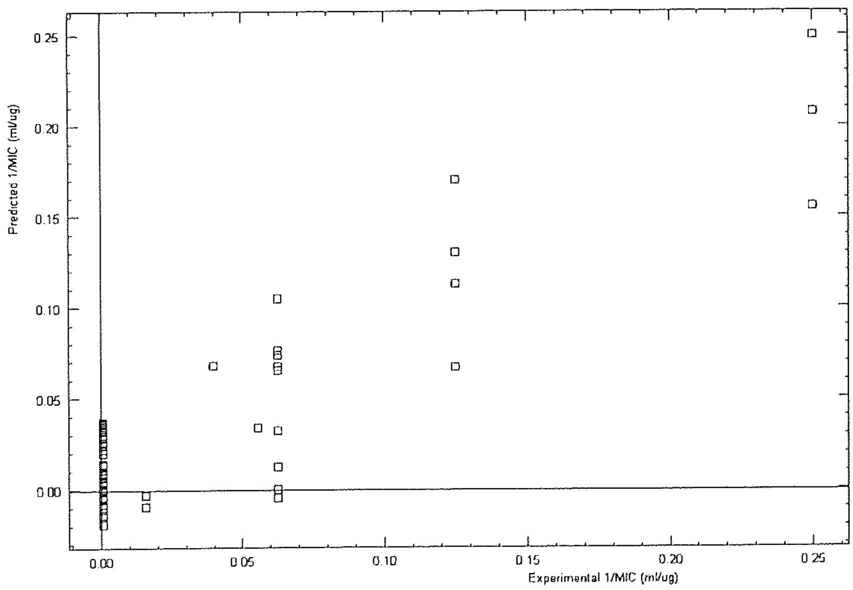

Figure 6.14 Graph of the pyridine-2-benzylidenecarboxamidrazone set against *M.fortuitum*

6.4.2.3 Discussion Of The Equations Found To Fit The M.fortuitum Data

Equation for the entire heteroaryl set::

Predicted 1/MIC= $1.839\times10^{-5}A^3 - 1.436\times10^{-5}B^3 + 5.683\times10^{-4}C^3 + 0.1934/D + 2.957\times10^{-3}E + 3.433\times10^{-3}/E + 0.0572/F + 7.979G - 0.1228$

Equation for the pyridine-2- set:

Predicted 1/MIC= $8.885\times10^{-5}A^3 - 5.560\times10^{-4}B^2 + 0.01143/C + 0.04798/D - 0.1220$

Table 6.3 Comparison of the two sets of data from the equations of activity against *M.fortuitum* for the entire benzylideneheteroarylcarboxamidrazone set and the pyridine-2-carboxamidrazone set.

	Entire Heteroaryl Set	**Pyridine-2- Set**
r^2	0.722	0.795
r^2(CV)	0.398	0.671
Properties in Eqn	N-Length (A) Aryl width (B) Log P (C) Total lipole (D) Lipole y (E) Total dipole (F) Dipole x (G)	N-Length (A) Aryl width (B) Lipole y (C) Total dipole (D)

As it was hypothesised, a better fitting equation was obtained when the benzylideneheteroaryl-carboxamidrazones were separated into their separate classes, and the calculations repeated for the pyridine-2- set alone. Table 6.3 shows the r^2 and r^2(CV) values for both equations and also the molecular properties which feature in these equations.

Although both equations have similar r^2 values, their r^2(CV) values are very different. The significance of this is that the predictive power of the equation for the pyridine-2- compounds is much better than that for the whole set of heteroaryl groups. The equation for the pyridine-2-set may also be expected to be more predictive than the other equation due to the smaller number of properties involved in the equation. The more terms the equation has, the more likely the chance of overfitting the data[118]. Since the pyridine-2- equation is the better one, it is this that shall now be discussed.

Table 6.4 Table to show the relative importance of each term in the pyridine-2- equation for compound **2PYbn**, with a predicted 1/MIC of 0.20μg^{-1}ml

Term	Value of A-D	Value of term in equation	% of term compared to final value
(A) N-Length	15.59	0.337	161
(B) Aryl width	7.02	0.027	13
(C) Lipole y	4.12	0.003	14
(D) Total dipole	2.67	0.018	9

The molecular properties which appear to be desirable in pyridine-2-benzylidenecarboxamidrazones for activity against *M.fortuitum* are N-length, aryl width, lipole y and total dipole. It is interesting to note that the length and width measurements proved important, and this agrees with the earlier hypothesis which was made in Section 6.3. According to the equation, a larger molecular length from the N-atom of the heteroaryl group and a larger width of the aryl group will improve activity. Table 6.4 shows that this is the most important term in the equation, in terms of its contribution to the final prediction. It must be remembered, however, that molecules which were both inactive and with lengths and/or widths greater than it was hypothesised would fit in the active site, were not included in the data set and so the equation cannot allow for these. This would not matter should the equation be used to predict activity, as one would simply apply the length and width limits (length <17.02Å, or width <12.26Å) prior to using the equation. It is not surprising that a lipole is also included in the equation, as this is effectively a vectorised log P value, and log P is known to be important in activity against mycobacteria. It is of interest though, why lipole in the y direction particular, is vital. (The vertical axis is the y axis, directions as in Figure 6.8). Total dipole is the final term in the equation and again there is an inverse relationship to activity, so a smaller dipole is required to improve activity.

6.4.3 Using Multiple Regression Analysis To Study The *M.tuberculosis* Results

The *M.tuberculosis* test results were better to work with for this procedure, as the percentage inhibition results provided a continuous data set. Unfortunately the *M.fortuitum* results, being MICs and converted to 1/MIC, gave discrete data, which obviously does not give as good a spread of results and did limit the ability of the program to produce a successful equation.

6.4.3.1 All Types of Heteroarylbenzylidenecarboxamidrazones

As the continuous *M.tuberculosis* test results were more agreeable for regression analysis, a valid equation was obtained without removing any of the data points. This equation is given below, and it must be noted that although the equation is valid, both the r^2 and r^2(CV) values are very low, so the equation does not fit the data particularly well [r^2=0.371] and the predictive power of the equation is extremely low [r^2(CV)=0.094].

Predicted %Inh.= 8.809A +1.410B -9.012/C -14.36

n=81 s value=20.641 F value=15.163 r^2=0.371 r^2 (CV)=0.094

A= Log P B= Lipole x C= Total dipole

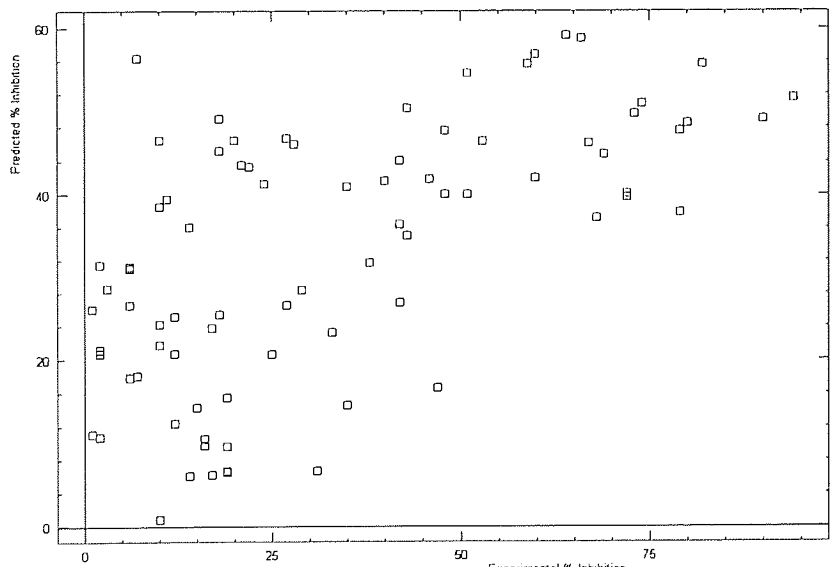

Figure 6.15 Graph of the entire set of heteroarylbenzylidenecarboxamidrazone data against *M.tuberculosis*

A more useful equation was required, so the greatest outliers at the lower end of activity were removed. The resulting equation is shown below.

Predicted %Inh.= $-3.7694 \times 10^{-7} A^3 + 27.828B + 61.183/C + 2.6206/D + 0.01578D^3 - 0.23406/E - 67.682$

n=55 s value=11.385 F value=48.630 r^2=0.859 r^2 (CV)=0.680

A= Molecular mass B= Log P C= Total lipole D= Lipole x E= Lipole z

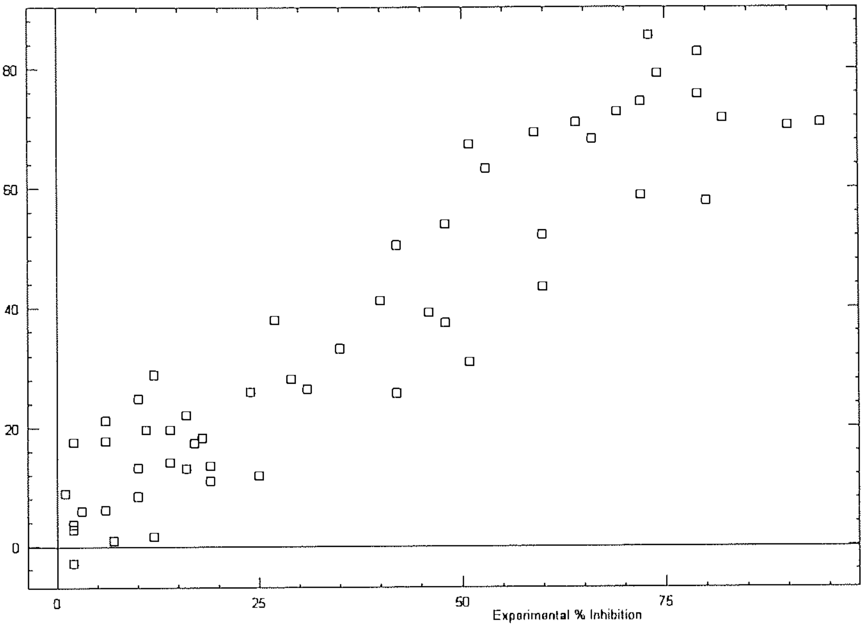

Figure 6.16 Graph of the reduced set of all types of heteroarylbenzylidenecarboxamidrazones against *M.tuberculosis*

6.4.3.2 The Pyridine-2-benzylidenecarboxamidrazone Set

Again, it was thought that a better equation could be obtained if the compounds were subdivided according to the heteroaryl group. Since the most data was available for the pyridine-2-benzylidenecarboxamidrazones these were subjected to multiple regression analysis, with the most significant outliers at the lower end of activity, being removed.

Predicted %Inh.= $-9957/A + 36.37B - 2.720 \times 10^{-3} C^4 - 8.491 \times 10^{-3} D^4 - 0.1727/E - 46.49$

n=31 s value=7.474 F value=93.573 r^2=0.949 r^2 (CV)=0.744

A= Molecular mass B= Log P C= Lipole x D= Lipole y E= Lipole z

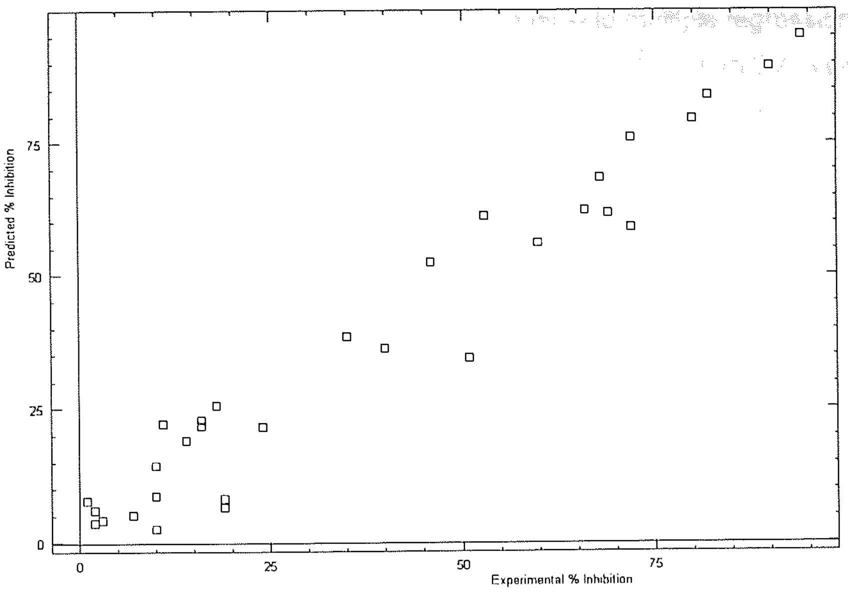

Figure 6.17 Graph of the pyridine-2-benzylidenecarboxamidrazone set against *M.tuberculosis*

6.4.3.3 Discussion Of The Equations Found To Fit The M.tuberculosis Data

Equation for the entire heteroaryl set:

Predicted %Inh.= $-3.7694\times10^{-7}A^3 + 27.828B + 61.183/C + 2.6206/D + 0.01578D^3 - 0.23406/E - 67.682$

Equation for the pyridine-2- set:

Predicted %Inh.= $-9957/A + 36.37B - 2.720\times10^{-3}C^4 - 8.491\times10^{-3}D^4 - 0.1727/E - 46.49$

Table 6.5 Comparison of the two sets of data from the equations of activity against *M.tuberculosis* for the entire heteroarylcarboxamidrazone set and the pyridine-2-carboxamidrazone set.

	Entire Heteroaryl Set	**Pyridine-2- Set**
r^2	0.859	0.949
r^2(CV)	0.680	0.744
Properties in Eqn	Molecular mass (A) Log P (B) Total lipole (C) Lipole x (D) Lipole z (E)	Molecular mass (A) Log P (B) Lipole x (C) Lipole y (D) Lipole z (E)

Once more, a better fitting equation was found when the heteroarylcarboxamidrazones were separated into their separate classes. Table 6.5 shows the r^2 and r^2(CV) values for both equations and also the molecular properties which feature in these equations.

As previously mentioned, the *M.tuberculosis* test results provide a continuous data set, as opposed to the discrete data for *M.fortuitum*, which is far more amenable to multiple regression analysis. This can be seen by the improved analyses of the equations: the r^2 and r^2(CV) values are much improved over those of the *M.fortuitum* equations. As before though, both values are much higher for the pyridine-2-carboxamidrazone set, indicating that the equation better fits this data, than the entire benzylideneheteroarylcarboxamidrazone set, and that it has better predictive power for untested compounds. Since the pyridine-2- equation is the better one, it is this that shall now be discussed.

The molecular properties which appear to be desirable in pyridine-2-benzylidenecarboxamidrazones for activity against *M.tuberculosis* are molecular mass, log P and each of the vectorised lipoles x, y and z (directions as in Figure 6.7). Log P would be expected to enter into the equation, and it does so, multiplied by a large number (thirty-six) such that a higher log P will give higher activity. This is so that the compound can penetrate the highly lipophillic mycobacterial cell wall more easily. Molecular mass also features in the equation. Although molecular mass could be closely correlated to log P, it was proven not to be in this case, by the use of a term correlation cut-off during multiple regression analysis, set at 0.5. It is not only lipophilicity (or log P) which is important, but also where in the molecule the lipophilicity lies, as shown by the appearance of the vectorised lipoles x,y and z in the equation.

Table 6.6 Table to show the relative importance of each term in the pyridine-2- equation for compound **2PYam**, with a predicted %Inh. of 89.6

Term	Value of A-E	Value of term in equation	% of term compared to final value
(A) Mol. Mass	324	-30.7	34
(B) Log P	4.86	177	197
(C) Lipole x	7.66	-9.36	10
(D) Lipole y	2.23	-0.210	0.2
(E) Lipole z	0.41	-0.421	0.5

Table 6.6 shows that the most important terms in the equation, which account for the majority of the final activity value are molecular mass and log P. As mentioned previously, this is to be expected when one considers the hydrophobic mycobacterial cell wall, which is more easily penetrated by lipophillic compounds. The various lipole values are used to 'fine tune' the equation.

6.4.3.4 Conclusion

The equations predict activity fairly well, and would certainly be a useful tool to use when considering which compounds from a virtual library would be worth synthesising, i.e. predicting in terms of dividing compounds into inactives and possible actives.

CHAPTER 7
ANTIBACTERIAL TESTING RESULTS

7.1 THE ANTIBACTERIAL TESTING

Each compound was initially tested for a zone of inhibition on agar, against both a methicillin-sensitive strain of *Staphylococcus aureus* (reference strain NCTC 6571) and a clinical isolate of MRSA (96-7475).

If a zone of inhibition was observed against the methicillin sensitive *S.aureus*, this was noted, but the MIC values against this strain were not measured and this is shown as a solitary 'tick' in Table 7.1. If a zone of inhibition was observed against the MRSA strain, the compound was purified where necessary, and then the MIC for that compound was measured against a panel of organisms, using a multi-point innoculator and the agar diffusion method. The MIC results for the panel of MRSA strains used, are given below in Table 7.1. The full set of results for the multi-point inoculation experiment, against all the organisms used along with a description of the bacteria, are given in the appendix, although the points of interest will be discussed in this chapter. The panel of Gram-positive organisms used comprised of three methicillin-sensitive *S.aureus* strains, ten MRSA clinical isolate strains, two *E.faecium* strains, and seven strains of *E.faecalis* (including six clinical isolates). A small selection of ten different Gram-negative bacteria were also tested, to investigate the possibility of any broad-spectrum activity.

Table 7.1 Antibacterial testing results of the heteroarylbenzylidenecarboxamidrazones. 'Staph' refers to the reference strain of *S.aureus* (NCTC 6571). A tick in the MRSA column refers to a positive zone against MRSA strain 96-7474, and the MIC range which follows is that found against a panel of ten MRSA strains (see Appendix). Where MIC values are given for MRSA, these are stated as a range of values, as testing was carried out on a panel of clinical isolates.

	2PY		3PY		4PY		HD		PZ		QN	
Ald	Staph	MRSA	Staph	MRSA	Staph	MRSA	Staph	MRSA	Staph	MRSA	Staph	MRSA
aa	X	X			X	X	X	X	X	X	X	X
ab	✓	X	X	X	X	X	X	X	X	X	X	X
ad	X	X							X	X	X	X
ae	X	X	X	X	X	X	X	X	X	X	X	X
af	✓	✓>256	✓	✓32-64	✓	✓32-64	X	X	X	X	X	X
ag	X	X	X	X	X	X	X	X	X	X	X	X
ah	✓	✓128-256	X	X	X	X	X	X	X	X	X	X
ai	✓	✓128-256	X	X	X	X	X	X	X	X	X	X
aj	✓	✓128-256	X	X	X	X	X	X	X	X	X	X
ak	X	X	X	X	X	X	X	X	X	X	X	X
al	✓	✓>256	✓	X	X	X	X	X	X	X	X	X
am	X	X	X	X	✓	✓16-64	X	X	X	X	X	X
an	X	X	X	X	X	X	X	X	X	X	X	X
ao	X	X							X	X	X	X
aq	X	X							X	X	X	X
as	X	X	X	X	X	X	X	X	X	X	X	X
ay	X	X	✓	✓>256	X	X	X	X	X	X	X	X
be	X	X	X	X	X	X	X	X	X	X	X	X
bf	X	X	X	X	X	X	X	X	X	X	X	X
bg	X	X	X	X	X	X	X	X	X	X	X	X
bh	X	X	X	X	X	X	X	X	X	X	X	X
bn	X	X	X	X	X	X	X	X	X	X	X	X
bs	X	X	X	X	X	X	X	X	X	X	X	X
bt	X	X	X	X	X	X	X	X	X	X	X	X
bu	X	X	X	X	X	X	X	X	X	X	X	X
bv	X	X			X	X						
bw	X	X			X	X			X	X	X	X
bx	X	X							X	X	X	X
by	X	X							X	X	X	X
bz	X	X	X	X	X	X	✓	X	X	X	X	X
ca	✓	X	X	X	X	X	X	X	✓	X	✓	✓64-128
cb	✓	✓	✓	X	✓	✓30-40	✓	✓	✓	✓128-256	✓	X
cc	✓	X	✓	✓128-256	✓	✓20-30	✓	X	✓	✓	✓	✓
cd	X	X	X	X	X	X	X	✓128-256	X	X	X	X
ce	X	X			X	X	✓	✓10-20	X	X	X	X
cf	X	✓	X	X	X	X	✓	✓20-30	X	X	X	X
cg	X	X			X	X			X	X	X	X
ch	X	X			X	X			X	X	X	X
ci	X	X			X	X			X	X	X	X
cj	✓	✓4-32	✓	✓2-8	✓	✓20-30	✓	✓16-64	✓	✓4-16	X	X
ck	X	X			X	X	X	X	X	X	X	X
cl	✓	✓	✓	✓16-64	✓	X	✓	✓64-128	X	X	X	X
cm	✓	✓	X	X			X	X	X	X	X	X
cn					✓	X	X	X				
co					✓	✓10-20	X	X				

	2PY		3PY		4PY		HD		PZ		QN	
Ald	Staph	MRSA	Staph	MRSA	Staph	MRSA	Staph	MRSA	Staph	MRSA	Staph	MRSA
cp	X	X			X	X						
cq	X	X	X	X	✓	✓2-4	X	X	X	X	X	X
cr	X	X	X	X	✓	✓>256	X	X	X	X	X	X
cs	X	X							X	X	X	X
ct	X	X							X	X	X	X
cu	X	X							X	X	X	X
cv	X	X							X	X	X	X
cw	X	X			X	X			X	X	X	X
cx	X	X							X	X	X	X
cy	X	X			X	X			X	X	X	X
cz	X	X			X	X			X	X	X	X
da	X	X			X	X						
db	✓	✓>256	✓	✓128-256	✓	X	✓	✓4-16	X	X	X	X
dc			X	X			X	X	X	X	X	X
dd	X	X	X	X	X	X	X	X	X	X	X	X
de	✓	X							X	X	X	X
df	X	X							X	X	X	X
dg	✓	✓64-128	X	X	X	X	X	X	X	X	X	X
dh	✓	X							X	X	X	X
di	X	X							X	X	X	X
dj	X	X							X	X	X	X
dk	✓	X							X	X	X	X
dl	X	X							X	X	X	X
dm	✓	X							X	X	X	X
dn	X	X			X	X			X	X	X	X
do	X	X			X	X			X	X	X	X
dp	X	X							✓	X	X	X
dq	✓	✓128-256	X	X	X	X	X	X	X	X	X	X
dr	X	X			X	X			X	X	X	X
ds	X	X	X	X	X	X	X	X	X	X	✓	✓32-128
dt	X	X	X	X	X	X	X	X	X	X	X	X
dv	X	X	X	X	X	X	✓	✓	X	X	X	X
dw	X	X	X	X	X	X	X	X	X	X	X	X
dx	X	X	X	X	✓	✓64-128	X	X	X	X	X	X
ea	X	X							X	X	X	X
eb	✓	X							X	X	X	X
ec	X	X							X	X	X	X
ed	X	X			X	X	X	X	X	X	X	X
ee	X	X			X	X			X	X	X	X
ef	X	X			X	X			X	X	X	X
eg	X	X	X	X	X	X	X	X	✓	✓>256	X	X
eh	✓	X	X	X	✓	✓8-64	X	X	X	X	X	X

7.2 ANTIBACTERIAL ACTIVITY OF THE STARTING MATERIALS

The amidrazone starting materials themselves **2PY**, **3PY**, **PZ** and **QN**, along with the 2-pyridyl-hydrazine **HD**, were all inactive against *S.aureus* and MRSA, in their unsubstituted form.

All the aldehyde reactants were tested against *S.aureus* and MRSA. A few aldehydes did display activity against these organisms, namely **cj** and **cl**. The activities of these aldehydes, and that of their active amidrazone adducts are shown in Table 7.2 and 7.3 respectively. Unfortunately, however, the activities of the aldehydes themselves proved to be superior to those of their amidrazone adducts.

Table 7.2 The activities of aldehyde **cj** and its amidrazone adducts against a panel of ten MRSA strains

Code	Structure	MIC (μgml^{-1})
aldehyde cj	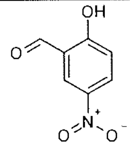	1-4
2PYcj	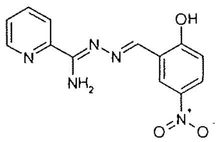	4-32
3PYcj	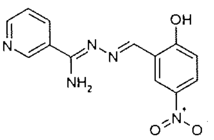	2-8

Code	Structure	MIC (μgml^{-1})
4PYcj	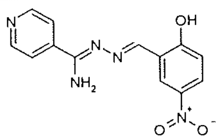	20-30
PZcj	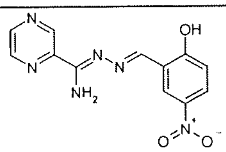	4-16
HDcj	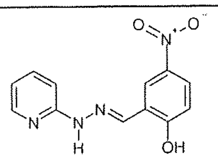	16-64

Table 7.3 The activities of aldehyde **cl** and its amidrazone adducts against a panel of ten MRSA strains

Code	Structure	MIC (μgml^{-1})
aldehyde cl	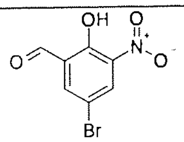	8-32
2PYcl	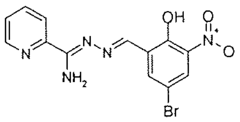	16-64
3PYcl	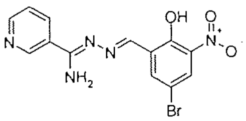	16-64

Code	Structure	MIC (μgml^{-1})
QNcl	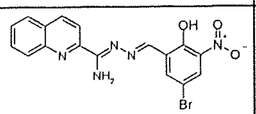	32-256
HDcl	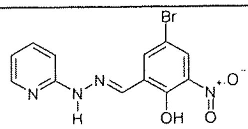	64-128

7.3 DISCUSSION OF THE MRSA TESTING RESULTS

The phenolic aldehydes **cj** and **cl** which have already been mentioned, show antibacterial activity against MRSA. The amidrazone adducts of these aldehydes also displayed some anti-MRSA activity, although it is somewhat reduced. Table 7.4, below, contains other phenolic compounds which were also active against MRSA. Of the seventeen active compounds discovered (with MIC of 64μgml^{-1} or less), fourteen are phenol derivatives. Perhaps this is not too surprising, as phenols are known to damage bacterial membranes, acting as detergents due to the polarity of the phenolic hydroxyl group. Phenols also denature proteins[33]. Due to this, it may be expected that activity was observed for all the phenolic aldehydes and derivatives produced. This was not the case, however, some were inactive, so there must be some other important factors which need to be identified. The generally less active, non-phenolic actives are shown in Table 7.5.

Table 7.4 Phenolic compounds possessing some activity against MRSA (<64μgml^{-1})

Code	Structure	MIC (μgml^{-1})
4PYcb	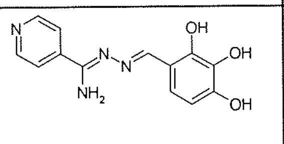	30-40
HDcb	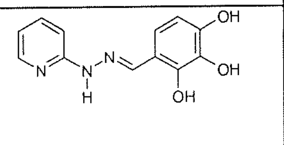	40-60
HDce	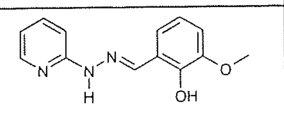	10-20
HDcf	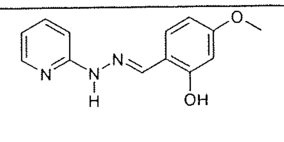	20-30

Code	Structure	MIC (μgml^{-1})
4PYco	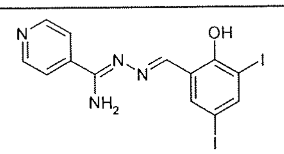	10-20
4PYcq	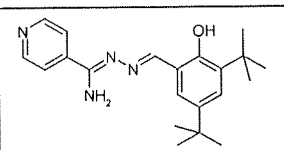	2-4
HDdb	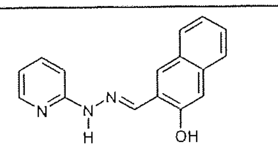	4-16

Table 7.5 Non-phenolic compounds possessing some activity against MRSA (<64μgml^{-1})

Code	Structure	MIC (μgml^{-1})
3PYaf	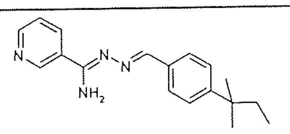	32-64
4PYaf	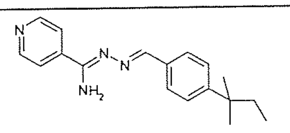	32-64

Code	Structure	MIC (μgml^{-1})
4PYam	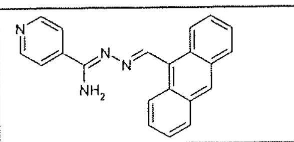	16-64
4PYeh	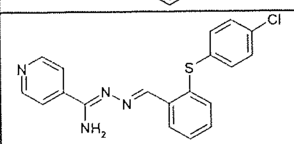	8-64

7.3.1 Comparison Of The Staphylococci Results With The Mycobacteria Results

Most of the compounds which were found to possess activity against *M.fortuitum* were pyridine-2-carboxamidrazone **2PY** derivatives. Only two **2PY** compounds were active against MRSA, and these were compounds for which the aldehyde itself was active. This suggests that most of the anti-mycobacterial compounds found in this study (Chapter 5), were actually specific for mycobacteria. The only compounds to share activity against both sets of organisms are those in Table 7.5. Again, it is of note that although **3PYaf** and **4PYaf** were active against MRSA, **2PYaf** was not.

7.3.2 Investigation Of 4PYcq; The Most Active Compound Against MRSA

*7.3.2.1 Activity of **4PYcq** Against Other Organisms*

The most active compound found against MRSA was **4PYcq**, which was active at 2-4μgml^{-1} against all the strains tested. At this concentration, the compound was also active against all the other Gram-positive bacteria tested. Due to this high activity, **4PYcq** was also tested against some vancomycin resistant enterococci (VREs), the results of which are shown in Table 7.6. The same high activity (2-4μgml^{-1}) was retained against these clinical VRE strains.

Table 7.6 Results of **4PYcq** against some vancomycin resistant enterococci

Culture	Vancomycin MIC (μgml^{-1})	**4PYcq** MIC (μgml^{-1})
3001562	4-8	2-4
3002043	4-8	2-4
3002066	4-8	2-4
3005323	>16	2-4
3005426	4-8	2-4
3005353	>16	2-4
3102095	>16	2-4

Despite its impressive activity against Gram-positive bacteria, **4PYcq** did not display any activity against Gram-negative bacteria. The structure of the two bacterial cell walls are very different. Gram-positive bacteria, such as staphylococci and enterococci, have a single, very thick cell wall, consisting largely of peptidoglycan. Gram-negative bacteria such as *Eschericha coli*, have a very thin inner membrane consisting of only 1-5% peptidoglycan, surrounded by an outer membrane consisting of a large amount of lipoproteins and lipopolysaccharides. It is this difference in structure that would account for the large difference in activity of **4PYcq** between the two bacterial types, particularly if the mode of action of this compound is associated with peptidoglycan or its synthesis.

*7.3.2.2 The Activity of **4PYcq** In Comparison With Structurally Similar Compounds*

Aldehyde **cr** is an isomer of **cq** and although **4PYcr** did give a zone of inhibition against MRSA, the MIC was very different; >256μgml^{-1} (compared with 2-4μgml^{-1} for **4PYcq**). Since the two compounds have the same calculated log P, and contain the same functional groups, there must be something important about the position of the groups in **cq**. Substituting the heteroaryl entity for pyridine-2- **2PY**, pyridine- 3- **3PY**, pyrazine **PZ** or quinoline **QN** groups resulted in loss of activity and the 2-pyridylhydrazone compound **HDcq** was also inactive. It is also of note that neither of the starting materials were active and neither was compound 2-hydroxybenzylidene-pyridine-4-carboxamidrazone (**4PYbw**), which lacks the alkyl groups.

Table 7.7 To compare the structure and activities against MRSA, of **4PYcq** and similar compounds

Code	Structure	MIC (μgml^{-1})
4PYcq	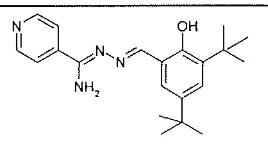	2-4
4PYcr	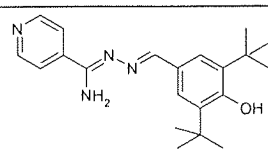	>256
4PYbv	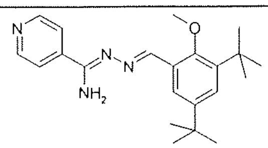	Inactive

Code	Structure	MIC (μgml^{-1})
4PYcp	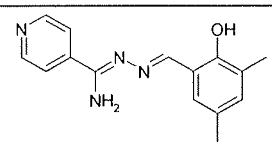	>256
4PYco	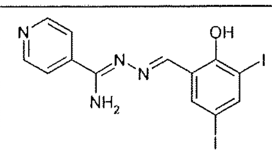	10-20
4PYda	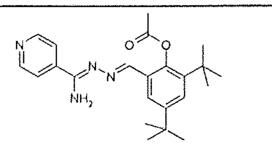	4-8

Synthesising **4PYbv** and putting a methoxy group in place of the hydroxyl group of **4PYcq**, negated the activity completely, indicating once more, that the phenolic-OH is vital to activity.

In **4PYcp**, the bulky *t*-butyl groups of **4PYcq** are replaced by small methyl groups, and although a zone of inhibition was observed for this compound, it was rather inactive, with an MIC>256μgml^{-1}. Compound **4PYco**, with iodide groups (which are approximately the same size as a methyl group), at positions 3- and 4-, however, was active, with a good MIC of 10-20μgml^{-1}. This may be explained by the log P of the compounds. **4PYcp**, which contains the methyl groups has a much lower log P (3.97) than the other two compounds **4PYcq** and **4PYco** (6.29 and 5.55 respectively). The higher lipophilicity of the latter two compounds could aid migration of the molecule through the lipophilic cell wall, and thus affording greater activity to the compound.

When the hydroxyl group of **4PYcq** is masked by an acetyl group, as in **4PYda**, biological activity is maintained, but slightly reduced at 4-8μgml^{-1}. The fact that this compound retains activity can be explained by the possible hydrolysis of the acetyl group *in vivo*, to give the free hydroxyl group, and so compound **4PYcq**, again.

Compound **4PYcq** made an interesting lead compound, unfortunately however, it was later found to be extremely toxic to human white blood cells (Section 8.2). This showed that the **4PYcq** was not viable as a potential drug and no further research on this compound was undertaken.

CHAPTER 8
TOXICOLOGY

In vitro toxicity testing is an important part of the drug discovery process. If a compound is too toxic compared with its activity, i.e. its therapeutic index is too low, then it will not progress through to further trials. The results of toxicity testing may mean that time spent developing toxic compounds is avoided, and the results can direct synthesis towards better lead compounds.

8.1 TOXICITY OF SOME ANTIMYCOBACTERIAL COMPOUNDS

As existing antitubercular drugs such as isoniazid, are toxic, it was thought to be important to evaluate the *in vitro* toxicity of some of the carboxamidrazones found to be active against *M.fortuitum*, in this study [119-121]. The toxicity of the pyridine-2-carboxamidrazone precursor and some aldehydes were also assessed. The *in vitro* assay used human mononuclear leucocytes (MNL, white blood cells) which were incubated with the test compound for 18 hours and cell death determined by tryptan blue exclusion (tryptan blue is a dye, which stains dead cells, whilst living cells exclude it). The main results of interest are shown in Table 8.1.

From Table 8.1, it can be seen that some direct MNL toxicity was encountered. The starting material pyridine-2-carboxamidrazone **2PY**, aldehyde **ae** and the compound **2PYal** were the most toxic compounds. However, the direct MNL toxicity for the other test compounds, **2PYae**, **2PYaf**, **2PYbe** and **2PYeh**, were indistinguishable from the background levels. Although not quite as potent as isoniazid, these compounds compare very favourably in terms of cytotoxicity.

It is interesting to note that the starting material pyridine-2-carboxamidrazone **2PY** was amongst the most cytotoxic compounds, but that generally, when it is combined with an aldehyde, even the very toxic aldehyde **ae**, the resulting benzylideneheteroarylcarboxamidrazone possesses no significant cytotoxicity. The exception to this is compound **2PYal**, which is more cytotoxic than both of its starting materials.

Table 8.1 Results of direct leucocyte toxicity testing on some antimycobacterial compounds[120]

Compound	Structure	*M.fortuitum* MIC (μgml^{-1})	Conc. (mM)	% Leucocyte Death
Control - acetone -DMSO	-	-	-	1.0±1.1 5.4±1.1
Isoniazid	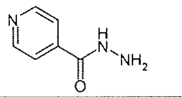	1-2	0.1 1.0	1.8±1.5 11.7±3.6
2PY	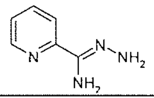	-	1.0	12.1±2.2
ae	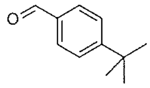	-	1.0	24.1±9.6
af	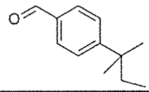	-	1.0	5.5±3.0
al	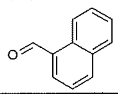	-	1.0	9.2±4.7
2PYae	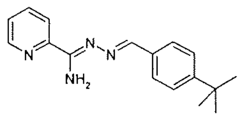	8-16	0.1	1.1±1.0
2PYaf	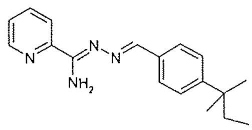	4-8	1.0	3.1±1.0
2PYal	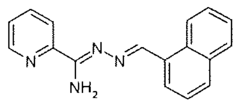	18-21	1.0	17.1±4.9
2PYbe	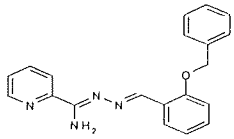	25-30	0.1	5.1±4.1
2PYeh	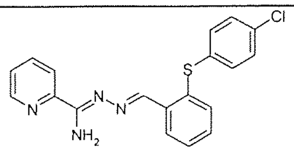	12.5-25	0.1	3.7±2.6

It is known that isoniazid is oxidatively metabolised to cytotoxic intermediate derivatives[67,121]. It was essential, therefore, to determine whether the amidrazones were oxidised to potentially reactive cytotoxic species. It is possible, for example, that the benzylideneheteroarylcarboxamidrazone could be cleaved, to produce the free pyridine-2-carboxamidrazone **2PY**, which has already been shown to be toxic.

To investigate the indirect toxicity of these compounds, Coleman *et al* [121] repeated the toxicology experiments, but also added to these, rat liver microsomes as a metabolising system. It was discovered that generally, there was negligible bioactivation of the amidrazones to toxic species. The only compound which was affected by the metabolising system was **2PYal**, which was also the only amidrazone to be directly toxic. For **2PYal** there was actually a marked reduction in cytotoxicity in the presence of the metabolising system, suggesting that a biotransformationally mediated partial detoxification occurred.

Four out of the five tested benzylideneheteroarylcarboxamidrazones were not significantly toxic, indicating that in the rat, the amidrazone links are not cleaved by oxidative metabolism and that potentially cytotoxic substituents are not likely to be liberated *in vivo*. Studies with human microsomes would be necessary to confirm this.

8.2 TOXICITY OF THE MOST ACTIVE ANTIBACTERIAL COMPOUND; 4PYcq

The most promising antibacterial compound found in this study was N^1-[3, 5-di-(tert-butyl)-2-hydroxy-benzylidene]-pyridine-2-carboxamidrazone **4PYcq**. It was active against the MRSA strains and the vancomycin resistant enterococci which were tested, all with an MIC of 2-4μgml^{-1} (Section 7.3.2).

The toxicity of **4PYcq** and the aldehyde **cq** and pyridine-4-carboxamidrazone precursors were assessed using the same *in vitro* assay with human mononuclear leucocytes that was mentioned in Section 8.1. The toxicity of related compounds, 2-hydroxybenzylidene-pyridine-2-carboxamidrazone **4PYbw** and benzylidenepyridine-2-carboxamidrazone **4PYaa** were also examined. The results are shown in Table 8.2.

Table 8.2 Results of direct leucocyte toxicity testing on **4PYcq**, its starting materials and related structures

Compound	Structure	Conc. (mM)	% Leucocyte Death
DMSO Control	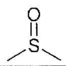	-	7.4±1.1
Isoniazid	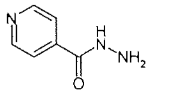	1	12.4±2.8
4PY	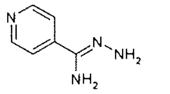	1	13.8±0.4
cq	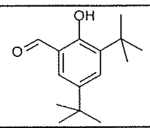	1	32.7±3.2
4PYcq	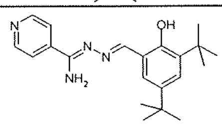	0.5	100
4PYbw	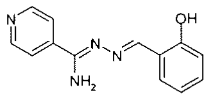	1	11.7±1.2
4PYaa	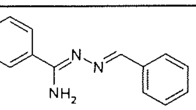	1	9.7±0.6

Unfortunately, **4PYcq** was found to be very toxic to leucocytes, causing lysis of the cells during the course of the experiment. Experiments on the two related compounds **4PYaa** and **4PYbw** (Table 8.2), show that these compounds are only mildly toxic in comparison, indicating that the *t*-butyl groups somehow afford huge cytotoxicity to **4PYcq**. This may be due to the steric properties of the bulky *t*-butyl groups, or due to their lipophilicity. Compound **4PYcq** initially proved to be an effective antimicrobial compound for Gram-positive bacteria, including those resistant to standard drugs, but it was later also found to be a highly cytotoxic compound, which prevented any further study of the compound as a potential drug.

CHAPTER 9

SYNTHESIS OF POTENTIAL ANTIMYCOBACTERIAL COMPOUNDS USING A SOLUBLE POLYMERIC SUPPORT

9.1 INTRODUCTION TO SOLUBLE POLYMERS

Soluble polymeric supports can be used to carry out liquid-phase synthesis, which is a relatively recent addition to synthetic chemistry. A polymeric support is employed which is soluble in some solvents and insoluble in others. The principle remains the same as for solid phase synthesis (Section 1.4.3.2), except that the polymeric support is completely soluble in the reaction medium and the reaction occurs under homogenous conditions. This approach retains the positive aspect of solid phase synthesis which is the ability to use excess reagents in order to drive a reaction to completion. Purification is simply achieved by the precipitation of the polymer in an appropriate solvent, followed by filtration to remove excess reagents, and by-products. Liquid phase synthesis also has the advantage of allowing characterisation of the reaction products, on the polymer, by routine analytical methods, without prior cleavage from the polymeric support[14,122,123].

The majority of examples of liquid phase synthesis use polyethylene glycol (PEG), **44**, as the support for organic synthesis of small molecules[14]. PEG will also be utilised in this study.

9.1.1 Polyethylene glycol (PEG)

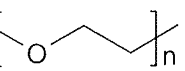

Figure 9.1 Polyethylene glycol **44**

Polyethylene glycol, shown in Figure 9.1, is produced by the polymerisation of ethylene oxide. It should be noted that these polymers do not exhibit one discrete molecular weight, but consist of macromolecules of various sizes. Commercially produced PEGs, however, tend to display quite a narrow range of molecular weights, it can be said that their polydispersity is low. PEGs of higher molecular weight (MW=200-20 000), are crystalline at room temperature, whilst the lower molecular weight PEGs are liquid[14].

Polyethylene glycol and its derivatives are non-toxic and non-immunogenic, and are used as chemical modifying reagents[128] in the pharmaceutical industry. PEG-drug conjugates are made, as the conjugation with PEG can enhance the stability of a drug during storage, delivery and end use.

The conjugate may exhibit reduced immune response and toxicity as well as a reduced rate of biotransformation in the liver and excretion by kidneys, thus prolonging circulation time. The aqueous solubility of hydrophobic drugs can also be increased by the hydrophilicity of the conjugated polymer[128]. PEG-drug conjugates have been shown to have potential in the treatment of cancer. Tumors passively accumulate synthetic polymers in the interstitial tissue, a process known as the enhanced permeation and retention effect (EPR). By conjugating an anticancer drug with PEG (so forming a PEG-prodrug), the tumors can be targeted, improving the selectivity and therefore general toxicity of the drug[130].

Different types of proteins, such as enzymes, antibodies and hormones can also be conjugated with PEG. This protects them from recognition by the bodys immune system, and to prolong the circulation time in the body[128,129].

PEG can also act as a soluble polymeric support, upon which organic chemistry can be carried out in the liquid phase[14,126,127,131].

9.1.2 Polyethylene glycol (PEG) As A Soluble Polymeric Support

PEG is soluble in a wide range of organic solvents and water, but is insoluble in diethyl ether, *tert*-butyl methyl ether and hexane. PEG is also insoluble in THF at low temperatures, which obviously limits the use of PEG in reactions requiring this as a solvent. Removal of inorganic materials during compound isolation can also be complicated by the solubility of PEG in water[14,122,123].

Polyethylene glycols are inexpensive and, as mentioned previously, are commercially available in a number of molecular weights (200-20 000). Larger molecular weight PEGs have the advantage of greater solubilising power, but the disadvantage of lower loading capacities, compared with the smaller PEGs. Thus, when choosing which molecular weight PEG to use as a polymeric-support, there is a trade-off between using a high MW for its solubilising power and crystalinity, and accepting that there will be lower loading onto the polymer as a result.

PEG has a strong propensity to crystalise, due to the helical structure of the polymer; therefore inclusions of unwanted excess reagents, due to gelatinous precipitation should be avoided. This precipitation/crystalisation is usually brought about by the addition of excess diethyl ether to the homogenous reaction mixture[128-130]. The higher the molecular weight of PEG, the stronger its propensity to crystalise.

The characterisation of PEG-bound organic entities is often straightforward as the polymer does not interfere with spectroscopic methods of analysis. Monitoring reactions by ^{1}H NMR is easily done, since the only signals from PEG itself are those from the methylene protons of the PEG backbone (3-4ppm)[131], as demonstrated in Figure 9.2. As this Figure shows, most of the spectrum of PEG is a clear 'window', where product spectra can be observed. ^{13}C NMR, UV-visible spectroscopy, IR spectroscopy and even TLC may also be used to monitor reactions without requiring preliminary cleavage from the polymer support[122].

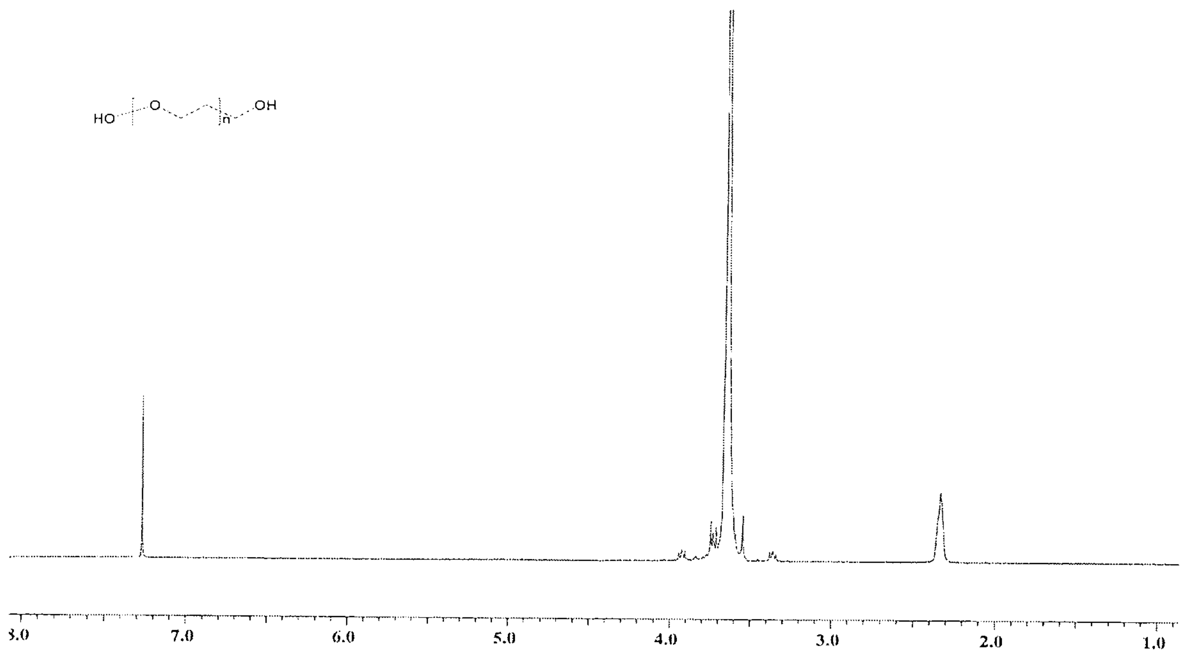

Figure 9.2 The ^{1}H NMR spectrum of 4000-PEG-OH in ($CDCl_3$)

9.2 REACTIONS ON POLYETHYLENE GLYCOL (PEG)

Liquid-phase synthesis should allow for the synthesis of any class of molecular entity, as long as the chemistry employed does not interact with, or adversely affect the polymers properties[132]. To follow are several examples of reactions which have been carried out on PEG.

The default linker on PEG is a hydroxyl group, however, modified linkers can be made[118]. In Section 9.2.3, a four carbon linker/spacer group is used, which is joined to PEG by an ester linkage and terminates with a carboxylic acid group.

9.2.1 Peptide Synthesis On PEG

Solid-phase synthesis was first introduced, by Merrifield, for peptide synthesis and this was also one of the first syntheses to be carried out in the liquid-phase, using PEG as the soluble polymeric support. Peptide synthesis on PEG has been carried out using PEGs of different molecular weights[122], and PEG has also been used for the synthesis of peptide libraries[14,122].

In both solid-phase and liquid-phase peptide synthesis, the polymer support is linked to C-terminus of the growing peptide and thus serves as a carboxylic acid protecting group (Figure 9.3). In liquid-phase synthesis, assuming a PEG of suitable molecular weight is used, this macromolecular protecting group also keeps the growing peptide in solution, to provide homogenous reaction conditions even with longer or hydrophobic peptides[14].

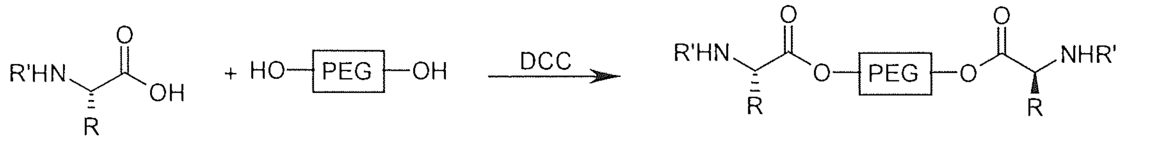

Figure 9.3 Direct esterification of PEG with amino acids

Optimisation of soluble polymer-supported peptide synthesis succeeded in the stepwise synthesis of a fourteen-mer on PEG-6000. A 33% yield of analytically pure peptide was reported[122].

9.2.2 PEG-Supported Library Synthesis of Arylsulfonamides

A library of arylsulfonamides **45** has been constructed by parallel synthesis, as shown in Figure 9.4[132]. Attachment to the polymeric support was formed quantitatively by reaction of 4-(chlorosulfonyl)-phenyl isocyanate with MeO-PEG in the presence of a catalytic amount of dibutyltinlaurate. There was no competing nucleophilic process at the chlorosulfonic acid moiety during this coupling reaction. The MeO-PEG-arylsulfonyl chloride was split among six reaction vessels containing different amines, which resulted in a library of MeO-PEG protected sulfonamides. Hydrolytic cleavage of the urethane linkage under basic conditions yielded the final library of six members in analytically pure form in yields over 95%[122,132].

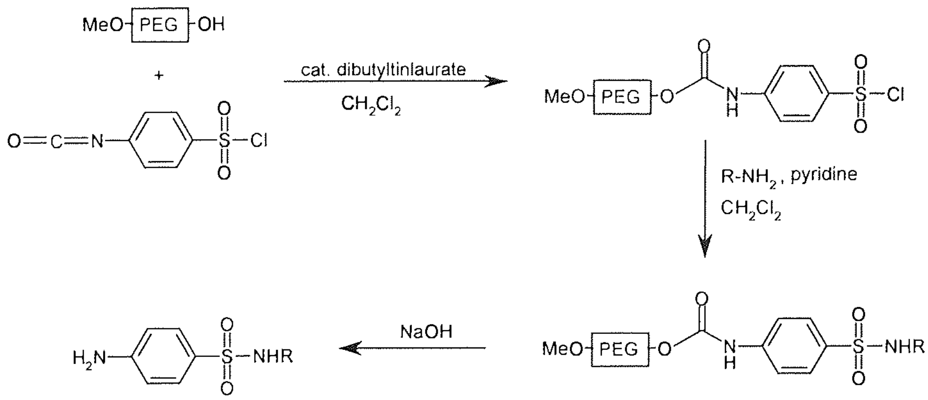

45

Figure 9.4 Construction of an arylsulfonamide **45** library[132]

9.2.3 Imine and β-Lactam Synthesis On PEG

Imines have been synthesised on MeO-PEG **46**, which have then been further reacted with ketenes to give β-lactams immobilised on MeO-PEG, as shown in Figure 9.5. Cleavage from the polymer resulted in yields between 30-56%, and both *cis* and *trans* isomers were present, *trans* being the dominant form in all cases[131]. No purity information was given for these compounds.

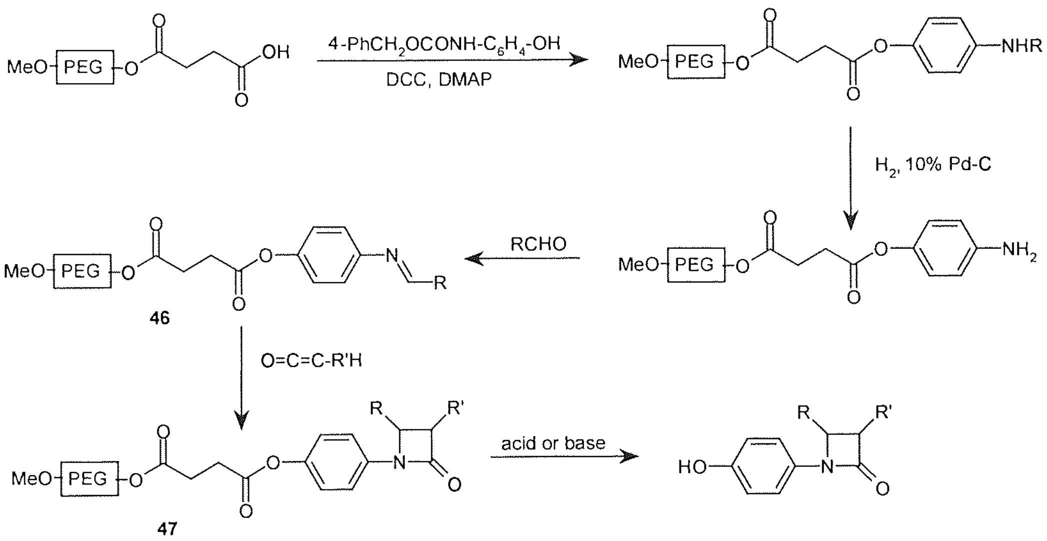

Figure 9.5 Soluble polymer supported synthesis of imines and β-lactams

As mentioned previously (Section 9.2), this synthesis involves adding a linker group onto the PEG support, although in this case, it may be mainly used as a spacer group to reduce steric hindrance of the polymer during the reactions. It is interesting to note that this synthesis involves amide reduction using hydrogen and palladium on charcoal. Palladium on charcoal, obviously itself a solid, can be used here, as the reaction is being carried out in the liquid-phase, but this would not be achievable if the reaction were carried out on solid phase. Cycloaddition of an imine with a ketene is also carried out on the polymeric support , prior to cleavage.

9.2.4 Piperidine and Piperazine Synthesis On PEG

Two papers by Sun and co-workers describe the synthesis of arylpiperazines and arylpiperidines[133] and benzylpiperazines and benzylpiperidines[134] on a soluble polymeric support.

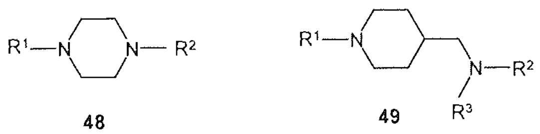

Figure 9.6 A piperazine **48** compared to a piperidine **49**

The syntheses for all four types of molecules are very similar, so only the synthesis of benzylpiperazines will be discussed for simplicity (see Figure 9.7). MeO-PEG-5000 was treated with 4-chloro-methylbenzoyl chloride to give a pseudo-Merrifield type molecule. This polymeric supported benzylic halide was then reacted with a variety of amines (piperidine in Figure 9.7). The PEG-bound products were then precipitated by the addition of ice-cold *t*-butyl methyl ether, and dried. Alkylation of the resin-bound piperidine can then be achieved by the addition of alkyl halide, monoalkylation occurring due to the polymer support acting as a macromolecular protecting group. After cleavage, high yields (86-98%) and purities of between 81-98% were obtained[134].

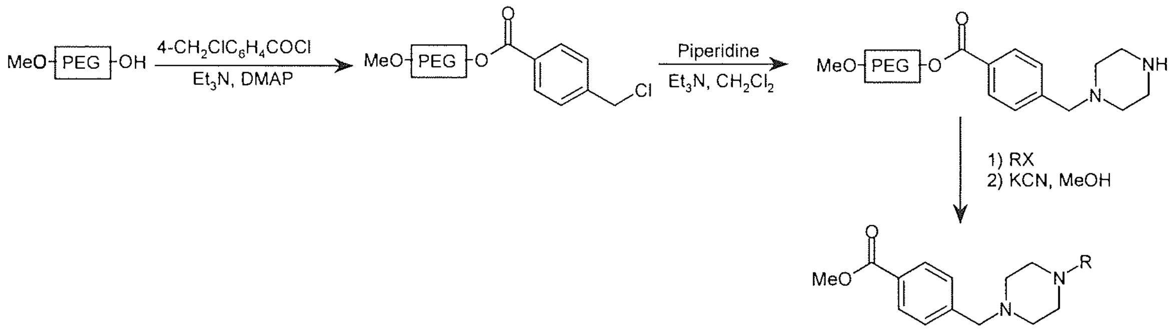

Figure 9.7 Soluble polymer supported synthesis of benzylpiperazines

9.2.5 Benzimidazole Synthesis On PEG

Benzimidazole based compounds have shown diverse biological activities including anti-ulcer and antiviral effects. The synthesis of these compounds has been carried out in the liquid phase, by Sun's research group, shown in Figure 9.8, utilising PEG as the soluble polymeric support. The reactions yielded between 72-88% after cleavage, and the crude products were between 80-94% pure[129].

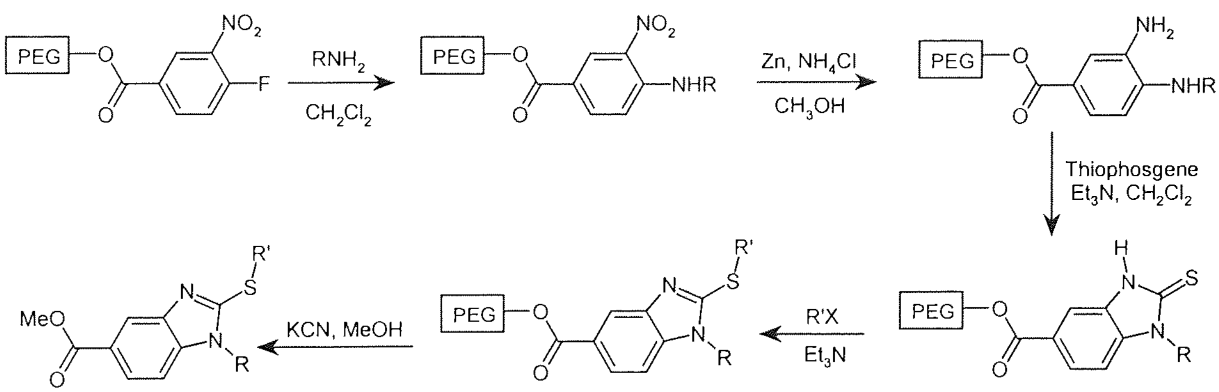

Figure 9.8 Soluble polymer supported synthesis of benzimidazoles

9.3 ISOXAZOLINE SYNTHESIS BY 1,3-DIPOLAR CYCLOADDITION

An effective, established method for the construction of isoxazoline or isoxazole rings is the 1,3-dipolar cycloaddition between nitrile oxides and alkenes or alkynes respectively[133]. This is a [3+2] cycloaddition reaction, where the 3π-electron component, called the 1,3-dipole reacts with the 2π-electron component, or dipolarophile which is a compound containing a double or triple bond, to produce a five-membered ring.

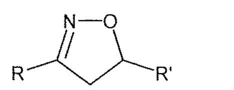

Figure 9.9 The general structure of Δ^2-isoxazolines

Δ^2-Isoxazoline rings are versatile intermediates for the synthesis of a variety of complex natural products[135,136] and are useful pharmacophores found in a number of pharmaceutical agents, such as glycoprotein GPIIb/IIIa inhibitors and human leukocyte elastase inhibitors[136].

9.3.1 Nitrile Oxides

Nitrile oxides **50** are compounds with the general structure R-C≡N$^+$-O$^-$, where R can be an aliphatic, aromatic or heterocyclic group. Nitrile oxides are generally very reactive, and spontaneous dimerisation can occur[137]. Due to this, nitrile oxides are usually formed *in situ*. This can be achieved by using oximes, which produce nitrile oxides when mixed with a weak solution of chlorine, such as bleach (sodium hypochlorite solution), as shown in Figure 9.10.

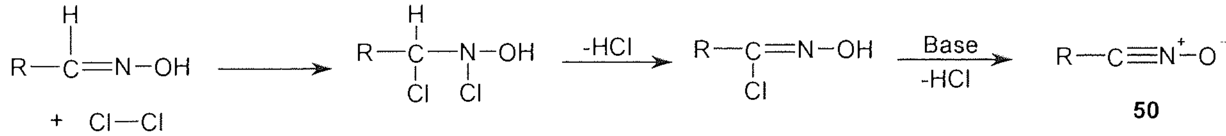

50

Figure 9.10 Formation of nitrile oxides from oximes[138] in bleach

As mentioned above, nitrile oxides are very reactive and they can dimerise in a number of ways, to give different products, as shown in Figure 9.11[139]. In the above synthesis, the nitrile oxides are produced from oximes, so it is also possible that a molecule of oxime could react with a molecule of nitrile oxide (Reaction C, Figure 9.11), to give yet more possible by-products. All the by-products formed from the nitrile oxides proposed in this thesis, will be highly lipophilic.

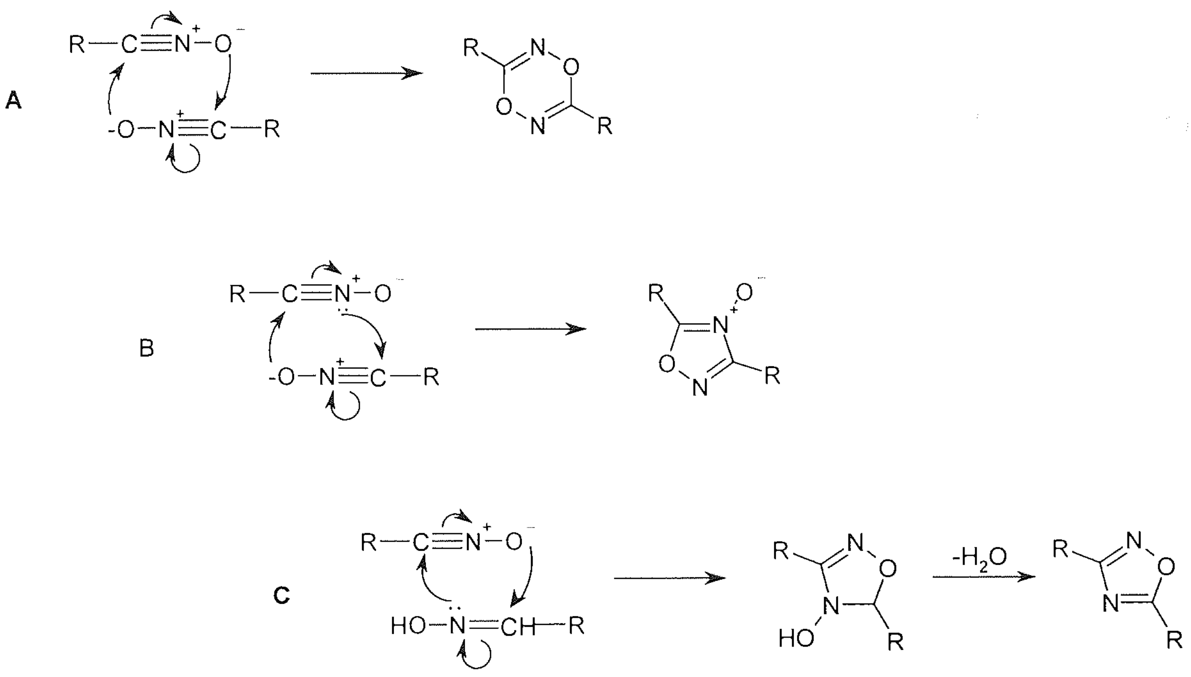

Figure 9.11 Possible dimerisation of nitrile oxides, **A** to form a 6-membered ring, **B** to form a 5-membered N-oxide. **C** reaction of a molecule of nitrile oxide with a molecule of oxime

Nitrile oxide cycloadditions to alkenes proceed regioselectively, such that the oxygen atom of the nitrile oxide usually connects to the more hindered position of monosubstituted alkenes[133,136].

9.3.1.1 Oximes

Oximes themselves are generally formed by the reaction of an aldehyde or ketone with hydroxylamine to form aldoxime or ketoxime respectively, as shown in Figure 9.12.

$$R^1R^2C{=}O + NH_2OH \rightarrow R^1R^2C{=}N\text{-}OH + H_2O$$

Figure 9.12 Reaction of aldehydes or ketones with hydroxylamine to give oximes

9.3.2 Isoxazolines

The preparation of five-membered heterocycles, in solution is well documented[140]. As previously mentioned, however, in this preparation of isoxazolines, the nitrile oxide readily dimerises. The resulting by-products are problematic in the solution phase synthesis of isoxazolines, as product purification becomes more difficult. In order to allow for this by-product formation, large excesses of the nitrile oxide are needed to be employed in the synthesis, which obviously wastes the reagent. It is not surprising therefore, that some solid-phase syntheses of these compounds have been carried out, which both eases the purification process and minimises the quantity of starting material to be used.

The solid-phase polymer supported synthesis of isoxazolines and isoxazoles has been reported, where the highly reactive nitrile oxide is immobilised, being covalently bonded to the polymeric support[136,137,141]. The major advantage of this, is the minimisation of the by-product formation which is observed. There is the disadvantage of using solid phase, however, that the product will always contain the linker group, which attaches the compound to the polymer.

General difficulties in solid phase work, however, also include the possibility of lower reactivity at the polymer-solvent interface and the difficulty of characterisation of intermediate products whilst still attached to the polymer[140].

9.3.3 Polyethylene Glycol Supported Dipolar Cycloaddition Of Alkynes

A dipolar cycloaddition reaction has been reported, using PEG as a soluble-polymer support. A soluble polymer-supported dipolarophile (an alkyne), was reacted with dipolar azides for the synthesis of triazole heterocycles (Figure 9.13)[140].

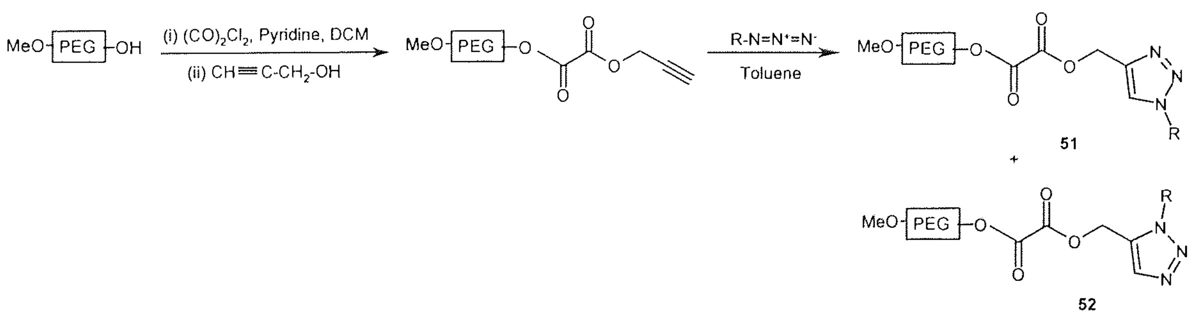

Figure 9.13 Synthesis of triazole heterocycles from an alkyne and an azide (R=carbohydrate)

The major isomer produced was isomer **51**, the product mixture being a 2:1 ratio of isomers. This would be the expected preferred isomer, as the bulk of the azidodeoxycarbohydrate (N_3R) is further away from the bulk of the polymer-supported dieneophile, which is sterically more favourable. The reaction afforded triazoles in 75% yield, no purity information is given[140].

9.4 SYNTHESIS OF POTENTIAL ANTIMYCOBACTERIAL ISOXAZOLINE SUBSTITUTED FATTY ACID ANALOGUES

9.4.1 Fatty Acid Analogues May Inhibit Mycolic Acid Synthesis

Mycolic acids (e.g. **32**) are a part of the cell wall structure specific to mycobacteria, as mentioned in Section 3.1. The biosynthesis pathway of these mycolic acids, which account for the unusual hydrophobicity of mycobacterial cells, offer potential drug targets[142].

It has been proposed that long chain fatty acid analogues, containing a non-standard atom or group, near the carboxyl end may inhibit mycolic acid production[141]. Barry *et al* reported long chain fatty acids containing a sulfur atom in the backbone[143] and Sacchetini *et al* reported a fatty acid with acetylenic unsaturation at the 2-position[144,145].

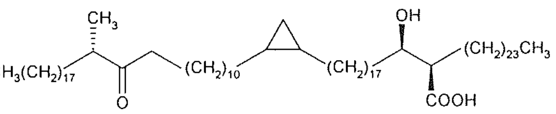

32

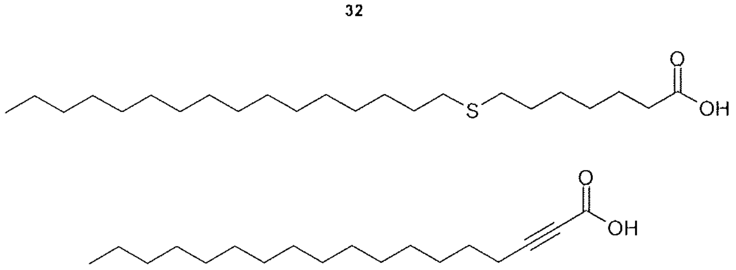

Figure 9.14 Top: A mycolic acid **32**. Middle and bottom: Some long chain fatty acid analogues which have been reported to possess antimycobacterial activity

9.4.2 Proposed Work

As discussed above, there have been reports in the literature of fatty acid derivatives possessing antimycobacterial, and in particular, antitubercular activity. As an extension of these findings, a series of fatty acid derivatives containing substituted Δ^2-isoxazolines at positions along the backbone was to be prepared Figure 9.15.

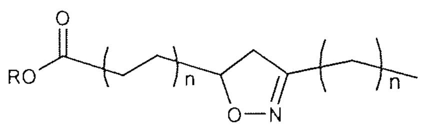

Figure 9.15 An example of a Δ^2-isoxazoline-substituted fatty acid

In Section 9.3.2 it was mentioned that during the preparation of isoxazolines in solution, by-products resulting from dimerisation of the nitrile oxide are a major impurity, which can be problematic to remove. Although the use of solid-phase synthesis could resolve this, the difficulty of characterisation of intermediate products whilst still attached to the polymer[140], makes this method less than ideal.

In these studies, therefore, a soluble polymeric support is to be utilised to carry out liquid-phase synthesis. Using this method, the major advantage of traditional solid-phase chemistry is retained, namely the ease of product separation from the reaction media, but in contrast, the chemistry is conducted under true solution phase conditions and the resin-bound products may be directly analysed by usual means, such as ^{1}H NMR[142].

Dihydroxy-polyethylene glycol of molecular weight 4000 (4000-PEG-OH) was used as the soluble-polymeric support, this has a loading capacity of 0.5mmol/g. Theoretically, any reaction occurring on PEG happens at both hydroxyl terminals of the molecule, in the Figures to follow, however, for reasons of clarity, the reaction will only be shown at one end of the molecule.

9.4.3 Discussion of The Synthesis of Some Isoxazoline Substituted Fatty Acid Analogues

9.4.3.1 Reaction of PEG with Unsaturated Acid Chlorides

Reaction of 4000-PEG-OH with an appropriate unsaturated acid chloride, results in a polymer bound ester, which would form the backbone of the fatty acid derivative. To investigate the affect of the position of the double bond comparative to the point of polymer attachment on the reaction, two acid chlorides were used. 10-Undecenoyl chloride was used as an example of a product where the double bond is distanced from the support **53**, and acrolyl chloride was used, as here, the double bond of the product is in conjugation with the ester group attached to the polymer **54** (see Scheme 9.1).

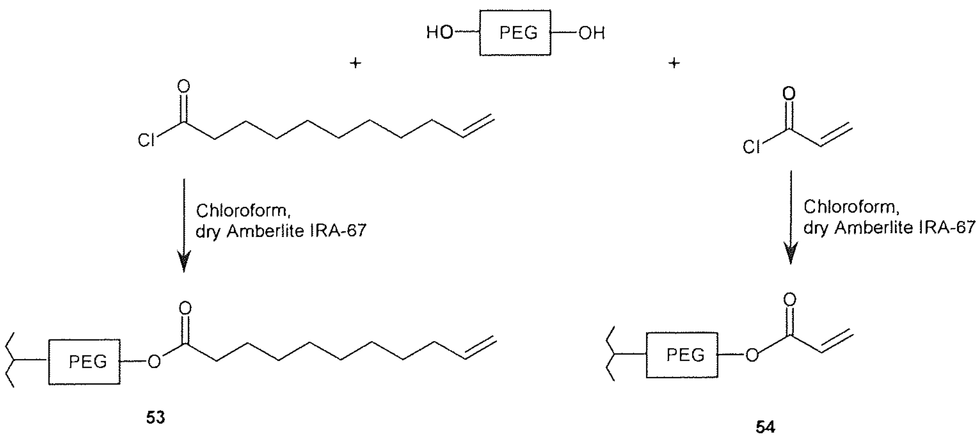

53

54

Scheme 9.1 Reaction of PEG with acid chlorides to give polymer supported compounds **53** and **54**

This reaction proceeded well, with crude reaction yields of 96-97%, the only impurity being the presence of unsubstituted PEG. The degree of substitution of the terminal hydroxyl groups of PEG, by other groups was determined from ^{1}H NMR in d_6-DMSO, using the method of Dust[131].

Dust *et al* reported that the ^{1}H NMR spectra of PEG derivatives in deuterated dimethylsulfoxide show a clean triplet (at 4.56ppm) for the hydroxyl protons at the polymer termini, which is well separated from the large PEG backbone peak , spinning side bands and ^{13}C satellites(3.0-4.0ppm). This hydroxyl peak does not shift or broaden with variation in the concentration of the PEG, or water. The percentage substitution of the hydroxyl groups of PEG can be calculated as shown in Figure 9.16.

$$\%\ \text{Substitution} = \left[\frac{\text{(integral of 1H from product)}}{\text{(integral of 1H from product)} + \text{(integral of OH from PEG)}} \right] \times 100$$

Figure 9.16 Calculation of the percentage substitution the hydroxyl groups of PEG

Applying this equation to the d_6-DMSO ^{1}H NMR spectra of **53** and **54**, the reaction in Scheme 9.1 went to 100% substitution for the long chain compound **53** and 62% for the acrolyl-PEG **54**.

9.4.3.2 *Isoxazoline Synthesis*

In order to form long chain fatty acid derivatives containing an isoxazoline heterocycle as in Figure 9.15, long chain nitriles would have to be used. For ease of analysis though, in this developmental phase of the chemistry, oximes **55** and **56** (Figure 9.17), derived from aldehydes **ae** and **bg** respectively were used, as the para-substitution of these molecules would ease the analysis of the ^{1}H NMR spectra. These two aldehyde derived oximes were also chosen, as these particular aldehyde fragments afforded antimycobacterial activity to some pyridinecarboxamidrazones (Chapter 5), and these isoxazoline compounds were also to be tested against *Mycobacterium fortuitum*.

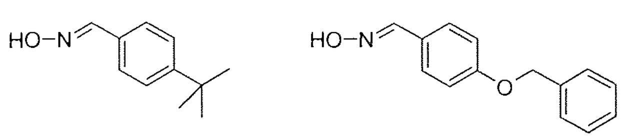

55 **56**

Figure 9.17 The two oximes used in the isoxazoline chemistry

The polymer bound esters undecanoyl-PEG **53** and acrolyl-PEG **54** were converted to the corresponding supported Δ^{2}-isoxazolines **57** in a 1,3-dipolar cycloaddition reaction by exposure to nitrile oxides, formed *in situ* from oximes, **55** and **56**, in an organic-aqueous biphasic system (Scheme 9.2).

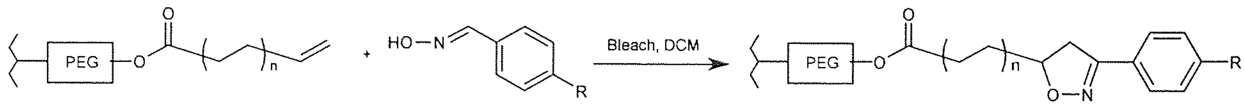

57

Scheme 9.2 Synthesis of supported Δ^2-isoxazolines **57**. n=4 for compound **53** and n= 0 for **54**

Table 9.1 Products and their codes, resulting from the synthesis in Scheme 9.2

Product Code	Oxime	Structure
58	**55**	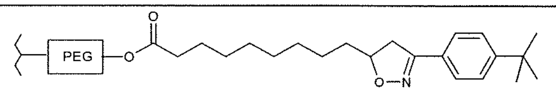
59	**56**	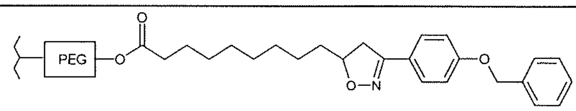
60	**55**	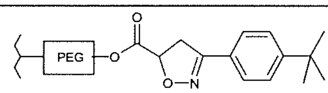
61	**56**	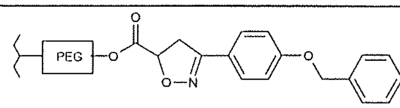

The cycloaddition of the oximes onto the alkenes of **53** and **54**, to give compounds **58-61**, worked well, to 100% completion judging by on-resin analysis via ^{1}H NMR spectroscopy, in recovered yields between 32 and 64%. The only impurities contaminating these PEG-bound products were very small quantities of the products of dimerisation of the nitrile oxide

Although it is possible for the cycloaddition of nitrile oxide to result in the formation of two isomers of isoxazoline, in the PEG-acrylate reactions with nitrile oxide, only one isomer was observed. As previously stated, nitrile oxide cycloadditions to alkenes proceed regioselectively, such that the oxygen atom of the nitrile oxide usually connects to the more hindered position of monosubstituted alkenes[129,132]. During the reaction of the longer chain alkene with the nitrile oxide from oxime **55**, however, two isomers of the isoxazoline were observed by ^{1}H NMR spectroscopy (see Figure 9.18). The major isomer was the more sterically preferred, **isomer 1**, where the oxygen atom of the nitrile oxide connects to the more hindered position of the alkene. The alternative isomer, **isomer 2**, was also present in a small amount. This is the only reaction in which both of the two possible isomers were seen.

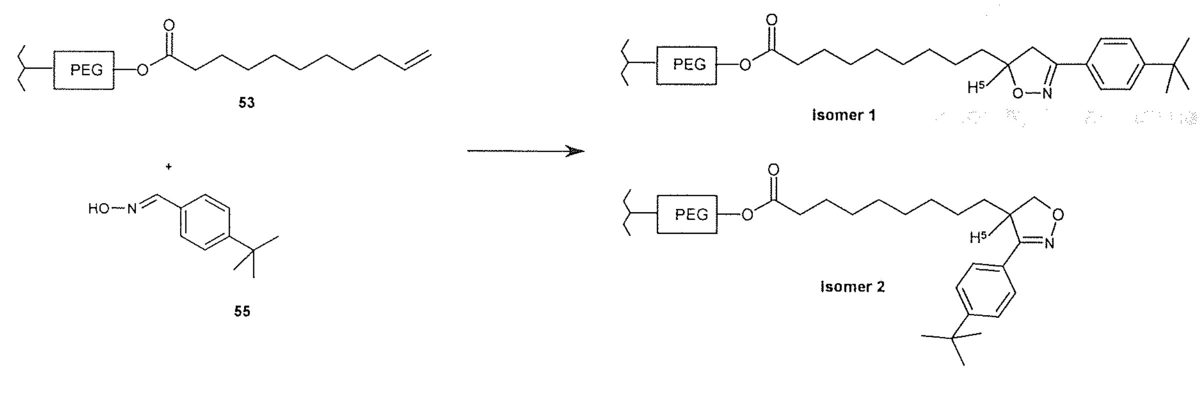

Figure 9.18 The two isomeric products formed when **53** is reacted with **55**

The ^{1}H NMR spectrum of the cleaved isoxazoline products is indicative of which compound isomer predominates. It is the signal from the hydrogen atom at the 5- position of the isoxazoline ring which is most useful in determining which isomer is which. The molecule has a chiral centre at this point, which is adjacent to the pro-chiral centre at position 4-, so the signal from the H5 proton is a complex multiplet. The chemical shifts of the two isomers are different and it is this which is most helpful. Referring to Figure 9.18, the major isomer is **isomer 1**; in this molecule, the H5 proton is adjacent to the oxygen atom in the heterocyclic ring, which will have deshielding effect upon H5 and the signal is shifted downfield to 4.72ppm. In the minor isomer, **isomer 2**, the hydrogen at position-5- is distanced from the heteroatoms of the isoxazoline ring and the chemical shift is further upfield at 4.31ppm.

The reason that the PEG-acrylate **54**, isoxazoline products resulted in only the more favoured isomer, is steric. The double bond of **54** is adjacent to the polymer itself, whose bulk will prevent the approach of the nitrile oxide in the more hindered manner. In the undecanoyl-PEG **53**, however, the double bond is at the terminus of a long alkyl chain, thus the difference in the steric natures of the two ends of the alkene bond is not as great, and the approach of the nitrile oxide in the more hindered manner, is possible.

The reaction of the undecanoyl-PEG **53** with the nitrile oxide from oxime **56** only resulted in the production of the one, sterically preferred isomer. The reason for this is not really understood. Oxime **56** is similar, both electronically and sterically to oxime **55**, which did result in two product isomers, as shown in Figure 9.18, and one would expect the two nitrile oxides to act in a similar fashion.

9.4.3.3 Cleavage from Polymeric Support

Cleavage was attempted in two ways, firstly, cleavage via methanol and secondly by an amine (isobutylamine) as shown in Scheme 9.3.

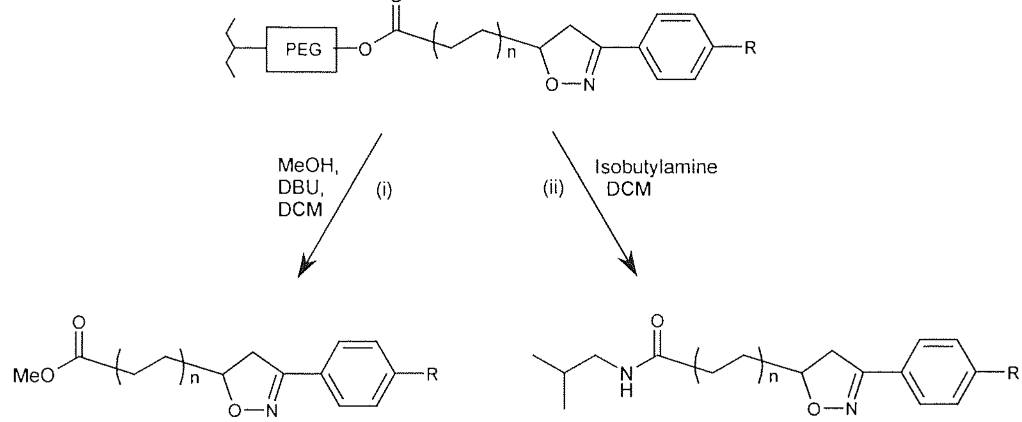

Scheme 9.3 Cleavage of isoxazoline products from the PEG-support, (i) via methanol and (ii) via isobutylamine

The methanolic cleavage from polyethylene glycol was aided by 1,8-diazabicycloundec-7-ene (DBU), a strong, hindered amine base (Figure 9.19). The base is used to facilitate the deprotonation of methanol, in order to produce small amounts of nucleophillic methoxide ions which are required for ester cleavage of the isoxazoline products from PEG, as shown in Figure 9.20.

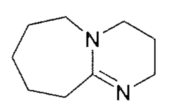

Figure 9.19 1,8-diazabicycloundec-7-ene (DBU)

$$\text{MeOH} + \text{DBU} \rightleftharpoons \text{MeO}^{-} + \text{DBU}^{+}\text{—H}$$

Figure 9.20 Production of methoxide ions by DBU proton abstraction from methanol

Table 9.2 Products and their codes, resulting from the cleavage in Scheme 9.3

Product Code	Cleaved with	Parent Compound	Structure
62	MeOH	**58**	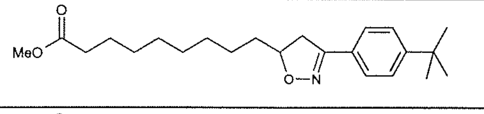
63	MeOH	**59**	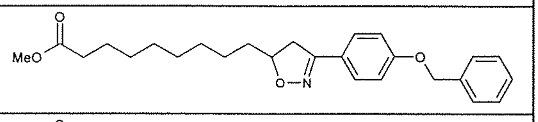
64	MeOH	**60**	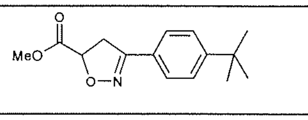
65	MeOH	**61**	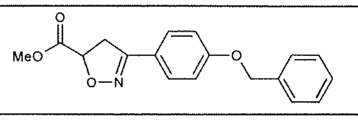
66	isobutylamine	**60**	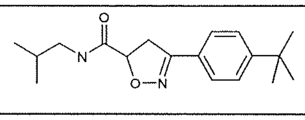
67	isobutylamine	**61**	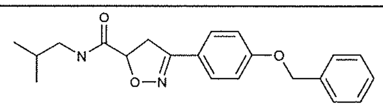

Methanolic cleavage of the isoxazoline products from the soluble polymeric support worked well for all compounds on both the undecanoyl-PEG **53** and acrolyl-PEG **54**, with crude cleavage yields between 41-96%, the PEG-acrylate compounds giving the better yields. The crude products were subjected to preparative TLC, after which the desired compounds were obtained with greater than 95% purity. The purified yields were, however, generally low, between 8 and 12%.

For compound **62**, where two isomers were observed on the polymer, the relative quantities of each isomer could be seen more clearly after cleavage. The major isomer (i.e. **isomer 1** in Figure 9.18) was approximately five times more abundant than the minor isomer (**isomer 2** in Figure 9.18).

Cleavage from the polymer by the amine isobutylamine, was only successful for the compounds attached to the acrolyl-PEG **54**, with crude cleavage yields of 61-98%. The crude products were subjected to preparative TLC, after which the desired compounds were obtained with greater than 95% purity. The purified yield for compound **66** was 38%, but only 7% for compound **67**, it is not known why there is such a large difference between these two yields, of structurally similar compounds.

Attempted aminolysis from undecanoyl-PEG **53**, did not result in the desired compounds. The isobutylamine cleavage was successful for the PEG-acrylate **54** compounds, perhaps because the isoxazoline ring, adjacent to the linker group in these compounds, electronically contributes to the reaction. The isoxazoline ring would have an electron-withdrawing effect on the carbonyl-carbon of the ester-link, rendering it more susceptible to nucleophillic attack by the amine. In the undecanoyl-PEG **53** compounds, the isoxazoline ring is electronically insulated from the ester-linkage being cleaved and would not be able to contribute to the mechanism.

9.4.3.4 On-Resin Analysis

The characterisation of PEG-bound organic entities was indeed found to be straightforward, as predicted in Section 9.1.2. The polymer does not interfere with the ^{1}H NMR spectra of the PEG-bound compounds, as demonstrated by Figure 9.21. The only signals from PEG itself are those from the methylene protons of the PEG backbone (3-4ppm)[131], and the PEG-OCH_2 which are separated out slightly from the main PEG signal, at around 4.2ppm.

The polyethylene glycol used in this study had an average molecular weight of 4000. If a larger molecular weight PEG (e.g. PEG 20 000) was used, whilst its solubilising power and crystalisation properties would be further improved, the loading capacity would be much reduced. Analytically, products bound to a higher molecular weight PEG would be more difficult to observe by ^{1}H NMR spectroscopy. The methylene protons peak from PEG itself will be more intense, and, due to the low loading of product, the product signals will be very small in comparison. The product signals would have to be amplified greatly in order to be viewed. The PEG peak would also be amplified at the same time, and as the slopes of this peak are amplified, they could conceal signals from the product, in the proximity.

4000-PEG-OH was a good compromise of molecular weight to use. It was large enough to have good solubilising and crystalising properties, but, at the same time, small enough to possess a reasonable loading capacity (0.5mmol per gramme) and so therefore, allowed the PEG-bound products to be viewed easily by ^{1}H NMR spectroscopy.

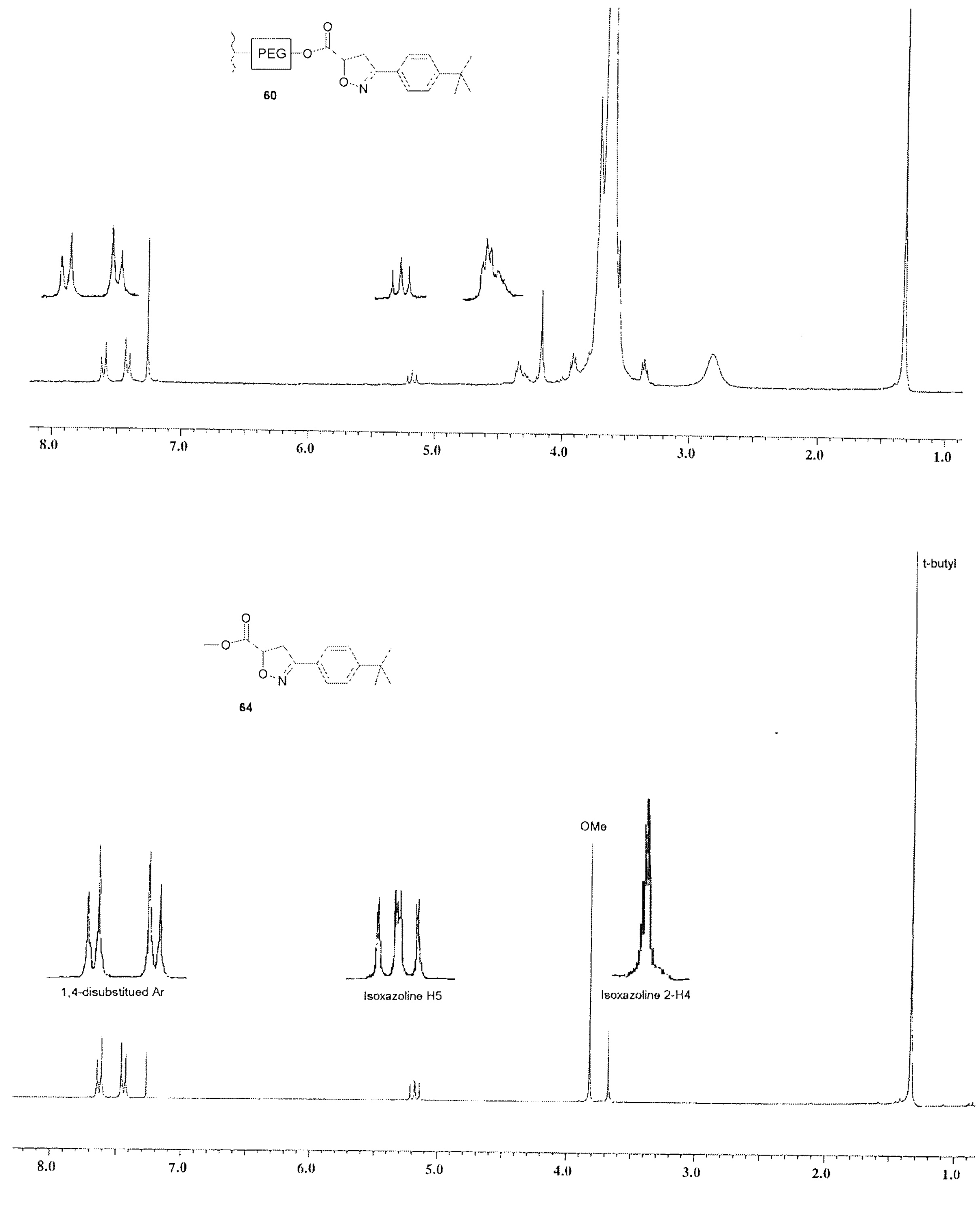

Figure 9.21 ^{1}H NMR spectra ($CDCl_3$) Top: an acrolyl-PEG isoxazoline product **60**, prior to cleavage from the polymer. Bottom: the final product **64**, after methanolic cleavage. When the two spectra are compared, it can be seen that the proton signals from PEG do not interfere with the product signals.

9.4.4 Results and Discussion of Antimycobacterial Testing of PEG-Bound and Cleaved Isoxazoline Products

Each of the isoxazoline compounds formed, including the polymer bound products, were tested against *Mycobacterium fortuitum*, using the 'gate' method described in Section 5.2. The cleaved products were tested at a single concentration of 32μgml^{-1}, as carried out for the benzylidene-pyridinecarboxamidrazones previously. The PEG-bound compounds were tested at the higher concentration of 320μgml^{-1}, due to their molecular weights being an order of magnitude larger than the cleaved products.

Table 9.3 Antimycobacterial testing results versus *Mycobacterium fortuitum* (*M.fort*).

Code	Structure	*M.fort* Gate ≤320μgml^{-1}	*M.fort* Gate ≤32μgml^{-1}	*M.fort* MIC (μgml^{-1})
58	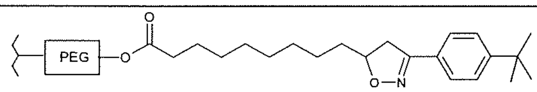	x		
59	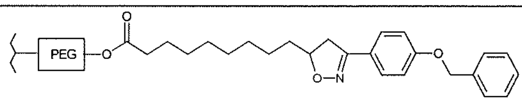	x		
60	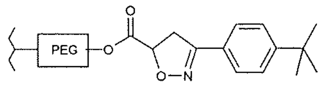	x		
61	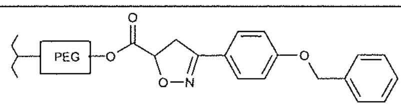	x		
62	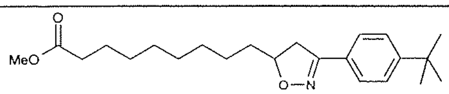		x	>256
63	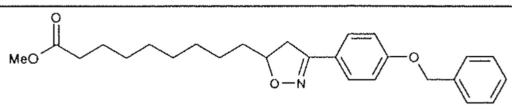		x	>256
64	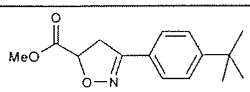		x	64-128
65	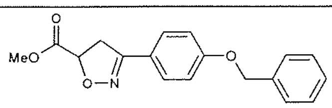		x	>256
66	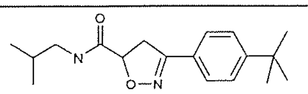		x	64-128
67	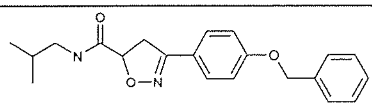		x	>256

Since none of the compounds displayed any activity at these 'gate' concentrations, and the class of compounds was novel, it was of interest to see whether the cleaved compounds possessed any weak antimycobacterial activity. For these reasons, the compounds were tested for an MIC, up to the concentration of 256μgml^{-1}. Two compounds, **64** and **66**, were observed to have weakly antimycobacterial activity, both displaying activities of 64-128μgml^{-1}. It is of interest that both of these compounds are cleavage products of PEG-acrylate **54**, and that the *t*-butylphenyl group afforded activity to these compounds as well as the pyridinecarboxamidrazones (Chapter 5).

This chemistry, to synthesise long chain fatty acid derivatives, has proved to be quite workable. It would be of interest to continue this work, using long chain nitrile oxides. The resulting compounds would be truer to the fatty acid derivative model containing an isoxazoline group (Figure 9.12), which was the original target of this work.

CHAPTER 10
CONCLUSIONS

10.1 ANTI-MYCOBACTERIAL STUDIES

The best compounds discovered against mycobacteria are shown below. It was unfortunate that, despite the number of compounds synthesised in this study, an MIC below 4μgml^{-1} was not achieved. **2PYaf** was, however, sufficiently active against *M.tuberculosis* for the TAACF to conduct further tests into the suitability of this compound as a potential drug candidate.

Table 10.1 The lead compounds discovered against *M.fortuitum* and *M.tuberculosis* (**2PYaf**)
(-) indicates that the compounds were not tested in that particular way

Code	Compound	*M.fortuitum* MIC (μgml^{-1})	*M.tuberculosis* % Inhibition	*M.tuberculosis* MIC (μgml^{-1})
2PYaf	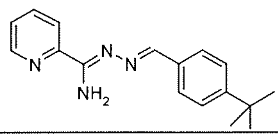	**4-8**	**94**	**-**
2PYbh	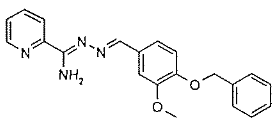	**4-8**	**42**	**-**
2PYbn	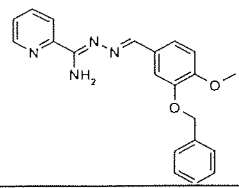	**4-8**	**72**	**8-16**
4PYbn	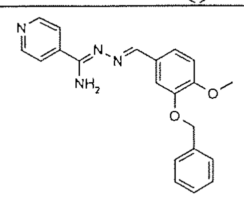	**4-8**	**-**	**-**

The results in Table 10.1 have proven that there is some interesting activity within the benzylideneheteroarylcarboxamidrazones, and perhaps if this class of compounds is probed further, then still more molecules possessing biological activity could be found.

The amidrazone starting materials are not just confined to reactions with aldehydes either. The chemistry with ketones has not been thoroughly investigated here. The amidrazones **2PY**, **4PY**, **PZ**, **QN** etc., could also be reacted with other classes of compounds, such as acid chlorides and sulfonyl chlorides, to produce similar compounds, but with a different functional group in place of the imine in the above compounds.

10.2 MOLECULAR MODELLING

QSAR studies were utilised in Chapter 6 to obtain equations to predict the biological activity of the benzylideneheteroarylcarboxamidrazones. When these compounds were separated into their separate heteroaryl groups, improved predictive power [higher r^2 and r^2(CV) values] and better graphs of correlation between predicted and observed activity, were obtained.

The next step would be to use these equations to predict where activity may lie in a 'virtual' library of compounds. For example, one could input all the compounds which could be made from all of the commercially available aldehydes into the TSAR database, which will then calculate all the molecular properties and finally use the relevant equation to predict which compounds are more likely to display activity against *M.tuberculosis*. Although TSAR may not predict the activities exactly, it should give an indication of which compounds are worth synthesising, and which are not.

It would be of interest to carry out the above procedure for all the possible benzylidene-pyridine-2-carboxamidrazones and to then actually synthesise the compounds with promising biological activities. The compounds would then be tested against the mycobacteria in the laboratory, and the results could be compared to identify whether or not the computational calculations gives a true picture of in which molecules activity lies.

10.3 ANTI-BACTERIAL STUDIES

The most active compound found against MRSA was **4PYcq**, which was active at 2-4μgml^{-1} against all the strains tested (Shown below). At this concentration, the compound was also active against all the other Gram-positive bacteria tested, including a panel of vancomycin resistant enterococci. No activity was observed for this compound against Gram-negative organisms .

Table 10.2 The lead compound discovered against MRSA, also active against VREs

Code	Structure	MRSA MIC(μgml^{-1})	VRE MIC(μgml^{-1})
4PYcq	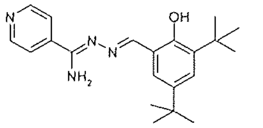	2-4	2-4

It was initially thought that **4PYcq** was a good lead compound, but the compound's activity was very sensitive to structure changes and any alteration attempted, such as a change from the 4- to a 2-pyridyl ring, replacement of the hydroxyl group by a methoxy group or using smaller alkyl groups resulted in loss of activity. **4PYcq** itself was also found to be very toxic, causing lysis of leucocytes. Further study of the compound as a potential drug was abandoned.

10.4 PEG CHEMISTRY

Polyethylene glycol (PEG) was used as a soluble polymeric support for the synthesis of some fatty acid derivatives, containing an isoxazoline group, which were thought could potentially inhibit mycolic acid synthesis in mycobacteria. The solution-phase chemistry: attachment of an unsaturated acid chloride to PEG, the 1,3-dipolar cycloaddition reaction of nitrile oxides with the PEG bound molecule and the methanolic cleavage of the final product from the solid support all proceeded well. The characterisation of PEG-bound organic entities by ^{1}H NMR was found to be straightforward.

Both the PEG-bound products and the cleaved, isolated products themselves were tested against *M.fortuitum* and some low levels of antimycobacterial activity were observed, which may serve as lead compounds for further studies. It would be of interest to continue this work, using long chain nitrile oxides. The resulting compounds would be truer to the fatty acid derivative model containing an isoxazoline group (Figure 9.12), which was the original target of this work.

CHAPTER 11
MATERIALS AND METHODS

11.1 INSTRUMENTATION

Robotic procedures were performed using a Tecan 5072 robotic sample processor. Proton NMR spectra were obtained on a Bruker AC 250 instrument operating at 250MHz as solutions either in d_6-DMSO and referenced from δDMSO=2.50ppm, or in $CDCl_3$ and referenced from δ$CDCl_3$= 7.27ppm. Carbon NMR spectra were obtained on the same instrument operating at 66MHz as solutions in $CDCl_3$ and referenced from δ$CDCl_3$=77ppm. Where it was not obvious which signals resulted from quaternary carbon atoms, DEPT spectra were obtained. R.f. values were obtained by thin layer chromatography, on aluminium silica gel 60 F_{254} plates; where two or more spots were observed, the dominant spot is underlined. Atmospheric pressure chemical ionisation mass spectrometry (APCI-MS) was carried out on a Hewlett-Packard 5989B quadrupole instrument connected to an electrospray 59987A unit with an APCI accessory and automatic injection using a Hewlett-Packard 1100 series autosampler. Positive APCI-MS was used, unless otherwise stated. Infrared (IR) spectra were recorded mainly as KBr discs, with a few spectra recorded as solutions in chloroform, on a Mattson 3000FTIR spectrophotometer. Interpretation of IR spectra and carbon NMR spectra were aided by relevant tables[146]. Melting points were obtained using a Reichert-Jung Thermo Galen hot stage microscope and are corrected by calibration against a compound of known melting point. Elemental analyses were performed by Butterworth Laboratories Ltd., Teddington, UK.

11.2 *N^1*-BENZYLIDENEHETEROARYLCARBOXAMIDRAZONE CHEMISTRY

11.2.2 Preparation of Heteroarylcarboxamidrazone

11.2.2.1 Pyridine-2-carboxamidrazone **2PY**

Hydrazine hydrate (15ml) was added to a solution of pyridine-2-carbonitrile (8.5g, 81mmol) in ethanol (15ml) and left at RT for 2 days. The solution was then diluted with an equal volume of water, extracted with ethyl acetate [rather than with ether as in the method proposed by Case[147], as this gave poor yields] and dried over sodium sulfate. The solvent was then removed by rotary evaporation, at 30°C-40°C, to give the product (8.17g, 73%). R.f. [EtOAc:MeOH (2:1)]: 0.10. ^{1}H NMR: 5.33 (bs, 2H, NH_2), 5.73 (bs, 2H, NH_2), 7.31 (ddd, 1H, J=4.9, 2.4, 1.3Hz, H4 or H5), 7.74

(ddd, 1H, J=6.9, 2.4, 1.8Hz, H4 or H5), 7.90 (m, 1H, H3 or H6), 8.48 (m, 1H, H3 or H6). APCI-MS m/z: 137 $(M+H)^+$.

11.2.2.2 Pyridine-3-carboxamidrazone[94] **3PY**

Hydrazine (80%, 21.5ml) was added to a solution of pyridine-3-carbonitrile (6.4g, 62mmol) in ethanol (10ml) and ether (10ml). The mixture was left at RT, with stirring for five days, after which the majority of the solvent was removed by rotary evaporation, at 30°C-40°C. The residual solution was cooled and a precipitate formed which was obtained by filtration and rapidly washed with ether to yield 6.00g (55%). R.f. [EtOAc:MeOH (2:1)]: 0.10. ^{1}H NMR: 5.78 (bs, 4H, $2(NH_2)$), 7.34 (m, 1H, H4 or H6), 7.99 (m, 1H, H4 or H6), 8.48 (dd, J=4.8, 1.6Hz, H5), 8.86 (d, J=1.8Hz, H2). APCI-MS m/z: 137 $(M+H)^+$.

11.2.2.3 Pyridine-4-carboxamidrazone **4PY**

Prepared from pyridine-4-carbonitrile, using the same method as pyridine-3-*carboxamidrazone* **3PY**, to yield 5.00g (67%). R.f. [EtOAc:MeOH (2:1)]: 0.18. ^{1}H NMR: 5.33 (bs, 2H, NH_2), 5.71 (bs, 2H, NH_2), 7.63 (d, 2H, J=6.3Hz, Pyr-H), 8.50 (d, 2H, J=6.3Hz, Pyr-H). APCI-MS m/z: 137 $(M+H)^+$.

11.2.2.4 Pyrazine-2-carboxamidrazone **PZ**

Prepared from pyrazine-2-carbonitrile, using the same method as pyridine-2-carboxamidrazone **2PY** to yield 8.61g (66%). R.f. [EtOAc:MeOH (9:1)]: 0.23. ^{1}H NMR: 5.62 (bs, 2H, NH_2), 5.71 (bs, 2H, NH_2), 8.52 (s, 2H, H5 and H6), 9.10 (d, 1H, J=1.2Hz, H3). APCI-MS m/z: 138 $(M+H)^+$.

11.2.2.5 Quinoline-2-carboxamidrazone **QN**

Prepared from quinoline-2-carbonitrile, using the same method as pyridine-2-carboxamidrazone **2PY** to yield 4.78g (81%). R.f. [EtOAc:MeOH (9:1)]: 0.39. ^{1}H NMR: 5.66 (bs, 2H, NH_2), 5.92 (bs, 2H, NH_2), 7.55 (m, 1H, H6 or H7), 7.73 (m, 1H, H6 or H7), 7.92 (d, 1H, J=8.4Hz, H5 or H8), 8.00 (d, 1H, J=8.6Hz, H5 or H8), 8.05 (d, 1H, J=8.8Hz, H3 or H4), 8.23 (d, 1H, J=8.8Hz, H3 or H4). APCI-MS m/z: 187 $(M+H)^+$.

11.2.3 Automated Synthesis of The N^1-Benzylideneheteroarylcarboxamidrazone and Hydrazone Library

Glass 4ml vials in a matrix were charged with 2-pyridylhydrazine **HD** (Aldrich) and each of the heteroarylcarboxamidrazones (0.4mmol) in methanol (1ml), with the exception 2-quinolylcarboxamidrazone , which was insoluble, so had to be weighed manually. This was followed by addition of an ethanolic solution of aldehyde (0.25M, 1.8ml, 1.1eq). The vials were heated in a heating block at 65°C for one hour to remove the methanol, then at 75°C for up to two hours, during which time the ethanol evaporated, to give the crude products. Purification was performed by robotic trituration (3x3ml ether or petroleum ether depending upon the lipophilicity of the material).The products were then dried under high vacuum prior to analysis (yield range 60-97%).

All compounds were analysed by thin layer chromatography and positive APCI-MS (Table 11.1). Initially 10% of the compounds were analysed by ^{1}H NMR, then any compounds which showed biological activity in the primary screen, were also analysed by ^{1}H NMR (Table 11.2) and purified, if necessary, usually by recrystalisation, prior to further biological testing. Compounds which displayed antimycobacterial activity at concentrations of 16-32μgml^{-1} or less were also subjected to ^{13}C NMR, infrared, melting point and elemental analyses.

Table 11.1 Analysis of the N^1-benzylideneheteroarylcarboxamidrazone library. In most cases R.f. values were determined using ethyl acetate as the eluent. (^{a}) denotes that an ethyl acetate/methanol (9:1) mixture was used as the TLC eluent. Where two R.f. or m/z values are given, the underlined value was the most prominent. * represents the m/z value for the **3PY** reaction bis-substituted by-product (See Section 4.3). %Yield refers to the crude product yield. Purity, where given, has been estimated by ^{1}H NMR. Where the NMR has been measured and the compound is of sufficient purity, the data is given in Table 11.2 and this is denoted by a tick in the column labelled '^{1}H NMR'.

Compound	Appearance	MW	% Yield	APCI-MS m/z	R.f.	% Purity	^{1}H NMR
2PYaa	Yellow crystals	224	59	225	0.48		
2PYab	Yellow crystals	238	66	239	0.59	90	✓
2PYac	Yellow solid	252	56	253	0.53	98	✓
2PYad	Yellow crystals	266	59	267	0.60	98	✓
2PYae	Yellow solid	280	66	281	0.62	98	✓
2PYaf	Yellow solid	294	80	295	0.63	98	✓
2PYag	Yellow solid	300	85	301	0.60		
2PYah	Yellow-brown solid	238	74	239	0.55	98	✓
2PYai	Yellow solid	252	55	253	0.58		
2PYaj	Beige solid	238	84	239	0.39		
2PYal	Yellow solid	274	90	275	0.53	95	✓
2PYam	Orange solid	324	78	325	0.65	98	✓
2PYan	Yellow solid	324	80	325	0.64		
2PYao	Yellow solid	250	63	251	0.75		
2PYar	Brown oil	302	97	303	0.55	92	
2PYas	Yellow crystals	254	90	255	0.25	98	✓

Compound	Appearance	MW	% Yield	APCI-MS m/z	R.f.	% Purity	^{1}H NMR
2PYat	Yellow solid	268	57	269	0.47		
2PYau	Yellow solid	282	82	283	0.51		
2PYav	Yellow crystals	296	80	97	0.54	98	
2PYaw	Yellow solid	352	56	353	0.60		
2PYax	Brown solid	254	92	255	0.53	98	✓
2PYay	Yellow solid	268	88	269	0.52	98	✓
2PYaz	Yellow solid	282	38	283	0.54	80	✓
2PYba	Yellow solid	296	82	297	0.54		
2PYbb	Yellow solid	310	41	311	0.55		
2PYbc	Yellow solid	324	55	325	0.55		
2PYbd	Yellow solid	254	73	255	0.22		
2PYbe	Yellow solid	330	65	331	0.70	98	✓
2PYbf	Yellow crystals	330	46	331	0.74	80	✓
2PYbg	Yellow crystals	330	94	331	0.67	90	✓
2PYbh	Yellow solid	360	74	361	0.47	89	✓
2PYbi	Yellow solid	374	92	375	0.45		
2PYbj	Yellow solid	388	77	389	0.46		
2PYbk	Yellow solid	374	79	375	0.49		
2PYbl	Yellow solid	416	83	417	0.49		
2PYbm	Yellow crystals	405	43	406	0.53		
2PYbn	Yellow solid	360	90	361	0.52	87	✓
2PYbo	Yellow solid	374	89	375	0.28	98	✓
2PYbp	Yellow solid	388	64	389	0.40	98	✓
2PYbq	Yellow solid	374	81	375	0.42	98	✓
2PYbr	Yellow solid	416	86	417	0.45		
2PYbs	Yellow crystals	436	67	437	0.68		
2PYbt	Light brown solid	360	90	361	0.69	75	✓
2PYbu	Yellow crystals	390	66	391	0.60		
2PYbv	Yellow solid	366	78	367	0.70		
2PYbw	Brown solid	240	45	241	0.35		
2PYbz	Orange crystals	256	38	257	0.29		
2PYca	Brown solid	256	73	257	0.30	72	
2PYcb	Dark brown solid	272	89	273	0.30	98	✓
2PYcc	Brown solid	272	66	273	0.25	68	
2PYcd	Orange-brown solid	272	52	273	0.09		
2PYce	Light brown crystals	270	57	271	0.64		
2PYcf	Yellow crystals	270	54	271	0.67	98	✓
2PYcg	Yellow solid	270	68	153, 271	0.31	66	
2PYch	Yellow solid	270	76	153, 271	0.29	75	
2PYci	Yellow solid	284	66	285	0.32		
2PYcj	Brown solid	285	82	286	0.30	98	✓
2PYck	Light brown solid	315	75	316	0.44		
2PYcl	Brown solid	364	88	365, 367	0.47	65	
2PYcm	Dark brown solid	330	90	331	0.06	85	
2PYcn	Brown solid	364	75	365, 367	0.10		
2PYco	Yellow solid	492	80	493	0.62		
2PYcp	Yellow solid	268	80	269	0.60		
2PYcq	Yellow solid	352	72	235, 353	0.79	80	
2PYcr	Yellow solid	352	95	353	0.75		
2PYcs	Yellow solid	284	53	285	0.53		
2PYct	Light brown crystals	284	66	285	0.35		
2PYcv	Yellow crystals	298	42	299	0.43	85	

Compound	Appearance	MW	% Yield	APCI-MS m/z	R.f.	% Purity	^{1}H NMR
2PYcw	Yellow crystals	298	69	299	0.33		
2PYcy	Yellow solid	312	50	313	0.40		
2PYcz	Brown solid	298	62	181, 299	0.19		
2PYdb	Yellow solid	290	48	291	0.69	98	✓
2PYdc	Brown crystals	304	67	305	0.73		
2PYdd	Yellow-brown solid	304	62	187, 305	0.54	78	✓
2PYdg	Yellow solid	258	57	259, 261	0.60	98	✓
2PYdm	Yellow solid	292	86	293	0.66	98	✓
2PYdn	Yellow-brown solid	269	57	270	0.50	98	✓
2PYdo	Orange-brown solid	269	73	270	0.49		
2PYdr	Yellow solid	281	77	164, 282	0.36	88	
2PYds	Yellow solid	325	89	208, 326	0.18	88	
2PYdu	Brown solid	228	90	229	0.06		
2PYdx	Brown solid	317	80	200, 318	0.56	82	✓
2PYeb	Light brown solid	292	76	105, 189, 293	0.85	98	✓
2PYec	Orange-brown solid	306	57	105, 203, 307	0.67		
2PYed	Yellow solid	230	68	231	0.55	98	✓
2PYee	Yellow solid	270	78	271	0.76		
2PYeh	Yellow solid	366	75	367, 369	0.59	98	✓
3PYab	Yellow solid	238	78	239, 237*	0.31, 0.70		
3PYac	Yellow solid	252	89	253, 265*	0.29		
3PYad	Yellow solid	266	60	267, 293*	0.30		
3PYae	Yellow crystals	280	42	281, 321*	0.25, 0.79	98	✓
3PYaf	Orange solid	294	59	295, 349*	0.26, 0.84	98	✓
3PYag	Yellow solid	300	76	301, 361*	0.21, 0.78		
3PYah	Orange solid	238	63	237*, 239	0.10, 0.42	70	
3PYai	Orange solid	252	60	253, 265*	0.40, 0.70		
3PYaj	Red solid	238	54	237*, 238	0.33, 0.66		
3PYak	Yellow solid	274	68	275, 309*	0.16, 0.79		
3PYal	Orange solid	274	76	275, 309*	0.22, 0.78	67	
3PYam	Orange solid	324	66	325, 409*	0.30, 0.77	60	
3PYan	Yellow solid	324	66	325, 409*	0.28, 0.77	60	
3PYas	Yellow solid	254	58	255, 269*	0.25, 0.78		
3PYat	Yellow solid	268	34	269, 296*	0.20, 0.70		
3PYau	Yellow solid	282	38	283, 324*	0.20, 0.74		
3PYav	Yellow solid	296	69	297, 353*	0.21, 0.74	60	
3PYaw	Yellow solid	352	50	353	0.29, 0.80		
3PYax	Orange solid	254	62	255, 269*	0.28, 0.74		
3PYay	Yellow solid	268	40	269, 297*	0.05, 0.51	98	✓
3PYaz	Yellow solid	282	44	283, 325*	0.36, 0.74		
3PYba	Yellow solid	296	70	297, 353*	0.39, 0.72	98	✓
3PYbb	Yellow solid	310	37	311, 381*	0.43, 0.75		
3PYbc	Yellow solid	324	46	325, 409*	0.44, 0.76		
3PYbe	Yellow solid	330	41	331, 421*	0.33		
3PYbf	Light yellow solid	330	76	331, 421*	0.31	98	✓
3PYbg	Light orange solid	330	79	331, 421*	0.23		
3PYbh	Yellow solid	360	42	361, 481*	0.27, 0.60	98	✓
3PYbm	Yellow solid	405	46	406	0.17		
3PYbn	Light yellow solid	360	48	361, 481*	0.35, 0.61	98	✓
3PYbs	Light yellow solid	436	68	437	0.28		
3PYbt	Yellow solid	360	44	361, 481*	0.39, 0.71	85	
3PYbu	Brown solid	390	54	391	0.06, 0.29		

Compound	Appearance	MW	% Yield	APCI-MS m/z	R.f.	% Purity	^{1}H NMR
3PYca	Yellow solid	256	55	257, 273*	0.68		
3PYcb	Brown solid	272	92	274, 305*	0.16		
3PYcc	Brown solid	272	79	273, 305*	[a]0.45	60	
3PYcd	Brown solid	272	89	273, 305*	[a]0.47, 0.61		
3PYcf	Orange solid	270	68	271, 301*	0.41, 0.65		
3PYcj	Yellow solid	285	83	285, 331*	[a]0.52, 0.80	60	
3PYcl	Orange solid	364	82	365, 367	[a]0.49	63	
3PYcm	Orange solid	330	77	331, 421*	[a]0.44		
3PYcq	Light orange crystals	352	40	353	0.43, 0.85		
3PYcr	Orange solid	352	43	353	0.39, 0.82		
3PYdb	Brown solid	290	92	291, 341*	0.30	67	
3PYdc	Orange solid	304	64	305, 369*	0.26		
3PYdd	Yellow solid	304	40	305, 369*	0.16, 0.72		
3PYdg	Yellow solid	258	40	259, 261, 277*, 279, 281	0.20		
3PYdq	Yellow-orange solid	267	50	267, 295*	0.81		
3PYds	Yellow solid	325	79	326, 411*	0.10, 0.48	67	
3PYdt	Red solid	213	82	187*, 214	0.11, 0.74		
3PYdv	Orange crystals	225	47	211*, 226	0.06		
3PYdw	Yellow solid	225	46	211*, 226	0.12		
3PYdx	Orange solid	317	60	317, 395*	0.23, 0.78		
3PYeg	Orange solid	354	52	354	0.93		
3PYeh	Yellow solid	366	76	367, 369	0.32, 0.82		
4PYaa	Yellow solid	224	82	225	0.50	98	✓
4PYab	Yellow solid	238	75	239	0.40		
4PYac	Yellow solid	252	38	253	0.56		
4PYad	Yellow solid	266	86	267	0.40		
4PYae	Yellow solid	280	55	281	0.37	98	✓
4PYaf	Yellow solid	294	60	295	0.38	98	✓
4PYag	Yellow crystals	300	93	301	0.33		
4PYah	Orange solid	238	40	239	0.47		
4PYai	Yellow solid	252	42	253	0.48	90	
4PYaj	Orange solid	238	40	239	0.42		
4PYak	Yellow solid	274	79	275	0.33		
4PYal	Yellow solid	274	60	275	0.33	98	✓
4PYam	Orange crystals	324	87	325	0.32	98	✓
4PYan	Orange solid	324	88	325	0.26		
4PYao	Yellow solid	250	64	251	0.35	90	
4PYar	Brown solid	302	42	303	0.48		
4PYas	Yellow solid	254	60	255	0.60		
4PYat	Yellow solid	268	36	269	0.56		
4PYau	Yellow solid	282	75	283	0.62		
4PYav	Yellow solid	296	54	297	0.67	98	✓
4PYaw	Yellow solid	352	85	353	0.70		
4PYax	Yellow solid	254	83	255	0.17	98	✓
4PYay	Yellow solid	268	40	269	0.39		
4PYaz	Yellow solid	282	36	283	0.38		
4PYba	Yellow solid	296	48	297	0.39	88	
4PYbb	Yellow solid	310	68	311	0.40		
4PYbc	Yellow solid	324	42	325	0.42		
4PYbe	Light yellow solid	330	67	331	0.40		
4PYbf	Light orange solid	330	81	331	0.33	98	✓

Compound	Appearance	MW	% Yield	APCI-MS m/z	R.f.	% Purity	^{1}H NMR
4PYbg	Yellow solid	330	96	331	0.30		
4PYbh	Yellow solid	360	78	361	0.39	98	✓
4PYbi	Yellow solid	374	88	375	0.20	92	
4PYbj	Yellow solid	388	77	389	0.20	98	✓
4PYbk	Yellow solid	374	82	375	0.18		
4PYbl	Yellow sold	416	87	417	0.20		
4PYbm	Yellow solid	405	58	406	0.19		
4PYbn	Yellow solid	360	65	361	0.40	98	✓
4PYbo	Yellow solid	374	78	375	0.25	98	✓
4PYbp	Yellow solid	388	56	389	0.29	98	✓
4PYbq	Yellow solid	374	68	375	0.23		
4PYbr	Yellow solid	416	71	417	0.27		
4PYbs	Yellow solid	436	97	437	0.36		
4PYbt	Yellow solid	360	50	361	0.40		
4PYbu	Yellow solid	390	56	391	0.30		
4PYbv	Yellow solid	366	45	367	0.44	98	✓
4PYbw	Yellow solid	240	85	241	0.21	90	
4PYbz	Brown solid	256	89	257	0.23		
4PYca	Dark orange solid	256	97	257	0.25		
4PYcb	Brown solid	272	99	273	0.25		
4PYcc	Red solid	272	96	273	[a]0.40		
4PYcd	Red solid	272	95	273	[a]0.42		
4PYce	Orange solid	270	71	271	0.20		
4PYcf	Orange solid	270	81	271	0.48	85	
4PYcg	Orange solid	270	80	271	0.33		
4PYch	Orange solid	270	84	271	0.39		
4PYci	Orange-yellow solid	284	68	285	0.31	90	
4PYcj	Yellow solid	285	86	286	[a]0.49		
4PYck	Yellow solid	315	82	316	[a]0.44		
4PYcl	Yellow solid	364	91	<u>365</u>, 367	[a]0.48		
4PYcm	Yellow solid	330	85	331	[a]0.45		
4PYcn	Orange solid	364	92	<u>365</u>, 367	0.02	98	✓
4PYco	Yellow solid	492	78	493	0.33		
4PYcp	Yellow solid	268	74	269	0.40	98	✓
4PYcq	Yellow crystals	352	60	353	0.48	98	✓
4PYcr	Yellow solid	352	57	353	0.48	74	
4PYcs	Orange solid	284	45	285	0.34		
4PYct	Orange solid	284	62	285	0.37		
4PYcw	Yellow solid	298	78	299	0.36		
4PYcy	Orange-yellow solid	312	51	313	0.28		
4PYcz	Yellow solid	298	59	299	0.19	89	
4PYda	Yellow solid	394	63	395	0.46	98	✓
4PYdb	Brown solid	290	55	291	0.41	98	✓
4PYdc	Yellow solid	304	48	305	0.30	75	
4PYdd	Yellow crystals	304	76	305	0.29		
4PYdg	Orange solid	258	43	<u>259</u>, 261	0.44		
4PYdm	Yellow solid	292	81	293	0.49		
4PYdn	Yellow solid	269	89	270	0.13	85	
4PYdo	Yellow solid	269	46	270	0.11		
4PYdq	Yellow-orange solid	267	64	268	0.30		
4PYdr	Yellow solid	281	75	282	0.28		
4PYds	Yellow solid	325	57	326	0.18		

Compound	Appearance	MW	% Yield	APCI-MS m/z	R.f.	% Purity	^{1}H NMR
4PYdt	Brown solid	213	66	214	0.37	68	
4PYdu	Brown solid	228	89	229	0.06		
4PYdv	Yellow solid	225	92	226	0.30		
4PYdw	Yellow crystals	225	90	226	0.22		
4PYdx	Orange solid	317	70	200, 318	0.20	83	✓
4PYeb	Dark orange solid	292	65	293	0.70		
4PYec	Orange-brown solid	306	61	105 203, 307	0.52		
4PYed	Yellow solid	230	90	231	0.40		
4PYee	Yellow solid	270	79	271	0.57		
4PYef	Yellow solid	312	80	312	0.60		
4PYeg	Yellow solid	354	67	355	0.66		
4PYeh	Yellow solid	366	56	367, 369	0.49	98	✓
PZaa	Yellow solid	225	97	226	0.60		
PZae	Orange solid	281	61	282	0.66	98	✓
PZaf	Yellow solid	295	84	296	0.54	98	✓
PZag	Yellow solid	301	83	302	0.58		
PZah	Yellow solid	239	46	240	0.63		
PZai	Orange solid	253	65	254	0.63	90	
PZam	Orange solid	325	78	326	0.60		
PZan	Orange solid	325	88	326	0.58		
PZar	Orange solid	303	64	304	0.64		
PZas	Yellow solid	255	80	256	0.48		
PZaw	Yellow solid	353	74	354	0.65	98	✓
PZax	Yellow solid	255	97	256	0.61		
PZaz	Yellow solid	283	51	284	0.60		
PZba	Yellow solid	297	66	298	0.61		
PZbb	Yellow solid	311	39	312	0.62		
PZbc	Yellow solid	325	46	326	0.63		
PZbf	Yellow solid	331	82	332	0.68	98	✓
PZbg	Light yellow solid	331	91	332	0.67		
PZbh	Yellow solid	361	76	362	0.61	98	✓
PZbm	Yellow solid	406	83	407	0.62		
PZbn	Light orange solid	361	87	362	0.61	98	✓
PZbs	Yellow solid	437	87	438	0.68	98	✓
PZbt	Yellow crystals	361	83	362	0.70		
PZbu	Yellow solid	391	93	392	0.72	98	✓
PZbw	Yellow solid	241	95	242	0.63		
PZbz	Brown solid	257	57	258	0.58	98	✓
PZca	Orange solid	257	54	258	0.48	98	✓
PZcb	Yellow solid	273	70	274	0.39	98	✓
PZcc	Yellow-brown solid	273	50	274	0.40	98	✓
PZcd	Brown solid	273	94	274	0.52		
PZce	Yellow solid	271	80	272	0.50	98	✓
PZcf	Yellow solid	271	82	272	0.61		
PZcg	Yellow solid	271	87	272	0.54		
PZch	Light orange solid	271	77	272	0.54		
PZci	Yellow solid	285	97	286	0.55		
PZcj	Yellow solid	286	93	287	0.41	98	✓
PZck	Light brown solid	316	95	317	0.54		
PZcl	Light yellow solid	365	90	357, 365	0.55		
PZcm	Orange solid	331	94	332	0.04	98	✓
PZcq	Yellow solid	353	40	354	0.66		

Compound	Appearance	MW	% Yield	APCI-MS m/z	R.f.	% Purity	^{1}H NMR
PZcr	Yellow solid	353	41	354	0.64		
PZcs	Yellow solid	285	72	286	0.49		
PZct	Yellow solid	285	80	286	0.54	98	✓
PZcv	Yellow solid	299	96	300	0.55		
PZcw	Yellow solid	299	94	300	0.53		
PZcy	Yellow solid	313	82	314	0.54	98	✓
PZcz	Orange solid	299	89	300	[a]0.50		
PZdb	Brown crystals	291	97	292	0.64		
PZdc	Yellow crystals	305	96	306	0.63		
PZdd	Orange solid	305	85	306	0.56		
PZdg	Orange solid	259	75	260, 262	0.63	90	
PZdn	Yellow solid	270	92	271	0.56		
PZdo	Yellow solid	270	95	271	0.56		
PZdq	Yellow-orange solid	268	79	269	0.48		
PZdr	Yellow solid	282	89	283	0.32		
PZds	Yellow solid	326	65	327	0.20	85	
PZdu	Yellow solid	229	72	230	0.08		
PZdv	Yellow solid	226	86	227	0.23		
PZdx	Yellow solid	318	75	319	0.56	98	✓
PZeb	Yellow solid	293	68	105, 189, 294	0.74	90	
PZec	Yellow solid	307	74	105, 203, 308	0.53		
PZeh	Yellow solid	367	70	368, 370	0.50		
QNaa	Yellow solid	274	74	275	0.76		
QNae	Yellow solid	330	83	331	0.88		
QNaf	Yellow solid	344	90	345	0.88	98	✓
QNag	Yellow solid	350	94	351	0.90		
QNah	Yellow solid	288	85	289	0.75		
QNam	Yellow solid	374	74	375	0.90		
QNan	Yellow solid	374	87	375	0.90		
QNar	Orange solid	352	61	353	0.79	85	
QNaw	Yellow solid	402	53	403	0.81		
QNax	Yellow solid	304	86	305	0.74		
QNaz	Yellow solid	332	39	333	0.76	90	
QNba	Yellow solid	346	53	347	0.78		
QNbb	Yellow solid	360	48	361	0.77		
QNbc	Yellow solid	374	60	375	0.78		
QNbf	Yellow solid	380	92	381	0.82	98	✓
QNbg	Yellow solid	380	92	381	0.82		
QNbh	Yellow solid	410	68	411	0.77	98	✓
QNbm	Yellow solid	455	72	456	0.80	75	
QNbn	Yellow solid	410	80	411	0.80	98	✓
QNbs	Yellow solid	486	89	487	0.83		
QNbt	Yellow crystals	440	84	441	0.70	93	
QNbu	Yellow solid	440	95	441	0.79		
QNbw	Yellow crystals	290	72	291	0.77		
QNbx	Yellow solid	290	93	291	0.68		
QNbz	Yellow solid	306	82	307	0.63		
QNca	Yellow solid	306	41	307	0.54	98	✓
QNcb	Yellow solid	322	63	155, 323	0.50		
QNcc	Brown solid	322	68	323	0.47	98	✓
QNcd	Orange solid	322	74	155, 323	0.29		
QNce	Yellow solid	320	92	321	0.69		

Compound	Appearance	MW	% Yield	APCI-MS m/z	R.f.	% Purity	^{1}H NMR
QNcf	Yellow solid	320	80	321	0.88		
QNci	Yellow solid	334	45	335	0.73		
QNcj	Yellow solid	335	66	336	[a]0.75		
QNck	Yellow solid	365	82	366	[a]0.70	80	
QNcl	Yellow solid	414	78	415, 417	[a]0.77	98	✓
QNcm	Orange solid	380	86	381	[a]0.49		
QNcq	Yellow solid	402	47	403	0.92		
QNcr	Yellow solid	402	63	403	0.90		
QNcs	Yellow solid	334	41	335	0.70		
QNct	Yellow solid	334	74	335	0.66		
QNcv	Yellow solid	348	88	349	0.62		
QNcw	Yellow solid	348	90	349	0.71	90	
QNcy	Yellow solid	362	87	363	0.73		
QNcz	Yellow-brown solid	348	98	349	0.40		
QNdb	Yellow solid	340	95	341	0.81		
QNdc	Yellow crystals	354	90	355	0.79	85	
QNdd	Yellow solid	354	72	355	0.86		
QNdn	Yellow solid	319	78	320	0.73		
QNdo	Yellow solid	319	98	320	0.76		
QNdr	Yellow solid	331	98	332	0.46		
QNds	Yellow solid	375	77	376	0.38	98	✓
QNdx	Yellow solid	367	60	368	0.90		
QNdy	Yellow solid	313	81	314	0.83		
QNec	Yellow solid	356	97	155, 203, 357	0.70	98	✓
QNee	Yellow solid	320	78	153, 321	0.68		
HDaa	Off white solid	197	60	198	0.76		
HDab	Light orange solid	211	72	212	0.74		
HDac	Light orange solid	225	66	226	0.77		
HDad	Light orange solid	239	70	240	0.75		
HDae	Light orange solid	253	68	254	0.74	98	✓
HDaf	White crystals	267	66	268	0.74		
HDag	Light orange crystals	273	54	274	0.71		
HDah	Red-brown solid	211	41	212	0.78		
HDai	Light orange solid	225	40	226	0.80		
HDaj	Light brown solid	211	444	212	0.78	90	
HDak	Light orange crystals	247	68	248	0.65		
HDal	Off-white solid	247	52	248	0.71		
HDam	Orange solid	297	59	298	0.62		
HDan	Orange solid	297	56	298	0.68		
HDas	Light orange solid	227	68	228	0.49		
HDaw	Light orange solid	325	80	326	0.61		
HDax	Light orange crystals	227	54	228	0.42	98	✓
HDay	Off-white crystals	241	63	242	0.43	98	✓
HDaz	Light orange solid	255	66	256	0.42		
HDba	Light orange solid	269	81	270	0.41		
HDbb	Light orange solid	283	61	284	0.43		
HDbc	Light orange solid	297	52	298	0.44		
HDbe	Light orange crystals	303	64	304	0.78		
HDbf	Light orange solid	303	68	304	0.71		
HDbg	Light orange solid	303	67	304	0.70		
HDbh	Off-white solid	333	53	334	0.75	98	✓
HDbm	Yellow-orange solid	378	53	379	0.62		

Compound	Appearance	MW	% Yield	APCI-MS m/z	R.f.	% Purity	^{1}H NMR
HDbn	Light orange solid	333	48	334	0.75		
HDbo	Off white solid	347	68	348	0.47		
HDbq	White solid	347	66	348	0.49	85	
HDbs	Off-white solid	409	57	410	0.70		
HDbt	Light orange crystals	333	71	334	0.76		
HDbu	Orange crystals	363	53	364	0.70		
HDbz	Red-brown solid	229	56	230	0.22		
HDca	Brown solid	229	82	230	0.20	98	✓
HDcb	Red-brown solid	245	59	246	0.26	98	✓
HDcc	Brown crystals	245	95	246	[a]0.43	80	
HDcd	Orange-brown solid	245	83	246	[a]0.50	98	✓
HDce	Brown solid	243	82	244	0.60		
HDcf	Brown solid	243	45	244	0.65		
HDcj	Yellow solid	258	66	259	[a]0.54	98	✓
HDck	Yellow solid	288	71	289	[a]0.50	98	✓
HDcl	Orange solid	337	76	<u>338</u>, 340	[a]0.53	98	✓
HDcm	Orange solid	303	92	304	0.50	85	
HDcn	Orange solid	337	70	<u>338</u>, 340	0.52		
HDco	Light orange solid	465	60	466	0.42		
HDcq	Light orange solid	325	47	326	0.78		
HDcr	Light orange solid	325	45	326	0.77		
HDdb	Brown solid	263	71	264	0.66	98	✓
HDdc	Orange crystals	277	78	278	0.67		
HDdd	Orange solid	277	66	278	0.66		
HDdg	Light orange solid	231	50	232	0.78		
HDdm	Light orange solid	265	74	266	0.73		
HDdn	Light orange solid	242	80	243	0.64		
HDdq	Light brown solid	240	40	241	0.47	98	✓
HDds	Orange crystals	298	55	299	0.31		
HDdt	Dark brown solid	186	67	187	0.61		
HDdv	Brown crystals	198	50	199	0.24	98	✓
HDdw	Light orange solid	198	62	199	0.29		
HDdx	Yellow crystals	290	51	291	0.69	95	
HDeb	Yellow solid	265	84	266	0.92		
HDed	Light orange solid	203	78	204	0.67		
HDeg	Light orange solid	327	44	213 (-SiC_6H_{14}), <u>328</u>	0.71		
HDeh	Off-white crystals	339	55	<u>340</u>, 342	0.80		

Table 11.2 ^{1}H NMR data of inactive compounds. If a compound was found to be active at a concentration of 16-32μgml^{-1} or less, then that compound was analysed in full (^{13}C NMR, IR, mp, CHN analysis). These compounds can be found in Section 11.2.3.1.

Compound	^{1}H NMR (d_6-DMSO)
2PYah	2.49 (s, 3H, Me), 7.04 (bs, 2H, NH_2), 7.29 (m, 3H, 3Ar-H), 7.54 (m, 1H, Pyr-H4), 7.93 (dt, 1H, J=7.7, 1.7Hz, Pyr-H5), 8.13 (m, 1H, Ar-H), 8.23 (d, 1H, J=8.0Hz, Pyr-H3), 8.67 (m, 1H, Pyr-H6), 8.73 (s, 1H, =CHAr)ppm.
2PYav	1.34 (s, 9H, $OCMe_3$), 6.99 (bs, 2H, NH_2), 7.03 (d, 2H, J=8.6Hz, 3'H and 5'H), 7.52 (ddd, 1H, J=7.5, 4.9, 1.1Hz, Pyr-H4), 7.83 (d, 2H, J=8.6Hz, 2'H and 6'H), 7.91 (td, 1H, J=7.8, 1.7Hz, Pyr-H5), 8.23 (d, 1H, J=8.0Hz, Pyr-H3), 8.45 (s, 1H, =CHAr), 8.65 (m, 1H, Pyr-H6)ppm.
2PYbp	2.05 (Qnt, 2H, J=7.1Hz, $OCH_2C\underline{H}_2CH_2Ph$), 2.79 (t, 2H, J=7.3Hz, $OCH_2CH_2C\underline{H}_2Ph$), 3.84 (s, 3H, OMe), 4.06 (t, 2H, J=6.4Hz, $OC\underline{H}_2CH_2CH_2Ph$), 7.02 (ov.m, 3H, NH_2 and 5'H), 7.19-7.34 (ov.m, 6'H and 5Phenyl-H), 7.53 (m, 1H, Pyr-H4), 7.62 (d, 1H, J=1.7Hz, 2'H), 7.91 (m, 1H, Pyr-H5), 8.22 (d, 1H, J=8.0Hz, Pyr-H3), 8.39 (s, 1H, =CHAr), 8.65 (m, 1H, Pyr-H6)ppm.
2PYcb	6.40 (d, 1H, J=8.4Hz, 6'H), 6.87 (ov.m, 3H, NH_2 and 5'H), 7.53 (m, 1H, Pyr-H4), 7.92 (m, 1H, Pyr-H5), 8.22 (d, 1H, J=7.9Hz, Pyr-H3), 8.54 (s, 1H, =CHAr), 8.64 (m, 1H, Pyr-H6)ppm.
2PYcf	3.78 (s, 3H, OMe), 6.52 (m, 2H, 3'H and 5'H), 6.96 (bs, 2H, NH_2), 7.52 (ov.m, Pyr-H4 and 6'H), 7.92 (dt, 1H, J=7.8, 1.7Hz, Pyr-H5), 8.22 (m, 1H, Pyr-H3), 8.62 (s, 1H, =CHAr), 8.65 (m, 1H, Pyr-H6), 11.25 (bs, 1H, NH)ppm.
2PYcj	7.11 (d, 1H, J=9.1Hz, 3'H), 7.28 (bs, 2H, NH_2), 7.57 (m, 1H, Pyr-H4), 7.94 (dt, 1H, J=7.8, 1.8Hz, Pyr-H5), 8.16 (dd, 1H, J=9.0, 2.9Hz, 4'H), 8.23 (m, 1H, Pyr-H3), 8.68 (m, 1H, Pyr-H6), 8.75 (ov.m, 2H, 6'H and =CHAr), 12.00 (bs, 1H, OH)ppm.
2PYdb	7.12 (bs, 2H, NH_2), 7.24 (d, 1H, J=9.0Hz, 3'H), 7.39 (m, 1H, Ar-H), 7.56 (ov.m, Pyr-H4 and Ar-H), 7.87-8.00 (ov.m, Pyr-H5 and 2Ar-H), 8.31 (d, 1H, J=8.0Hz, Pyr-H3), 8.43 (m, 1H, Ar-H), 8.67 (m, 1H, Pyr-H6), 9.53 (s, 1H, =CHAr), 12.79 (bs, 1H, OH)ppm.
2PYdg	7.25 (bs, 2H, NH_2), 7.46 (m, 2H, 4'H and 5'H), 7.55 (m, 1H, Pyr-H4), 7.83 (m, 1H, 6'H), 7.92 (dt, 1H, J=7.8, 1.7Hz, Pyr-H5), 8.11 (m, 1H, 2'H), 8.23 (d, 1H, J=8.0Hz, Pyr-H3), 8.47 (s, 1H, =CHAr), 8.67 (m, 1H, Pyr-H6)ppm.
2PYeb	7.22 (bs, 2H, NH_2), 7.54 (ov.m, 2H, Pyr-H4 and Ar-H), 7.73 (m, 1H, Ar-H), 7.86 (ov.m, 2H, Pyr-H5 and Ar-H), 8.15 (dd, 1H, J=8.0, 1.6Hz, 3'H or 6'H), 8.23 (m, 1H, Pyr-H3), 8.51 (s, 1H, =CHAr or 8'H), 8.66 (m, 1H, Pyr-H6), 9.28 (s, 1H, =CHAr or 8'H)ppm.
3PYay	1.37 (t, 3H, J=6.9Hz, $OCH_2C\underline{H}_3$), 4.10 (q, 2H, J=7.0Hz, $OC\underline{H}_2CH_3$), 6.97 (m, 1H, 4'H or 5'H), 7.06 (d, 1H, J=8.3Hz, 3'H), 7.14 (bs, 2H, NH_2), 7.37 (m, 1H, 4'H or 5'H), 7.47 (m, 1H, Pyr-H4), 8.18 (dd, 1H, J=7.8, 1.6Hz, 6'H), 8.26 (dt, 1H, J=8.0, 1.8Hz, Pyr-H5), 8.65 (dd, 1H, J=4.9, 1.7Hz, Pyr-H6), 8.73 (s, 1H, =CHAr), 9.09 (d, 1H, J=1.9Hz, Pyr-H2)ppm.
3PYba	0.95 (t, 3H, J=7.4Hz, $OCH_2CH_2CH_2C\underline{H}_3$), 1.47 (hex, 2H, J=7.2Hz, $OCH_2CH_2C\underline{H}_2CH_3$), 1.74 (pent, 2H, J=6.4Hz, $OCH_2C\underline{H}_2CH_2CH_3$), 4.06 (t, 2H, J=6.3Hz, $OC\underline{H}_2CH_2CH_2CH_3$), 6.98 (t, 1H, J=7.5Hz, 4'H or 5'H), 7.08 (d, 1H, J=8.2Hz, 3'H), 7.16 (bs, 2H, NH_2), 7.38 (m, 1H, 4'H or 5'H), 7.48 (m, 1H, Pyr-H4), 8.20 (dd, 1H, J=7.7, 1.7Hz, 6'H), 8.27 (dt, 1H, J=8.0, 2.1Hz, Pyr-H5), 8.66 (dd, 1H, J=4.8, 1.6Hz, Pyr-H6), 8.73 (s, 1H, =CHAr), 9.09 (d, 1H, J=1.6Hz, Pyr-H2)ppm.

Compound	^{1}H NMR (d_6-DMSO)
3PYbf	5.17 (s, 2H, OC<u>H</u>$_2$Ph), 7.06 (m, 1H, Ar-H), 7.22 (bs, 2H, NH_2), 7.34-7.51 (m, 7H, Pyr-H4 and 2Ar-H and 5Phenyl-H), 7.66 (s, 1H, 2'H), 8.25 (m, 1H, Pyr-H5), 8.43 (s, 1H, =CHAr), 8.66 (dd, 1H, J=4.8, 1.7Hz, Pyr-H6), 9.10 (d, 1H, J=1.8Hz, Pyr-H2)ppm.
3PYbh	3.86 (s, 3H, OMe), 5.14 (s, 2H, C<u>H</u>$_2$Ph), 7.10 (d, 3H, NH_2 and 5'H), 7.27-7.51 (ov.m, 7H, Pyr-H4, 6'H, 5Phenyl-H), 7.66 (d, 1H, J=1.8Hz, 2'H), 8.26 (m, 1H, Pyr-H5), 8.37 (s, 1H, =CHAr), 8.65 (m, 1H, Pyr-H6), 9.10 (m, 1H, Pyr-H2)ppm.
3PYbn	3.82 (s, 3H, OMe), 5.18 (s, 2H, C<u>H</u>$_2$Ph), 7.01 (d, 1H, J=8.3Hz, 5'H), 7.05 (bs, 2H, NH_2), 7.30-7.52 (ov.m, 7H, Pyr-H4, 6'H, 5Phenyl-H), 7.77 (d, 1H, J=1.8Hz, 2'H), 8.26 (dt, 1H, J=8.1, 1.8Hz, Pyr-H5), 8.36 (s, 1H, =CHAr), 8.66 (dd, 1H, J=4.8, 1.7Hz, Pyr-H6), 9.10 (d, 1H, J=1.8Hz, Pyr-H2)ppm.
4PYaa	7.25 (bs, 2H, NH_2), 7.43 (ov.m, 3H, 3Ar-H), 7.89 (ov.m,. 4H, Pyr-H3 and H5 and 2Ar-H), 8.47 (s, 1H, =CHAr), 8.67 (dd, 2H, J=4.6, 1.7Hz, Pyr-H2 and H6)ppm.
4PYav	1.35 (s, 9H, $OCMe_3$), 7.03 (d, 2H, J=8.5Hz, 3'H and 5'H), 7.14 (bs, 2H, NH_2), 7.86 (ov.m, 4H, Pyr-H3 and H5 and 2'H and 6'H), 8.43 (s, 1H, =CHAr), 8.68 (dd, 2H, J=4.5, 1.5Hz, Pyr-H2 and H6)ppm.
4PYax	6.99 (m, 1H, 4'H or 5'H), 7.08 (d, 1H, J=8.4Hz, 3'H), 7.20 (bs, 2H, NH_2), 7.41 (m, 1H, 4'H or 5'H), 7.88 (dd, 2H, J=4.6, 1.6Hz, Pyr-H3 and H5), 8.18 (dd, 1H, J=7.7, 1.7Hz, 3'H), 8.66 (dd, 2H, J=J=4.6, 1.6Hz, Pyr-H2 and H6), 8.73 (s, 1H, =CHAr)ppm.
4PYbf	5.17 (s, 2H, OC<u>H</u>$_2$Ph), 7.06 (m, 1H, Ar-H), 7.24 (bs, 2H, NH_2), 7.34-7.50 (m, 7H, 2Ar-H and 5Phenyl-H), 7.67 (s, 1H, 2'H), 7.88 (dd, 2H, J=4.5, 1.6Hz, Pyr-H3 and H5), 8.43 (s, 1H, =CHAr), 8.67 (dd, 2H, J=4.5, 1.6Hz, Pyr-H2 and H6)ppm.
4PYbj	2.04 (Qnt, 2H, J=7.4Hz, OCH_2C<u>H</u>$_2$$CH_2$Ph), 2.76 (t, 2H, J=7.4Hz, OCH_2CH_2C<u>H</u>$_2$Ph), 3.87 (s, 3H, OMe), 3.99 (t, 2H, J=6.4Hz, OC<u>H</u>$_2$$CH_2CH_2$Ph), 6.98 (d, 1H, J=8.3Hz, 5'H), 7.15-7.30 (ov.m, NH_2 and 6'H and 5Phenyl-H), 7.66 (d, 1H, J=2.0Hz, 2'H), 7.88 (dd, 2H, J=4.6, 1.6Hz, Pyr-H3 and H5), 8.38 (s, 1H, =CHAr), 8.67 (dd, 2H, J=4.6, 1.6Hz, Pyr-H2 and H6)ppm.
4PYbo	3.08 (t, 2H, J=5.6Hz, OCH_2C<u>H</u>$_2$Ph), 3.81 (s, 3H, OMe), 4.28 (t, 2H, J=5.6Hz, OC<u>H</u>$_2$$CH_2$Ph), 7.00-7.35 (ov.m, NH_2 and 5'H and 6'H and 5Phenyl-H), 7.65 (d, 1H, J=1.8Hz, 2'H), 7.86 (d, 2H, J=5.7Hz, Pyr-H3 and H5), 8.37 (s, 1H, =CHAr), 8.67 (d, 2H, J=5.7Hz, Pyr-H2 and H6)ppm.
4PYbp	2.05 (Qnt, 2H, J=7.4Hz, OCH_2C<u>H</u>$_2$$CH_2$Ph), 2.78 (t, 2H, J=7.4Hz, OCH_2 CH_2C<u>H</u>$_2$Ph), 3.83 (s, 3H, OMe), 4.06 (t, 2H, J=6.4Hz, OC<u>H</u>$_2$$CH_2CH_2$Ph), 7.02 (d, 1H, J=8.4Hz, 5'H), 7.13 (bs, 1H, NH_2), 7.18-7.35 (ov.m, 6'H and 5Phenyl-H), 7.62 (d, 1H, J=1.7Hz, 2'H), 7.88 (dd, 2H, J=4.6, 1.6Hz, Pyr-H3 and H5), 8.37 (s, 1H, =CHAr), 8.67 (dd, 2H, J=4.6, 1.6Hz, Pyr-H2 and H6)ppm.
4PYbv	1.32 (s, 9H, CMe_3), 1.38 (s, 9H, CMe_3), 3.74 (s, 3H, OMe), 7.18 (bs, 2H, NH_2), 7.36 (d, 1H, J=2.5Hz, 4'H), 7.89 (dd, 2H, J=4.6, 1.6Hz, Pyr-H3 and H5), 8.03 (d,1H, J=2.5Hz, 6'H), 8.61(s, 1H, =CHAr), 8.68 (dd, 2H, J=4.6, 1.6Hz, Pyr-H2 and H6)ppm.
4PYcn	7.10 (bs, 2H, NH_2), 7.87 (dd, 2H, J=4.6, 1.6Hz, Pyr-H3 and H5), 8.35 (bs, 1H, OH), 8.38 (d, 1H, J=2.8Hz, 4'H or 6'H), 8.68 (d, 1H, J=2.8Hz, 4'H or 6'H), 8.77 (dd, 2H, J=4.6, 1.6Hz, Pyr-H2 and H6), 8.85 (s, 1H, =CH Ar)ppm.

Compound	^{1}H NMR (d_6-DMSO)
4PYcp	2.21 (s, 3H, Me), 2.23 (s, 3H, Me), 7.30 (s, 1H, 4'H), 7.18 (bs, 2H, NH_2), 7.34 (s, 1H, 6'H), 7.87 (dd, 2H, J=4.6, 1.5Hz, Pyr-H3 and H5), 8.59 (s, 1H, =CHAr), 8.67 (dd, 2H, J=4.6, 1.5Hz, Pyr-H2 and H6), 11.09 (bs, 1H, OH)ppm.
4PYda	1.33 (s, 9H, CMe_3), 1.35 (s, 9H, CMe_3), 2.39 (s, 3H, CCO<u>Me</u>), 7.18 (bs, 2H, NH_2), 7.46 (d, 1H, J=2.4Hz, 4'H), 7.87 (d, 2H, J=6.0Hz, Pyr-H3 and H5),7.34 (d, 1H, J=2.4Hz, 6'H), 8.26 (s, 1H, =CHAr), 8.69 (ov.m, 3H, Pyr-H2 and H6 and OH)ppm.
4PYdb	7.23 (ov.m, 3H, NH_2 and Ar-H), 7.39 (m, 1H, Ar-H), 7.55 (m, 1H, Ar-H), 7.86-7.94 (ov.m, 4H, Pyr-H3 and H5 and 2Ar-H), 8.41 (d, 1H, J=8.4Hz, 4'H), 8.70 (d, 2H, J=5.3Hz, Pyr-H2 and H6), 9.49 (s, 1H, =CHAr), 12.66 (bs, 1H, OH)ppm.
PZae	1.30 (s, 9H, CMe_3), 7.10 (bs, 2H, NH_2), 7.46 (d, 2H, J=8.3Hz, 3'H and 5'H), 7.86 (d, 2H, J=8.3Hz, 2'H and 6'H), 8.48 (s, 1H, =CHAr), 8.72 (m, 1H, Pz-H5), 8.76 (d, 1H, J=2.6Hz, Pz-H6), 9.37 (d, 1H, J=1.4Hz, Pz-H3)ppm.
PZaw	0.85 (t, 3H, J=6.9Hz, $O(CH_2)_7C\underline{H}_3$), 1.28 (m, 10H, $OCH_2CH_2(C\underline{H}_2)_5CH_3$), 1.73 (pent, 2H, J=7.8Hz, $OCH_2C\underline{H}_2(CH_2)_5CH_3$), 4.02 (t, 2H, J=6.5Hz, $OC\underline{H}_2(CH_2)_6CH_3$), 6.98 (d, 2H, J=8.8Hz, 3'H and 5'H), 7.06 (bs, 2H, NH_2), 7.87 (d, 2H, J=8.8Hz, 2'H and 6'H), 8.46 (s, 1H, =CHAr), 8.72 (m, 1H, Pz-H5), 8.76 (d, 1H, J=2.6Hz, Pz-H6), 9.37 (d, 1H, J=1.5Hz, Pz-H3)ppm.
PZbf	5.17 (s, 2H, $O\underline{CH}_2Ph$), 7.08 (m, 1H, Ar-H), 7.20 (bs, 2H, NH_2), 7.32-7.50 (m, 7H, 2Ar-H and 5Phenyl-H), 7.71 (m, 1H, 2'H), 8.48 (s, 1H, =CHAr), 8.73 (m, 1H, Pz-H5), 8.77 (d, 1H, J=2.6Hz, Pz-H6), 9.38 (d, 1H, J=1.5Hz, Pz-H3)ppm.
PZbh	3.86 (s, 3H, OMe), 5.15 (s, 2H, $OC\underline{H}_2Ph$), 7.10 (d, 1H, 8.4Hz, 5'H), 7.16 (bs, 2H, NH_2), 7.300-7.45 (ov.m, 6H, Ar-H and 5Phenyl-H), 7.71 (d, 1H, J=1.8Hz, 2'H), 8.43 (s, 1H, =CHAr), 8.72 (m, 1H, Pz-H5), 8.76 (d, 1H, J=2.6Hz, Pz-H6), 9.37 (d, 1H, J=1.5Hz, Pz-H3)ppm.
PZbn	3.82 (s, 3H, OMe), 5.18 (s, 2H, $O\underline{CH}_2Ph$), 7.04 (d, 1H, 8.4Hz, 5'H), 7.15 (bs, 2H, NH_2), 7.33-752 (ov.m, 6H, Ar-H and 5Phenyl-H), 7.82 (d, 1H, J=1.8Hz, 2'H), 8.43 (s, 1H, =CHAr), 8.73 (m, 1H, Pz-H5), 8.76 (d, 1H, J=2.6Hz, Pz-H6), 9.37 (d, 1H, J=1.5Hz, Pz-H3)ppm.
PZbs	5.19 (s, 2H, $OC\underline{H}_2Ph$), 5.22 (s, 2H, $OC\underline{H}_2Ph$), 7.13 (ov.m, 3H, NH_2 and 5'H or 6'H), 7.31-7.52 (m, 11H, 10Phenyl-H and 5'H or 6'H), 7.82 (d, 1H, J=1.7Hz, 2'H), 8.41 (s, 1H, =CHAr), 8.72 (m, 1H, Pz-H5), 8.76 (d, 1H, J=2.6Hz, Pz-H6), 9.36 (d, 1H, J=1.5Hz, Pz-H3)ppm.
PZbu	3.80 (s, 3H, OMe), 3.82 (s, 3H, OMe), 5.20 (s, 2H, OCH_2Ph), 6.85 (s, 1H, 3'H), 7.45 (bs, 2H, NH_2), 7.34-7.50 (m, 5H, 5Phenyl-H), 7.75 (s, 1H, 6'H), 8.71 (ov.m, 2H, Pz-H5 and =CHAr), 8.74 (d, 1H, J=2.5Hz, Pz-H6), 9.35 (d, 1H, J=1.5Hz, Pz-H3)ppm.
PZbz	6.74 (m, 1H, 5'H), 6.86 (dd, 1H, J=7.8, 1.6Hz, 4'H or 6'H), 7.10-7.16 (ov.m, 3H, NH_2 and 4'H or 6'H), 8.69 (s, 1H, =CHAr), 8.73 (m, 1H, Pz-H5), 8.78 (d, 1H, J=2.6Hz, Pz-H6), 9.39 (d, 1H, J=1.5Hz, Pz-H3)ppm.
PZca	6.78 (d, 1H, J=8.0Hz, 5'H), 6.89 (bs, 2H, NH_2), 7.17 (dd, 1H, J=8.1, 1.9Hz, 6'H), 7.34 (d, 1H, J=1.9Hz, 2'H), 8.33 (s, 1H, =CHAr), 8.71 (m, 1H, Pz-H5), 8.74 (d, 1H, J=2.6Hz, Pz-H6), 9.35 (d, 1H, J=1.5Hz, Pz-H3)ppm.

Compound	^{1}H NMR (d_6-DMSO)
PZcb	6.40 (d, 1H, J=8.4Hz, 6'H), 6.90 (d, 1H, J=8.4Hz, 5'H), 6.98 (bs, 2H, NH_2), 8.35 (bs, 1H, OH), 8.56 (s, 1H, =CHAr), 8.71 (m, 1H, Pz-H5), 8.75 (d, 1H, J=2.6Hz, Pz-H6), 9.36 (d, 1H, J=1.4Hz, Pz-H3), 9.55 (bs, 1H, OH), 10.95 (bs, 1H, OH)ppm.
PZcc	5.69 (s, 1H, 3'H), 6.92 (bs, 2H, NH_2), 6.96 (s, 1H, 6'H), 8.51 (bs, 1H, OH), 8.54 (s, 1H, =CHAr), 8.71 (m, 1H, Pz-H5), 8.75 (d, 1H, J=2.6Hz, Pz-H6), 9.36 (d, 1H, J=1.4Hz, Pz-H3), 9.63 (bs, 1H, OH), 10.39 (bs, 1H, OH)ppm.
PZce	3.83 (s, 3H, OMe), 6.86 (m, 1H, 5'H), 7.05 (dd, 1H, J=8.2, 1.5Hz, 4'H), 7.19 (bs, 2H, NH_2), 7.30 (dd, 1H, J=7.9, 1.5Hz, 6'H), 8.73 (ov.m, 2H, Pz-H5 and =CHAr), 8.78 (d, 1H, J=2.8Hz, Pz-H6), 9.39 (d, 1H, J=1.5Hz, Pz-H3), 10.60 (bs, 1H, OH)ppm.
PZcj	7.12 (d, 1H, J=9.1Hz, 3'H), 7.40 (bs, 2H, NH_2), 8.18 (dd, 1H, J=9.1, 2.9Hz, 4'H), 8.75 (m, 1H, Pz-H5), 8.81 (ov.m, 4H, Pz-H5 and H6 and 6'H and =CHAr), 9.40 (d, 1H, J=1.5Hz, Pz-H3), 11.95 (bs, 1H, OH)ppm.
PZcm	7.10 (bs, 2H, NH_2), 8.62 (d, 1H, J=3.2Hz, Ar-H), 8.93 (d, 1H, J=3.3Hz, Ar-H), 8.95 (m, 1H, Pz-H5), 9.03 (d, 1H, J=2.5Hz, Pz-H6), 9.05 (s, 1H, =CHAr), 9.43 (d, 1H, J=1.4Hz, Pz-H3), 9.90 (bs, 1H, OH)ppm.
PZct	3.80 (s, 3H, OMe), 3.84 (s, 3H, OMe), 7.01 (d, 1H, 8.2Hz, 5'H), 7.12 (bs, 2H, NH_2), 7.32 (dd, 1H, J=8.2, 1.8Hz, 6'H), 7.68 (d, 1H, J=1.6Hz, 2'H), 8.43 (s, 1H, =CHAr), 8.72 (m, 1H, Pz-H5), 8.75 (d, 1H, J=2.6Hz, Pz-H6), 9.37 (d, 1H, J=1.5Hz, Pz-H3) ppm.
PZcy	2.28 (s, 3H, OOCMe), 3.87 (s, 3H, OMe), 7.16 (d, 1H, J=8.1Hz, 5'H), 7.30 (bs, 2H, NH_2), 7.44 (dd, 1H, J=8.2, 1.8Hz, 6'H), 7.81 (d, 1H, J=1.7Hz, 2'H), 8.50 (s, 1H, =CHAr), 8.74 (m, 1H, Pz-H5), 8.77 (d, 1H, J=2.6Hz, Pz-H6), 9.39 (d, 1H, J=1.5Hz, Pz-H3)ppm.
PZdx	2.90 (s, 6H, CMe_2), 7.03 (bs, 2H, NH_2), 7.15 (d, 1H, J=8.0Hz, 2'H or 3'H), 7.60 (m, 2H, 2Ar-H), 8.11 (d, 1H, J=8.0Hz, 2'H or 3'H), 8.18 (m, 1H, Ar-H), 8.77 (ov.m, 2H, Pz-H5 and H6), 9.00 (m, 1H, Ar-H), 9.09 (s, 1H, =CHAr), 9.44 (d, 1H, J=1.5Hz, Pz-H3)ppm.
QNbf	(s, 2H, OCH_2Ph), 7.08 (m, 1H, Ar-H), 7.23 (bs, 2H, NH_2), 7.34-7.51 (m, 7H, 2Ar-H and 5Phenyl-H), 7.68 (ov.m, 2H, Qn-H6 and 2'H), 7.84 (m, 1H, Qn-H7), 8.05 (m, 1H, Qn-H5), 8.14 (m, 1H, Qn-H8), 8.35 (d, 1H, J=8.6Hz, Qn-H4), 8.47 (d, 1H, J=8.6Hz, Qn-H3), 8.52 (s, 1H, =CHAr)ppm.
QNbh	3.88 (s, 3H, OMe), 5.15 (s, 2H, OCH_2Ph), 7.12 (ov.m, 3H, 5'H and NH_2), 7.32-7.48 (m, 6H, Ar-H and 5Phenyl-H), 7.67 (ov.m, 2H, Qn-H6 and 2'H), 7.83 (m, 1H, Qn-H7), 8.04 (m, 1H, Qn-H5), 8.14 (m, 1H, Qn-H8), 8.34 (m, 1H, J=8.6Hz, Qn-H4), 8.45 (ov.m, 2H, Qn-H3 and =CHAr)ppm.
QNbn	3.82 (s, 3H, OMe), 5.19 (s, 2H, OCH_2Ph), 7.05 (d, 1H, J=8.4Hz, 5'H), 7.14 (bs, 2H, NH_2), 7.35-7.52 (m, 6H, Ar-H and 5Phenyl-H), 7.67 (m, 1H Qn-H6), 7.81 (ov.m, 2H, 2'H and Qn-H7), 8.05 (m, 1H, Qn-H5), 8.14 (m, 1H, Qn-H8), 8.35 (d, 1H, 8.6Hz, Qn-H4), 8.44 (ov.m, 2H, Qn-H3 and =CHAr)ppm.
QNca	6.30 (d, 1H, J=8.1Hz, 5'H), 7.92 (bs, 2H, NH_2), 7.18 (dd, 1H, J=8.1, 1.9Hz, 6'H), 7.37 (d, 1H, J=1.9Hz, 2'H), 7.66 (m, 1H, Qn-H6 or H7), 7.83 (m, 1H, Qn-H6 or H7), 8.04 (m, 1H, Qn-H5), 8.11 (d, 1H, J=8.6Hz, Qn-H8), 8.32 (d, 1H, J=8.6Hz, Qn-H4), 8.36 (s, 1H, =CHAr), 8.44 (d, 1H, J=8.6Hz, Qn-H3), 9.06 (bs, 1H, OH), 9.46 (bs, 1H, OH)ppm.

Compound	^{1}H NMR (d_6-DMSO)
QNcc	6.36 (s, 1H, 3'H), 6.98 (ov.m, 3H, NH_2 and 5'H), 7.68 (m, 1H, Qn-H6), 7.84 (m, 1H, Qn-H7), 8.05 (d, 1H, J=7.6Hz, Qn-H5), 8.13 (d, 1H, J=8.4Hz, Qn-H8), 8.33 (d, 1H, J=8.6Hz, Qn-H4), 8.46 (d, 1H, J=8.8Hz, Qn-H3), 8.53 (bs, 1H, OH), 8.58 (s, 1H, =CHAr), 9.64 (bs, 1H, OH), 10.57 (s, 1H, OH)ppm.
QNcl	7.09 (bs, 2H, NH_2), 7.73 (m, 1H, Qn-H6 or H7), 7.89 (m, 1H, Qn-H6 or H7), 8.10 (m, 1H, Qn-H5), 8.17 (m, 1H, Qn-H8), 8.34 (d, 1H, J=8.6Hz, Qn-H4), 8.42 (m, 1H, Ar-H), 8.55 (m, 1H, Qn-H3), 8.69 (d, 1H, J=2.3Hz, Ar-H), 8.96 (s, 1H, =CHAr)ppm.
QNds	1.85 (t, 2H, J=6.8Hz, $OCH_2C\underline{H}_2CH_2NMe_2$), 2.13 (s, 6H, NMe_2), 2.35 (t, 2H, J=7.0Hz, $OCH_2CH_2C\underline{H}_2NMe_2$), 4.05 (t, 2H, J=6.4Hz, $OC\underline{H}_2CH_2CH_2NMe_2$), 7.00 (d, 2H, J=8.8Hz, 3'H and 5'H), 7.07 (bs, 2H, NH_2), 7.66 (m, 1H, Qn-H6 or H7), 7.7.79-7.89 (ov.m, 3H, Qn-H6 or H7 and 2'H and 6'H), 8.03 (m, 1H, Qn-H5), 8.12 (m, 1H, Qn-H8), 8.33 (d, 1H, J=8.7Hz, Qn-H4), 8.44 (d, 1H, J=8.7Hz, Qn-H3), 8.49 (s, 1H, =CHAr)ppm.
QNec	2.46 (s, 3H, Me), 7.33 (bs, 2H, NH_2), 7.66-7.72 (ov.m, 3H, Qn-H6 and 2Ar-H), 7.85 (m, 1H, Qn-H7), 7.94 (m, 1H, Ar-H), 807 (m, 1H Qn-H5), 8.14 (d, 1H, J=8.2Hz, Qn-H8), 8.37 (d, 1H, J=8.6Hz, Qn-H4), 8.48 (d, 1H, J=8.5Hz, Qn-H3), 8.59 (s, 1H, =CHAr), 9.29 (s, 1H, 8'H)ppm.
HDax	3.83 (s, 3H, OMe), 6.72 (ddd, 1H, J=7.1, 4.9, 1.1Hz, Pyr-H4), 6.96 (m, 1H, Ar-H), 7.04 (m, 1H, Pyr-H3), 7.21 (d, 1H, J=8.4Hz, 3'H or 6'H), 7.30 (m, 1H, 4'H or 5'H), 7.60 (m, 1H, Pyr-H5), 7.86 (dd, 1H, J=7.8, 1.7Hz, 3'H or 6'H), 8.08 (m, 1H, Pyr-H6), 8.34 (s, 1H, =CHAr)ppm.
HDay	1.37 (t, 3H, J=6.9Hz, $CH_2C\underline{H}_3$), 4.09 (q, 2H, J=6.9Hz, $C\underline{H}_2CH_3$), 6.73 (m, 1H, Pyr-H4), 6.96 (m, 1H, 4'H or 5'H), 7.03 (d, 1H, J=8.1Hz, Pyr-H3), 7.21 (d, 1H, J=8.4Hz, 3'H or 6'H), 7.28 (m, 1H, 4'H or 5'H), 7.60 (m, 1H, Pyr-H5), 7.86 (dd, 1H, J=7.7, 1.7Hz, 3'H or 6'H), 8.08 (m, 1H, Pyr-H6), 8.37 (s, 1H, =CHAr), 10.82 (bs, 1H, NH)ppm.
HDbh	3.84 (s, 3H, OMe), 5.11 (s, 2H, $OC\underline{H}_2Ph$), 6.72 (m, 1H, Pyr-H4), 7.07 (ov.m, Pyr-H3 and Ar-H), 7.23 (d, 1H, J=8.4Hz, 5'H), 7.32-7.47 (m, 6H, 6'H and 5Phenyl-H), 7.62 (m, 1H, Pyr-H5), 7.94 (s, 1H, =CHAr), 8.08 (m, 1H, Pyr-H6), 10.71 (bs, 1H, NH)ppm.
HDca	6.66-6.71 (ov.m, Pyr-H4 and 5'H), 6.84 (dd, 1H, J=8.2, 1.9Hz, Pyr-H3), 7.13 (m, 2H, 2'H and 6'H), 7.59 (m, 1H, Pyr-H5), 7.84 (s, 1H, =CHAr), 8.05 (m, 1H, Pyr-H6), 10.52 (bs, 1H, OH)ppm.
HDcb	6.35 (d, 1H, J=8.5Hz, Ar-H), 6.74 (ov.m, 2H, Pyr-H4 and Ar-H), 6.86 (m, 1H, Pyr-H3), 7.62 (m, 1H, Pyr-H5), 8.10 (ov.m, 2H, Pyr-H6 and =CHAr), 9.00 (bs, 1H, OH), 10.68 (bs, 1H, OH)ppm.
HDcd	5.81 (s, 2H, 3'H and 5'H), 6.72 (ov.m, 2H, Pyr-H4 and H3), 7.61 (m, 1H, Pyr-H5), 8.10 (m, 1H, Pyr-H6), 8.43 (s, 1H, =CHAr), 9.61 (bs, 1H, NH), 10.65 (bs, 1H, p-OH), 10.74 (bs, 2H, 2OH)ppm.
HDcj	6.79 (m, 1H, Pyr-H4), 7.05 (m, 1H, Pyr-H3), 7.15 (d, 1H, J=8.4Hz, 3'H), 7.67 (m, 1H, Pyr-H5), 8.06 (dd, 1H, J=9.0, 3.0Hz, 4'H), 8.13 (m, 1H, Pyr-H6), 8.54 (d, 1H, J=2.9Hz, 6'H), 11.13 (bs, 1H, NH or OH), 11.80 (bs, 1H, NH or OH)ppm.
HDcl	6.90 (m, H, Pyr-H4), 6.96 (m, 1H, Pyr-H3), 7.74 (m, 1H, Pyr-H5), 8.19 (m, 1H, Pyr-H6), 8.33 (d, 1H, J=2.9Hz, Ar-H), 8.36 (s, 1H, =CHAr), 8.50 (d, 1H, 2.7Hz, Ar-H), 11.65 (bs, 1H, NH or OH)ppm.

Compound	^{1}H NMR (d_6-DMSO)
HDdb	6.82 (m, 1H, Pyr-H4), 6.96 (m, 1H, Pyr-H3), 7.21 (d, 1H, J=8.9Hz, 3'H), 7.37 (m, 1H, Ar-H), 7.57 (m, 1H, Ar-H), 7.69 (m, 1H, Pyr-H5), 7.85 (m, 2H, 2Ar-H), 8.18 (m, 1H, Pyr-H6), 8.34 (d, 1H, J=8.5Hz, 4'H), 9.07 (s, 1H, =CHAr), 10.99 (bs, 1H, NH or OH), 11.95 (bs, 1H, NH or OH)ppm.
HDdq	2.93 (s, 6H, NMe_2), 6.67 (ov.m, 3H, Pyr-H4 and 2'H and 6'H), 7.14 (m, 1H, Pyr-H3), 7.45 (d, 2H, J=8.8Hz, 3'H and 5'H), 7.57 (m, 1H, Pyr-H5), 7.89 (s, 1H, =CHAr), 8.04 (m, 1H, Pyr-H6), 10.46 (bs, 1H, NH)ppm.
HDdv	6.80 (m, 1H, Pyr-H4), 7.27 (m, 2H, Pyr-H3 and Pyr'-H), 7.66 (m, 1H, Pyr-H5), 7.79 (m, 1H, Pyr'-H), 7.95 (d, 1H, J=8.0Hz, Pyr'-H), 8.05 (s, 1H, =CHAr), 8.12 (m, 1H, Pyr-H6), 8.52 (m, 1H, Pyr'-H), 11.13 (bs, 1H, NH)ppm.

11.2.3.1 Full Characterisation of Compounds Displaying Activity of 16-32μgml^{-1} or Less

2PYab *N^1-(4-Methylbenzylidene)-pyridine-2-carboxamidrazone*[93]

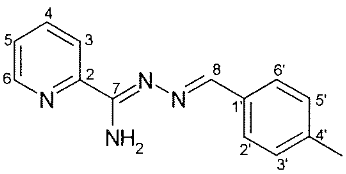

Recrystallised from ethanol to give a yellow crystalline solid, 35% yield. R.f. [EtOAc]: 0.54. ^{1}H NMR (d_6-DMSO): 2.35 (s, 3H, Me), 7.02 (bs, 2H, NH_2), 7.26 (d, 2H, J=8.0Hz, 3'H and 5'H), 7.53 (ddd, 1H, J=7.4, 4.8, 1.2Hz, Pyr-H4), 7.81 (d, 2H, J=8.0Hz, 2'H and 6'H), 7.92 (dt, 1H, J=7.7, 1.8Hz, Pyr-H5), 8.22 (d, 1H, J=7.9Hz, Pyr-H3), 8.46 (s, 1H, =CHAr), 8.65 (m, 1H, Pyr-H6)ppm. ^{13}C NMR ($CDCl_3$): 21.5 (CH_3), 121.2 (C5), 125.0 (C3), 127.9 (C2' and C6'), 129.3 (C3' and C5'), 132.4 (C1'), 136.5 (C4), 140.4 (C4'), 148.3 (C6), 150.2 (C2), 156.0 (C8), 156.8 (C7)ppm. IR (KBr disc): 3474 (ν_{as} NH_2), 3344 (ν_s NH_2), 3080 (ν Ar-CH), 3021 (ν Ar or Pyr-CH), 2956 (ν_{as} Me), 2870 (ν_s Me), 1622 (ν C=N), 1590 (ν skeletal Ar or Pyr),1558 (ν skeletal Pyr), 1510 (ν skeletal Ar or Pyr), 1467 (δ_{as} Me or ν skeletal Ar or Pyr), 1370 (δ_s Me), 1255, 1178, 1107 (ν C-N), 1047, 983, 970, 869, 811 (γ CH, p-subst. Ar),763 (γ CH, 2-Pyr), 744 (β ring, 2-Pyr), 690, 619cm^{-1}. APCI-MS m/z: 239 $(M+H)^+$. mp (corrected): 122.7-123.7°C. CHN Analysis, %m/m (%calculated/%found): C 70.57/70.57, H 5.92/ 5.87, N 23.51/23.56.

2PYac *N^1-(4-Ethylbenzylidene)-pyridine-2-carboxamidrazone*

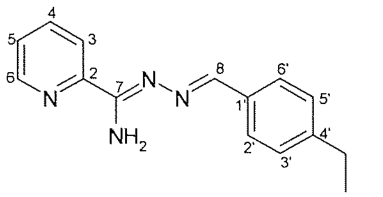

Recrystallised from 40-60 PE twice, to give a yellow crystalline solid, 45%. R.f. [EtOAc]: 0.53. ^{1}H NMR (d_6-DMSO): 1.20 (t, 3H, J=7.6Hz, $CH_2C\underline{H}_3$), 2.65 (q, 2H, J=7.6Hz, $C\underline{H}_2CH_3$), 7.01 (bs, 2H, NH_2), 7.28 (d, 2H, J=8.1Hz, 3'H and 5'H), 7.53 (ddd, 1H, J=7.4, 4.9, 1.2Hz, Pyr-H4), 7.83 (d, 2H, J=8.1Hz, 2'H and 6'H), 7.93 (dt, 1H, J=7.6, 1.7Hz, Pyr-H5), 8.23 (d, 2H, J=8.0Hz, Pyr-H3), 8.46 (s, 1H, =CHAr), 8.66 (m, 1H, Pyr-H6)ppm. ^{13}C NMR ($CDCl_3$): 15.4 ($CH_2\underline{C}H_3$), 28.8 ($\underline{C}H_2CH_3$),121.2 (C5), 125.1 (C3), 128.0, (C2' and C6' or C3' and C5'), 128.1 (C2' and C6' or C3' and C5'), 132.7 (C1'), 136.5 (C4), 146.8 (C4') 148.3 (C6), 150.2 (C2), 156.0 (C8), 156.8 (C7)ppm. IR (KBr disc): 3496 (ν_{as} NH_2), 3375 (ν_s NH_2), 3050 (ν Ar- or Pyr-CH), 2956 (ν_{as} Me), 2925 (ν_{as} CH_2), 2867 (ν_s Me), 1622 (ν C=N), 1589 (ν skeletal Ar or Pyr), 1554 (ν skeletal Pyr), 1500 (ν skeletal Ar or Pyr), 14(δ_{as} Me or ν skeletal Ar or Pyr), 1364 (δ_s Me), 1176, 1109 (ν C-N), 1049, 1005, 964, 836 (γ CH, p-subst. Ar), 802, 767 (γ CH, 2-Pyr), 746 (β ring, 2-Pyr), 686, 622cm^{-1}. APCI-MS m/z: 253 $(M+H)^+$. mp (corrected): 97.5-98.7°C. CHN Analysis, %m/m (%calculated/%found): C 71.40/71.05, H 6.39/6.31, N 22.20/22.22.

2PYad *N^1-(4-Isopropylbenzylidene)-pyridine-2-carboxamidrazone*

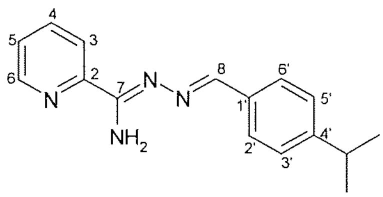

Recrystallised from ethanol twice, to give a yellow crystalline solid, 61% yield. R.f. [EtOAc]: 0.54. ^{1}H NMR (d_6-DMSO): 1.21 (s, 3H, Me), 1.24 (s, 3H, Me), 2.93 (sept, 1H, J=6.9Hz, $C\underline{H}Me_2$), 7.01 (bs, 2H, NH_2), 7.31 (d, 2H, J=8.2Hz, 3'H and 5'H), 7.53 (ddd, 1H, J=7.4, 4.8, 1.2Hz, Pyr-H4), 7.84 (d, 2H, J=8.2Hz, 2'H and 6'H), 7.92 (dt, 1H, J=7.7, 1.7Hz, Pyr-H5), 8.23 (d, 1H, 7.9Hz, Pyr-H3), 8.46 9s, 1H, =CHAr), 8.67 (m, 1H, Pyr-H6)ppm. ^{13}C NMR ($CDCl_3$): 23.7 ($CH\underline{Me}_2$), 34.0 ($\underline{C}HMe_2$), 121.2 (C5), 125.0 (C3), 126.6 (C2' and C6'), 127.9 (C3' and C5'), 132.8 (C1'), 136.4 (C4), 148.3 (C6), 150.1 (C2), 151.3 (C4'), 155.9 (C8), 156.7 (C7)ppm. IR (KBr disc): 3494 (ν_{as} NH_2), 3360 (ν_s NH_2), 3100 (ν Ar-CH), 3048 (ν Ar or Pyr-CH), 2954 (ν_{as} Me), 2863 (ν_s Me), 1623 (ν C=N), 1600 (ν skeletal Ar or Pyr), 1558 (ν skeletal Pyr), 1519 (ν skeletal Ar or Pyr), 1467 (δ_{as} Me or ν skeletal Ar or Pyr), 1372 (δ_s Me), 1334, 1280, 1108 (ν C-N), 1049, 833 (γ CH, p-subst. Ar), 766 (δ_{as} Me), 742 (β ring, 2-Pyr), 678, 624cm^{-1}. APCI-MS m/z: 267 $(M+H)^+$. mp (corrected): 66.7-67.6°C. CHN Analysis, %m/m (%calculated/ %found): C 72.15/72.18, H 6.81/6.78, N 21.04/21.05.

2PYae *N^1-(4-tert-Butylbenzylidene)-pyridine-2-carboxamidrazone*

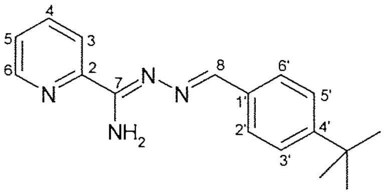

Recrystallised from ethanol twice, to give a yellow crystalline solid, 72%yield. R.f. [EtOAc]: 0.62. ^{1}H NMR (d_6-DMSO): 1.31 (s, 9H, CMe_3), 7.00 (bs, 2H, NH_2), 7.46 (d, 2H, J=8.4Hz, 3'H and 5'H), 7.53 (m, 1H, Pyr-H4), 7.83 (d, 2H, J=8.4Hz, 2'H and 6'H), 7.92 (dt, 1H, J=7.1, 1.7Hz, Pyr-H5), 8.23 (d, 1H, J=8.0Hz, Pyr-H3), 8.46 (s, 1H, =CHAr), 8.66 (d, 1H, J=4.8, Pyr-H6)ppm. ^{13}C NMR ($CDCl_3$): 31.2 ($C\underline{Me}_3$), 34.9 ($\underline{C}Me_3$), 121.4 (C5), 125.2 (C3), 125.6 (C2' and C6'), 127.7 (C3' and C5'), 132.4 (C1'), 136.6 (C4), 148.4 (C6), 150.0 (C2), 153.7 (C4'), 156.0 (C8), 156.8 (C7)ppm. IR (KBr disc): 3490 (ν_{as} NH_2), 3364 (ν_s NH_2), 3091 (ν Ar-CH), 3015 (ν Ar or Pyr-CH), 2954 (ν_{as} Me), 2862 (ν_s Me), 1619 (ν C=N), 1590 (ν skeletal Ar or Pyr),1558 (ν skeletal Pyr), 1515 (ν skeletal Ar or Pyr), 1453 (δ_{as} Me or ν skeletal Ar or Pyr), 1378 (δ_s Me), 1365, 1336, 1263, 1105 (ν C-N), 1039, 1000, 946, 832 (γ CH, p-subst. Ar), 802, 780 (γ CH, 2-Pyr), 748 (β ring, 2-Pyr), 705, 605cm^{-1}. APCI-MS m/z: 281 $(M+H)^+$. mp (corrected): 121.8-122.7°C. CHN Analysis, %m/m (%calculated/%found): C 72.83/72.84, H 7.19/7.22, N 19.98/19.90.

3PYae *N^1-(4-tert-Butylbenzylidene)-pyridine-3-carboxamidrazone*

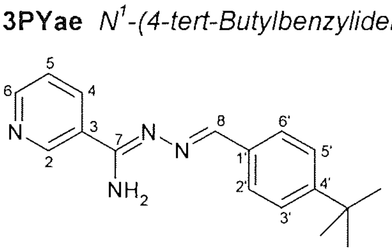

Recrystallised from ethanol three times, to give a yellow crystalline solid, 56% yield. R.f. [EtOAc]: 0.25. ^{1}H NMR (d_6-DMSO): 1.30 (s, 9H, CMe_3), 7.12 (bs, 2H, NH_2), 7.47 (ov.m, 3H, Pyr-H4 and 3'H and 5'H), 7.82 (d, 2H, J=8.4Hz, 2'H and 6'H), 8.26 (dt, 1H, J=8.0, 1.9Hz, Pyr-H5), 8.42 (s, 1H, =CHAr), 8.65 (dd, 1H, J=4.8, 1.7Hz, Pyr-H6), 9.10 (d, 1H, J=1.8Hz, Pyr-H2)ppm. ^{13}C NMR ($CDCl_3$): 31.2 ($C\underline{Me}_3$), 34.9 ($\underline{C}Me_3$), 123.4 (C5), 125.6 (C3' and C5'), 127.8 (C2' and C6'), 129.7 (C4), 132.2 (C1'), 134.3 (C6), 147.7 (C2), 151.5 (C3), 153.9 (C4'), 156.7 (C7), 156.8 (C8)ppm. IR (KBr disc): 3434 (ν_{as} NH_2), 3282 (ν_s NH_2), 3095 (ν Ar-CH), 3020 (ν Ar or Pyr-CH), 2956 (ν_{as} Me), 2861 (ν_s Me), 1616 (ν C=N), 1585 (ν skeletal Ar or Pyr), 1560 (ν skeletal Pyr), 1517 (ν skeletal Ar or Pyr), 1453 (δ_{as} Me or ν skeletal Ar or Pyr), 1376 (δ_s Me), 1359, 1263, 1185, 1105 (ν C-N), 1028, 1014, 997, 950, 833 (γ CH, p-subst. Ar), 809 (γ CH, 3-Pyr), 748, 715 (β ring, 3-Pyr), 630cm^{-1}. APCI-MS m/z: 281 $(M+H)^+$. mp (corrected): 165.2-166.6. CHN Analysis, %m/m (%calculated/%found): C 72.83/72.78, H 7.19/7.19, N 19.98/19.88.

4PYae *N¹-(4-tert-Butylbenzylidene)-pyridine-4-carboxamidrazone*

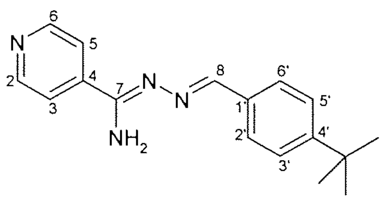

Recrystallised from ethanol to give a yellow crystalline solid, 54% yield. R.f. [EtOAc]: 0.36. ^{1}H NMR (d_6-DMSO): 1.25 (s, 9H, CMe_3), 7.15 (bs, 2H, NH_2), 7.46 (d, 2H, J=8.3Hz, 3'H and 5'H), 7.84 (d, 2H, J=8.3Hz, 2'H and 6'H), 7.88 (dd, 2H, J=4.7,1.5Hz, Pyr-H3 and H5), 8.44 (s, 1H. =CHAr), 8.68 (dd, 2H, J=4.7, 1.5Hz, Pyr-H2 and H6)ppm. ^{13}C NMR ($CDCl_3$): 31.1 (C$\underline{Me}_3$), 34.8 ($\underline{C}Me_3$), 120.6 (C3 and C5), 125.6 (C2' and C6'), 127.8 (C3' and C5'), 132.0 (C1'), 141.3 (C4), 150.1 (C2 and C6), 154.0 (C4'), 156.6 (C7), 157.1 (C8)ppm. IR (KBr disc): 3432 (ν_{as} NH_2), 3282 (ν_s NH_2), 3100 (ν Ar-CH), 3009 (ν Ar or Pyr-CH), 2952 (ν_{as} Me), 2868 (ν_s Me), 1630 (ν C=N), 1601 (ν skeletal Ar or Pyr), 1558 (ν skeletal Pyr), 1527 (ν skeletal Ar or Pyr), 1459 (δ_{as} Me or ν skeletal Ar or Pyr), 1415 (ν skeletal Ar or Pyr), 1368 (δ_s Me), 1265, 1215, 1182, 1109 (ν C-N), 1066, 1001, 879, 832 (γ CH, p-subst. Ar), 800 (γ CH, 4-Pyr), 748 (β ring, 4-Pyr), 704, 671cm^{-1}. APCI-MS m/z: 281 $(M+H)^+$. mp (corrected): 174.2-175.7°C. CHN Analysis, %m/m (%calculated/%found): C 72.83/72.95, H 7.19/ 7.26, N 19.98/20.14.

2PYaf *N¹-[4-(1,1-Dimethylpropyl)benzylidene]-pyridine-2-carboxamidrazone*[97]

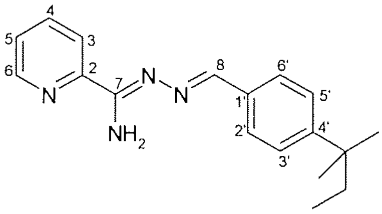

Recrystallised from ether/PE to give a yellow crystalline solid, 34% yield. R.f. [EtOAc]: 0.64. ^{1}H NMR (d_6-DMSO): 0.70 (t, 3H, J=7.4Hz, $CH_2C\underline{H}_3$), 1.32 (s, 6H, CMe_2), 1.68 (q, 2H, J=7.4Hz, $C\underline{H}_2CH_3$), 6.53 (bs, 2H, NH_2), 7.36 (m, 1H, Pyr-H4), 7.39 (d, 2H, J=8.4Hz, 3'H and 5'H), 7.77 (d, 2H, J=8.4Hz, 2'H and 6'H), 7.85 (m, 1H, Pyr-H5), 8.35 (d, 1H, J=8.0Hz, Pyr-H3), 8.56 (s, 1H, =CHAr), 8.61 (m, 1H, Pyr-H6)ppm. ^{13}C NMR ($CDCl_3$): 9.1 ($CH_2\underline{C}H_3$), 28.3 (C$\underline{Me}_2$), 36.7 ($\underline{C}Me_2$), 38.1 ($\underline{C}H_2CH_3$), 121.3 (C5), 125.1 (C3), 125.1 (C2' and C6'), 127.6 (C3' and C5'), 132.3 (C4'), 136.5 (C4), 148.3 (C6), 150.1 (C2), 152.0 (C1'), 155.9 (C8), 156.8 (C7)ppm. IR (KBr disc): 3443 (ν_{as} NH_2), 3274 (ν_s NH_2), 3122 (ν Ar-CH), 3055 (ν Ar or Pyr-CH), 2962 (ν_{as} Me), 2872 (ν_s Me), 1626 (ν C=N), 1594 (ν skeletal Ar or Pyr), 1560 (ν skeletal Pyr), 1521 (ν skeletal Ar or Pyr), 1450 (δ_{as} Me or ν skeletal Ar or Pyr), 1407 (ν skeletal Ar or Pyr), 1378 (δ_s Me),1344, 1307, 1230, 1178, 1117, 1058 (ν C-N), 997, 887, 832 (γ CH, p-subst. Ar), 778 (γ CH, 2-Pyr), 748 (β ring, 2-Pyr), 702, 674cm^{-1}. APCI-MS m/z: 295 $(M+H)^+$. mp (corrected): 86.3-88.4°C. CHN Analysis, %m/m (%calculated/%found): C 73.44/73.44, H 7.53/7.54, N 19.03/18.94.

3PYaf *N^1-[4-(1,1-Dimethylpropyl)benzylidene]-pyridine-3-carboxamidrazone*

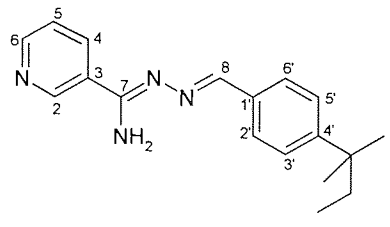

Recrystallised from ethanol three times, to give a yellow crystalline solid, 49% yield. R.f. [EtOAc]: 0.26. ^{1}H NMR (d_6-DMSO): 0.63 (t, 3H, J=7.4Hz, $CH_2\underline{CH_3}$), 1.26 (s, 6H, CMe_2), 1.63 (q, 2H, J=7.4Hz, $\underline{CH_2}CH_3$), 7.12 (bs, 2H, NH_2), 7.38 (d, 2H, J=8.3Hz, 3'H and 5'H), 7.47 (m, 1H, Pyr-H4), 7.82 (d, 2H, J=8.3Hz, 2'H and 6'H), 8.26 (m, 1H, Pyr-H5), 8.42 (s, 1H, =CHAr), 8.65 (m, 1H, Pyr-H6), 9.10 (m, 1H, Pyr-H2)ppm. ^{13}C NMR ($CDCl_3$): 9.0 ($CH_2\underline{C}H_3$), 28.2 ($C\underline{Me_2}$), 36.6 ($\underline{C}Me_2$), 38.1 ($\underline{C}H_2CH_3$), 123.3 (C5), 126.2 (C3' and C5'), 127.6 (C2' and C6'), 129.8 (C4), 132.0 (C1'), 134.2 (C6), 147.7 (C2), 151.3 (C3), 152.2 (C4'), 156.6 (C8), 156.7 (C8)ppm. IR (KBr disc): 3446 (ν_{as} NH_2), 3286 (ν_s NH_2), 3110 (ν Ar-CH), 3035 (ν Ar or Pyr-CH), 2963 (ν_{as} Me), 2869 (ν_s Me), 1622 (ν C=N), 1590 (ν skeletal Ar or Pyr),1551 (ν skeletal Pyr), 1525 (ν skeletal Ar or Pyr), 1450 (δ_{as} Me or ν skeletal Ar or Pyr), 1378 (δ_s Me), 1332, 1303, 1193, 1106 (ν C-N), 1016, 960, 839 (γ CH, p-subst. Ar), 817 (γ CH, 3-Pyr), 711 (β ring, 3-Pyr), 630cm^{-1}. APCI-MS m/z: 295$(M+H)^+$. mp (corrected): 160.5-161.3°C. CHN Analysis, %m/m (%calculated/%found): C 73.44/73.56, H 7.53/7.53, N 19.03/19.06.

4PYaf *N^1-[4-(1,1-Dimethylpropyl)benzylidene]-pyridine-4-carboxamidrazone*

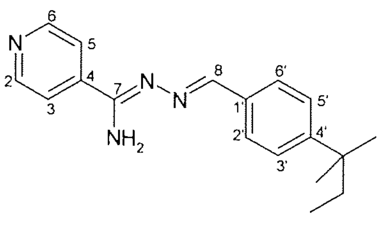

Recrystallised from toluene twice, to give a yellow crystalline solid, 42% yield. R.f. [EtOAc]: 0.38. ^{1}H NMR (d_6-DMSO): 0.63 (t, 3H, J=7.5Hz, $CH_2\underline{CH_3}$), 1.26 (s, 6H, CMe_2), 1.64 (q, 2H, J=7.5Hz, $\underline{CH_2}CH_3$), 7.14 (bs, 2H, NH_2), 7.39 (d, 2H, J=8.3Hz, 3'H and 5'H), 7.83 (d, 2H, J=8.3Hz, 2'H and 6'H), 7.88 (dd, 2H, J=4.6, 1.6Hz, Pyr-H3 and H5), 8.44 (s, 1H, =CHAr), 8.67 (dd, 2H, J=4.6, 1.6Hz, Pyr-H2 and H6)ppm. ^{13}C NMR ($CDCl_3$): 9.1 ($CH_2\underline{C}H_3$), 28.3 ($C\underline{Me_2}$), 36.7 ($\underline{C}Me_2$), 38.1 ($\underline{C}H_2CH_3$), 120.6 (C3 and C5), 126.3 (C2' andC6'), 127.8 (C3' and C5'), 131.9 (C1'), 141.3 (C4), 150.2 (C2 and C6), 152.5 (C4'), 156.6 (C7), 157.3 (C8)ppm. IR (KBr disc): 3443 (ν_{as} NH_2), 3274 (ν_s NH_2), 3122 (ν Ar-CH), 3019 (ν Ar or Pyr-CH), 2962 (ν_{as} Me), 2860 (ν_s Me), 1625 (ν C=N), 1595 (ν skeletal Ar or Pyr), 1568 (ν skeletal Pyr),1521 (ν skeletal Ar or Pyr), 1449 (δ_{as} Me or ν skeletal Ar or Pyr), 1378 (δ_s Me), 1344, 1307, 1230, 1178, 1117, 1086 (ν C-N), 996, 878, 832 (γ CH, p-subst. Ar), 802 (γ CH, 4-Pyr), 748 (β ring, 4-Pyr), 701, 675cm^{-1}. APCI-MS m/z: 295 $(M+H)^+$. mp (corrected): 144.0-145.8°C. CHN Analysis, %m/m (%calculated/%found): C 73.44/73.51, H 7.53/7.41, N 19.03/19.14.

PZaf *N^1-[4-(1,1-Dimethylpropyl)benzylidene]-pyrazine-2-carboxamidrazone*

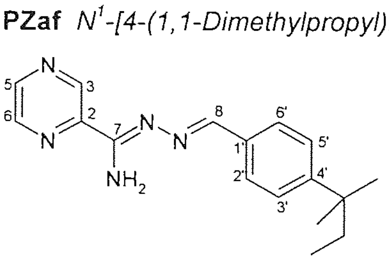

Recrystallised from 40-60 PE to give a orange/yellow solid, 64% yield. R.f. [EtOAc]: 0.62. ^{1}H NMR (d_6-DMSO): 0.67 (t, 3H, J=7.5Hz, $CH_2C\underline{H_3}$), 1.27 (s, 6H, $C\underline{Me_2}$), 1.65 (q, 2H, J=7.5Hz, $C\underline{H_2}CH_3$), 7.10 (bs, 2H, NH_2), 7.41 (d, 2H, J=8.4Hz, 3'H and 5'H), 7.86 (d, 2H, J=8.4Hz, 2'H and 6'H), 8.49 (s, 1H, =CHAr), 8.73 (m, 1H, Pz-H5), 8.77 (d, 1H, J=2.5Hz, Pz-H6), 9.38 (d, 1H, J=1.4Hz, Pz-H3)ppm. ^{13}C NMR ($CDCl_3$): 9.1 ($CH_2\underline{C}H_3$), 28.3 ($C\underline{Me_2}$), 36.7 ($\underline{C}Me_2$), 38.2 ($\underline{C}H_2CH_3$), 126.3 (C2' and C6'), 127.8 (C3' and C5'), 132.0 (C1'), 142.7 (C3 or C5 or C6), 143.8 (C3 or C5 or C6), 145.6 (C3 or C5 or C6), 152.5 (C4'), 155.0 (C2), 156.9 (C7), 157.2 (C8)ppm. IR (KBr disc): 3419 (ν_{as} NH_2), 3305 (ν_s NH_2), 3090 (ν Ar-CH), 3010 (ν Ar or Pz-CH), 2968 (ν_{as} Me), 2872 (ν_s Me), 1612 (ν C=N), 1560 (ν skeletal Pz), 1506 (ν skeletal Ar or Pz), 1471, 1450 (δ_{as} Me or ν skeletal Ar or Pz), 1429 (ν skeletal Ar or Pz), 1375 (δ_s Me), 1151, 1108 (ν C-N), 1018, 823, 715cm^{-1}. APCI-MS m/z: 296 $(M+H)^+$. mp (corrected): 141.7-142.8°C. CHN Analysis, %m/m (%calculated/%found): C 69.13/68.88, H 7.17/7.14, N 23.71/ 23.99.

QNaf *N^1-[4-(1,1-Dimethylpropyl)benzylidene]-quinoline-2-carboxamidrazone*

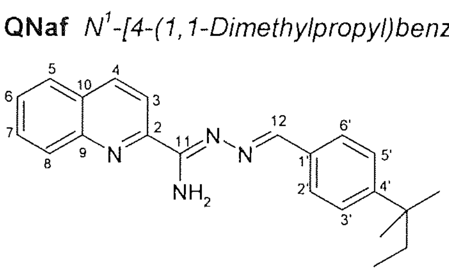

Recrystallised from methanol to give a yellow solid, 81% yield. R.f. [EtOAc]: 0.88. ^{1}H NMR (d_6-DMSO): 0.65 (t, 3H, J=7.4Hz, $CH_2C\underline{H_3}$), 1.28 (s, 6H, $C\underline{Me_2}$), 1.66 (q, 2H, J=7.4Hz, $C\underline{H_2}CH_3$), 7.12 (bs, 2H, NH_2), 7.42 (d, 2H, J=8.3Hz, 3'H and 5'H), 7.69 (t, 1H, J=7.4Hz, Qn-H6), 7.86 (ov.m, 3H, 2'H and 6'H and Qn-H7), 8.05 (d, 1H, J=7.9Hz, Qn-H5), 8.15 (d, 1H, J=8.4Hz, Qn-H8), 8.35 (d, 1H, J=8.6Hz, Qn-H3 or H4), 8.47 (d, 1H, J=8.8Hz, Qn-H3 or H4), 8.53 (s, 1H, =CHAr)ppm. ^{13}C NMR ($CDCl_3$): 9.1 ($CH_2\underline{C}H_3$), 28.3 ($C\underline{Me_2}$), 36.7 ($\underline{C}Me_2$), 38.1 ($\underline{C}H_2CH_3$), 118.6 (Qn $\underline{C}$H), 126.3 (C3' and C5'), 127.2 (Qn $\underline{C}$H), 127.6 (Qn $\underline{C}$H), 12.7 (C2' and C6'), 128.9 (C9), 129.5 (Qn $\underline{C}$H), 129.6 (Qn $\underline{C}$H), 132.3 (C1'), 136.3(Qn $\underline{C}$H), 146.9 (C10), 150.3 (C2), 152.1 (C4'), 156.4 (C12), 156.8 (C11)ppm. IR (KBr disc): 3475(ν_{as} NH_2), 3322 (ν_s NH_2), 3080 (ν Ar-CH), 2962 (ν_{as} Me), 2871 (ν_s Me), 1618 (ν C=N), 1593 (ν skeletal Ar or Qn), 1562, 1500 (ν skeletal Ar or Qn), 1459 (δ_{as} Me or ν skeletal Ar or Qn), 1370 (δ_s Me), 1336, 1213, 1172, 1103 (ν C-N), 1009, 970, 839, 769, 702, 624 cm^{-1}. APCI-MS m/z: 344 $(M+H)^+$. mp (corrected): 151.6-152.4°C. CHN Analysis,%m/m (% calculated/%found): C 76.71/76.54 , H 7.02/6.87 , N 16.26/16.26.

2PYal *N*[1]*-(1-Naphthylidene)-pyridine-2-carboxamidrazone*[97]

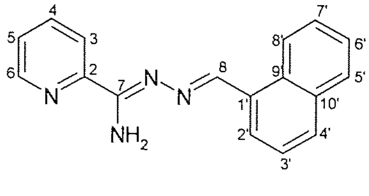

Recrystallised from ethanol three times, to give a yellow crystalline solid, 55%yield. R.f. [EtOAc]: 0.53. ^{1}H NMR (d_6-DMSO): 7.09 (bs, 2H, NH_2), 7.43-7.68 (ov.m, 4H, Pyr-H4 and 3Ar-H), 7.93-8.06 (ov.m, 3H, 3Ar-H), 8.26 (d, 1H, J=7.3Hz, Pyr-H5), 8.32 (d, 1H, J=8.0Hz, Ar-H), 8.69 (m, 1H, Pyr-H3), 8.90 (d, 1H, J=8.3 Hz, Pyr-H6), 9.20 (s, 1H, =CHAr)ppm. ^{13}C NMR ($CDCl_3$): 121.3 (C5), 124.1 (naphthalene CH), 125.1 (C3), 125.2 (naphthalene CH), 125.9 (naphthalene CH), 126.8 (naphthalene CH), 127.6 (naphthalene CH), 128.6(naphthalene CH), 130.5 (naphthalene CH), 130.7 (C9' or C10'), 131.2 (C9' or C10'), 133.7 (C1'), 136.5 (C4), 148.3 (C6), 150.0 (C2), 155.1 (C8), 156.9 (C7)ppm. IR (KBr disc): 3550 (ν_{as} NH_2), 3456 (ν_s NH_2), 3115 (ν Ar-CH), 3030 (ν Ar or Pyr-CH), 1610 (ν C=N), 1597 (ν skeletal Ar or Pyr), 1578, 1474 (ν skeletal Ar or Pyr), 1401 (ν skeletal Ar or Pyr), 1386, 1166, 1141, 1125, 1106 (ν C-N), 1089, 1000, 801, 779 (γ CH, 2-Pyr), 750 (β ring, 2-Pyr), 690, 619cm^{-1}. APCI-MS m/z: 275 $(M+H)^+$. mp (corrected): 112.7-115.9°C. CHN Analysis, %m/m (%calculated/%found): C 74.43/74.08, H 5.14/4.93, N 20.42/20.18.

4PYal *N*[1]*-(1-Naphthylidene)-pyridine-4-carboxamidrazone*

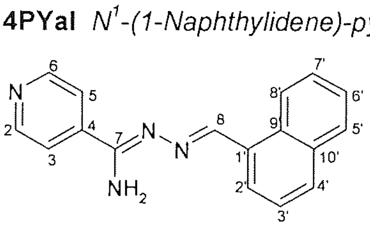

Recrystallised from ethanol three times, to give a yellow crystalline solid, 60%yield. R.f. [EtOAc]: 0.33. ^{1}H NMR (d_6-DMSO): 7.23 (bs, 2H, NH_2), 7.55-7.67 (m, 2H, 2Ar-H), 7.93 (dd, 2H, J=4.5, 1.6Hz, Pyr-H3 and H5), 8.00 (m, 2H, 2Ar-H), 8.28 (m, 1H, Ar-H), 8.70 (dd, 2H, J=4.5, 1.6Hz, Pyr-H2 and H6), 8.82 (m, 1H, Ar-H), 9.19 (s, 1H, =CHAr)ppm. ^{13}C NMR ($CDCl_3$): 120.5 (C3 and C5), 124.1 (naphthalene CH), 124.3 (naphthalene CH), 124.8 (naphthalene CH), 126.1 (C2 and C6), 126.6 (naphthalene CH), 127.9 (naphthalene CH), 128.6 (naphthalene CH), 131.1 (naphthalene CH), 130.7 (C9' or C10'), 131.9 (C9' or C10'), 133.6 (C1'), 142.5 (C4), 155.6 (C8), 156.9 (C7)ppm. IR (KBr disc): 3548 (ν_{as} NH_2), 3449 (ν_s NH_2), 3115 (ν Ar-CH), 3020 (ν Ar or Pyr-CH), 1616 (ν C=N), 1595 (ν skeletal Ar or Pyr), 1567, 1470 (ν skeletal Ar or Pyr), 1401 (ν skeletal Ar or Pyr), 1386, 1307, 1176, 1118, 1102 (ν C-N), 1089, 1000, 801, 779 (γ CH, 2-Pyr), 749 (β ring, 4-Pyr), 700, 669cm^{-1}. APCI-MS m/z: 275 $(M+H)^+$. mp (corrected): 162.4-163.7°C. CHN Analysis, %m/m (%calculated/%found): C 74.43/74.21, H 5.14/5.01, N 20.42/20.21.

2PYas *N[1]-(4-Methoxybenzylidene)-pyridine-2-carboxamidrazone*[97]

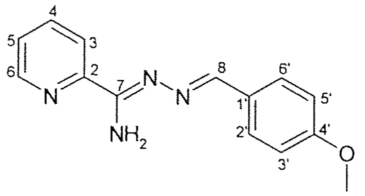

Recrystallised from 40-60 PE to give a yellow crystalline solid, 66% yield. R.f. [EtOAc]: 0.51. ^{1}H NMR (d$_6$-DMSO): 3.82 (s, 3H, OMe), 6.96 (bs, 2H, NH_2), 7.00 (d, 2H, J=8.8Hz, 3'H and 5'H), 7.52 (m, 1H, Pyr-H4), 7.86 (d, 2H, J=8.8Hz, 2'H and 6'H), 7.93 (m, 1H, Pyr-H5), 8.22 (m, 1H, Pyr-H3), 8.43 (s, 1H, =CHAr), 8.65 (m, 1H, Pyr-H6)ppm. ^{13}C NMR ($CDCl_3$): 55.2 (OMe), 114.0 (C3' and C5'), 121.1 (C5), 125.0 (C3), 128.0 (C1'), 129.4 (C2' and C6'), 136.4 (C4), 148.2 (C6), 150.2 (C2), 155.5 (C8), 156.5 (C7) , 161.3 (C4')ppm. IR (KBr disc): 3422 (ν_{as} NH_2), 3312 (ν_s NH_2), 3100 (ν Ar-CH), 3005 (ν Ar or Pyr-CH), 2933 (ν_{as} sat. CH), 2833 (ν_s sat. CH), 1617 (ν C=N), 1566, 1508, 1477 (ν skeletal Ar or Pyr), 1423 (ν skeletal Ar or Pyr), 1311, 1245, 1108 (ν C-N or C-O), 1026 (ν C-N or C-O), 1004, 962, 848, 830 (γ CH, p-subst. Ar),786 (γ CH, 2-Pyr), 746 (β ring, 2-Pyr), 684, 604cm^{-1}. APCI-MS m/z: 255 $(M+H)^+$. mp (corrected): 113.2-114.1°C. CHN Analysis, %m/m (%calculated/%found): C 66.13/65.87, H 5.55/5.47, N 22.03/21.95.

2PYax *N[1]-(2-Methoxybenzylidene)-pyridine-2-carboxamidrazone*

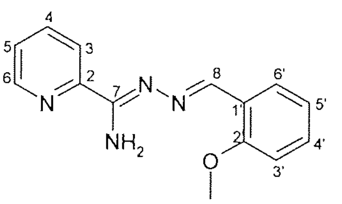

Recrystallised from 40-60 PE to give a yellow crystalline solid, 70% yield. R.f. [EtOAc]: 0.53. ^{1}H NMR (d$_6$-DMSO): 3.87 (s, 3H, OMe), 7.04 (ov.m, 4H, NH_2 and 2Ar-H), 7.41 (m, 1H, Ar-H), 7.53 (m, 1H, Pyr-H4), 7.92 (dt, 1H, J=7.8Hz, 1.8Hz, Pyr-H5), 8.22 (ov.m, 2H, Pyr-H3, and Ar-H), 8.65 (m, 1H, Pyr-H6), 8.76 (s, 1H, =CHAr)ppm. ^{13}C NMR ($CDCl_3$): 55.5 (OMe), 111.1 (C3'), 120.6 (C5'), 121.3 (C5), 123.8 (C3), 125.0 (C1'), 126.9 (C6'), 131.3 (C4'), 136.5 (C4), 148.3 (C6), 150.4 (C2), 151.9 (C2'), 156.7 (C7), 158.6 (C8)ppm. IR (KBr disc): 3421 (ν_{as} NH_2), 3310 (ν_s NH_2), 3083 (ν Ar), 3024 (ν Ar or Pyr-CH), 2973 (ν_{as} Me), 2881 (ν_s Me), 1615 (ν C=N), 1598 (ν skeletal Ar or Pyr), 1566 (ν skeletal Pyr), 1526, 1493 (ν skeletal Ar or Pyr), 1438 (δ_{as} Me or ν skeletal Ar or Pyr), 1392, 1330, 1293, 1238, 1161, 1111 (ν C-N or C-O), 1039 (ν C-N or C-O), 997, 918, 800, 745 (γ CH, o-subst. Ar or β ring, 2-Pyr), 680cm^{-1}. APCI-MS m/z: 255 $(M+H)^+$. mp (corrected): 114.7-115.6°C. CHN Analysis, %m/m (%calculated/%found): C 66.13/65.93, H 5.55/5.51, N 22.03/21.99.

2PYay *N^1-(2-Ethoxybenzylidene)-pyridine-2-carboxamidrazone*

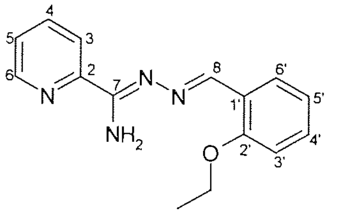

Recrystallised from 40-60 PE twice, to give a yellow crystalline solid, 39% yield. R.f. [EtOAc]: 0.62. ^{1}H NMR (d$_6$-DMSO): 1.39 (t, 3H, J=7.0Hz, OCH$_2$C$\underline{H_3}$), 4.12 (q, 2H, J=7.0Hz, OC$\underline{H_2}$CH$_3$), 7.02 (ov.m, 4H, NH$_2$ and 2Ar-H), 7.39 (m, 1H, Ar-H), 7.53 (m, 1H, Pyr-H4), 7.91 (dt, 1H, J=7.8Hz, 1.8Hz, Pyr-H5), 8.22 (ov.m, 2H, Pyr-H3, and Ar-H), 8.66 (m, 1H, Pyr-H6), 8.77 (s, 1H, =CHAr)ppm. ^{13}C NMR (CDCl$_3$): 14.8 (OCH$_2\underline{C}$H$_3$), 63.9 (O$\underline{C}$H$_2$CH$_3$), 112.0 (C3'), 120.4 (C5'), 121.3 (C5), 123.8 (C3), 125.0 (C1'), 126.8 (C6'), 131.3 (C4'), 136.5 (C4), 148.3 (C6), 150.3 (C2), 152.0 (C2'), 156.7 (C7), 158.0 (C8)ppm. IR (KBr disc): 3414 (ν_{as} NH$_2$), 3307 (ν_s NH$_2$), 3080 (ν Ar), 3025 (ν Ar or Pyr-CH), 2973 (ν_{as} Me), 2930 (ν_{as} CH$_2$), 2880 (ν_s Me), 1618 (ν C=N), 1598 (ν skeletal Ar or Pyr), 1566 (ν skeletal Pyr), 1526, 1493 (ν skeletal Ar or Pyr), 1438 (δ_{as} Me or ν skeletal Ar or Pyr), 1392, 1332, 1294, 1238, 1161, 1102 (ν C-N or C-O), 1039 (ν C-N or C-O), 997, 921, 802, 745 (γ CH, o-subst. Ar or β ring, 2-Pyr), 686cm^{-1}. APCI-MS m/z: 269 (M+H)$^+$. mp (corrected): 110.0-111.3°C. CHN Analysis, %m/m (%calculated/%found): C 67.15/67.06, H 6.01/5.97, N 20.88/20.77.

2PYaz *N^1-(2-Propoxybenzylidene)-pyridine-2-carboxamidrazone*

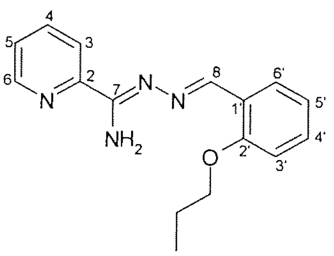

Recrystallised from ethanol three times, to give a yellow solid, 39% yield. R.f. [EtOAc]: 0.57. ^{1}H NMR (d$_6$-DMSO): 1.03 (t, 3H, J=7.4Hz, OCH$_2$CH$_2$C$\underline{H_3}$), 1.80 (hex, 2H, J=7.1Hz, OCH$_2$C$\underline{H_2}$CH$_3$), 4.02 (t, 2H, J=6.4Hz, OC$\underline{H_2}$CH$_2$CH$_3$), 7.02 (ov.m, 4H, NH$_2$ and 2Ar-H), 7.38 (m, 1H, Ar-H), 7.53 (m, 1H, Pyr-H4), 7.91 (m, 1H, Pyr-H5), 8.22 (ov.m, Pyr-H3 and Ar-H), 8.65 (m, 1H, Pyr-H6), 8.78 (s, 1H, =CHAr)ppm. ^{13}C NMR (CDCl$_3$): 10.7 (OCH$_2$CH$_2\underline{Me}$), 22.6 (OCH$_2\underline{C}$H$_2$Me), 69.8 (O$\underline{C}$H$_2$CH$_2$Me), 112.0 (C3' or C4' or C5' or C6'), 120.3 (C3' or C4' or C5' or C6'), 121.3 (C5), 123.8 (C1' or C2'), 125.0 (C3), 126.9 (C3' or C4' or C5' or C6'), 131.3 (C3' or C4' or C5' or C6'), 136.5 (C4), 148.3 (C6), 150.4 (C2), 151.9 (C1' or C2'), 156.8 (C7), 158.1 (C8)ppm. IR (KBr disc): 3451 (ν_{as} NH$_2$), 3268 (ν_s NH$_2$), 3052 (ν Ar- or Pyr-CH), 2962 (ν_{as} Me), 2930 (ν_{as} CH$_2$), 2873 (ν_s Me), 1623 (ν C=N), 1586 (ν skeletal Ar or Pyr), 1566 (ν skeletal Pyr), 1473 (ν skeletal Ar or Pyr), 1454 (δ_{as} Me or ν skeletal Ar or Pyr), 1340, 1252, 1161, 1106 (ν C-N) 1041, 997, 978, 798, 755 (γ CH, o-subst. Ar, or γ CH, 2-Pyr) 686cm^{-1}. APCI-MS m/z: 282 $(M+H)^+$. mp (corrected): 77.8-78.6°C. CHN Analysis, %m/m (%calculated/%found): C 68.06/67.79, H 6.43/6.31, N 19.84/19.63.

2PYbe *N[1]-(2-Benzyloxybenzylidene)-pyridine-2-carboxamidrazone*[97]

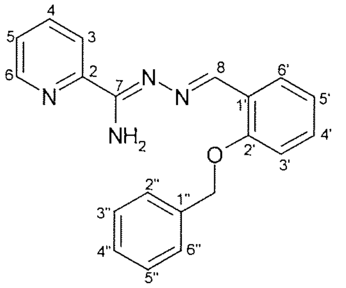

Recrystallised from ethanol twice, to give a yellow crystalline solid, 66%yield. R.f. [EtOAc]: 0.60. ^{1}H NMR (d_6-DMSO): 5.21 (s, 2H, OC<u>H</u>$_2$Ph), 6.98-7.08 (ov.m, 3H, NH_2 and Ar-H), 7.19 (d, 1H, J=8.4Hz, Ar-H), 7.32 (ov.m, 7H, Pyr-H4 and 5Phenyl-H and Ar-H), 7.89 (m, 1H, Pyr-H5), 8.20-8.25 (ov.m, 2H, Pyr-H3 and Ar-H), 8.65 (m, 1H, Pyr-H6), 8.79 (s, 1H, =CHAr)ppm. ^{13}C NMR ($CDCl_3$): 70.2 (O<u>C</u>H$_2$Ph), 112.4 (C3'), 120.8 (C5), 121.4 (C5'), 124.0 (C6'), 125.0 (C3), 127.1 (C4"), 127.4 (C2" and C6"), 127.9 (C4'), 128.5 (C3" and C5"), 131.3 (C1'), 136.5 (C4), 136.6 (C1"), 148.3 (C6), 150.1 (C2), 151.8 (C2'), 156.8 (C8), 157.7 (C7)ppm. IR (KBr disc): 3412 (ν_{as} NH_2), 3370 (ν_s NH_2), 3068 (ν Ar or Pyr-CH), 3031 (ν Ar or Pyr-CH), 1613 (ν C=N), 1578 (ν skeletal Ar or Pyr), 1556 (ν skeletal Pyr), 1516 (ν skeletal Ar or Pyr), 1486 (ν skeletal Ar or Pyr), 1473 (ν skeletal Ar or Pyr), 1451 (ν skeletal Ar or Pyr), 1334, 1287, 1240, 1168, 1159, 1100 (ν C-N or C-O), 1044 (ν C-N or C-O), 996, 963, 798, 753 (γ CH, o-subst. Ar or γ CH, 2-Pyr), 744 (β ring, 2-Pyr)cm^{-1}. APCI-MS m/z: 330 $(M+H)^+$. mp (corrected): 110.7-112.4°C. CHN Analysis, %m/m (%calculated/%found): C 72.71/ 72.43, H 5.49/5.35, N 16.96/16.65.

2PYbf *N[1]-(3-Benzyloxybenzylidene)-pyridine-2-carboxamidrazone*

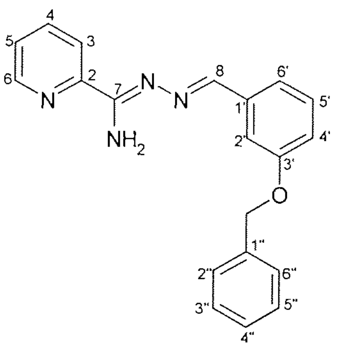

Recrystallised from ethanol to give a yellow crystalline solid, 64% yield. R.f. [EtOAc]: 0.74. ^{1}H NMR (d_6-DMSO): 5.18 (s, 2H, OC<u>H</u>$_2$Ph), 7.06-7.21 (ov.m, 3H, NH_2 and Ar-H), 7.32- 7.56 (ov.m, 8H, Pyr-H4 and 2Ar-H and 5Phenyl-H), 7.69 (s, 1H, 2'H), 7.93 (dt, 1H, J=7.7, 1.7Hz, Pyr-H5), 8.24 (d, 1H, J=8.0Hz, Pyr-H3), 8.46 (s, 1H, =CHAr), 8.67 (m, 1H, Pyr-H6)ppm. ^{13}C NMR ($CDCl_3$): 70.0

(O<u>C</u>H_2Ph), 113.0 (C2'), 117.1 (C4'), 121.3 (C5 or C6'), 121.4 (C5 or C6'), 125.1 (C3), 127.5 (C2" and C6"), 127.9 (C4"), 128.5 (C3" and C5"), 129.6 (C5'), 136.5 (C4), 136.6 (C1' or C1"), 136.8 (C1' or C1"), 148.3 (C6), 150.1 (C2), 155.7 (C3'), 157.0 (C7 or C8), 158.9 (C7 or C8)ppm. IR (KBr disc): 3428 (ν_{as} NH_2), 3316 (ν_s NH_2), 3062 (ν Ar or Pyr-CH), 2881 (ν sat. CH), 1618 (ν C=N), 1584 (ν skeletal Ar or Pyr), 1562 (ν skeletal Pyr), 1525, 1477 (ν skeletal Ar or Pyr), 1450 (ν skeletal Ar or Pyr), 1374, 1334, 1287, 1246, 1161, 1051 (ν C-N or C-O), 1012 (ν C-N or C-O), 954, 896, 804, 775 (γ CH, 2-Pyr), 742 (β ring, 2-Pyr), 690 (γ CH, m-subst), 628cm^{-1}. APCI-MS m/z: 331$(M+H)^+$. mp (corrected): 108.2-110.1°C. CHN Analysis, %m/m (%calculated/%found): C 72.71/72.35, H 5.49/ 5.46, N 16.96/16.82.

2PYbg *N^1-(4-Benzyloxybenzylidene)-pyridine-2-carboxamidrazone*

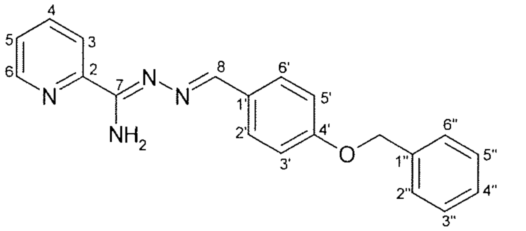

Recrystallised from ethanol to give a yellow solid, 68% yield. R.f. [EtOAc]: 0.67. ^{1}H NMR (d_6-DMSO): 5.18 (s, 2H, C<u>H</u>$_2$Ph), 6.97 (bs, 2H, NH_2), 7.09 (d, 2H, J=8.7Hz, 3'H and 5'H), 7.34-7.55 (ov.m, 6H, Pyr-H4 and 5Phenyl-H), 7.69-7.95 (ov.m, 3H, Pyr-H5 and 2'H and 6'H), 8.22 (m, 1H, Pyr-H3), 8.43 (s, 1H, =CHAr), 8.65 (m, 1H, Pyr-H6)ppm. ^{13}C NMR ($CDCl_3$): 70.0 (O<u>C</u>H_2Ph), 114.9 (C3' and C5'), 121.3 (C5), 125.0 (C3), 127.5 (C2" and C6"), 128.1 (C4"), 128.2 (C1'), 128.6 (C3" and C5"), 129.5 (C2' and C6'), 136.5 (C4), 148.4 (C6), 150.2 (C2), 155.6 (C4' or C1"), 156.7 (C4' or C1"), 160.5 (C8)ppm. IR (KBr disc): 3422 (ν_{as} NH_2), 3318 (ν_s NH_2), 3032 (ν Ar or Pyr-CH), 2906 (ν sat. CH), 1621 (ν C=N), 1560 (ν skeletal Pyr), 1508 (ν skeletal Ar or Pyr), 1465 (ν skeletal Ar or Pyr), 1390, 1305, 1242, 1170, 1090 (ν C-N or C-O), 1018 (ν C-N or C-O), 974, 812 (γ CH, p-subst. Ar), 788 (γ CH, 2-Pyr), 746 (β ring, 2-Pyr), 686, 647cm^{-1}. APCI-MS m/z: 331 $(M+H)^+$. mp (corrected): 160.7-162.3°C. CHN Analysis, %m/m (%calculated/%found): C 72.71/72.67, H 5.49/5.44, N 19.96/ 16.86.

2PYbh *N^1-(4-Benzyloxy-3-methoxybenzylidene)-pyridine-2-carboxamidrazone*

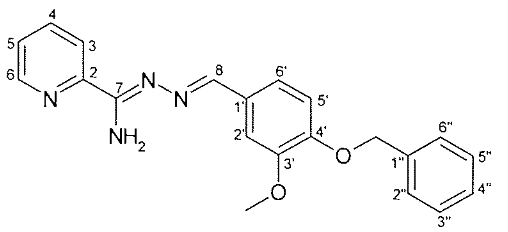

Recrystallised from ethanol twice, to give a yellow crystalline solid, 64% yield. R.f. [EtOAc]: 0.47. ^{1}H NMR (d_6-DMSO): 3.86 (s, 3H, OMe), 5.14 (s, 2H, OC$\underline{H}_2$Ph), 7.02-7.10 (ov.m, 3H, NH_2 and 5'-H), 7.27-7.54 (ov.m, 7H, Pyr-H4, 6'-H, 5Phenyl H), 7.66 (d, 1H, J=1.7Hz, 2'H), 7.90 (dt, 1H, J=7.7, 1.7Hz, Pyr-H5), 8.22 (d, 1H, J=7.9Hz, Pyr-H3), 8.39 (s, 1H, =CHAr), 8.65 (bd, 1H, J=4.2Hz, Pyr-H6)ppm. ^{13}C NMR ($CDCl_3$): 56.0 (OMe), 70.7 (O$\underline{C}H_2$Ph), 109.1 (C2' or C5'), 113.0 (C2' or C5'), 121.1 (C5), 122.7 (C6'), 124.9 (C3), 127.1 (C2" and C6"), 127.9 (C4"), 128.5 (C3" and C5"), 128.6 (C1'), 136.4 (C4), 136.6 (C1"), 148.2 (C6), 149.7 (C3' or C4'), 150.1 (C3' or C4') , 150.3 (C2), 155.8 (C8), 156.4 (C7)ppm. IR (KBr disc): 3486 (ν_{as} NH_2), 3349 (ν_s NH_2), 3050 (ν Ar or Pyr-CH), 3000 (ν Ar or Pyr-CH), 2939 (ν sat. CH), 2870 (ν sat. CH), 1600 (ν C=N), 1580 (ν skeletal Ar or Pyr), 1558 (ν skeletal Pyr), 1512 (ν skeletal Ar or Pyr), 1469 (ν skeletal Ar or Pyr), 1396, 1351, 1261, 1158, 1137 (ν C-N or C-O), 1031 (ν C-N or C-O), 995, 790 (γ CH, 2-Pyr), 732 (β ring, 2-Pyr), 696, 800, 866, 638cm^{-1}. APCI-MS m/z: 361 $(M+H)^+$. R.f. [EtOAc]: 0.47. mp (corrected): 143.2-144.0°C. CHN Analysis, %m/m (%calculated/%found): C 69.98/69.59, H 5.59/5.52, N 15.54/15.15.

4PYbh *N^1-(4-Benzyloxy-3-methoxybenzylidene)-pyridine-4-carboxamidrazone*

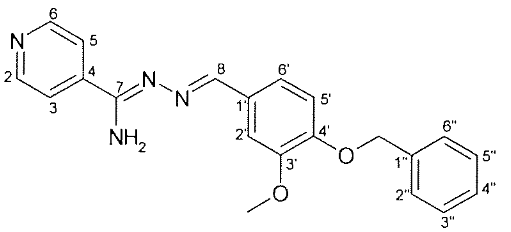

Recrystallised from ethanol twice, to give a yellow crystalline solid, 60% yield. R.f. [EtOAc]: 0.49. ^{1}H NMR (d_6-DMSO): 3.87 (s, 3H, OMe), 5.14 (s, 2H, C$\underline{H}_2$Ph), 7.10 (d, 1H, J=8.3Hz, 5'H) 7.16 (bs, 2H, NH_2), 7.28-7.49 (ov.m, 6'H and 5Phenyl H), 7.67 (d, 1H, J=1.8Hz, 2'H), 7.88 (dd, 2H, J=4.5, 1.6Hz, Pyr-H3 and H5), 8.38 (s, 1H, =CHAr), 8.68 (dd, 2H, J=4.5, 1.6Hz, Pyr-H2 and H6)ppm. ^{13}C NMR ($CDCl_3$): 56.0 (OMe), 70.8 (O$\underline{C}H_2$Ph), 109.3 (C2' or C5'), 113.0 (C2' or C5'), 120.6 (C3 and C5), 123.0 (C6'), 127.2 (C2" and C6" or C3" and C5"), 127.9 (C2" and C6" or C3" and C5"), 128.0 (C4"), 128.6 (C1'), 136.5 (C1"), 141.3 (C4), 149.7 (C3' or C4'), 150.3 (C2 and C6), 150.5 (C3' or C4'), 156.2 (C7), 157.3 (C8)ppm. IR (KBr disc): 3473 (ν_{as} NH_2), 3347 (ν_s NH_2), 3039 (ν Ar or Pyr-CH), 3008 (ν Ar or Pyr-CH), 2937 (ν sat. CH), 2872 (ν sat. CH),1621 (ν C=N), 1587 (ν skeletal Ar or Pyr), 1537 (ν skeletal Pyr), 1510 (ν skeletal Ar or Pyr), 1464 (ν skeletal Ar or Pyr), 1405, 1377, 1354, 1257, 1228, 1167, 1135 (ν C-N or C-O), 1037 (ν C-N or C-O), 997, 806 (γ CH, 4-Pyr), 760 (β ring, 4-Pyr), 673cm^{-1}. APCI-MS m/z: 361 $(M+H)^+$. mp (corrected): 168.0-169.1°C. CHN Analysis, %m/m (%calculated/%found): C 69.98/69.75, H 5.59/5.54, N 15.54/15.28.

2PYbi *N[1]-(3-Methoxy-4-phenethyloxybenzylidene)-pyridine-2-carboxamidrazone*

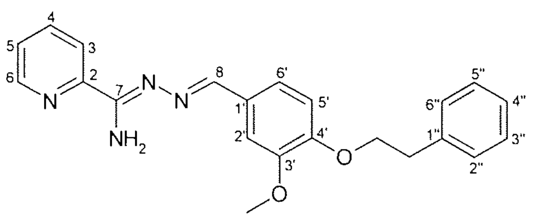

Recrystallised from ethanol twice, to give a yellow solid, 57% yield. R.f. [40-60 PE]: 0.59. ^{1}H NMR (d_6-DMSO): 3.07 (t, 2H, J=7.0Hz, $OCH_2C\underline{H}_2Ph$), 3.85 (s, 3H, OMe), 4.23 (t, 2H, J=7.0Hz, $OC\underline{H}_2CH_2Ph$), 7.02-7.05 (ov.m, 3H, NH_2 and 5'H), 7.23-7.34 (m, 6H, 6'H and 5Phenyl-H), 7.53, (m, 1H, Pyr-H4), 7.66 (d, 1H, J=1.5Hz, 2'H), 7.91 (dt, 1H, J=7.8Hz, 1.7Hz, Pyr-H5), 8.22 (m, 1H, Pyr-H3), 8.40 (s, 1H, =CHAr), 8.66 (m, 1H, Pyr-H6)ppm. ^{13}C NMR ($CDCl_3$): 35.6 ($OCH_2\underline{C}H_2Ph$), 56.0 (OMe), 69.6 ($O\underline{C}H_2CH_2Ph$), 109.2 (C2' or C5'), 112.1 (C2' or C5'), 121.2 (C5), 122.8 (C6'), 125.0 (C3), 126.5 (C1'), 128.2 (C4"), 128.5 (C2" and C6" or C3" and C5"), 129.0 (C2" and C6" or C3" and C5"), 136.5 (C4), 137.6 (C1"), 148.3 (C6), 149.4 (C4'), 150.0 (C3'), 150.3 (C2), 155.9 (C8), 156.4 (C7)ppm. IR (KBr disc): 3428 (ν_{as} NH_2), 3318 (ν_s NH_2), 3056 (ν Ar or Pyr-CH), 3016 (ν Ar or Pyr-CH), 2922 (ν sat. CH), 2882 (ν sat. CH), 1621(ν C=N), 1584 (ν skeletal Ar or Pyr), 1568 (ν skeletal Pyr), 1508 (ν skeletal Ar or Pyr), 1467 (ν skeletal Ar or Pyr), 1417, 1331, 1261, 1230, 1137 (ν C-N or C-O), 1024 (ν C-N or C-O), 958, 873, 788 (γ CH, 2-Pyr), 740 (β ring, 2-Pyr), 686, 613cm^{-1}. APCI-MS m/z: 375 $(M+H)^+$. mp (corrected): 113.4-115.3°C. CHN Analysis, %m/m (%calculated/%found): C 70.57/70.27, H 5.92/5.95, N 14.96/14.68.

2PYbn *N[1]-(3-Benzyloxy-4-methoxybenzylidene)-pyridine-2-carboxamidrazone*

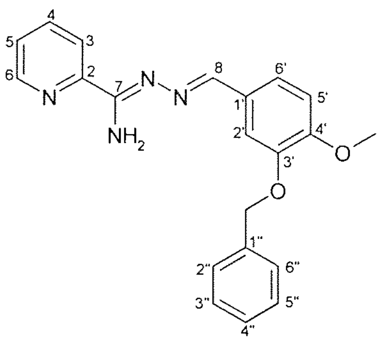

Recrystallised from ethanol twice, to give a yellow crystalline solid, 68% yield. R.f. [EtOAc]: 0.52. ^{1}H NMR (d_6-DMSO): 3.81 (s, 3H, OMe), 5.17 (s, 2H, $C\underline{H}_2Ph$), 7.01-7.04 (ov.m, 3H, NH_2 and 5'H), 7.30-7.54 (ov.m, 7H, Pyr-H4, 6'H, 5Phenyl-H), 7.78 (d, 1H, J=1.8Hz, 2'H), 7.90 (dt, 1H, J=7.7, 1.7Hz, Pyr-H5), 8.22 (d, 1H, J=7.9Hz, Pyr-H3), 8.39 (s, 1H, =CHAr), 8.65 (bd, 1H, J=4.1Hz, Pyr-H6)ppm. ^{13}C NMR ($CDCl_3$): 55.9 ($O\underline{C}H_2Ph$), 71.0 (OMe), 111.1 (C2' or C5'), 121.2 (C5), 123.1 (C6'), 125.0

(C3), 127.4 (C2" and C6"), 127.9 (C4"), 128.1 (C1'), 128.5 (C3" and C5"), 136.5 (C4), 136.9 (C3'), 148.3 (C6), 150.1 (C2), 151.7 (C4'), 155.6 (C8), 156.5 (C7)ppm. IR (KBr disc): 3486 (ν_{as} NH_2), 3352 (ν_s NH_2), 3082 (ν Ar or Pyr-CH), 3033 (ν Ar or Pyr-CH), 2933 (ν sat. CH), 2876 (ν sat. CH), 1614 (ν C=N), 1604 (ν skeletal Ar or Pyr), 1581 (ν skeletal Ar or Pyr), 1558 (ν skeletal Pyr), 1506 (ν skeletal Ar or Pyr), 1469 (ν skeletal Ar or Pyr), 1433 (ν skeletal Ar or Pyr), 1371, 1348, 1325, 1259, 1161, 1134 (ν C-N or C-O), 1004 (ν C-N or C-O), 918, 864, 850, 806, 784 (γ CH, 2-Pyr), 748 (β ring, 2-Pyr), 699, 620cm^{-1}. APCI-MS m/z: 361 $(M+H)^+$. mp (corrected): 149-151.1°C. CHN Analysis, %m/m (%calculated/%found): C 69.98/69.95, H 5.59/5.44, N 15.54/15.28.

4PYbn *N^1-(3-Benzyloxy-4-methoxybenzylidene)-pyridine-4-carboxamidrazone*

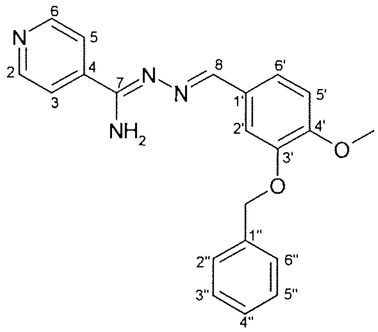

Recrystallised from ethanol twice, to give a yellow crystalline solid, 55% yield. R.f. [EtOAc]: 0.43. ^{1}H NMR (d_6-DMSO): 3.82 (s, 3H, OMe), 5.18 (s, 2H, C<u>H</u>$_2$Ph), 7.03 (m, 1H, 5'-H), 7.16 (bs, 2H, NH_2), 7.32-7.52 (ov.m, 6H, 6'H and 5Phenyl-H), 7.79 (m, 1H, 2'H), 7.88 (dd, 2H, J=4.5,1.3Hz, Pyr-H3 and H5), 8.38 (s, 1H, =CHAr), 8.68 (dd, 2H, J=4.5,1.3Hz, Pyr-H2 and H6)ppm. ^{13}C NMR ($CDCl_3$): 56.0 (OMe), 71.1 (O<u>C</u>H$_2$Ph), 111.1 (C2' or C5'), 111.7 (C2' or C5'), 120.5 (C3 and C5), 123.4 (C6'), 127.4 (C2" and C6"), 127.6 (C1'), 127.9 (C4"), 128.5 (C3" and C5"), 136.8 (C3'), 141.3 (C4), 148.3 (C4'), 150.3 (C2 and C6), 152.0 (C2), 156.2 (C7), 157.1 (C8)ppm. IR (KBr disc): 3469 (ν_{as} NH_2), 3351 (ν_s NH_2), 3029 (ν Ar or Pyr-CH), 2929 (ν sat. CH), 2842 (ν sat. CH), 1616 (ν C=N), 1602 (ν skeletal Ar or Pyr), 1554 (ν skeletal Pyr), 1514, 1431 (ν skeletal Ar or Pyr), 1410 (ν skeletal Ar or Pyr), 1328, 1269, 1240, 1166, 1135 (ν C-N or C-O), 1006 (ν C-N or C-O), 832, 808 (γ CH, 4-Pyr), 746 (β ring, 4-Pyr), 696, 679, 619cm^{-1}. APCI-MS m/z: 361 $(M+H)^+$. mp (corrected):158.5-159.9°C. CHN Analysis, %m/m (%calculated/%found): C 69.98/69.58, H 5.59/5.51, N 15.54/15.46.

2PYbo *N[1]-(4-Methoxy-3-phenethyloxybenzylidene)-pyridine-2-carboxamidrazone*

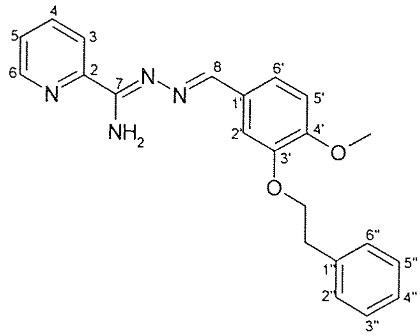

Recrystallised from methanol to give a yellow solid, 70% yield. R.f. [EtOAc]: 0.50. ^{1}H NMR (d_6-DMSO): 3.09 (t, 2H, J=5.6Hz, OCH$_2$C<u>H</u>$_2$Ph), 3.81 (s, 3H, OMe), 4.28 (t, 2H, J=5.6Hz, OC<u>H</u>$_2$CH$_2$Ph), 7.00-7.03 (ov.m, NH$_2$ and 5'H), 7.26-7.36 (ov.m, 6H, 6'H, and 5Phenyl-H), 7.52 (m, 1H, Pyr-H4), 7.65 (d, 1H, J=1.8Hz, 2'H), 7.91 (m, 1H, Pyr-H5), 8.20 (m, 1H, Pyr-H3), 8.38 (s, 1H, =CHAr), 8.64 (m, 1H, Pyr-H6)ppm. ^{13}C NMR (CDCl$_3$): 35.8 (OCH$_2$<u>C</u>H$_2$Ph), 56.0 (OMe), 69.7 (O<u>C</u>H$_2$CH$_2$Ph), 110.4 (C2' or C5'), 111.1 (C2' or C5'), 121.3 (C5), 123.2 (C6'), 125.1 (C3), 126.5 (C1') , 128.2 (C4"), 128.5 (C2" and C6"), 129.1 (C3", C5"), 136.5 (C4), 137.8(C1') , 148.3 (C6), 148.4 (C3') , 150.0 (C2) , 151.5 (C4'), 155.9 (C8), 156.4 (C7)ppm. IR (KBr disc): 3430 (ν_{as} NH$_2$), 3316 (ν_s NH$_2$), 3060 (ν Ar or Pyr-CH), 3005 (ν Ar or Pyr-CH), 2931 (ν sat. CH), 2884 (ν sat. CH), 1621 (ν C=N), 1583 (ν skeletal Ar or Pyr), 1562 (ν skeletal Pyr), 1510, 1466 (ν skeletal Ar or Pyr), 1429 (ν skeletal Ar or Pyr), 1348, 1269, 1232, 1168, 1140 (ν C-N or C-O), 1028 (ν C-N or C-O), 954, 780 (γ CH, 2-Pyr), 744 (β ring, 2-Pyr), 690, 620cm^{-1}. APCI-MS m/z: 375 (M+H)$^+$. mp (corrected): 122.8-123.3°C. CHN Analysis, %m/m (%calculated/%found): C 70.57/70.43, H 5.92/ 5.78, N 14.96/14.71.

2PYbq *N[1]-[3-Methoxy-4-(4-methylbenzyloxy)benzylidene]-pyridine-2-carboxamidrazone*

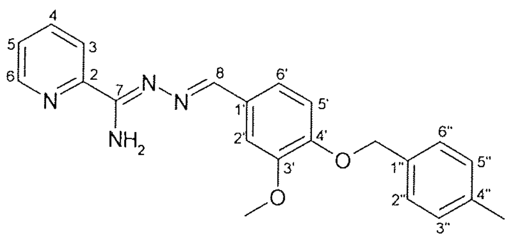

Recrystallised from methanol to give a yellow solid, 63% yield. R.f. [EtOAc]: 0.49. ^{1}H NMR (d_6-DMSO): 2.32 (s, 3H, Ph<u>Me</u>), 3.81 (s, 3H, OMe), 5.12 (s, 2H, OC<u>H</u>$_2$PhMe), 7.01-7.04 (ov.m, 3H, NH$_2$ and 5'H), 7.23 (d, 2H, J=7.8Hz, 3"H and 5"H), 7.31 (m, 1H, 6'H), 7.40 (d, 2H, J=7.8Hz, 2"H and 6"H), 7.52 (m, 1H, Pyr-H4), 7.77 (m, 1H, 2'H), 7.92 (dt, J=7.7, 1.7Hz, Pyr-H5), 8.24 (m, 1H, Pyr-H3), 8.39 (s, 1H, =CHAr), 8.65 (m, 1H, Pyr-H6)ppm. ^{13}C NMR (CDCl$_3$): 21.2 (OCH$_2$Ph<u>Me</u>), 55.9 (OMe), 70.9 (O<u>C</u>H$_2$PhMe), 111.1 (C2' or C5'), 111.6 (C2' or C5'), 121.2 (C5), 122.9 (C6'), 125.0 (C3), 127.5 (C2" and C6"),128.1 (C4"), 129.2 (C3" and C5"), 133.8 (C1'), 136.5 (C4), 137.6 (C4'), 148.3 (C1"), 148.4 (C6), 150.3 (C2), 151.66 (C3'), 155.7 (C8), 156.5 (C7)ppm. IR (KBr disc): 3423 (ν_{as} NH$_2$), 3315 (ν_s NH$_2$), 3062 (ν Ar or Pyr-CH), 3008 (ν Ar or Pyr-CH), 2927 (ν sat. CH), 2836 (ν sat. CH), 1617 (ν C=N), 1584 (ν skeletal Ar or Pyr), 1563 (ν skeletal Pyr), 1511 (ν skeletal Ar or Pyr), 1475 (ν skeletal Ar or Pyr), 1429 (ν skeletal Ar or Pyr), 1375, 1346, 1323, 1271, 1137 (ν C-N or C-O), 1008 (ν C-N or C-O), 782 (γ CH, 2-Pyr), 752 (β ring, 2-Pyr), 686, 623cm^{-1}. APCI-MS m/z: 375 $(M+H)^+$. mp (corrected):154.0-155.6°C. CHN Analysis, %m/m (%calculated/%found): C 70.57/70.49, H 5.92/5.98, N 14.96/14.92.

2PYbt *N[1]-(2-Benzyloxy-3-methoxybenzylidene)-pyridine-2-carboxamidrazone*

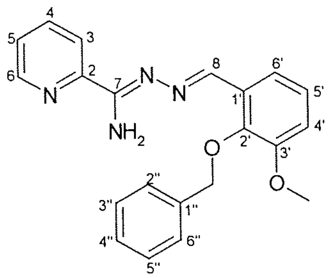

Recrystallised from ethanol to give a yellow crystalline solid, 65% yield. R.f. [EtOAc]: 0.69. ^{1}H NMR (d_6-DMSO): 3.88 (s, 3H, OMe), 5.05 (s, 2H, OC$\underline{H}_2$Ph), 7.04 (bs, 2H, NH_2), 7.13 (m, 2H, 4',6'H), 7.31-7.55 (ov.m, 6H, Pyr-H4 and 5Phenyl-H), 7.81 (dd, 1H, J=6.0, 3.5Hz, 5'H), 7.90 (dt, 1H, J=7.7, 1.8Hz, Pyr-H5), 8.21 (m, 1H, Pyr-H3), 8.65 (ov.m, 2H, Pyr-H6 and =CHAr)ppm. ^{13}C NMR ($CDCl_3$): 55.6 (OMe), 75.4 (O$\underline{C}H_2$Ph), 113.5 (C5'), 118.4 (C4'), 121.2 (C5), 124.0 (C6'), 124.9 (C3), 127.8 (C4"), 128.0 (C2" and C6" or C3" and C5"), 128.2 (C2" and C6" or C3" and C5"), 129.2 (C1'), 136.3 (C4), 137.1 (C1"), 147.4 (C2' or C3'), 148.1 (C6), 150.1 (C2), 151.5 (C2' or C3'), 152.8 (C7 or C8), 156.8 (C7 or C8)ppm. IR (KBr disc): 3467 (ν_{as} NH_2), 3366 (ν_s NH_2), 3085 (ν Ar CH), 3027 (ν Ar or Pyr-CH), 2935 (ν sat. CH), 2851 (ν sat. CH), 1620 (ν C=N), 1590 (ν skeletal Ar or Pyr), 1564 (ν skeletal Pyr), 1523 (ν skeletal Ar or Pyr), 1473 (ν skeletal Ar or Pyr), 1375, 1336, 1299, 1265, 1213, 1180, 1066 (ν C-N or C-O), 1020 (ν C-N or C-O), 798, 772 (γ CH, 2-Pyr), 730 (β ring, 2-Pyr), 688cm^{-1}. APCI-MS m/z: 361 $(M+H)^+$. mp (corrected): 89.6-90.5°C. CHN Analysis, %m/m (%calculated/%found): C 69.98/69.99, H 5.59/5.56, N 15.54/15.52.

2PYdd *N[1]-(4-Methoxy-1-napthylidene)-pyridine-2-carboxamidrazone*

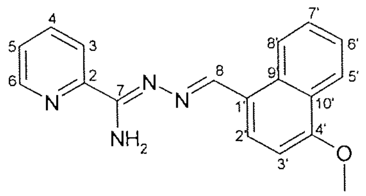

Recrystallised from methanol twice, to give a yellow solid, 57% yield. R.f. [EtOAc]: 0.54. ^{1}H NMR (d_6-DMSO): 4.05 (s, 3H, OMe), 6.96 (bs, 2H, NH_2), 7.09 (d, 1H, J=8.3Hz, Ar-H), 7.52-7.72 (ov.m, 3H, Pyr H4 and 2Ar-H), 7.95 (dt, 1H, J=7.8, 1.7Hz, Pyr-H5), 8.13 (d, 1H, J=8.3Hz, Ar-H), 8.24-8.32 (ov.m, 2H, Pyr-H3 and Ar-H), 8.67 (m, 1H, Pyr-H6), 9.04-9.07 (ov.m, 2H, =CHAr and Ar-H)ppm. ^{13}C NMR ($CDCl_3$): 55.6 (OMe), 113.6 (C3'), 121.3 (C5), 122.5 (C2' or C5' or C6' or C7' or C8'), 123.3

(C10'), 124.4 (C2' or C5' or C6' or C7' or C8'), 125.0 (C3), 125.4 (C2' or C5' or C6' or C7' or C8'), 125.7 (C1' or C9'), 127.6 (C2' or C5' or C6' or C7' or C8'), 129.7 (C2' or C5' or C6' or C7' or C8'), 132.2 (C1' or C9'), 136.6 (C4), 148.4 (C6), 150.2 (C2), 156.0 (C4'), 156.4 (C7), 157.4 (C8)ppm. IR (KBr disc): 3457 (ν_{as} NH_2), 3342 (ν_s NH_2), 3064 (ν Ar or Pyr-CH), 2925 (ν Sat. CH), 1616 (ν C=N), 1605 (ν skeletal Ar or Pyr), 1575 (ν skeletal Pyr), 1459(ν skeletal Ar or Pyr), 1396, 1317, 1226, 1097 (ν C-N or C-O), 993, 769 (γ CH, 2-Pyr), 741 (β ring, 2-Pyr), 681, 621cm^{-1}. APCI-MS m/z: 305 $(M+H)^+$. mp (corrected): 98.2-99.3°C. CHN Analysis, %m/m (%calculated/%found): C 71.04/71.02, H 5.30/4.94, N 18.41/18.39.

2PYdm *N^1-(2-Trifluoromethylbenzylidene)-pyridine-2-carboxamidrazone*

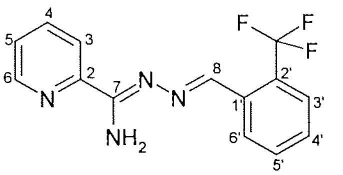

Recrystallised from 40-60 PE twice, to give a yellow solid, 46% yield. R.f. [EtOAc]: 0.66. ^{1}H NMR (d_6-DMSO): 7.31 (bs, 2H, NH_2), 7.56 (m, 1H, Pyr-H4), 7.63 (d, 1H, J=7.5Hz, 3'H or 6'H), 7.75 (ov.m, 2H, 2Ar-H), 7.93 (dt, 1H, J=7.7, 1.8Hz, Pyr-H5), 8.28 (d, 1H, J=7.9Hz, Pyr-H3), 8.68 (ov.m, 3H, Pyr-H6 and Ar-H and =CHAr)ppm. ^{13}C NMR ($CDCl_3$): 121.6 (C5), 125.3 (C3), 125.8 (q,CF_3), 126.2 (C3'), 127.8 (C6'), 129.0 (C2'), 129.4 (C5'), 131.6 (C4'), 133.3 (C1'), 136.7 (C4), 148.4 (C6), 149.9 (C2), 151.8 (C8), 157.7 (C7)ppm. IR (KBr disc): 3510 (ν_{as} NH_2), 3386(ν_s NH_2), 3066 (ν Ar or Pyr - CH), 3013 (ν Ar or Pyr -CH), 2924, 1635 (ν C=N), 1591 (ν skeletal Ar or Pyr), 1589 (ν skeletal Ar or Pyr), 1557 (ν skeletal Pyr), 1519, 1473 (ν skeletal Ar or Pyr), 1351, 1315, 1280 (ν CF), 1164, 1114, 1031 (ν C-N), 821, 771 (γ CH, 2-Pyr), 750 (β ring, 2-Pyr or γ CH, o-subst. Ar), 680 (γ CH, p-subst. Ar)cm^{-1}. APCI-MS m/z: 293 $(M+H)^+$. mp (corrected): 78.7-79.9°C. CHN Analysis, %m/m (%calculated/%found): C 57.54/57.78, H 3.79/3.82, N 19.17/19.08.

2PYdn *N^1-(3-Nitrobenzylidene)-pyridine-2-carboxamidrazone*

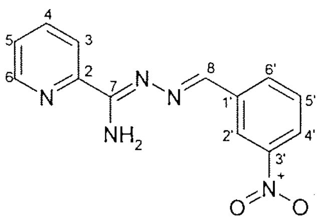

Recrystallised from 40-60 PE twice, to give a yellow crystalline solid, 64% yield. R.f. [EtOAc]: 0.50. ^{1}H NMR (d_6-DMSO): 7.25 (bs, 1H, NH), 7.44 (bs, 1H, NH), 7.56 (m, 1H, Pyr-H4), 7.73 (dd, 1H, J=8.0Hz, 5'H), 7.94 (dt, 1H, J=7.7Hz, 1.7Hz, Pyr-H5), 8.25 (m, 2H, Pyr-H3 and 4'or 6'H), 8.40 (m, 1H, 4' or 6'H), 8.62 (s, 1H, =CHAr), 8.68 (m, 1H, Pyr-H6), 8.77 (m, 1H, 2'H)ppm. ^{13}C NMR ($CDCl_3$): 121.5 (C5), 122.1 (C2'), 124.2 (C4'), 125.5 (C3), 129.5 (C5'), 133.5 (C6'), 136.7 (C4), 137.0 (C1'), 148.4 (C6), 148.5 (C3'), 149.7 (C2), 153.0 (C8), 157.9 (C7)ppm. IR (KBr disc): 3472 (ν_{as} NH_2), 3330

(ν_s NH_2), 3069 (ν Ar or Pyr-CH), 1622 (ν C=N), 1591 (ν skeletal Ar or Pyr), 1568 (ν skeletal Pyr), 1521 (ν_{as} NO_2), 1471 (ν skeletal Ar or Pyr), 1386, 1353 (ν_s NO_2), 1251, 1095 (ν C-N), 997, 802, 770 (γ CH, 2-Pyr), 747 (β ring, 2-Pyr), 709 (γ CH, m-subst. Ar), 678, 622cm^{-1}. APCI-MS m/z: 269 $(M+H)^+$. mp (corrected): 145.0-146.2°C. CHN Analysis, %m/m (%calculated/%found): C 57.99/57.87, H 4.12/4.02, N 26.01/26.06.

2PYdx *N^1-[(4-Dimethylamino)-1-naphthylidene]-pyridine-2-carboxamidrazone*

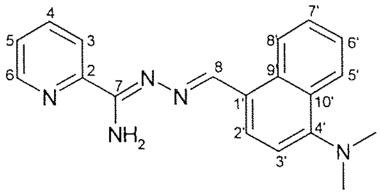

Recrystallised from ethanol twice, to give a yellow crystalline solid, 84% yield. R.f. [EtOAc]: 0.56. ^{1}H NMR (d_6-DMSO): 2.90 (s, 6H, NMe_2), 6.95 (bs, 2H, NH_2), 7.15 (d, 1H, J=8.0Hz, 2' or 3'H), 7.52-7.66 (ov.m, 3H, Pyr-H4 and 2Ar-H), 7.95 (dt, 1H, J=7.7Hz, 1.7Hz, Pyr-H5), 8.08 (d, 1H, J=8.0Hz, 2' or 3'H), 8.21 (m, 1H, Ar-H), 8.30 (d, 1H, J=7.9Hz, Pyr-H3), 8.68 (m, 1H, Pyr-H6), 9.01 (m, 1H, Ar-H), 9.06 (s, 1H, =CHAr)ppm. ^{13}C NMR ($CDCl_3$): 44.9 (NMe_2), 113.2 (C3'), 121.2 (C5), 124.9-125.0 (C5' and C6' and C7' and C8'), 125.1 (C3), 126.8 (C2'), 128.4 (C10'), 129.0 (C1' or C9'), 132.6 (C1'or C9'), 136.4 (C4), 148.3 (C6), 150.2 (C2), 153.2 (C4'), 155.9 (C8), 156.4 (C7)ppm. IR (KBr): 3417 (ν_{as} NH_2), 3291 (ν_s NH_2), 3092 (ν Ar-CH), 3014 (ν Ar or Pyr-CH), 2950 (ν sat. CH), 2870 (ν sat. CH), 1621 (ν C=N), 1592 (ν skeletal Ar or Pyr), 1564 (ν skeletal Pyr), 1477 (ν skeletal Ar or Pyr), 1396, 1319, 1286, 1143, 1049 (ν C-N), 993, 962, 914, 833, 806, 775 (γ CH, 2-Pyr), 748 (β ring, 2-Pyr), 688cm^{-1}. APCI-MS m/z: 317 $(M+H)^+$. mp (corrected): 88.8-89.9°C. CHN Analysis, %m/m (%calculated/%found): C 71.9/71.50, H 6.03/6.06, N 22.06/21.66.

4PYdx *N^1-[(4-Dimethylamino)-1-naphthylidene]-pyridine-4-carboxamidrazone*

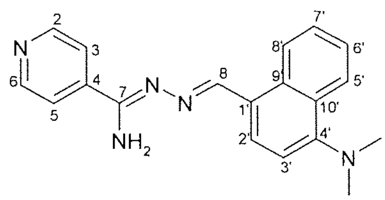

Orange oil, obtained by trituration with 60-80 petroleum ether, 86% yield. R.f. [EtOAc]: O.20. ^{1}H NMR (d_6-DMSO): 2.90 (s, 6H, NMe_2), 7.11 (bs, 2H, NH_2), 7.15 (d, 1H, J=8.0Hz, 2' or 3'H), 7.54-7.66 (ov.m, 2H, 2Ar-H), 7.93 (dd, 2H, J=4.5, 1.5Hz, Pyr-H3 and H5), 8.12 (d, 1H, J=8.0Hz, 2' or 3'H), 8.22 (m, 1H, Ar-H), 8.70 (dd, 2H, J=4.5, 1.5Hz, Pyr-H2 and H6), 8.94 (m, 1H, Ar-H), 9.07 (s, 1H, =CHAr)ppm. ^{13}C NMR ($CDCl_3$): 44.8 (NMe_2), 113.0 (C3'), 120.6 (C3 and C5), 124.4 (C5' or C6' or C7' or C8'), 124.7 (C5' or C6' or C7' or C8'), 124.9 (C5' or C6' or C7' or C8'), 125.0 (C5' or C6' or C7' or C8'),126.9 (C2'), 128.3 (C10'), 129.3 (C1' or C9'), 132.6 (C1'or C9'), 141.5 (C4), 150.1 (C2 and

C6), 153.6 (C4'), 156.1 (C7), 157.2 (C8)ppm. IR ($CHCl_3$): 3505 (ν_{as} NH_2), 3388 (ν_s NH_2), 3006 (ν Ar or Pyr-CH), 2968 (ν sat. CH), 1619 (ν C=N), 1599 (ν skeletal Ar or Pyr), 1556 (ν skeletal Pyr), 1539, 1454 (ν skeletal Ar or Pyr)cm^{-1}. APCI-MS m/z: 317 $(M+H)^+$. CHN Analysis, %m/m (%calculated/ %found): C 71.90/69.97, H 6.03/6.06, N 22.06/22.21.

2PYed *N^1-(2-Thiophenylidene)-pyridine-2-carboxamidrazone*

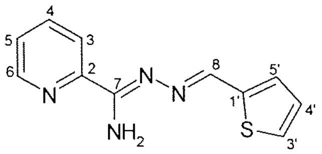

Recrystallised from ethanol twice, to give a yellow solid, 42% yield. R.f. [EtOAc]: 0.55. ^1H NMR (d_6-DMSO): 6.64 (bs, 1H, NH), 6.89 (bs, 1H, NH), 7.16 (m, 1H, Pyr-H4), 7.52 (ov.m, 2H, Pyr-H5 and 2' or 5'H), 7.66 (m, 1H, 2' or 5'H), 7.92 (dd, 1H, J=7.8 Hz, 1.8Hz, 4'H), 8.21 (m, 1H, Pyr-H3), 8.66 (ov.m, =CHAr, and Pyr-H6)ppm. ^{13}C NMR ($CDCl_3$): 121.3 (C5), 125.1 (C3' or C4' or C5'), 127.5 (C3), 128.3 (C3' or C4' or C5'), 130.3 (C2 or C1'), 136.5 (C4), 140.5 (C3' or C4' or C5'), 145.9 (C6), 150.0 (C2), 156.7 (C8)ppm. IR (KBr disc): 3427 (ν_{as} NH_2), 3311 (ν_s NH_2), 3104 (ν Ar-CH), 3053 (ν Ar or Pyr-CH), 1608 (ν C=N), 1598 (ν skeletal Ar or Pyr), 1562 (ν skeletal Ar or Pyr), 1529 (ν skeletal Ar or Pyr), 1475 (ν skeletal Ar or Pyr), 1394 (ν skeletal Ar), 1210, 1005 (ν C-N), 802, 776 (γ CH, 2-Pyr), 749 (β ring, 2-Pyr), 690, 620cm^{-1}. APCI-MS m/z: 231 $(M+H)^+$. mp (corrected): 131.2-132.3°C. CHN Analysis, %m/m (%calculated/%found): C 57.37/57.42, H 4.38/4.34, N 24.33/24.37.

2PYeh *N^1-[2-(4-Chlorothiophenyl)benzylidene]-pyridine-2-carboxamidrazone*[97]

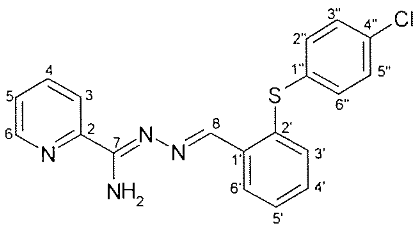

Recrystallised from ethanol to give a yellow crystalline solid, 57%yield. R.f. [EtOAc]: 0.59. ^1H NMR (d_6-DMSO): 7.17 (bs, 2H, NH_2), 7.26 (d, 2H, J=8.6Hz, 2"H and 6"H), 7.34 (m, 1H, Pyr-H4), 7.42 (m, 1H, Ar-H), 7.44 (d, 2H, J=8.6Hz, 3"H and 5"H), 7.46 (m, 1H, Ar-H), 7.54 (m, 1H, Ar-H), 7.91 (m, 1H, Ar-H), 8.22 (m,1H, Pyr-H5), 8.14 (m, 1H, Pyr-H3), 8.66 (m, 1H, Pyr-H6), 8.83 (s, 1H, =CHAr)ppm. ^{13}C NMR ($CDCl_3$): 121.6 (C5), 125.3 (C3), 127.1 (C5'), 129.4 (C3'), 129.5 (C2" and C6"), 130.2 (C6'), 131.9 (C4'), 132.7 (C3" and C5"), 133.4 (C4"), 134.0 (C1'), 135.9 (C1"), 136.6 (C4), 148.4 (C6), 149.8 (C2), 157.4 (C8), 166.4 (C7)ppm. IR (KBr disc): 3411 (ν_{as} NH_2), 3234 (ν_s NH_2), 3100 (ν Ar-CH), 3056 (ν Ar or Pyr-CH), 1631 (ν C=N), 1617 (ν skeletal Ar or Pyr), 1577, 1560, 1552 (ν skeletal Pyr), 1507 (ν skeletal Ar or Pyr), 1475 (ν skeletal Ar or Pyr), 1464 (ν skeletal Ar or Pyr), 1383, 1329, 1087 (ν C-N), 1006, 994, 832 (γ CH, p-subst. Ar), 808, 797, 763 (γ CH, 2-Pyr or γ CH, o-subst. Ar), 742 (β ring, 2-Pyr)cm^{-1}. APCI-MS m/z: 367 (M+H)$^+$, 369. mp (corrected): 141.2-143.5°C. CHN Analysis, %m/m (%calculated/%found): C 62.20/61.87, H 4.12/3.99, N 15.27/15.27.

4PYeh *N^1-[2-(4-Chlorothiophenyl)benzylidene]-pyridine-4-carboxamidrazone*

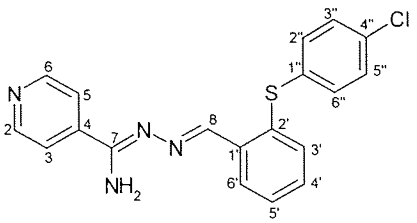

Recrystallised from ethanol three times, to give a yellow crystalline solid, 30% yield. R.f. [EtOAc]: 0.49. ^{1}H NMR (d_6-DMSO): 7.22-7.37 (ov.m, 5H, NH_2 and and Ar-H), 7.41-7.48 (ov.m, 4H, 2"H and 6"H and 2Ar-H), 7.86 (dd, 2H, J=4.5, 1.6Hz, Pyr-H3 and H5), 8.35 (m, 1H, Ar-H), 8.67 (dd, 2H, J=4.5, 1.6Hz, 3"H and 5"H), 8.81 (s, 1H, =CHAr)ppm. ^{13}C NMR ($CDCl_3$):120.7 (C3 and C5), 127.0 (C5'), 129.6 (C2" and C6"), 129.7 (C3'), 130.4 (C6'), 131.5 (C4'), 133.0 (C3" and C5"), 133.5 (C1' or C1" or C4"), 133.7 (C1' or C1" or C4"), 133.9 (C1' or C1" or C4"), 136.4 (C2"), 141.1 (C4), 150.3 (C2 and C6), 155.7 (C8), 157.3 (C7)ppm. IR (KBr disc): 3409 (ν_{as} NH_2), 3295 (ν_s NH_2), 3089 (ν Ar-CH), 3059 (ν Ar or Pyr-CH), 2972, 1610 (ν C=N), 1533 (ν skeletal Pyr), 1473 (ν skeletal Ar or Pyr), 1436 (ν skeletal Ar or Pyr), 1410, 1340, 1284, 1209, 1095 (ν CN), 1016, 999, 819 (γ CH, 4-Pyr or γ CH, p-subst. Ar), 766 (γ CH, o-subst. Ar), 741 cc, 667cm^{-1}. APCI-MS m/z: 367, 369 (M+H)$^+$. mp (corrected): 154.8-156.0°C. CHN Analysis, %m/m (%calculated/%found): C 62.20/61.59, H 4.12/3.87, N 15.27/14.91.

4PYam *N^1-(9-Anthrylidene)-pyridine-2-carboxamidrazone*

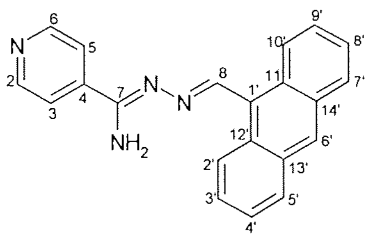

Recrystallised from methanol twice, to give an orange crystalline solid, 53% yield. R.f. [EtOAc]: 0.32. ^{1}H NMR (d_6-DMSO): 7.17 (bs, 2H, NH_2), 7.61 (m, 4H, 4Ar-H), 8.00 (dd, 2H, J=4.5Hz, 1.6Hz, Pyr-H3 and H5), 8.16 (m, 2H, 2Ar-H), 8.71(ov.m, 5H, Pyr-H2 and H6 and 3Ar-H), 9.66 (s, 1H, =CHAr)ppm. ^{13}C NMR ($CDCl_3$): 120.7 (C3 and C5), 125.3 (C2' and C10' or C3' and C9' or C4' and C8' or C5' and C7'), 125.4 (C2' and C10' or C3' and C9' or C4' and C8' or C5' and C7'), 126.6 (C1'), 126.8 (C2' and C10' or C3' and C9' or C4' and C8' or C5' and C7'), 128.9 (C2' and C10' or C3' and C9' or C4' and C8' or C5' and C7'), 129.7 (C6' or C11' and C12' or C13' and C14'), 130.4 7 (C6' or C11' and C12' or C13' and C14'), 131.4 7 (C6' or C11' and C12' or C13' and C14'), 141.3 (C4), 150.5 (C2 and C6), 156.4 (C8), 157.3 (C7)ppm. IR (KBr disc): 3427 (ν_{as} NH_2), 3305 (ν_s NH_2), 3106 (ν Ar-CH), 3037 (ν Ar or Pyr-CH), 1621 (ν C=N), 1594 (ν skeletal Ar or Pyr), 1511 (ν skeletal Ar or Pyr), 1415 (ν skeletal Ar or Pyr), 1133 (ν C-N), 997, 889, 820 (γ CH, 4-Pyr), 734 (β ring, 4-Pyr), 674cm^{-1}. APCI-MS m/z: 325 $(M+H)^+$. mp (corrected): 241.9-244.1°C. CHN Analysis, %m/m (%calculated/ %found): C 77.76/77.46, H 4.97/5.02, N 17.27/ 6.93.

4PYcq *N^1-[3, 5-Di-(tert-butyl)-2-hydroxybenzylidene]-pyridine-2-carboxamidrazone*

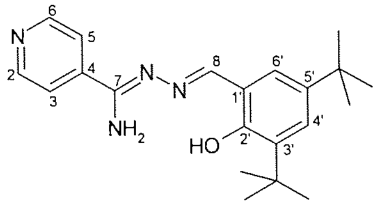

Recrystallised from methanol/40-60 PE to give a yellow solid, 68% yield. R.f. [EtOAc]: 0.48. ^{1}H NMR (d_6-DMSO): 1.27 (s, 9H, CMe_3), 1.42 (s, 9H, CMe_3), 7.18 (bs, 2H, NH_2), 7.30 (d, 1H, J=2.4Hz, 4'H), 7.34 (d, 1H, J=2.3Hz, 6'H), 7.87 (d, 2H, J=6.1Hz, Pyr-H3 and H5), 8.67-8.69 (ov.m, 3H, =CHAr and Pyr-H2 and H6), 11.60 (bs, 1H, OH)ppm. ^{13}C NMR ($CDCl_3$): 29.4 (C<u>Me</u>$_3$), 31.4 (C<u>Me</u>$_3$), 34.1 (<u>C</u>Me_3), 35.0 (<u>C</u>Me_3), 117.4 (C1'), 120.6 (C3 and C5), 126.5 (C4'), 127.2 (C6'), 136.3 (C3'), 141.2 (C4), 150.3 (C2 and C6), 154.3 (C5'), 156.1 (C2'), 162.4 (C8)ppm. IR (KBr disc): 3468 (ν_{as} NH_2), 3282 (ν_s NH_2), 3250-3000(ν OH, overlapping ν Ar-CH), 2954 (ν sat. CH), 2865 (ν sat. CH), 1633 (ν C=N), 1610 (ν skeletal Ar or Pyr), 1595 (ν skeletal Ar or Pyr), 1534 (ν skeletal Pyr), 1463 (ν skeletal Ar or Pyr), 1436 (ν skeletal Ar or Pyr), 1374, 1247, 1178, 1070 (ν C-N), 997, 968, 877, 818 (γ CH, 4-Pyr), 746 (β ring, 4-Pyr), 713, 642cm^{-1}. APCI-MS m/z: 353 $(M+H)^+$. mp corrected: 156.7-158.0°C. CHN Analysis, %m/m (%calculated/%found): C 71.56/71.70, H 8.01/7.96, N 15.89/16.01.

HDck *N^1-(2-Hydroxy-3-methoxy-5-nitrobenzylidene)-pyridine-2-hydrazone*

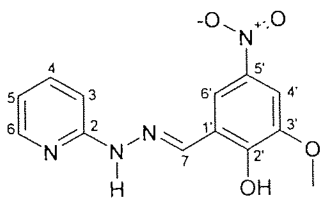

Recrystallised from ethanol three times, to give a yellow solid, 30% yield. R.f. [EtOAc/MeOH (9:1)]: 0.50. ^{1}H NMR (d_6-DMSO): 3.95 (s, 3H, OMe), 6.81 (m, 1H, Pyr-H4), 7.15 (d, 1H, J=8.4Hz, Pyr-H3), 7.68 (m, 2H, Pyr-H5 and 4' or 6'H), 8.14 (m, 1H, Pyr-H6), 8.25 (d, 1H, J=2.6Hz, 4' or 6'H), 8.34 (s, 1H, =CHAr), 11.14 (bs, 1H, NH or OH)ppm. ^{13}C NMR (d_6-DMSO): 57.0 (OMe), 106.3, 107.0, 114.5, 116.0, 121.7, 135.1, 138.7, 140.1, 148.4, 148.5, 151.7, 156.8ppm. IR (KBr disc): 3300-2800 (ν OH, overlapping ν NH, ν CH), 1600 (ν C=N), 1598 (ν skeletal Ar or Pyr), 1585 (ν skeletal Ar or Pyr), 1577, 1525 (ν_{as} NO_2), 1436 (ν skeletal Ar or Pyr), 1336 (ν_s NO_2), 1266, 1149, 1089 (ν C-N), 993, 918, 873, 786 (γ CH, 2-Pyr), 743 (β ring, 2-Pyr), 711, 624cm^{-1}. APCI-MS m/z: 289 $(M+H)^+$. mp (corrected): 252.4-263.3°C. CHN Analysis, %m/m (%calculated/%found): C 54.17/54.21, H 4.20/ 4.19, N 19.44/19.40.

11.2.4 Synthesis Of Aldehydes

11.2.4.1 3-Methoxy-4-(phenethyloxy)benzaldehyde **bi**

4-Hydroxy-3-methoxybenzaldehyde **ch** (2.25g, 14.8mmol), 1-(2-bromoethyl)benzene (3.012g, 1.1eq) and potassium carbonate (2.850g, 1.4eq) were placed in a dry flask under argon. Dry acetonitrile (20ml) was added and the mixture heated under reflux for 16 hours. The mixture was allowed to cool, the potassium carbonate removed by filtration and the mixture concentrated under vacuum. This was then partitioned between DCM (50ml) and water (50ml) and the DCM extraction repeated (2x50ml). The combined organic fractions were dried over anhydrous sodium sulfate, filtered and the solvent removed under vacuum, to obtain a brown oil. This residue was subjected to flash column chromatography, eluted with 60-80PE/ethyl acetate (1:1). The title compound was collected as an orange oil (2.955g, 78%). R.f. [60-80PE/ EtOAc (1:1)]: 0.67. ^{1}H NMR (d_6-DMSO): 3.71 (t, 2H, J=7.0Hz, $OCH_2C\underline{H}_2Ph$), 3.82 (s, 3H, OMe), 4.29 (t, 2H, J=7.0Hz, $OC\underline{H}_2CH_2Ph$), 7.18 (d, 1H, J=8.3Hz, H5), 7.22-7.38 (ov.m, 6H, H2 and 5Ar-H), 7.52 (dd, 1H, J=8.3, 1.9Hz, H6), 9.84 (s, 1H, CHO)ppm. APCI-MS m/z: 257 $(M+H)^+$.

11.2.4.2 3-Methoxy-4-(3-phenylpropoxy)benzaldehyde **bj**

4-Hydroxy-3-methoxybenzaldehyde **ch** (2.877g, 18.9mmol), 1-(3-bromopropyl)benzene (3.767g, 1.1eq) and potassium carbonate (3.657g, 1.4eq) were placed in a dry flask under argon. Dry acetonitrile (20ml) was added and the mixture heated under reflux for 16 hours. The mixture was allowed to cool and water was added (60ml). The solution was extracted with DCM (3x30ml), the combined organic layers dried over sodium sulfate, filtered and the solvent removed under vacuum. The title compound was collected as a yellow oil (3.501g, 69%). R.f. [EtOAc]: 0.66. ^{1}H NMR (d_6-DMSO): 2.06 (quint, 2H, J=6.5z, $OCH_2C\underline{H}_2CH_2Ph$), 2.75 (m, 2H, $OCH_2CH_2C\underline{H}_2Ph$), 3.85 (s, 3H, OMe), 4.07 (t, 2H, J=6.5Hz, $OC\underline{H}_2CH_2CH_2Ph$), 7.12-7.32 (ov.m, H5 and 5Ar-H), 7.40 (d, 1H, J=1.8Hz, H2), 7.53 (dd, 1H, J=8.2, 1.8Hz, H6)ppm. APCI-MS m/z: 271 $(M+H)^+$.

11.2.4.3 3-Methoxy-4-[(4-methylbenzyl)oxy]benzaldehyde **bk**

4-Hydroxy-3-methoxybenzaldehyde **ch** (2.137g, 14.1mmol), 1-(bromomethyl)-4-methyl-benzene (2.860g, 1.2eq) and potassium carbonate (2.722g, 1.4eq) were placed in a dry flask under argon. Dry acetonitrile (20ml) was added and the mixture heated under reflux for 16 hours. The mixture was allowed to cool, the potassium carbonate removed by filtration and the mixture concentrated under vacuum. This was then partitioned between DCM (50ml) and water (50ml) and the DCM extraction repeated (2x50ml). The combined organic fractions were dried over anhydrous sodium sulfate, filtered and the solvent removed under vacuum, to obtain an brown oil. This residue was then placed on top of a plug of silica and eluted with 60-80 PE, until no more alkyl halide was observed by TLC. The silica was then eluted with ethyl acetate to displace the product from the silica. The title compound was collected as an off white solid (2.617g, 73%). R.f. [EtOAc]: 0.63. ^{1}H NMR (d_6-DMSO): 2.31 (s, 3H, Ph<u>Me</u>), 3.83 (s, 3H, OMe), 5.11 (s, 2H, $OC\underline{H}_2PhMe$), 7.21 (d, 2H, J=8.0Hz, 3'H and 5'H), 7.26 (d, 1H, J=8.3Hz, H5), 7.35 (d, 2H, J=8.0Hz, 2'H and 5'H), 7.41 (d, 1H, J=1.8Hz, H2), 7.53 (dd, 1H, J=8.3, 1.8Hz, H6), 9.84 (s, 1H, CHO)ppm. APCI-MS m/z: 257 $(M+H)^+$.

11.2.4.4 4-{[4-(tert-Butyl)benzyl]oxy}-3-methoxybenzaldehyde **bl**

4-Hydroxy-3-methoxybenzaldehyde **ch** (2.924g,19.2mmol), 1-(bromomethyl)-4-(*tert*-butyl)-benzene (4.803, 1.1eq) and potassium carbonate (4.648g, 1.4eq) were placed in a dry flask under argon. Dry acetonitrile (20ml) was added and the mixture heated under reflux for 16 hours. The mixture was allowed to cool and water was added (60ml). This was then stirred for 15 minutes to dissolve the potassium carbonate, and the solution filtered off. The solid remaining was further washed with water (2x40ml), then ether (2x40ml) and dried under vacuum. The title compound was collected as a white solid (4.712g, 82%). R.f. [EtOAc]: 0.65. ^{1}H NMR (d_6-DMSO): 1.28 (s, 9H, CMe_3), 3.83 (s, 3H, OMe), 5.17 (s, 2H, $OC\underline{H}_2PhCMe_3$), 7.28 (d, 2H, J=8.3Hz, 3'H and 5'H), 7.40 (ov.m, 4H, H2 and H5 and 2'H and 6'H), 7.55 (dd, 1H, J=8.2, 1.8Hz, H6), 9.84 (s, 1H, CHO)ppm. APCI-MS m/z: 299 $(M+H)^+$.

11.2.4.5 4-Methoxy-3-(3-phenylpropoxy)benzaldehyde **bp**

3-Hydroxy-4-methoxybenzaldehyde **cg** (10.00g, 65.7mmol), 1-bromo-3-phenylpropane (17.21g, 1.3eq) and potassium carbonate (12.85g, 1.4eq) were placed in a dry flask under argon. Dry acetonitrile (35ml) was then added and the mixture heated under reflux for 16 hours. The mixture was allowed to cool, the potassium carbonate removed by filtration and the mixture concentrated under vacuum. This was then partitioned between DCM (50ml) and water (50ml) and the DCM extraction repeated (2x50ml). The combined organic fractions were dried over anhydrous sodium sulfate, which was subsequently filtered off and the solvent removed by rotary evaporation, to obtain an brown oil. This residue was then placed on top of a plug of silica and eluted with 60-80 PE, until no more alkyl halide was observed by TLC. The silica was then eluted with ethyl acetate to displace the product from the silica. The title compound was collected as a brown oil (10.371g, 58%). R.f. [Et_2O]: 0.67. ^{1}H NMR (d_6-DMSO): 2.04 (quint, 2H, J=6.4Hz, $OCH_2C\underline{H}_2CH_2Ph$), 2.75 (t, 2H, J=7.2Hz, $OCH_2CH_2C\underline{H}_2Ph$), 3.89 (s, 3H, OMe), 4.01 (m, 2H, $OC\underline{H}_2CH_2CH_2Ph$), 7.14-7.32 (ov.m, 6H, H5 and

5Phenyl-H), 7.36 (d, 1H, J=1.8Hz, H2), 7.55 (dd, 1H, J=8.2, 1.8Hz, H6), 9.82 (s, 1H, CHO)ppm. APCI-MS m/z: 271 $(M+H)^+$.

11.2.4.6 4-Methoxy-3-[(4-methylbenzyl)oxy]benzaldehyde **bq**

3-Hydroxy-4-methoxybenzaldehyde **cg** (10.00g, 65.7mmol), 1-(bromomethyl)-4-methyl-benzene (14.59g, 1.2eq) and potassium carbonate (12.85g, 1.4eq) were placed in a dry flask under argon. Dry acetonitrile (35ml) was then added and the mixture heated under reflux for 16 hours. The mixture was allowed to cool, the potassium carbonate removed by filtration and the mixture concentrated under vacuum. This was then partitioned between DCM (50ml) and water (50ml) and the DCM extraction repeated (2x50ml). The combined organic fractions were dried over anhydrous sodium sulfate, filtered and the solvent removed under vacuum, to obtain an orange oil. This residue was then placed on top of a plug of silica and eluted with 60-80PE, until no more alkyl halide was observed by TLC. The silica was then eluted with ethyl acetate to displace the product from the silica. The title compound was collected as a pale yellow solid (10.597g, 63%). R.f. [EtOAc/60-80PE (2:1)]: 0.55. ^{1}H NMR (d_6-DMSO): 2.31 (s, 3H, Ph<u>Me</u>), 3.87 (s, 3H, OMe), 5.11 (s, 2H, OC<u>H</u>$_2$PhMe), 7.19 (ov.m, 3H, H5 and 3'H and 5'H), 7.35 (d, 2H, J=8.0Hz, 2'H and 6'H), 7.47 (d, 1H, J=1.8Hz, H2), 7.56 (dd, 1H, J=8.2, 1.8Hz, H6), 9.82 (s, 1H, CHO)ppm. APCI-MS m/z: 257 $(M+H)^+$.

11.2.4.7 3-{[4-(tert-Butyl)benzyl]oxy}-4-methoxybenzaldehyde **br**

3-Hydroxy-4-methoxybenzaldehyde **cg** (2.91g, 19.2mmol), 1-(bromomethyl)-4-(*tert*-butyl)-benzene (5.22g, 1.2eq) and potassium carbonate (3.71g, 1.4eq) were placed in a dry flask under argon. Dry acetonitrile (35ml) was then added and the mixture heated under reflux for 16 hours. The mixture was allowed to cool, the potassium carbonate removed by filtration and the mixture concentrated under vacuum. This was then partitioned between DCM (50ml) and water (50ml) and the DCM extraction repeated (2x50ml). The combined organic fractions were dried over anhydrous sodium sulfate, filtered and the solvent removed under vacuum, to obtain an orange oil. This residue was then placed on top of a plug of silica and eluted with 60-80PE, until no more alkyl halide was observed by TLC. The silica was then eluted with ethyl acetate to displace the product from the silica. The title compound was collected as an off white solid (4.29g, 75%). R.f. [EtOAc/60-80PE (2:1)]: 0.61. ^{1}H NMR (d_6-DMSO): 1.28 (s, 9H, CMe_3), 3.87 (s, 3H, OMe), 5.11 (s, 2H, OC<u>H</u>$_2$PhCMe$_3$), 7.21 (d, 1H, J=8.2Hz, H5), 7.39 (ov.m, 4H, 3'H and 5'H and 2'H and 6'H), 7.50 (d, 1H, J=1.9Hz, H2), 7.57 (dd, 1H, J=8.2, 1.9Hz, H6), 9.83 (s, 1H, CHO)ppm. APCI-MS m/z: 299 $(M+H)^+$.

11.2.4.8 *3,5-Di(tert-butyl)-2-methoxybenzaldehyde* **bv**

3,5-Di(*tert*-butyl)-2-hydroxybenzaldehyde **cq** (3.042g, 13.0mmol), anhydrous potassium carbonate (1.98g, 1.1eq), dry acetonitrile (20ml) and iodomethane (2.5ml, 3eq) were stirred together at 50°C under argon for 16 hours. A second portion of iodomethane (2.5 ml, 3eq) was then added and the mixture left under the same conditions for a further 6 hours. The mixture was allowed to cool, the potassium carbonate filtered off, and the solution washed with water (2x30ml), dried over sodium sulfate, filtered and the solvent removed under vacuum. The light brown oil obtained was subjected to flash column chromatography, eluted with 60-80PE/ethyl acetate (20:1). The title compound was obtained as a pale yellow oil (2.24g, 69%). R.f. [60-80PE/EtOAc (20:1)]: 0.50. ^{1}H NMR (d_6-DMSO): 1.28 (s, 9H, CMe_3), 1.38 (s, 9H, CMe_3), 3.88 (s, 3H, OMe), 7.60 (d, 1H, J=2.6Hz, Ar-H), 7.63 (d, 1H, J=2.6Hz, Ar-H), 10.23 (s, 1H, CHO)ppm. APCI-MS m/z: 249 $(M+H)^+$.

11.2.4.9 *2-Hydroxy-3,5-dimethylbenzaldehyde* **cp**[103]

2,4-Dimethylphenol (12ml, 100mmol), anhydrous toluene (20ml), tri-n-butylamine (7ml, 40mmol) and tin tetrachloride (1.2ml, 10mmol) were stirred in a flask, fitted with a reflux condenser under argon for 20 minutes at RT. Paraformaldehyde (6.6g, 220mmol) was then added and the reaction heated at 100°C for 8 hours. The mixture was allowed to cool and then poured onto water (500ml), which was then acidified to pH2 with 2M HCl. This mixture was extracted with ether (3x200ml), the combined organic layers washed with a saturated sodium chloride solution (2x200ml), dried over sodium sulfate, filtered and the solvent removed under vacuum. The brown oil obtained was subjected to flash column chromatography, eluted with 60-80PE/ether (20:1). The title compound was collected as a yellow oil (5.11g, 34%). R.f. [60-80PE/ether (20:1)]: 0.41. ^{1}H NMR (d_6-DMSO): 2.16 (s, 3H, Me), 2.24 (s, 3H, Me), 7.29 (s, 1H, Ar-H), 7.36 (s, 1H, Ar-H), 9.97 (s, 1H, CHO), 10.77 (bs, 1H, OH)ppm. APCI-MS m/z: 151 $(M+H)^+$.

11.2.4.10 *2,4-Di(tert-butyl)-6-formylphenyl acetate* **da**

3,5-Di(*tert*-butyl)-2-hydroxybenzaldehyde **cq** (2.41g, 10.3mmol) was dissolved in pyridine (10ml). Acetic anhydride (10ml, 10eq) and DMAP (2mg) was added and the reaction stirred at 100°C for 16 hours. The solvent was removed under vacuum, and the resulting solid was washed with water (3x20ml), then methanol (3x20ml). The title compound was obtained as a pale yellow solid (2.180g, 77%). R.f. [EtOAc]: 0.61. ^{1}H NMR (d_6-DMSO): 1.34 (s, 18H, $(CMe_3)_2$), 2.38 (s, 3H, OCOMe), 7.70 (d, 1H, J=2.5Hz, Ar-H), 7.82 (d, 1H, J=2.5Hz, Ar-H), 9.92 (s, 1H, CHO)ppm. APCI-MS m/z: 235 $[(M-COMe)+H]^+$, 277 $(M+H)^+$.

11.2.5 Synthesis of N^1-[4,6-di-(tert-butyl)-2-acetyl)benzylidene]-pyridine-4-carboxamidrazone

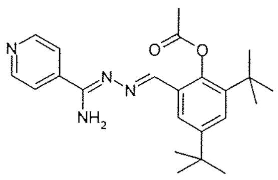

Pyridine-4-carboxamidrazone **4PY** (46mg, 0.34mmol), 2,4-di(tert-butyl)-6-formylphenyl-acetate **da** (103mg, 1.1eq), and toluene (25ml) were heated under reflux with stirring for 16 hours. The solution was allowed to cool, then the solvent removed under vacuum. Addition of ether (25ml) to the resulting oil caused precipitation, and the solid was obtained by filtration and washed with ether (3x20ml). The title compound was collected a yellow solid (80mg, 60%). R.f. [EtOAc]: 0.46. ^{1}H NMR (d_6-DMSO): 1.33 (s, 9H, CMe_3), 1.35 (s, 9H, CMe_3), 2.39 (s, 3H, CCO<u>Me</u>), 7.18 (bs, 2H, NH_2), 7.46 (d, 1H, J=2.4Hz, 4'H), 7.87 (d, 2H, J=6.0Hz, Pyr-H3 and H5),7.34 (d, 1H, J=2.4Hz, 6'H), 8.26 (s, 1H, =CHAr), 8.69 (ov.m, 3H, Pyr-H2 and H6 and OH)ppm. APCI-MS m/z: 353 $[(M\text{-}COMe)+H]^+$, 395 $(M+H)^+$.

11.2.6 Study Of The Effect Of Temperature On The Reaction Between Pyridine-3-carboxamidrazone (3PY) and Aldehydes

Pyridine-3-carboxamidrazone **3PY** (54mg, 0.4mmol) was weighed into 6 vials. 3,4,5-Tri-methoxy-benzaldehyde **cu** (0.25M, 1.8ml) was added to 3 vials, one was heated at 80°C, one at 40°C and one was left at RT. The same was carried out with 4-(dimethylamino)-benzaldehyde **dq**. All samples were given a reaction time of 3 hours, after which each was triturated with ether (3x3ml) and the samples dried under high vacuum.

*Attempted Synthesis of **3PYcu** at RT:* Pale yellow solid. R.f. [EtOAc]: 0.69. ^{1}H NMR (d_6-DMSO): 3.72 (s, 6H, 4-OMe and 4'-OMe), 3.83 (s, 12H, 3- and 5-OMe and 3'- and 5'-OMe), 7.20 (s, 4H, H2 and H6 and H2' and H6'), 8.65 (s, 2H, 2x CH=N)ppm. APCI-MS m/z: 465 $(M+H)^+$.

*Attempted Synthesis of **3PYcu** at 40°C:* Pale yellow solid. R.f. [EtOAc]: 0.69. ^{1}H NMR (d_6-DMSO): 3.72 (s, 6H, 4-OMe and 4'-OMe), 3.83 (s, 12H, 3- and 5-OMe and 3'- and 5'-OMe), 7.20 (s, 4H, H2 and H6 and H2' and H6'), 8.65 (s, 2H, 2x CH=N)ppm. APCI-MS m/z: 465 [bis-substituted by-product $(M+H)^+$].

*Attempted Synthesis of **3PYcu** at 80°C:* Orange-yellow solid. R.f. [EtOAc]: 0.09, 0.69. ^{1}H NMR analysis showed the main product was the aldehyde bis-hydrazone product, with a trace of the expected pyridine-3-carbohydrazonamide product. APCI-MS m/z: 315 [**3PYcu** $(M+H)^+$], 465 [bis-substituted by-product $(M+H)^+$].

*Attempted Synthesis of **3PYdq** at RT:* Yellow solid. R.f. [EtOAc]: 0.68. ^1H NMR (d_6-DMSO): 2.98 (s, 12H, 4-NMe_2 and 4'-NMe_2), 6.75 (d, 4H, J=8.9Hz, H2 and H4 and H2' and H4'), 7.63 (d, 4H, J=8.9Hz, H3 and H5 and H3' and H5'), 8.49 (s, 2H, 2x CH=N)ppm. APCI-MS m/z: 295 [bis-substituted by-product $(M+H)^+$].

*Attempted Synthesis of **3PYdq** at 40°C:* Yellow solid. R.f. [EtOAc]: 0.68. ^1H NMR analysis showed the main product was the aldehyde bis-hydrazone product, with a trace of the expected pyridine-3-carbohydrazonamide product. APCI-MS m/z: 268 [**3PYdq** $(M+H)^+$], 295 [bis-substituted by-product $(M+H)^+$].

*Attempted Synthesis of **3PYdq** at 80°C:* Orange solid. R.f. [EtOAc]: 0.13, 0.68. ^1H NMR analysis showed that the residue was approximately a 50:50 mixture of the aldehyde bis-hydrazone product and the expected pyridine-3-carbohydrazonamide product. APCI-MS m/z: 268 [**3PYdq** $(M+H)^+$], 295 [bis-substituted by-product $(M+H)^+$].

11.2.7 Reaction With Ketones Instead of Aldehydes

Glass 4ml vials in a matrix were charged with 2-pyridylhydrazine (Aldrich) and each of the pyridinecarboxamidrazones (0.4mmol) in methanol (1ml). This was followed by addition of an ethanolic solution of ketone **ep**,**eq** or **er** (0.25M, 1.8ml, 1.1eq). The vials were heated in a heating block at 65°C for one hour to remove the methanol, then at 75°C for up to two hours, during which time the ethanol evaporated, to give the crude products. Purification was performed by robotic trituration with petroleum ether (3x2ml) and the products dried under high vacuum prior to analysis.

Table 11.3 Analysis of the reaction products from **ep** and the heteroarylcarboxamidrazones. %Yield refers to the crude product yield. Purity, where given, has been estimated by ^{1}H NMR.

Compound	Appearance	MW	% Yield	APCI-MS m/z	R.f.	^{1}H NMR (d_6-DMSO)	% Purity
2PYep	Yellow solid	294	54	295	0.79	1.29 (s, 9H, CMe_3), 2.25 (s, 3H, Me), 6.89 (bs, 2H, NH_2), 7.39 (d, 2H, J=8.4Hz, 3'H and 5'H), 7.56 (m, 1H, Pyr-H4), 7.82 (d, 2H, J=8.4Hz, 2'H and 6'H), 8.04 (dt, 1H, J=7.8, 1.7Hz, Pyr-H5), 8.24 (d, 1H, J=8.0Hz, Pyr-H3), 8.72 (m, 1H, Pyr-H6)ppm.	95
3PYep	Yellow solid	294	40	295	0.41	1.30 (s, 9H, CMe_3), 2.23 (s, 3H, Me), 6.93 (bs, 2H, NH_2), 7.45 (ov.m, 2H, Pyr-H4 and 3'H and 5'H), 7.86 (d, 2H, J=8.1Hz, 2'H and 6'H), 8.30 (m, 1H, Pyr-H5), 8.66 (dd, 1H, J=4.8, 1.7Hz, Pyr-H6), 9.13 (m, 1H, Pyr-H2)ppm.	95
4PYep	Yellow solid	294	47	295	0.45	1.30 (s, 9H, CMe_3), 2.41 (s, 3H, Me), 6.93 (bs, 2H, NH_2), 7.42 (d, 2H, J= 8.5Hz, 3'H and 5'H), 7.91 (ov.m, 4H, Pyr-H3 and Pyr-H5 and 2'H and 6'H), 8.66 (dd, 2H, J=4.5, 1.5Hz, Pyr-H2 and Pyr-H6)ppm.	95
HDep	Light pink crystals	267	32	268	0.73	1.28 (s, 9H, CMe_3), 2.27 (s, 3H, Me), 6.76 (ddd, 1H, J=6.8, 4.9, 1.0Hz, Pyr-H4), 7.26 (d, 1H, J=8.4Hz, Pyr-H3), 7.40 (d, 2H, J=8.6Hz, 3'H and 5'H), 7.63 (m, 1H, Pyr-H5), 7.70 (d, 2H, J=8.6Hz, 2'H and 6'H), 8.12 (m, 1H, Pyr-H6), 9.65 (bs, 1H, NH)ppm.	95

[4-(*tert*-Butyl)phenyl](cyclopropyl)methanone **eq** and [4-(*tert*-butyl)phenyl](phenyl)-methanone **er** were unreactive and no reaction occurred for these ketones under these conditions. The procedure was repeated using *iso*-propanol as the solvent and the mixture was heated at 100°C for 16 hours. TLC analysis showed that no reaction had taken place.

11.2.8 Synthesis of 3,5-dipyridin-2-yl-4*H*-1,2,4-triazol-4-amine-pyridinecarbox-amidrazone dimer

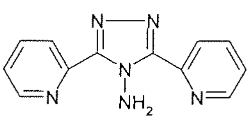

Pyridine-2-carboxamidrazone **2PY** (1.226g, 9.01mmol) was dissolved in ethanol (20ml) and heated under reflux for 53 hours. The solvent was then removed under vacuum, the title compound was collected as an orange solid (2.144g, 99%). R.f. [EtOAc]: 0.73. ^{1}H NMR ($CDCl_3$): 7.36 (ddd, 2H, J=7.5, 4.9, 1.2Hz, Pyr -4 and Pyr -4'), 7.77 (td, 2H, J=7.7, 1.8Hz, Pyr-H5 and Pyr-H5'), 8.06 (dt, 2H, J=8.0, 1.1Hz, Pyr-H3 and Pyr-H3'), 8.59 (ov.m, 4H, Pyr-H6 and Pyr-H6' and NH_2)ppm. NH_2 signal did not disappear on D_2O shake- stabilised due to intramolecular hydrogen bonding. IR (KBr): 3346 (ν_{as} NH_2), 3300 (ν_s NH_2), 3060 (ν Ar CH), 1625 (ν C=N), 1584 (ν skeletal Pyr), 1561(ν skeletal Pyr), 1473 (ν skeletal Pyr), 1384, 1286, 1249, 1152, 1114, 1079 (ν C-N), 1043 (ν C-N), 983, 882, 769 (γ CH, 2-Pyr), 723 (β ring, 2-Pyr), 675cm^{-1}. APCI-MS m/z: 224 $[(M-NH_2)+H]^+$, 239 $(M+H)^+$.

11.2.9 Attempted Synthesis Of A Bis-Substituted Pyridylcarboxamidrazone

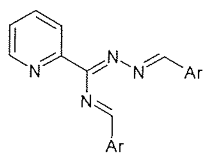

Method A

N'-(4-Methylbenzylidene)-pyridine-2-carboxamidrazone **2PYah** (40mg, 0.17mmol), was put into one vial and *N'*-(4-nitrobenzylidene)-pyridine-2-carboxamidrazone **2PYdo** (45mg, 0.17mmol) was put into another. Into each vial was added an ethanolic solution of 4-(*tert*-butyl)-benzaldehyde **ae** (0.25M, 0.62ml, 1.1eq) and ethanol (2ml). The mixtures were heated at 78°C for 3 hours, and the solvent allowed to evaporate. Purification was carried out by trituration with ether (3x2ml) and the products dried under vacuum. Both reactions failed. TLC, APCI-MS and ^{1}H NMR studies showed only the pure, respective starting materials to be present.

Method B

Pyridine-2-carboxamidrazone **2PY** (100mg, 0.74mmol) was dissolved in ethanol (30ml), and 4-(*tert*-butyl)benzaldehyde **ae** (264mg, 2.2eq) added. The mixture was heated under reflux for 16 hours. A yellow precipitate formed and was isolated by filtration and washed with ether. TLC, APCI-MS and ^{1}H NMR studies showed the only product to be the mono-substituted carboxamidrazone **2PYae**.

11.2.10 Synthesis Of Other Carboxamidrazones

11.2.10.1 Attempted synthesis of 2-chlorobenzenecarboxamidrazone **2ClBZ**

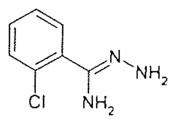

Hydrazine (80%, 18ml) was added to a solution of 2-chlorobenzonitrile (5.80g, 33.9mmol) in ethanol (10ml) and ether (10ml). The mixture was left at RT, with stirring for ten days. TLC of the reaction mixture showed that no reaction had occurred.

11.2.10.2 Synthesis of 2-nitrobenzenecarboxamidrazone **$2NO_2BZ$**

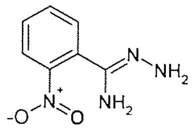

Hydrazine (80%, 18ml) was added to a solution of 2-nitrobenzonitrile (5.17g, 33.9mmol) in ethanol (10ml) and ether (10ml). The mixture was left at RT, with stirring for ten days, after which the majority of the solvent was removed by rotary evaporation. The residual solution was cooled and a precipitate formed which was obtained by filtration and rapidly washed with toluene. The title compound was collected as a light brown solid (3.325g, 54%). R.f. [EtOAc]: 0.58. ^{1}H NMR (d_6-DMSO): 6.46 (m, 1H, H4), 6.54 (bs, 2H, NH_2), 6.67 (dd, 1H, J=8.1, 1.2Hz, H3), 7.04 (bs, 1H, NH), 7.12 (m, 1H, H5), 7.52 (dd, 1H, J=8.0, 1.4Hz, H6), 7.69 (bs, 1H, NH)ppm. APCI-MS m/z: 120, 135 $(M+H-NO_2)^+$, 137,.138.

11.2.10.3 Synthesis of a small set of benzylidene-2-nitrobenzylcarboxamidrazones

2-Nitrobenzylcarboxamidrazone **$2NO_2BZ$** (0.180g) was dissolved in ethanol (25ml), the relevant aldehyde (1.1eq) added and the mixture heated under reflux for 4 hours. The solutions were allowed to cool and the solvent was removed under vacuum. The residues were triturated with ether (20ml), to give the final products and dried under high vacuum prior to analysis.

Table 11.4 Analysis of reaction products from 2-nitrobenzylcarboxamidrazone **$2NO_2BZ$** and aldehydes. %Yield refers to the crude product yield. Purity, where given, has been estimated by ^1H NMR. * refers to the common peak $(M+H-NO_2)^+$, in the mass spectrum of these compounds.

Compound	Appearance	MW	% Yield	APCI-MS m/z	R.f.	^1H NMR (d_6-DMSO)	% Purity
$2NO_2BZae$	Beige solid	324	65	264, 279*, 281, 282	0.53		
$2NO_2BZaf$	Beige solid	338	72	278, 293*, 295, 296	0.53	0.64 (t, 3H, J=7.3Hz, $CMe_2CH_2\underline{Me}$), 1.22 (s, 6H, $C\underline{Me_2}CH_2Me$), 1.65 (q, 2H, J=7.3Hz, $CMe_2C\underline{H_2}Me$), 7.22 (m, 1H, H4), 7.34 (m, 1H, H3), 7.54 (ov.m, 3H, H5 and 3'H and 5'H), 7.63 (bs, 1H, NH), 7.91 (ov.m, 3H, H6 and 2'H and 6'H), 8.29 (bs, 1H, NH), 8.57 (s, 1H, =CHAr)ppm.	98
$2NO_2BZbh$	Beige solid	404	76	344, 359*, 361, 362	0.58		
$2NO_2BZbn$	Orange glass	404	83	344, 359*, 361, 362	0.57	3.87 (s, 3H, OMe), 5.17 (s, 2H, $O\underline{CH_2}$ Ph), 7.19 (m, 1H, H4), 7.29-7.54 (ov.m, 10H, 5Phenyl-H and H3 and H5 and 5'H and 6'H and NH), 7.64 (d, 1H, J=1.7Hz, 2'H), 7.96 (m, 1H, H6), 8.36 (bs, 1H, NH), 8.50 (s, 1H, =CHAr)ppm.	95
$2NO_2BZ$ dx	Orange glass	361	61	301, 316*, 318, 319	0.56		
$2NO_2BZ$ eh	Beige solid	410	87	350, 365*, 367, 368	0.50	6.97 (m, 1H, H4), 7.36 (ov.m, 4H, H3 and Ar-H' and 3"H and 5"H), 7.46-7.60 (ov.m, 6H, 3Ar-H and 2"H and 6"H and NH), 7.85 (m, 1H, H6 or Ar-H), 8.09 (ov.m, 2H, NH and H6 or Ar-H), 8.85 (s, 1H, =CHAr)ppm.	95

11.2.11 Attempted Reduction Of The Carboxamidrazone Imine Bond of *N'*-[3,5-di-(tert-butyl)-2-hydroxybenzylidene]-pyridine-4-carboxamidrazone, 4PYcq

11.2.11.1 Attempted Reduction With Lithium Aluminium Hydride

A pressure equalised dropping funnel containing *N'*-[3,5-di-(tert-butyl)-2-hydroxy-benzylidene]-pyridine-4-carboxamidrazone **4PYcq** (1.04g, 2.95mmol) dissolved in dry THF (20ml) was fitted to a flask containing lithium aluminium hydride in dry THF (0.113g, 1eq /15ml), under an atmosphere of argon. The flask was placed in an ice bath, and the solution in the funnel was added dropwise, with stirring, over 20 minutes. The flask was then allowed to warm to RT and the reaction followed by TLC. After 1 hour a saturated solution of ammonium chloride (50ml) was added to the reaction mixture. The resulting grey precipitate was removed by filtration and washed with ethyl acetate, the ethyl acetate washing was kept. The THF filtrate was extracted with ethyl acetate (3x30ml), and the organic fractions combined with the previous ethyl acetate wash, were dried over magnesium sulfate, filtered and the solvent removed under vacuum. The resulting beige solid was found to be starting material with the pyridyl nitrogen atom being protonated. R.f. [Et_2O]: 0.44 (compared to 0.65 for unprotonated form). ^{1}H NMR (d_6-DMSO): 1.28 (s, 9H, CMe_3), 1.44 (s, 9H, CMe_3), 7.15 (bs, 2H, NH_2), 7.31 (m, 1H, 4'H), 7.34 (m, 1H, 6'H), 7.90 (bs, 2H, Pyr-H3 and Pyr-H5), 8.67 (s, 1H, =CHAr), 11.61 (s, 1H, OH)ppm. APCI-MS m/z: 353 $(M+H)^+$. In order to prove that this was the protonated form, the solid was dissolved in DCM (30ml) and extracted with aqueous potassium carbonate (3x30ml). The DCM layers were combined and the solvent removed under vacuum. ^{1}H NMR analysis of the pale yellow solid obtained showed that it was the starting material, *N'*-[3,5-di-(tert-butyl)-2-hydroxybenzylidene]-pyridine-4-carboxamidrazone **4PYcq**.

11.2.11.2 Attempted Catalytic Hydrogenation Using Palladium-on-Charcoal

N'-[3,5-Di-(tert-butyl)-2-hydroxybenzylidene]-pyridine-4-carboxamidrazone **4PYcq** (1.517g, 4.31mmol) was dissolved in ethanol (25ml) and Pd-C (0.152g, 10%w/w) added. The reaction was carried out under positive hydrogen pressure (120Psi) with agitation for 72 hours. The Pd-C was removed by filtration through celite and the solvent removed under vacuum. ^{1}H NMR analysis of the pale yellow solid showed that it was the starting material, **4PYcq**.

11.2.11.3 Attempted Catalytic Hydrogenation Using Raney Nickel, Cyclohexadiene and Heat

N'-[3,5-Di-(tert-butyl)-2-hydroxybenzylidene]-pyridine-4-carboxamidrazone **4PYcq** (0.42g, 1.19mmol) was dissolved in ethanol (40ml) and cyclohexadiene (2ml, 18eq) added. Raney nickel (0.162mg) was added, and the mixture was heated under reflux, in an atmosphere of argon for 16 hours. The mixture was allowed to cool, the Raney nickel removed by filtration through celite and the solvent and benzene formed, evaporated under vacuum. ^{1}H NMR analysis of the pale yellow solid obtained showed that it was the starting material, **4PYcq**

11.2.11.4 Attempted Catalytic Hydrogenation Using Raney Nickel, Cyclohexadiene and Pressure

N'-[3,5-Di-(tert-butyl)-2-hydroxybenzylidene]-pyridine-4-carboxamidrazone **4PYcq** (0.49g, 1.39mmol) was dissolved in ethanol (40ml) and cyclohexadiene (2.3ml, 18eq) added. Raney nickel (0.286mg) was added and the reaction was carried out under positive hydrogen pressure (140Psi) with agitation for 16 hours. The Raney nickel was removed by filtration through celite and the solvent, and benzene formed, evaporated under vacuum. ^{1}H NMR analysis of the pale yellow solid obtained showed that it was the starting material, *N'*-[3,5-di-(tert-butyl)-2-hydroxybenzyl]pyridine-4-carboxamidrazone **4PYcq**.

11.3 PEG AS A SOLUBLE POLYMERIC SUPPORT FOR 1,3- DIPOLAR-CYCLOADDITION CHEMISTRY

4000-PEG-OH refers to the dihydoxy 4000-PEG, so all of the reactions below theoretically occur on both ends of the molecule, however, for simplicity, the structures show only reaction site.

In the following section, the when 'bleach' is mentioned, this refers to sodium hypochlorite solution containing 4.5%w/w available chlorine.

11.3.1 Synthesis Of Oximes

*11.3.1.1 Synthesis of 4-(tert-butyl)benzaldehyde oxime **55***

4-tert-Butylbenzaldehyde **ae** (28.61g, 0.18mol) was dissolved in ethanol (90ml). Hydroxylamine hydrochloride (14.79g, 1.2eq) was added and the mixture was stirred at RT. An aqueous solution of sodium hydroxide (7.9g,1.1eq, 35ml) was added dropwise. The mixture was heated under reflux for 1 hour and then poured onto water (200ml). The precipitate formed was collected by filtration and dried under vacuum. The title compound was collected as an off white solid. R.f. [EtOAc]: 0.76. ^{1}H NMR (d_6-DMSO): 1.28 (s, 9H, $CCMe_3$), 7.40 (d, 2H, J=8.5Hz, 3H and 5H), 7.52 (d, 2H, J=8.5Hz, 2H and 6H), 8.09 (s, 1H, C<u>H</u>=NOH), 11.10 (d, 1H, 2.1Hz, CH= NO<u>H</u>)ppm. APCI-MS m/z: 178 $(M+H)^+$.

*11.3.1.2 Synthesis of 4-benzyloxybenzaldehyde oxime **56***

4-Benzyloxybenzaldehyde **bg** (15.256g, 72.0mmol) was dissolved in ethanol (60ml). Hydroxylamine hydrochloride (6.00g, 1.2eq) was added and the mixture was stirred at RT. An aqueous solution of sodium hydroxide (3.2g,1.1eq, 30ml) was added dropwise over 20 minutes. The mixture was heated under reflux for 1 hour and then poured onto water (200ml). The title compound precipitated as a white solid which was collected by filtration and dried under vacuum (15.749g, 96%). R.f. [Et_2O]: 0.72. ^{1}H NMR (d_6-DMSO):5.14 (s, 2H, OC<u>H</u>$_2$Ph), 7.03 (dd, 2H, J=6.8, 1.9Hz, 3H and 5H), 7.39 (m, 5H, 5Phenyl-H), 7.52 (d, 2H, J=6.8, 1.9Hz, 2H and 6H), 8.06 (s, 1H, C<u>H</u>=NOH), 10.96 (bs, 1H, CH=NO<u>H</u>)ppm. APCI-MS m/z: 228 $(M+H)^+$.

11.3.2 Reaction of PEG With Unsaturated Acid Chlorides

*11.3.2.1 Synthesis of PEG-undec-10-enoate **53***

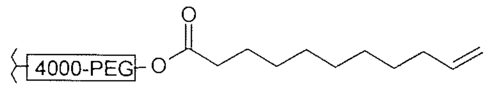

4000-PEG-OH (191.3g) was dissolved in chloroform, and dry Amberlite® IRA-67 (35g) and 10-undecenoyl chloride (35ml) added dropwise. The mixture was stirred at RT for 70 hours. After this time, methanol (50ml) was added and the mixture stirred for 30 minutes to quench any excess acid chloride. The reaction mixture was filtered to remove the ion exchange resin, the filtrate reduced to half volume, under vacuum and then poured onto ether (800ml). The title product formed as a white precipitate which was obtained by filtration, and dried under vacuum overnight (193.5g, 97% yield, 100% substitution). ^{1}H NMR (d_6-DMSO): 1.25 (m, 10H, 5CH_2), 1.51(m, 2H, CH_2), 2.02 (q, 2H, J=6.9Hz, CH_2), 2.28 (t, 2H, J=7.3Hz, CH_2), 3.20-3.79 (PEG backbone), 4.11 (t, 2H, J=4.9Hz, PEG-OCH_2), 4.95 (m, 2H, CH=C$\underline{H}_2$), 5.79 (m, 1H, C$\underline{H}$=CH_2)ppm.

*11.3.2.2 Synthesis of PEG-acrylate **54***

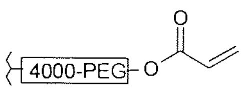

4000-PEG-OH (190.5g) was dissolved in chloroform, and dry Amberlite® IRA-67 (35g) and acrolyl chloride (35ml) added dropwise. The mixture was stirred at RT for 16 hours. After this time, methanol (50ml) was added and the mixture stirred for 30 minutes to quench any excess acid chloride. The reaction mixture was filtered to remove the ion exchange resin, the filtrate reduced to half volume, under vacuum and then poured onto ether (800ml). The title product formed as a white precipitate which was obtained by filtration, and dried under vacuum overnight (185.6g, 96% crude yield, 62% purity)*. ^{1}H NMR (d_6-DMSO): 3.20-3.79 (PEG backbone), 4.22 (t, 2H, J=4.9Hz, PEG-OCH_2), 4.55 (bt, 0.61H, unreacted PEG-OH), 5.95 (m, 1H, C$\underline{H}$=CH_2), 6.24 (m, 2H, CH=C$\underline{H}_2$)ppm.

*The only impurity observed by ^{1}H NMR was unreacted PEG. The purity, i.e. the degree of substitution was calculated from the ratio of the integral for the vinyl CH (5.95ppm) compared to the ratio of the OH triplet (4.55ppm)[131].

11.3.3 1.3-Dipolar Cycloadditions Onto PEG Derivatives

11.3.3.1 Synthesis of PEG-10-{3-[4-(tert-butyl)phenyl]-4,5-dihydroisoxazol-5-yl}-undecanoate **58**

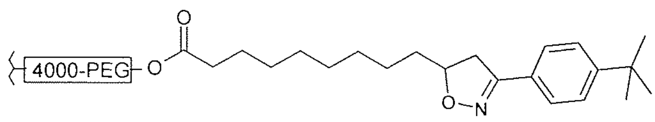

PEG-undec-10-enoate **53** (6.11g, 3.1mmol alkene equivalents) was dissolved in DCM (50ml) and bleach (30ml) added. 4-(tert-Butyl)benzaldehyde oxime **55** (0.649g, 1.2eq) in DCM (25ml) was added dropwise over 25 minutes with rapid stirring, then the mixture was left at RT for 16 hours. The organic and aqueous layers were then separated and the aqueous layer extracted with DCM (3x40ml). The combined organic layers were dried over sodium sulfate, filtered and the bulk of the solution removed under vacuum. This was then poured onto ether (200ml), with stirring. The white precipitate which formed was collected by filtration, then Recrystallised from *iso*-propanol. The title compound was collected as a white solid (4.256g, 32% yield). ^{1}H NMR ($CDCl_3$): 1.30 (s, 12H, $6CH_2$), 1.33 (s, 9H, CMe_3), 1.61 (m, 2H, CH_2), 2.32 (t, 2H, J=7.4Hz, CH_2), 2.95 (m, 1H, isoxazoline-H4), 3.34-3.94 (PEG backbone), 4.19 (m, 2H, J=4.9Hz, PEG-OCH_2), 4.73 (m, 1H, isoxazoline-H4), 6.20 (m, 1H, isoxazoline-H5), 7.42 (d, 2H, J=8.5Hz, Ar-H3 and Ar-H5), 7.60 (d, 2H, J=8.5Hz, Ar-H2 and Ar-H6)ppm. Peaks from alternative isomer: 4.31 (m, 1H, isoxazoline-H4), 6.05 (m, 1H, isoxazoline-H5)ppm.

11.3.3.2 Synthesis of PEG-10-[3-(4-benzyloxyphenyl)-4,5-dihydroisoxazol-5-yl]-undecanoate **59**

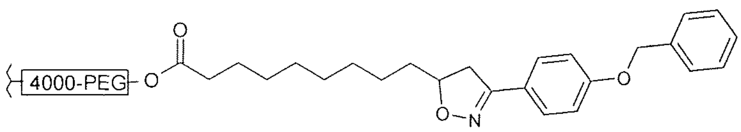

PEG-undec-10-enoate **53** (11.06g, 5.5mmol alkene equivalents) was dissolved in DCM (100ml) and bleach (60ml) added. 4-Benzyloxybenzaldehyde oxime **56** (1.26, 1.2eq) in DCM (25ml) was added dropwise over 35 minutes with rapid stirring, then the mixture was left at RT for 16 hours. The organic and aqueous layers were then separated and the aqueous layer extracted with DCM (3x40ml). The combined organic layers were dried over sodium sulfate, filtered and the bulk of the solution removed under vacuum. This was then poured onto ether (200ml), with stirring. The white precipitate which formed was collected by filtration, then Recrystallised from iso-propanol. The title compound was collected as a white solid (8.051g, 33% yield). ^{1}H NMR ($CDCl_3$): 1.29 (s, 12H, $6CH_2$), 1.60 (m, 2H, CH_2), 2.32 (t, 2H, J=7.4Hz, CH_2), 2.92 (m, 1H, isoxazoline-H4), 3.34-3.94 (PEG backbone), 4.21 (overlapping m, 3H, J=4.7Hz, PEG-OCH_2, isoxazoline-H4), 4.69 (m, 1H, isoxazoline-H5), 5.09 (s, 2H, $OC\underline{H_2}Ph$), 6.99 (d, 2H, J=8.9Hz, Ar-H3 and Ar-H5), 7.39 (m, 5H, 5Phenyl-H), 7.60 (d, 2H, J=8.9Hz, Ar-H2 and Ar-H6)ppm.

11.3.3.3 Synthesis of PEG-{3-[4-(tert-butyl)phenyl]-4,5-dihydroisoxazol-5-yl}acetate ***60***

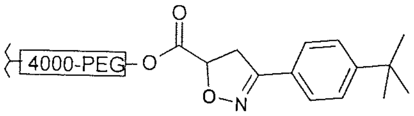

PEG-acrylate **54** (5.87g, 1.8mmol alkene equivalents) was dissolved in DCM (50ml) and bleach (20ml) added. 4-(tert-Butyl)benzaldehyde oxime **55** (0.412g, 1.2eq) in DCM (25ml) was added dropwise over 25 minutes with rapid stirring, then the mixture was left, with stirring, at RT for 16 hours. The organic and aqueous layers were then separated and the aqueous layer extracted with DCM (3x40ml). The combined organic layers were dried over sodium sulfate, filtered and the bulk of the solution removed under vacuum. This was then poured onto ether (200ml), with stirring. The white precipitate which formed was collected by filtration, then Recrystallised from iso-propanol. The title compound was collected as a white solid (2.739g, 36% yield). ^{1}H NMR ($CDCl_3$): 1.32 (s, 9H, CMe_3), 3.35-3.92 (PEG backbone), 4.30 (m, 2H, (2)isoxazoline-H4), 4.35 (m, 2H, J=4.9Hz, PEG-OCH_2), 5.18 (m, 1H, isoxazoline-H5), 7.42 (d, 2H, J=8.5Hz, Ar-H3 and Ar-H5), 7.61 (d, 2H, J=8.5Hz, Ar-H2 and Ar-H6)ppm.

11.3.3.4 Synthesis of PEG-[3-(4-benzyloxyphenyl)-4,5-dihydroisoxazol-5-yl]acetate ***61***

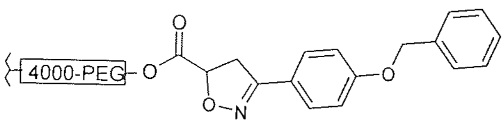

PEG-acrylate **54** (10.25g, 3.4mmol alkene equivalents) was dissolved in DCM (100ml) and bleach (45ml) added. 4-Benzyloxybenzaldehyde oxime **56** (0.94g, 1.2eq) in DCM (40ml) was added dropwise over 45 minutes with rapid stirring, then the mixture was left at RT for 16 hours. The organic and aqueous layers were then separated and the aqueous layer extracted with DCM (3x40ml). The combined organic layers were dried over sodium sulfate, filtered and the bulk of the solution removed under vacuum. This was then poured onto ether (200ml), with stirring. The white precipitate which formed was collected by filtration, then Recrystallised from iso-propanol. The title compound was collected as a white solid (9.290g, 64% yield). ^{1}H NMR ($CDCl_3$): 3.35-3.92 (PEG backbone), 4.30 (m, 2H, (2)isoxazoline-H4), 4.35 (m, 2H, J=4.9Hz, PEG-OCH_2), 5.09 (s, 2H, $O\underline{CH_2}Ph$), 5.18 (m, 1H, isoxazoline-H5), 6.99 (d, 2H, J=8.9Hz, Ar-H3 and Ar-H5), 7.39 (m, 5H, 5Phenyl-H), 7.61 (d, 2H, J=8.9Hz, Ar-H2 and Ar-H6)ppm.

11.3.4 Cleavage Of PEG-Bound Cycloaddition Products By Methanol

11.3.4.1 Harvest of methyl 10-{3-[4-(tert-butyl)phenyl]-4,5-dihydroisoxazol-5-yl}-undecanoate ***62***

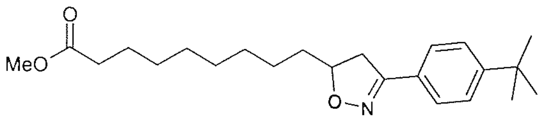

Methanol (5ml) and DBU (15mg) were added to PEG-10-[3-(4-(*tert*-butyl)phenyl)-4,5-dihydro-isoxazol-5-yl]undecanoate **58** (1.032g) dissolved in DCM (20ml) and the mixture heated with stirring at 30°C for 16 hours. The mixture was then concentrated under vacuum, and poured onto ether (100ml). The precipitate which formed was filtered off and washed with ether (2x20ml). The filtrate and ether washes were combined and the solvent removed under vacuum. The orange glass (95mg, 53% crude yield) obtained was subjected to preparative TLC (silica, 1000μm), eluted with 60:80PE/ether (1:1). The yellow glass (20mg, 11% yield) obtained was a mixture of the title compound, and the isoxazol-4-yl-undecanoate isomer (7:1). R.f. [60:80PE/ether (1:1)]: 0.60. ^{1}H NMR ($CDCl_3$): 1.31 (s, 12H, 6CH_2), 1.33 (s, 9H, CMe_3), 1.62 (m, 2H, CH_2), 2.31 (t, 2H, J=7.4Hz, CH_2), 2.95 (dd, 1H, J=16.4, 8.0Hz, isoxazoline-H5 cis to isoxazoline-H4), 3.40 (dd, 1H, J=16.4, 10.3Hz, isoxazoline-H5 trans to isoxazoline-H4), 3.67 (s, 3H, OMe), 4.72 (m, 1H, isoxazoline-H4), 7.42 (d, 2H, J=6.6, Ar-H3 and Ar-H5), 7.60 (d, 2H, J=6.6, Ar-H2 and Ar-H6)ppm. Peaks from alternative isomer: 2.47 (dd, 1H, J=5.0, 2.8Hz, isoxazoline-H5), 2.75 (m, 1H, isoxazoline-H5), 4.31 (m, 1H, J=6.7Hz, isoxazoline-H4)ppm. APCI-MS m/z: 360 $(M+H)^+$. Major isomer:minor isomer, 5:1.

11.3.4.2 Harvest of methyl 10-{3-[4-(benzyloxy)phenyl]-4,5-dihydroisoxazol-5-yl}-undecanoate ***63***

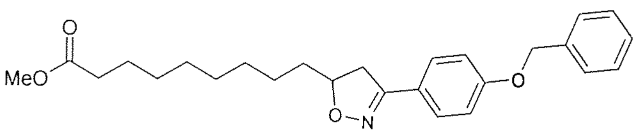

Methanol (5ml) and DBU (15mg) were added to PEG-10-[3-(4-benzyloxyphenyl)-4,5-dihydro-isoxazol-5-yl]undecanoate **59** (1.359g) dissolved in DCM (30ml) and the mixture heated with stirring at 30°C for 16 hours. The mixture was then concentrated under vacuum, and poured onto ether (50ml). The precipitate which formed was filtered off and washed with ether (2x20ml). The filtrate and ether washes were combined and the solvent removed under vacuum. The orange oil obtained (110mg, 41% crude yield) was subjected to preparative TLC (silica, 1000μm), eluted with 60:80PE/ether (1:1). The title compound was obtained as a beige solid (10mg, 12% yield). R.f. [60:80PE/ether (1:1)]: 0.31. ^{1}H NMR ($CDCl_3$): 1.28 (m, 14H, $MeOCOCH_2(C\underline{H_2})_7R$), 2.31 (t, 2H, J=7.4Hz, $MeOCOC\underline{H_2}(CH_2)_7R$), 2.93 (dd, 1H, J=17.5, 7.5Hz, isoxazoline-H4 cis to isoxazoline-H5), 3.37 (dd, 1H, J=17.5, 10.0Hz, isoxazoline-H4 trans to isoxazoline-H5), 4.70 (m, 1H, isoxazoline-H5), 3.67 (s, 3H, OMe), 5.11 (s, 2H, OC$\underline{H}_2$Ph), 6.99 (d, 2H, J=7.0 Ar-H3 and Ar-H5), 7.41 (m, 5H, 5Phenyl-H), 7.61 (d, 2H, J=7.0, Ar-H2 and Ar-H6)ppm. APCI-MS m/z: 424 $(M+H)^+$.

11.3.4.3 Harvest of methyl 3-[4-(tert-butyl)phenyl]-4,5-dihydroisoxazole-5-carboxylate **64**

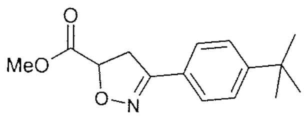

Methanol (5ml) and DBU (15mg) were added to PEG-{3-[4-(*tert*-butyl)phenyl]-4,5-dihydroisoxazol-5-yl}acetate **60** (0.806g) dissolved in DCM (20ml) and the mixture heated with stirring at 30°C for 16 hours. The mixture was then concentrated under vacuum, and poured onto ether (50ml). The precipitate which formed was filtered off and washed with ether (2x20ml). The filtrate and ether washes were combined and the solvent removed under vacuum. The orange glass (100mg, 96% crude yield) obtained was subjected to preparative TLC (silica, 1000μm), eluted with 60:80PE/ether (1:1). The title compound was obtained as a colourless glass (10mg, 10% yield). R.f. [60:80PE/ether (1:1)]: 0.41. ^{1}H NMR ($CDCl_3$):1.34 (s, 9H, CMe_3), 3.65 (ov.m, 2H, (2)isoxazoline-H4), 3.82 (s, 3H, OMe), 5.19 (dd, 1H, J=10.0, 8.0Hz, isoxazoline-H5), 7.44 (d, 2H, J=6.6, Ar-H3 and Ar-H5), 7.63 (d, 2H, J=6.6, Ar-H2 and Ar-H6)ppm. APCI-MS m/z: 262 $(M+H)^+$.

11.3.4.4 Harvest of methyl 3-[4-(benzyloxy)phenyl]-4,5-dihydroisoxazole-5-carboxylate **65**

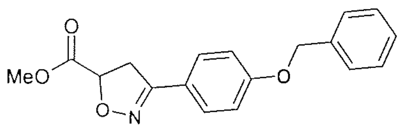

Methanol (5ml) and DBU (15mg) were added to PEG-{3-[4-(benzyloxy)phenyl]-4,5-dihydro-isoxazol-5-yl}acetate **61** (1.110g) dissolved in DCM (20ml) and the mixture heated with stirring at 30°C for 16 hours. The mixture was then concentrated under vacuum, and poured onto ether (100ml). The precipitate which formed was filtered off and washed with ether (2x20ml). The filtrate and ether washes were combined and the solvent removed under vacuum. The brown-green oil obtained (146mg, 72% crude yield) was subjected to preparative TLC (silica, 1000μm), eluted with 60:80PE/ether (1:1). The title compound was obtained as a orange oil (9mg, 8% yield). R.f. [60:80PE/ether (1:1)]: 0.17. ^{1}H NMR ($CDCl_3$): 3.63 (ov.m, 2H, (2)isoxazoline-H4), 3.83 (s, 3H, OMe), 5.11 (s, 2H, OC$\underline{H}_2$Ph), 5.16 (dd, 1H, J=10.0, 7.5Hz, isoxazoline-H5), 7.00 (d, 2H, J=7.0, Ar-H3 and Ar-H5), 7.41 (m, 5H, 5Phenyl-H), 7.62 (d, 2H, J=7.0, Ar-H2 and Ar-H6)ppm. APCI-MS m/z: 312 $(M+H)^+$.

11.3.5 Cleavage Of PEG-Bound Cycloaddition Products By Amine

11.3.5.1 Attempted harvest of 9-{3-[4-(tert-butyl)phenyl]-4,5-dihydroisoxazol-5-yl}-N-isobutyl-nonanamide

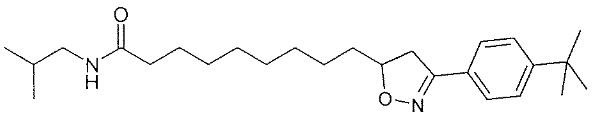

PEG-10-[3-(4-(*tert*-butyl)phenyl)-4,5-dihydro-isoxazol-5-yl]undecanoate **58** (1.011g) was dissolved in DCM (18ml) and isobutylamine (2ml) added. The mixture was left stirring at RT for 16 hours, then the solution concentrated under vacuum and ether added (50ml). The precipitate which formed was filtered off and washed with ether (2x20ml). The filtrate and ether washes were combined and the solvent removed under vacuum, to give a brown oil (15mg) in low yield. The attempted cleavage was unsuccessful, as judged by ^{1}H NMR and APCI-MS and the title compound was not obtained.

11.3.5.2 Attempted harvest of 9-{3-[4-benzyloxyphenyl]-4,5-dihydroisoxazol-5-yl}-N-isobutyl-nonanamide

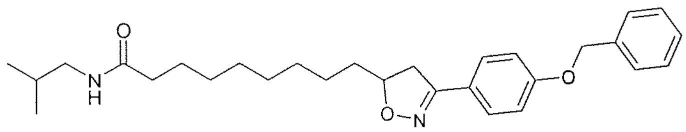

PEG-10-[3-(4-benzyloxyphenyl)-4,5-dihydro-isoxazol-5-yl]undecanoate **59** (1.248g) was dissolved in DCM (20ml) and isobutylamine (2.5ml) added. The mixture was left stirring at RT for 16 hours, then the solution concentrated under vacuum and ether added (50ml). The precipitate which formed was filtered off and washed with ether (2x20ml). The filtrate and ether washes were combined and the solvent removed under vacuum, to give an orange oil (15mg) in low yield. The attempted cleavage unsuccessful, as judged by ^{1}H NMR and APCI-MS and the title compound was not obtained.

11.3.5.3 Harvest of 3-[4-(tert-butyl)phenyl]-N-isobutyl-4,5-dihydroisoxazole-5-carboxamide ***66***

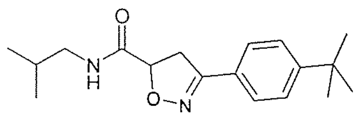

PEG-10-[3-(4-(*tert*-butyl)phenyl)-4,5-dihydro-isoxazol-5-yl]acetate **58** (0.825g) was dissolved in DCM (18ml) and isobutylamine (2ml) added. The mixture was left stirring at RT for 16 hours, then the solution concentrated under vacuum and ether added (50ml). The precipitate which formed was filtered off and washed with ether (2x20ml). The filtrate and ether washes were combined and the solvent removed under vacuum. The brown oil (117g, 98% crude yield) was subjected to preparative TLC (silica, 1000μm), eluted with ether. The title compound was obtained as an off white solid (31mg, 38% yield). R.f. [Et_2O]: 0.65. ^1H NMR ($CDCl_3$): 0.88 (d, 3H, J=6.8Hz, $NHCH_2CH\underline{Me_2}$), 0.91 (d, 3H, J=6.8Hz, $NHCH_2CH\underline{Me_2}$), 1.33 (s, 9H, $C\underline{Me_3}$), 1.78 (nonet, 1H, J=6.8Hz, $NHCH_2C\underline{H}Me_2$), 3.10 (m, 2H, $NHC\underline{H_2}CHMe_2$), 3.67 (ov.m, 2H, (2)isoxazoline-H4), 5.13 (dd, 1H, J=9.4, 7.6Hz, isoxazoline-H5), 6.88 (bt, 1H, $N\underline{H}CH_2CHMe_2$), 7.44 (d, 2H, J=6.6, Ar-H3 and Ar-H5), 7.61 (d, 2H, J=6.6, Ar-H2 and Ar-H6)ppm. MS ($M+H^+$) m/z: 303.

11.3.5.4 Harvest of 3-[4-benzyloxyphenyl]-N-isobutyl-4,5-dihydroisoxazole-5-carboxamide ***67***

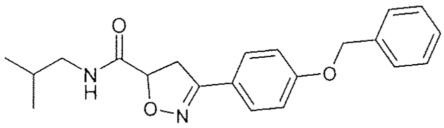

PEG-10-[3-(4-benxyloxyphenyl)-4,5-dihydro-isoxazol-5-yl]acetate **61** (1.224g) was dissolved in DCM (20ml) and isobutylamine (2.5ml) added. The mixture was left stirring at RT for 16 hours, then the solution concentrated under vacuum and ether added (50ml). The precipitate which formed was filtered off and washed with ether (2x20ml). The filtrate and ether washes were combined and the solvent removed under vacuum. The off white solid (127mg, 61% crude yield) obtained was subjected to preparative TLC (silica, 1000μm), eluted with ether. The title compound was obtained as an off white solid (10mg, 7% yield). R.f. [Et_2O]: 0.60. ^1H NMR ($CDCl_3$): 0.87 (d, 3H, J=6.8Hz, $NHCH_2CH\underline{Me_2}$), 0.91 (d, 3H, J=6.8Hz, $NHCH_2CH\underline{Me_2}$), 1.76 (m, 1H, $NHCH_2C\underline{H}Me_2$), 3.10 (m, 2H, $NHC\underline{H_2}CHMe_2$), 3.68 (ov.m, 2H, (2)isoxazoline-H4), 5.09 (ov.m, 1H, $OC\underline{H_2}Ph$ and isoxazoline-H5), 6.89 (bt, 1H, $N\underline{H}CH_2CHMe_2$), 6.98 (d, 2H, J=6.6, Ar-H3 and Ar-H5), 7.40 (m, 5H, 5Phenyl-H), 7.58 (d, 2H, J=6.6, Ar-H2 and Ar-H6)ppm. MS ($M+H^+$) m/z: 353.

11.4 MICROBIOLOGY

11.4.1 Mycobacterial Testing

11.4.1.1 Zones of Inhibition

Columbia agar plates, supplemented with horse blood (5%) were inoculated with *M.fortuitum* (NCTC 10394) (100µl, 10^7CFU). Seven wells (3mm diameter) were cut into the agar, one in the centre and six around the periphery. Isoniazid (20µl of 0.5mgml^{-1} solution in DMSO), was put in the centre well as a control. The crude *N*^{1}-benzylideneheteroarylcarboxamidrazone products (20µl of 5mgml^{-1} solution in DMSO) were placed in the peripheral wells. Zones of inhibition were recorded after three days incubation at 37°C.

11.4.1.2 'Gate' Testing of compounds at 32µgml^{-1}

The medium used was Middlebrook 7H9 broth, supplemented with glycerol (0.2%) and Middlebrook ADC enrichment (10%). A DMSO solution of the test compound (0.64mgml^{-1}, 50µl)* was added to the medium (1ml), which was then inoculated with *M.fortuitum* (10µl, 10^6CFU), and incubated at 37°C for four days. Control tubes containing broth and inoculum, and broth alone were also set up. The compound was recorded as active at this concentration if a 99% reduction of mycobacterial growth was observed, as judged by appearance.

* For PEG-bound products (6.4mgml^{-1}, 50µl) dissolved in chloroform.

11.4.1.3 Minimum Inhibitory Concentrations (MICs)

The MICs were determined using the broth dilution method. The medium used was Middlebrook 7H9 broth, supplemented with glycerol (0.2%) and Middlebrook ADC enrichment (10%). Serial two-fold dilutions of the *N*^{1}-benzylideneheteroarylcarboxamidrazone stock solution (5.1mgml^{-1} solution in DMSO) with broth were carried out to give solutions of 128, 64, 32, 16, 8, 4, 2, 1µgml^{-1}. Each tube was inoculated with *M.fortuitum* (10µl, 10^6CFU), and incubated at 37°C for four days. Control tubes containing broth and inoculum, and broth alone were also set up. The MIC values were recorded as the minimum concentration which resulted in a 99% reduction of mycobacterial growth, based on appearance.

11.4.2 Bacterial Testing

11.4.2.1 Zones of Inhibition versus S.aureus

Testing was carried out in the same way as for zones versus *M.fortuitum* (10.4.1.1), with the exception that two test organisms, on separate plates, were used and the agar utilised was Mueller-Hinton. The strains used were a methicillin-sensitive strain of *S.aureus* (NCTC 6571), and an MRSA strain (96-7475). Zones of inhibition were recorded after overnight incubation at 37°C.

11.4.2.2 Broad Spectrum and MIC Testing

This was carried out by the agar diffusion method. Mueller-Hinton agar was used to prepare plates with serial DMSO twofold dilutions of the compound being tested, to give test agar plates of 128, 64, 32, 16, 8, 4, 2, 1μgml^{-1}. A multi-point innoculator was used to deliver 35 different organisms (approximately 10^5CFU per spot) onto each plate. After overnight incubation at 37°C, MICs were read for each test organism. The MICs were recorded as the lowest concentration at which the bacteria did not grow.

11.5 TOXICOLOGY

Phosphate buffered saline (PBS): 1 PBS tablet (Dulbecco A) in distilled water (100ml), adjusted to pH7.4.

HEPES-buffered salt medium (HEPES): HEPES (0.894g), NaCl (1.828g), KCl (0.112g), $MgSO_4$ (0.074g), NaH_2PO_4 (0.039g), $CaCl_2$ (0.037g), Glucose (0.45g), distilled water (250ml), adjusted to pH7.4.

11.5.1 Direct Mononuclear Leucocyte Toxicity

11.5.1.1 Preparation of leucocytes

Blood was taken from a suitable donor, and layered onto Lymphoprep® (Nycomed Pharma, 7ml per 10ml blood per tube). This was centrifuged for 20 minutes at 2000rpm. The leucocytes were collected, washed with 10ml of PBS and the suspension centrifuged for 4 minutes at 1100rpm. The PBS was removed and the cells counted, then resuspended in HEPES to give a final concentration of $1x10^6$ cells per ml.

11.5.1.2 Compound Testing

Each experiment was carried out in triplicate, by adding the test compound (10μl of a 100mM solution in DMSO) to the stock leucocyte solution (1ml) resulting in a 1mM solution. Control tubes of cells only and cells plus DMSO were also included. The tubes were incubated in a water bath (37°C), with agitation for 1hr. The tubes were then centrifuged for 4 minutes at 1100rpm, and the supernatent discarded. The pellet of leucocytes was then resuspended in bovine serum albumin (BSA) in HEPES, (1ml of a 5mgml^{-1} per tube). Control incubations were also set up with isoniazid and DMSO with cells. The tubes were incubated for 18hrs at 37°C, without agitation.

11.5.1.3 Assessment of Toxicity

Following overnight incubation, the number of cell deaths was determined using tryptan blue exclusion (tryptan blue being a dye, which stains dead cells, whilst living cells extrude it)[148] and the percentage cell death calculated.

REFERENCES

1. Petsko, G. For medicinal purposes. *Nature* 1996, **384** (Suppl), 7-9.
2. Balkenhohl, F., Bussche-Hunnefeld von dem, C., Lansky, A., Zechel, C. Combinatorial synthesis of small organic molecules. *Angew. Chem. Int. Ed. Engl.* 1996, **35**, 2288-2337.
3. Billington, D. Drug discovery in the new millenium. *Education in Chemistry* 2001, *in press.*
4. Bormon, S. Combinatorial Chemistry. *C&EN.* 1997, 24/02, 43-62.
5. Bormon, S. Combinatorial Chemistry. *C&EN.* 1998, 6/04, 47-67.
6. Hogan Jr, J.C. Directed combinatorial chemistry. *Nature* 1996, **384** (Suppl), 17-19.
7. Terrett, N.K., Gardner, M., Gordon D.W., Kobylecki, R.J., Steele, J. Combinatorial synthesis - The design of compound libraries and their application to drug discovery. *Tetrahedron* 1995, **51** (30), 8135-8173.
8. Gallop, M.A., Barrett, R.W., Dower, W.J., Fodor, S.P.A., Gordon, E.M. Applications of combinatorial technologies to drug discovery 1. Background and peptide combinatorial libraries. *J. Med. Chem.* 1994, **37** (9), 1233-1251.
9. Thompson, L.A., Ellman, J.A. Synthesis and applications of small molecule libraries. *Chem. Rev.* 1996, **96**, 555-600.
10. Storer, R. Solution-phase synthesis in combinatorial chemistry: Applications in drug discovery. *DDT.* 1996, **1** (6), 248-254.
11. Nielson, J. Combinatiorial chemistry and automation. *DDT.* 1996, **1** (11), 458-460.
12. Cheng, S., Comer, D.D., Williams, J.P., Myers, P.L., Boger, D.L. Novel solution-phase strategy for the synthesis of chemical libraries containing small organic molecules. *J. Am. Chem. Soc.* 1996, **118**, 2567-2573.
13. Sim, M.M., Ganesan, A. Solution-phase synthesis of a combinatorial thiohydantoin library. *J. Org. Chem.* 1997, **62**, 3230-3235.
14. Gravert, D.J., Janda, K. Organic synthesis on soluble polymer supports: Liquid phase methodologies. *Chem. Rev.* 1997, **97**, 489-509.
15. Setti, E.L., Micetich, R. Modern drug design and lead discovery: An overview. *Cur. Med. Chem.* 1996, **3**, 317-324.
16. Gordon, E.M., Barrett, R.W., Dower, W.J., Fodor, S.P.A., Gallop, M.A. Applications of combinatorial chemistry technologies to drug discovery 2. Combinatorial organic synthesis, library screening strategies and future directions. *J. Med. Chem* 1994, **37** (10), 1385-1401.
17. McKeown, S., Watson, S.P., Carr, R.A.E., Marshall, P. A photolabile carbamate based dual linker analytical construct for facile monitoring of solid phase chemistry: 'TLC' for solid phase?. *Tet. Lett.* 1999, **40**, 2407-2410.

18. Murray, P.J., Kay, C., Scicinski, J.J., McKeown, S., Watson, S.P., Carr, R.A.E. Rapid reaction scanning of solid phase chemistry using resins incorporating analytical constructs. *Tet. Lett.* 1999, **40**, 5609-5612.

19. Vetter, D. Miniaturization for drug discovery applications. *DDT.* 1998, **3** (9), 404-408.

20. Moellering Jr., R.C. Past, present, and future of antimicrobial agents. *Am. J. Med.* 1995, **99** (Suppl. 6A), 11-18.

21. Chopra, I., Hodgson, J., Metcalf, B., Poste, G. The search for antimicrobial agents effective against bacteria resistant to multiple antibiotics. *Antimicrob. Agents Chemother.* 1997, **41** (3), 497-503.

22. Jawetz, E., Melnick, J.L., Adelberg, E.A., Brooks, G.F., Butel, J.S., Orhston, L.N. *Medical Microbiology*: 19th Ed., Prentice Hall International, London, 1991.

23. Chambers, H.F. Methicillin resistance in staphylococci: Molecular and biochemical basis and clinical implications. *Clin. Microbiol. Rev.* 1997, **10** (4), 781-791.

24. Degener, J. *J. Clin. Microb.* 1994, **32**, 2260-2265.

25. Noble, D.C., Virani, Z., Cree, R.G. *FEMS Microbiol. Lett.* 1992, **72**, 195-198.

26. Hiramatsu, K., Hanaki, H., Ino, T., Yabuta, K., Oguri, T., Tenover, F.C. Methicillin-resistant *Staphylococcus aureus* clinical strain with reduced vancomycin susceptibility. *J. Antimicrob. Chemother.* 1997, **40**, 135-146.

27. Johnson, A.P., James, D. Continuing increase in invasive methicillin-resistant infection. *Lancet* 1997, **350**, 6/12, 1710.

28. Bartley, J., First Case of VRSA identified in Michigan. *Infect. Control Hosp. Epidemiol.* 2002, Aug.23, (8), 480.

29. Anon. Vancomycin-resistant Staphylococcus aureus- Pennsylvania 2002. *Morb. Mortal. Wkly. Rep.* 2002, **51** (40), 902.

30. Henry, C. Antibiotic resistance. *C&EN.* 2000, 6/03, 41-58.

31. Crosley & Archer. *The Staphylococci in Human Disease*, Churchill Livingstone Inc., 1997.

32. Abraham, E.P., Chain, E. *Nature* 1940, **146**, 837.

33. Nogrady, T. *Medicinal Chemistry A Biochemical Approach*, 2nd Ed., Oxford University Press, New York, 1988.

34. Dax, S.L. *Antibacterial Chemotherapeutic Agents*, 1st Ed., Blackie Academic & Professional, London, 1997.

35. Neu, H. The crisis in antibiotic resistance. *Science* 1992, **257**, 1064-1073.

36. Nicas, T.I., Zeckel, M.L., Braun, D.K. Beyond vancomycin: New therapies to meet the challenge of glycopeptide resistance. *Trends Microbiol.* 1997, **5** (6), 240-249.

37. Arthur, M., Reynolds, P., Courvalin, P. Glycopeptide resistance in enterococci. *Trends Microbiol.* 1996, **4** (10), 401-407.

38. Luh, K.T., Hsueh, P.R., Teng, L.J., Pan, H.J., Chen, Y.C., Lu, J.J., Wu, J.J., Ho, S.W. Quinupristin-Dalfopristin resistance among gram-positive bacteria in Taiwan. *Antimicrob. Agents Chemother.* 2000, **44** (12), 3374-3380.

39. Soltani, M., Beighton, D., Philpott-Howard, J., Woodford, N. Mechanisms of resistance to Quinupristin-Dalfopristin among isolates of *Enterococcus faecium* from animals, raw meat and hospital patients in western Europe. *Antimicrob. Agents Chemother.* 2000, **44** (2), 43-436.

40. Eustice, D.C., Feldman, P.A., Zajac, I., Slee, A.M. Mechanism of action of DuP 721: Inhibition of an early event during initiation of protein synthesis. *Antimicrob. Agents Chemother.* 1988, **32** (8), 1218-1222.

41. Brickner, S. Multidrug-resistant bacterial infections: Driving the search for new antibiotics. *Chem. Industry* 1997, 17/02, 131-135.

42. Entenza, J.M., Marchetti, O., Glauser, M.P., Moreillon, P. Y-688, A new quinolone active against quinolone-resistant *Staphylococcus aureus*: lack of *in vivo* efficacy in experimental endocarditis. *Antimicrob. Agents Chemother.* 1998, **42** (8), 1889-1894.

43. Fukuda, H., Hori, S., Hiramatsu, K. Antibacterial activity of gatifloxacin (AM-1155, CG5501, BMS-206584), a newly developed fluoroquinolone, against sequentially acquired quinolone-resistant mutants and the *norA* ytransformant of *Staphylococcus aureus*. *Antimicrob. Agents Chemother.* 1998, **42** (8), 1917-1922.

44. Dougherty, T.J., Beaulieu, D., Barrett, J.F. New quinolones and the impact on resistance. *DDT.* 2001, **6** (10), 529-536.

45. Ishiguro, M., Tanaka, R., Namikawa, K., Nasu, T., Inoue, H., Nakatsuka, T., Oyama, Y., Imajo, S. 5,6-*cis*-Penems: Broad spectrum anti-methicillin-resistant *Staphylococcus aureus* beta-lactam antibiotics. *J. Med. Chem.* 1997, **40**, 2126-2132.

46. Barbachyn, M.R., Hutchinson, D.K., Brickner, S.J., Cynamon, M.H., Kilburn, J.O., Klemens, S.P., Glickman, S.E., Grega, K.C., Hendges, S.K., Toops, D.S., Ford, C.W., Zurenko, G.E. Identification of a novel oxazolidinone (U-100480) with potent antimycobacterial activity. *J. Med. Chem.* 1995, **39** (3), 680-685.

47. Gleave, D.M., Brickner, S.J., Manninen, P.R., Allwine, D.A., Lovasz, K.D., Rohrer, D.C., Tucker, J.A., Zurenko, G.E., Ford, C.W. Synthesis and antibacterial activity of [6,5,5] and [6,6,5] tricyclic fused oxazolidinones. *Bioorg. Med. Chem. Lett.* 1998, **8**, 1231-1236.

48. Brickner, S.J., Hutchinson, D.K., Barbachyn M.R., Manninen, P.R., Ulanowicz, D.A., Garmon, S.A., Grega, K.C., Hendges, S.K., Toops, D.S., Ford, C.W., Zurenko, G.E. Synthesis and antibacterial activity of U-100592 and U-100766, two oxazolidinone antibacterial agents for the potential treatment of multidrug-resistant gram-positive bacterial infections. *J. Med. Chem.* 1996, **39**, 673-679.

49. Ford, C. First of a kind. *Chem. Britain* 2001, March, 22-24.

50. Haddad, J., Vakulenko, S., Mobashery, S. An antibiotic cloaked by its own resistance enzyme. *J. Am. Chem. Soc.* 1999, **121**, 11922-11923.

51. Lee, W., Li, Z.H., Vakulenko, S., Mobashery, S. A light-inactivated antibiotic. *J. Med. Chem.* 2000, **43**, 128-132.

52. Bloom, B.R., Murray, C.J.L. Tuberculosis: Commentary on a reemergent killer. *Science* 1992, **257**, 1055-1064.

53. Evans, J. TB: Know your enemy. *Chem. Britain* 1998, Nov., 38-42.

54. Duncan, K. Towards the next generation of drugs and vaccines for tuberculosis. *Chem. Industry* 1997, 3/11, 861-865.

55. The Times, Schools set for mass screening after TB outbreak. 2001, Thursday 5th April. 4.

56. Ellner, J.J. Review: The immune response in human tuberculosis, implications for tuberculosis control. *J. Infect. Dis.* 1997, **176**, 1351-1359.

57. BBC online. http://news.bbc.co.uk/hi/english/health. 27/01, 2001

58. Rouhi, A.M. Tuberculosis: A tough adversary. *C&EN.* 1999, 17/05, 52-69.

59. Krause, R.M. The origin of plagues: Old and new. *Science* 1992, **257**, 1073-1077.

60. The Times, Times 2. 2001,*Thursday 5th April.* 2.

61. Chatterjee, D. The mycobacterial cell wall: Structure, biosynthesis and sites of drug action. *Curr. Opin. Chem. Biol.* 1997, **1**, 579-588.

62. Baker, W.R., Mitscher, L.A., Arain, T.M., Sharwar, R., Kendall-Stover, C. Recent advances in the chemistry and biology of antimycobacterial agents. *Ann. Rep. Med. Chem.* 1996, **31**, 161-170.

63. Stryer, L. *Biochemistry*; 3rd Ed., W.H. Freeman and Company, New York, 1988.

64. Kling, J. Russian jailhouse genomics. Enlisting a genome to fight MDR tuberculosis. *Modern Drug Discov.* 1999, Jan/Feb, 32-45.

65. Petrini, B., Hoffner S. Drug-resistant and multidrug-resistant tubercle bacilli. *Int. J. Antimicrob. Agents* 1999, **13**, 93-97.

66. Rattan, A., Kalia, A., Ahmad, N. Multidrug-resistant *Mycobacterium tuberculosis*: Molecular perspectives. *Emerg. Infect. Dis.* 1998, **4** (2), 195-209.

67. Barry III, C.E. New horizons in the treatment of tuberculosis. *Biochem. Pharmacol.* 1997, **54**, 1165-1172.

68. Johnsson, K., Schultz, P.G. Mechanistic studies of the oxidation of isoniazid by the catalase peroxidase from *Mycobacterium tuberculosis*. *J. Am. Chem. Soc.* 1994, **116**, 7425-7426.

69. Slayden, R., Barry III., C.E. The genetics and biochemistry of isoniazid resistance in *Mycobaterium tuberculosis*. *Microb. Infect.* 2000, **2**, 659-669.

70. Magliozzo, R.S., Marcinkeviciene, J.A. Evidence for isoniazid oxidation by oxyferrous mycobacterial catalase-peroxidase. *J. Am. Chem. Soc.* 1996, **118**, 11303-11304.

71. Wang, J.Y., Burger, R.M., Drlica, K. Role of superoxide in catalase-peroxidase mediated isoniazid action against mycobacteria. *Antimicrob. Agents Chemother.* 1998, **42** (3), 709-711.

72. Warek, U., Falkinham III, J.O. Action of clofazimine on the *Mycobacterium avium* complex. *Res. Microbiol.* 1995, **147**, 43-48.

73. Reddy, V.M., Nadadhur, G., Daneluzzi, D., O'Sullivan, J.F., Gangadharam, P.R.J. Antituberculosis activities of clofazimine and its new analogs B4154 and B4157. *Antimicrob. Agents Chemother.* 1996, **40** (3), 633-636.

74. Mdluli, K., Sherman, D.R., Hickey, M.J., Kreiswirth, B.N., Morris, S., Stover, C.K., Barry III, C.E. Biochemical and genetic data suggest that InhA is not the primary target for activated isoniazid in *Mycobacterium tuberculosis*. *J. Infect. Dis.* 1996, **174**, 1085-1090.

75. Bardou, F., Quemard, A., Dupont, M.A., Horn, C., Marchal, G., Daffe, M. Effects of isoniazid on ultrastructure of *Mycobacterium aurum* and *Mycobacterium tuberculosis* and on production of secreted proteins. *Antimicrob. Agents Chemother.* 1996, **40** (11), 2459-2467.

76. Mdluli, K., Slayden, R.A., Zhu, Y.Q., Ramaswamy, S., Pan, X., Mead, D., Crane, D.D., Musser, J.M., Barry III, C.E. Inhibition of a *Mycobacterium tuberculosis* beta-ketoacyl ACP synthase by isoniazid. *Science* 1998, **280**, 1607-1610.

77. Manca, C., Paul, S., Barry III, C.E., Freedman, V.H., Kaplan, G. Mycobacterium tuberculosis catalase and peroxidase activities and resistance to oxidative killing in human monocytes *in-vitro*. *Infect. Immun.* 1999, **67** (1), 74-79.

78. Baulard, A.R., Betts, J.C., Engohang-Ndong, J., Quan, S., McAdams, R.A., Brennan, P.J., Locht, C., Besra, G.S. Activation of the pro-drug ethionamide Is regulated in mycobacteria. *J. Biol. Chem.* 2000, **275** (36), 28326-28331.

79. Toman, K. Tuberculosis, Case-finding and Chemotherapy, Questions and Answers. <http://www.who.int/>. 2001.

80. Watt, B. *In-vitro* sensitivities and treatment of less common mycobacteria. *J. Antimicrob. Chemother.* 1997, **39**, 567-574.

81. Saito, H., Tomioka, H., Sato, K., Emori, M., Yamane, T., Yamashita, K., Hosoe, K., Hidaka, T. *In-vitro* antimycobacterial activities of newly synthesised benzoxazinorifamycins. *Antimicrob. Agents Chemother.* 1991, **35** (1), 542-547.

82. De Logu, A., Onnis, V., Saddi, B., Congui, C., Schivo, M.L., Cocco, M.T. Activity of a new class of isonicotinylhydrazones used alone and in combination with isoniazid, rifampicin, ethambutol, para-aminosalicylic acid and clofazimine against *Mycobacterium tuberculosis*. *J. Antimicrob. Chemother.* 2002, **49**, 275-282.

83. Renau, T.E., Sanchez, J.P., Shapiro, M.A., Dever, J.A., Grachek, S.J., Domagala, J.M. Effect of lipophilicity at N-1 on activity of fluoroquinolones against mycobacteria. *J. Med. Chem.* 1995, **38**, 2974-2977.

84. Klemens, S.P., Sharpe, C.A., Rogge, M.C., Cynamon, M.H. Activity of levofloxacin in a murine model of tuberculosis. *Antimicrob. Agents Chemother.* 1994, **38** (7), 1476-1479.

85. Savini, L., Chiasserini, L., Gaeta, A., Pellerano, C. Synthesis and anti-tubercular evaluation of 4-quinolylhydrazones. *Bioorg. Med. Chem.* 2002, **10**, 2193-2198.

86. Stover, C.K., Warrener, P., VanDevanter, D.R., Sherman, D.R., Arain, T.M., Langhorne, M.H., Anderson, S.W., Towell, J.A., Yuan, Y., McMurray, D.N., Kreiswirth, B.N., Barry III, C.E., Baker, W.R. A small molecule nitroimidazopyran drug candidate for the treatment of tuberculosis. *Nature* 2000, **405**, 22/06, 962-966.

87. Rouhi, A.M. Potential new weapon in tuberculosis war. *C&EN*. 2000, 26/06.

88. Amaral, L., Kristiansen, J.E., Abebe, L.S., Millet, W. Inhibition of the respiration of multidrug resistant clinical isolates of *Mycobacterium tuberculosis* by thioridazine: Potential use for initial therapy of freshly diagnosed tuberculosis. *J. Antimicrob. Chem.* 1996, **38** (6), 1049-1053.

89. Amaral, L., Kristiansen, J.E. Phenothiazines: An alternative to conventional therapy for the initial management of suspected multidrug resistant tuberculosis. A call for studies. *Int. J. Antimicrob. Agents* 2000, **14**, 173-176.

90. Betttencourt, M.V., Bosne-David, S., Amaral, L. Comparative *in vitro* activity of phenothiazines against multidrug resistant *Mycobacterium tuberculosis*. *Int. J. Atimicrob. Agents* 2000, **16**, 69-71.

91. De Smet, K.A.L. *Mycobacterium tuberculosis*: Beyond genome sequencing. *Trends Microbiol.* 1997, **5** (11), 429-431.

92. Cole, S.T., Parkhill, J., Garnier, T., Churcher, C., Harris, D., Gordon, S.V., Eiglmeier, K., Gas, S., Barry III, C.E., *et al.* Deciphering the biology of *Mycobacterium tuberculosis* from the complete genome sequence. *Nature* 1998, **393**, 537.

93. Mamalo, M.G., Vio L., Banfi, E., Predominato, M., Fabris, C., Asaro, F. Synthesis and antimycobacterial activity of some 2-pyridinecarboxyamidrazone derivatives. *Farmaco* 1992, **47** (7), 1055-1066.

94. Mamalo, M.G., Vio, L., Banfi, E., Predominato, M., Fabris, C., Asaro, F. Synthesis and antimycobacterial activity of some 4-pyridinecarboxyamidrazone derivatives. *Farmaco* 1993, **48** (4), 529-538.

95. Mamalo, M.G., Vio, L., Banfi, E. Synthesis and antimycobacterial activity of some indole derivatives of pyridine-2-carboxamidrazone and quinoline-2-carboxamidrazone. *Farmaco* 1996, **51** (1), 65-70.

96. Banfi, E., Mamalo, M.G., Vio, L., Predominato, M. *In-vitro* antimycobacterial activity of new synthetic amidrazone derivatives. *J. Chemother.* 1993, **5** (3), 164-167.

97. Billington, D.C., Coleman, M.D., Ibiabuo, J., Lambert, P.A., Rathbone, D.L., Tims, K.J. Synthesis and antimycobacterial activity of some heteroarylcarboxamidrazone derivatives. *Drug Design Discov.* 1998, **15**, 269-275.

98. Vio, L., Mamalo, M.G., Ronsisvalle, G., Oliveri, S., Grego, A.M. Synthesis and antifungal activities of some amidrazone derivatives. *Farmaco* 1989, **44** (9), 819-829.

99. Foks, H., Buraczewska, M., Manowska, W., Sawlewicz, J. Investigations on pyrazine derivatives. *Dissert. Pharm. Pharmacol.* 1971, **23** (1), 49-58.

100. Neilson, D.G., Roger, R., Heatlie, J.W.M., Newlands, L.R. The chemistry of amidrazones. *Chem. Rev.* 1970, **70**, 151-170.

101. Billington, D.C., Tims, K.J., Rathbone, D.L. Automated synthesis and antimycobacterial activity of a series of 2-heteroarylcarboxamidrazones and related compounds. *J. Pharm. Pharmacol.* 1998, **50** (Suppl), 262.

102. March, J. *Advanced Organic Chemistry*; 2nd Ed.,McGraw-Hill Kogakusha, Tokyo, 1977.

103. Casiraghi, G., Casnati, G., Puglia, G., Sartori, G., Terenghi, G. Selective reactions between phenols and formaldehyde. A novel route to salicylaldehydes. *J. Chem. Soc. Perkin Trans. 1* 1980, 1862-1865.

104. Pavia, D.L., Lampman, G.M., Kriz, G.S. *Introduction to Spectroscopy,* 2nd Ed., Harcourt Brace College, Florida, 1996.

105. House, H. *Modern Synthetic Reactions,* 2nd Ed., The Benjamin/Cummings Publishing Company, California, 1972.

106. Koneman, E.W., Allen, S.D., Janda, W.M., Schreckenberger, P.C., Winn Jr, W.C. *Colour Atlas and Textbook of Diagnostic Microbiology*: J.B. Lippencott Company, 1992.

107. Attkins, N. Screening of potential antimicrobial compounds. *4th Yr. Biology Project for Degree of B.Sc. Applied and Human Biology.* Aston University, Birmingham, 2000.

108. Tims, K.J., Rathbone, D.L., Lambert, P.A., Attkins, N., Cann, S.W., Billington, D.C. *Mycobacterium fortuitum* as a screening model for *Mycobacterium tuberculosis. J. Pharm. Pharmacol.* 2000, **52** (Suppl), 135.

109. Coleman, M.D., Rathbone, D.L., Chima, R., Lambert, P.A., Billington, D.C. Preliminary *in-vitro* toxicological evaluation of a series of 2-pyridylcarboxamidrazone candidate anti-tuberculosis compounds: III. *Environ. Tox. Pharmacol.* 2001, **9**, 99-102.

110. Griffiths, P. *Hospital Infection Research Laboratory*, City Hospital, NHS Trust, Dudley Road, Birmingham, 1998.

111. Schwalbe, C.H., Lowe, P.R., Gordon, B., Rathbone, D.L., Billington, D.C. Relationship of structural and electronic properties to antimycobacterial activity of a series of 2-heteroarylcarboxamidrazones. *J. Pharm. Pharmacol.* 1998, **50** (Suppl), 245.

112. Billington, D.C., Lowe, P.R., Rathbone, D.L., Schwalbe, C.H. A new amidrazone derivative with antimycobacterial activity. *Acta. Cryst.* 2000, **C56**, e211-e212.

113. Schwalbe, C.H., Gallgher, C., Lowe, P.R., Rathbone, D.L., Billington, D.C., Tims, K.J. Comparison of structural features and antimycobacterial activity in isomeric pyridyl-carboxamidrazones. *J. Pharm. Pharmacol.* 1999, **51** (Suppl), 262.

114. Schwalbe, C.H., Rathbone, D.L., Tims, K.J., Billington, D.C., Sandbhor, U., Padhye, S. Effects of functional group deletion on structural features and antimycobacterial activity in pyridylcarboxamidrazones. *J. Pharm. Pharmacol.* 2000, **52** (Suppl), 105.

115. Dewar, M.J.S., *et al. J. Am. Chem. Soc.* 1985, **107**, 3902-3909.

116. Schmidt, M., *et al. J. Comput. Chem.* 1993, **14**, 1347-1363.

117. Rathbone, D.L., Tims, K.J., Attkins, N., Cann, S.W., Billington, D.C. QSAR studies on a large set of antimycobacterial N^1-benzylideneheteroarylcarboxamidrazones. *J. Pharm. Pharmacol.* 2000, **52** (Suppl), 97.

118. *Oxford Molecular Ltd. TSAR™ 3.3 for Windows -Reference Guide: Oxford Molecular Ltd., 2000.*

119. Coleman, M.D., Endersby, C., Hovey, M.C., Tims, K.J., Rathbone, D.L., Billington, D.C. *In-vitro* toxicity evaluation of two novel anti-tubercular 2-pyridylheteroarylcarboxamidrazone derivatives. *J. Pharm. Pharmacol.* 1999, **51** (Suppl), 243.

120. Coleman, M.D., Rathbone, D.L., Endersby, C.R., Hovey, M.C., Tims, K.J., Lambert P.A., Billington, D.C. Preliminary *in-vitro* toxicological evaluation of a series of 2-pyridylcarboxamidrazone candidate anti-tuberculosis compounds: II. *Environ. Tox. Pharmacol.* 2000, **8**, 167-172.

121. Coleman, M.D., Rathbone, D.L., Abberly, L., Lambert, P.A., Billington, D.C. Preliminary *in-vitro* toxicological evaluation of a series of 2-pyridylcarboxamidrazone candidate anti-tuberculosis compounds. *Environ. Tox. Pharmacol.* 1999, **7**, 59-65.

122. Gravert, D.J., Janda, K. Soluble polyethylene glycol supports for liquid phase combinatorial synthesis. *Drugs of the Future* 1997, **22** (10), 1147-1150.

123. Gravert, D.J., Janda, K. Bifunctional initiators for free radical polymerisation of non-cross linked block copolymers. *Tet. Lett.* 1998, **39**, 1513-1516.

124. Kodera, Y., Tanaka, H., Matsushima, A., Inada, Y. Chemical modification of L-asparaginase with a comb-shaped copolymer of polyethylene glycol derivative and maleic anhydride. *Biochem. Biophys. Res. Com.* 1992, **184** (1), 144-148.

125. Hoffman, A.S. *Biorelated Polymers and Gels.* Academic Press, 1998.

126. Greenwald, R.B., Pendri, A., Cononver, C.D., Zhao, H., Choe, Y.H., Martinez, A., Shum, K., Guan, S. Drug delivery systems employing 1,4- or 1,6-elimination: Poly(ethylene glycol) produgs of amine-containing compounds. *J. Med. Chem.* 1999, **42**, 3657-3667.

127. Geckeler, K.E. Soluble polymer supports for liquid-phase synthesis. *Adv. Polym. Sci.* 1995, **121**, 31-79.

128. Blettner, C.G., Konig, W.A., Stenzel, W., Schotten, T. Poly(ethylene glycol) supported liquid phase synthesis of biaryls. *Synlett.* 1998, *March*, 295-297.

129. Yeh, C.M., Sun, C.M. Rapid parallel synthesis of benzimidazoles. *Synlett.* 1999, **6**, 810-812.

130. Molteni, V., Annunziata, R., Cinguini, M., Cozzi, F., Benaglia, M. Soluble polymer-supported synthesis of imines and beta-lactams. *Tet. Lett.* 1998, **39**, 1257-1260.

131. Dust, J.M., Fang, J.M., Harris, J.M. Proton NMR characterisation of poly(ethylene glycols) and derivatives. *Macromolecules* 1990, **23**, 3742-3746.

132. Han, H, Wolfe, M.M., Brenner, S., Janda, K.D. Liquid-phase combinatorial synthesis. *Proc. Natl. Acad. Sci. USA.* 1995, **92**, 6419-6423.

133. Pan, P.C., Sun, C.M. Soluble polymer-supported synthesis of arylpiperazines. *Tet. Lett.* 1998, **39**, 9505-9508.

134. Shey, J.Y., Sun, C.M. Liquid phase combinatorial synthesis of benzylpiperazines. *Bioorg. Med. Chem. Lett.* 1999, **9**, 519-522.

135. Boyd, E.C., Paton, M. Stereoselective cycloaddition of nitrile oxides to 4-vinyl-oxazolines and -oxazolidines. *Tet. Lett.* 1993, **34** (19*)*, 3169-3172.

136. Cheng, J.F., Mjalli, A.M.M. Solid-phase synthesis of isoxazolines. *Tet. Lett.* 1998, **39**, 939-942.

137. Cereda, E., Ezhaya, A., Quai, M., Barbaglia, W. Solid-phase synthesis of 3-hydroxymethyl isoxazoles via resin bound nitrile oxides. *Tet. Lett.* 2001, **42**, 4951-4953.

138. Norman, R.O.C. *Principles of Organic Synthesis,* 2nd Edition; Chapman and Hall: London, 1968.

139. De Sarlo, F. Behaviour of nitrile oxides towards nucleophiles. Part 1. Pyridine-catalysed dimerisation of aromatic nitrile oxides. *J. Chem. Soc. Perkin Trans. 1* 1974, 1951-1953.

140. Moore, M., Norris, P. Dipolar cycloaddition reactions on a soluble polymer-supported dipolarophile: Synthesis of sugar-derived triazoles. *Tet. Lett.* 1998, **39**, 7027-7030.

141. Beebee, X., Schore, N.E., Kurth, M.J. Polymer-supported synthesis of cyclic ethers: Electrophilic cyclisation. *J. Org. Chem.* 1995, **60**, 4196-4203.

142. Rathbone, D.L. Solution-phase polymer-supported synthesis of potential antimycobacterial fatty acid analogues. *J. Pharm. Pharmacol.* 1999, **51** (Suppl.), 219.

143. Barry III, C.E., *et al.* Antimycobacterial compositions and their use for the treatment of tuberculosis and related diseases. *US Patent* 1997, *5,610,198.*

144. Sacchetini, J.,*et al.* Antimycobacterial compounds and method of using same. *US Patent* 1997, 5,648,392.

145. Sacchetini, J., *et al.* Antimycobacterial compounds and method of using same. *US Patent* 1998, 5,837,732.

146. Silverstein, R.M., Bassler, G.C., Morril, T.C. *Spectrometric Identification of Organic Compounds*, 5th Ed., John Wiley & Sons Inc., New York, 1991.

147. Case, F.H. The preparation of hydrazidines and as-triazines related to substituted 2-cyanopyridines. *J. Org. Chem.* 1965, **30**, 931-933.

148. Spielberg, S.P. *Brit. J. Clin. Pharmacol.* 1984, **30**, 829-838.

APPENDICES

A.1 MOLECULAR TEMPLATE (2PYab)FOR MOLECULAR MODELLING

File generated by Oxford Molecular Ltd

```
 32 33  0  0  0  0  0  0  0  0  1 V2000
  -6.1754    1.6948   -0.5739 C   0  0  0  0  0  0
  -5.9968    0.3303   -0.4569 C   0  0  0  0  0  0
  -4.7902   -0.2146   -0.3285 N   0  0  0  0  0  0
  -3.7188    0.5672   -0.3105 C   0  0  0  0  0  0
  -3.8060    1.9430   -0.4202 C   0  0  0  0  0  0
  -5.0565    2.5125   -0.5544 C   0  0  0  0  0  0
  -2.3987   -0.1051   -0.1673 C   0  0  0  0  0  0
  -2.4407   -1.4418   -0.0847 N   0  0  0  0  0  0
  -1.3570    0.6382   -0.1384 N   0  0  0  0  0  0
  -0.1445   -0.1175   -0.0068 N   0  0  0  0  0  0
   0.8930    0.5962    0.0536 C   0  0  0  0  0  0
   2.2399    0.0210    0.1822 C   0  0  0  0  0  0
   2.4376   -1.3556    0.2054 C   0  0  0  0  0  0
   3.7068   -1.8763    0.3246 C   0  0  0  0  0  0
   4.8166   -1.0419    0.4259 C   0  0  0  0  0  0
   4.6155    0.3282    0.4043 C   0  0  0  0  0  0
   3.3406    0.8551    0.2826 C   0  0  0  0  0  0
   6.2080   -1.6330    0.5372 C   0  0  0  0  0  0
  -7.1587    2.1038   -0.6760 H   0  0  0  0  0  0
  -6.8304   -0.3403   -0.4665 H   0  0  0  0  0  0
  -2.9094    2.5202   -0.3991 H   0  0  0  0  0  0
  -5.1607    3.5754   -0.6430 H   0  0  0  0  0  0
  -1.5863   -1.9425    0.0088 H   0  0  0  0  0  0
  -3.3249   -1.8988   -0.1175 H   0  0  0  0  0  0
   0.8227    1.6708    0.0122 H   0  0  0  0  0  0
   1.5864   -1.9997    0.1273 H   0  0  0  0  0  0
   3.8445   -2.9404    0.3420 H   0  0  0  0  0  0
   5.4565    0.9894    0.4847 H   0  0  0  0  0  0
   3.2049    1.9198    0.2665 H   0  0  0  0  0  0
   6.5135   -2.0644   -0.4114 H   0  0  0  0  0  0
   6.2349   -2.4170    1.2858 H   0  0  0  0  0  0
   6.9335   -0.8773    0.8122 H   0  0  0  0  0  0
```

Three carriage returns here.

Then the next column which should read directly underneath this one.

```
  1  2  1  0  0  0  0
  1  6  2  0  0  0  0
  1 19  1  0  0  0  0
  2  3  2  0  0  0  0
  2 20  1  0  0  0  0
  3  4  1  0  0  0  0
  4  5  2  0  0  0  0
  4  7  1  0  0  0  0
  5  6  1  0  0  0  0
  5 21  1  0  0  0  0
  6 22  1  0  0  0  0
  7  8  1  0  0  0  0
  7  9  2  0  0  0  0
  8 23  1  0  0  0  0
  8 24  1  0  0  0  0
  9 10  1  0  0  0  0
 10 11  2  0  0  0  0
 11 12  1  0  0  0  0
 11 25  1  0  0  0  0
 12 13  1  0  0  0  0
 12 17  2  0  0  0  0
 13 14  2  0  0  0  0
 13 26  1  0  0  0  0
 14 15  1  0  0  0  0
 14 27  1  0  0  0  0
 15 16  2  0  0  0  0
 15 18  1  0  0  0  0
 16 17  1  0  0  0  0
 16 28  1  0  0  0  0
 17 29  1  0  0  0  0
 18 30  1  0  0  0  0
 18 31  1  0  0  0  0
 18 32  1  0  0  0  0
M  END
$$$$
```

The tables A2-A5 all use the same abbreviations in the table headings. 1/MIC (Exptl) is the inverse of the MIC found by experiment. N-length is the length of the molecule, measuring from the heteroaryl-nitrogen atom. Mol. Mass = Molecular mass. Mol. S. A. = Molecular Surface Area. Mol. Vol. = Molecular Volume.
Molar Refrac = Molar Refractivity. Mean Polar. = Mean Polarisability. LUMO = Lowest Unoccupied Molecular Orbital. HOMO = Highest Occupied Molecular Orbital.

A.2 TSAR RESULTS TABLE FOR HETEROARYLCARBOXAMIDRAZONES ACTIVE AGAINST *M.FORTUITUM*

Code	1/MIC	N-Length	Aryl Width	Mol. Mass	Mol S.A.	Mol. Vol.	Log P	Total Lipole	Lipole x	Lipole y	Lipole z	Molar Refrac.	Mean Polar.	LUMO	HOMO	Total Dipole	Dipole x	Dipole y	Dipole z
2PYaa	0.0010	10.69	4.91	224.29	237.59	149.60	3.32	3.64	2.809	2.308	0.022	67.36	32.68	-0.400	-8.771	1.498	-0.742	-1.301	-0.023
2PYab	0.0625	11.80	4.90	238.32	255.97	162.46	3.32	3.98	2.457	3.130	-0.036	72.44	34.99	-0.387	-8.697	0.892	0.891	-0.041	-0.027
2PYac	0.0625	12.75	4.90	252.35	277.45	175.99	4.18	4.32	-2.196	3.592	-0.949	77.01	37.20	-0.384	-8.707	0.902	0.869	0.077	-0.231
2PYad	0.1250	12.69	4.90	266.38	293.08	188.64	4.05	4.05	0.147	4.041	-0.264	81.59	39.45	-0.385	-8.696	0.746	0.744	0.059	-0.009
2PYae	0.1250	13.17	4.89	280.41	309.18	200.94	4.48	3.97	-0.379	3.939	-0.278	86.06	41.69	-0.374	-8.691	0.479	0.472	-0.073	0.039
2PYaf	0.2500	13.03	4.89	294.44	323.54	214.23	4.88	4.08	-0.806	3.946	-0.672	90.66	43.95	-0.371	-8.682	0.525	0.505	-0.143	-0.008
2PYah	0.0010	10.85	5.87	238.32	250.54	162.34	3.79	4.09	1.579	3.769	-0.128	72.40	35.07	-0.393	-8.740	1.632	-1.090	-1.214	-0.025
2PYai	0.0160	10.87	7.25	252.35	265.84	175.16	3.72	5.85	3.621	4.594	-0.011	77.04	37.31	-0.393	-8.736	1.518	1.406	0.573	0.016
2PYaj	0.0010	10.68	5.86	238.32	261.44	162.30	3.79	3.99	0.435	3.954	-0.254	72.40	34.96	-0.389	-8.745	1.227	-0.917	-0.815	-0.001
2PYak	0.0010	12.57	7.13	274.35	279.87	181.13	3.86	7.49	7.346	1.318	0.576	83.85	41.74	-0.497	-8.604	1.463	1.461	-0.069	0.050
2PYal	0.0556	11.89	7.13	274.35	271.61	181.88	4.32	5.48	4.536	3.074	0.242	83.81	41.74	-0.548	-8.534	1.530	1.520	-0.158	-0.064
2PYam	0.0010	11.41	9.47	324.41	309.84	232.84	4.86	7.99	7.658	2.229	0.411	100.30	50.28	-0.900	-8.127	1.780	1.778	0.083	-0.012
2PYao	0.0010	13.23	4.91	250.33	267.36	169.60	3.73	5.13	4.415	2.597	0.186	77.61	37.53	-0.479	-8.623	1.482	-0.579	-1.364	0.008
2PYaq	0.0010	10.99	4.85	228.33	253.90	167.24	2.63	4.42	-3.037	3.202	-0.290	68.75	31.82	-0.297	-8.979	1.485	-0.467	-1.395	0.206
2PYas	0.0625	12.65	4.90	254.32	265.58	169.93	2.60	5.27	-1.648	4.976	-0.494	73.86	35.13	-0.364	-8.558	1.592	1.130	1.121	0.047
2PYaw	0.0010	21.91	4.90	352.53	403.21	259.76	5.86	12.17	-11.276	4.459	-1.098	106.10	50.81	-0.350	-8.529	1.511	-0.994	1.138	0.001
2PYax	0.0625	10.82	7.08	254.32	257.05	169.56	2.60	6.52	2.642	5.959	-0.224	73.86	35.22	-0.295	-8.525	0.438	0.067	0.432	0.030
2PYay	0.0625	10.81	8.29	268.35	279.34	182.77	2.95	6.89	2.736	6.322	0.202	78.61	37.44	-0.289	-8.506	0.814	-0.751	0.103	0.296
2PYaz	0.0625	10.82	9.60	282.38	295.62	195.30	3.41	7.03	2.767	6.455	-0.302	83.13	39.66	-0.291	-8.505	0.881	0.172	0.864	0.024
2PYba	0.0010	10.77	9.37	296.41	308.97	213.45	4.28	6.70	-0.534	6.159	2.596	87.70	41.61	-0.407	-8.729	2.096	1.336	-0.575	-1.509
2PYbb	0.0010	10.82	12.15	310.44	340.88	220.92	4.67	8.33	0.001	8.335	-0.046	92.30	44.11	-0.292	-8.509	1.004	-0.915	0.249	0.329
2PYbc	0.0010	10.79	11.52	324.47	346.77	239.37	5.07	7.72	-0.966	6.878	3.369	96.90	46.13	-0.406	-8.733	2.073	1.230	-0.806	1.461
2PYbf	0.0310	13.77	11.20	330.42	334.99	221.33	4.38	3.57	3.539	0.345	0.324	98.47	47.80	-0.403	-8.769	1.129	0.849	-0.741	-0.072
2PYbg	0.0625	16.91	4.90	330.42	338.37	219.81	4.38	6.86	6.374	2.511	0.287	98.47	47.95	-0.379	-8.584	1.704	1.439	-0.912	0.045
2PYbi	0.1250	17.02	7.04	374.48	383.27	259.00	4.38	9.45	3.887	7.839	3.563	109.69	52.36	-0.399	-8.593	2.193	1.372	-1.586	-0.643
2PYbj	0.0010	19.06	7.05	388.51	408.92	277.83	4.78	7.06	5.951	3.609	-1.180	114.29	53.78	-0.373	-8.545	2.364	1.084	1.855	-0.987

Code	1/MIC	N-Length	Aryl Width	Mol. Mass	Mol S.A.	Mol. Vol.	Log P	Total Lipole	Lipole x	Lipole y	Lipole z	Molar Refrac.	Mean Polar.	LUMO	HOMO	Total Dipole	Dipole x	Dipole y	Dipole z
2PYbk	0.0010	17.78	7.09	374.48	385.50	264.98	4.59	7.76	4.398	6.331	0.878	109.98	52.05	-0.455	-8.642	3.189	2.878	-0.868	-1.066
2PYbl	0.0010	19.10	7.08	416.57	430.84	303.53	5.75	6.65	2.078	6.295	0.507	123.60	58.84	-0.455	-8.634	2.870	2.291	-1.032	-1.386
2PYbm	0.0010	17.85	7.01	405.45	385.28	274.70	4.08	9.67	-6.249	7.311	-1.037	112.26	50.23	-1.276	-8.960	8.957	8.940	-0.475	0.286
2PYbn	0.2500	12.62	11.21	360.45	361.44	251.93	4.13	1.30	-0.644	0.047	-1.126	104.93	49.17	-0.471	-8.773	2.357	2.288	-0.518	0.232
2PYbo	0.1250	12.67	11.79	374.48	390.01	265.43	4.38	3.95	-3.881	0.085	0.719	109.69	51.54	-0.440	-8.648	3.182	2.807	0.949	-1.159
2PYbp	0.0010	12.92	13.73	388.51	403.99	266.18	4.78	3.26	-1.894	-2.635	0.306	114.29	54.92	-0.395	-8.421	2.537	-2.153	1.342	-0.015
2PYbq	0.0625	12.93	12.26	374.48	386.21	264.66	4.59	2.00	-1.920	0.434	-0.347	109.98	51.56	-0.384	-8.578	2.408	1.259	1.859	0.869
2PYbr	0.0010	12.94	13.61	416.57	428.59	291.69	5.75	3.21	-2.024	2.434	-0.520	123.60	59.48	-0.393	-8.434	1.650	1.566	0.417	-0.310
2PYbu	0.0010	12.79	10.71	390.48	378.35	275.16	3.87	6.04	-3.555	-0.708	-4.826	111.40	51.50	-0.400	-8.546	1.301	-0.207	-1.284	0.014
2PYbw	0.0010	10.75	5.65	240.29	232.63	156.72	2.57	5.61	4.286	3.606	0.236	69.09	32.86	-0.516	-8.751	2.831	2.680	-0.795	0.448
2PYby	0.0010	11.61	4.90	240.29	249.99	156.36	3.04	3.16	-1.260	2.883	-0.322	69.06	32.75	-0.393	-8.633	2.262	0.007	-2.259	-0.114
2PYbz	0.0010	10.73	5.70	256.29	251.54	162.74	2.75	5.75	-1.547	5.516	-0.473	70.75	32.82	-0.330	-8.569	1.144	1.128	-0.189	0.003
2PYcb	0.0010	11.20	6.62	272.29	260.87	170.50	2.47	7.52	-3.959	6.327	-0.901	72.45	32.74	-0.382	-8.561	1.381	-0.786	-0.906	-0.685
2PYcd	0.0010	11.35	6.28	272.29	260.73	169.83	2.47	5.49	-3.932	3.798	-0.538	72.45	32.85	-0.226	-8.395	1.274	0.035	1.272	0.057
2PYce	0.0010	12.52	5.60	270.32	268.61	176.11	2.78	8.30	-3.946	7.255	-0.815	75.52	35.21	-0.296	-8.519	1.185	-0.979	-0.667	0.029
2PYcf	0.0010	12.71	5.64	270.32	268.62	175.33	2.32	5.46	-1.443	5.245	-0.524	75.55	35.37	-0.468	-8.536	2.065	2.062	-0.055	0.086
2PYcg	0.0010	12.66	6.00	270.32	277.71	177.04	2.78	8.47	-5.825	5.992	-1.389	75.52	35.08	-0.478	-8.717	3.467	3.192	0.458	1.273
2PYch	0.0010	11.09	7.09	270.32	270.44	177.47	2.78	8.34	-4.178	7.110	-1.254	75.52	35.15	-0.428	-8.556	3.483	3.099	1.589	0.041
2PYci	0.0010	11.07	8.31	284.35	293.02	188.72	3.13	8.89	-4.493	7.656	-0.483	80.27	37.39	-0.421	-8.528	3.359	2.778	1.887	-0.077
2PYcl	0.0010	11.05	6.47	364.18	281.51	196.89	3.78	8.94	-2.586	8.562	0.051	84.01	35.30	-1.378	-9.384	9.041	-1.368	-8.879	-1.015
2PYcs	0.0010	11.77	9.19	284.35	284.44	193.36	2.82	5.25	-4.417	2.835	-0.026	80.29	37.43	-0.423	-8.681	3.112	2.541	-1.235	-1.304
2PYct	0.0010	12.64	7.08	284.35	295.53	189.96	2.82	9.94	-6.691	7.338	-0.430	80.29	37.49	-0.455	-8.659	3.385	2.991	1.045	-1.193
2PYcv	0.0010	12.67	8.29	298.38	313.06	203.68	3.16	10.13	-6.793	7.487	-0.646	85.04	39.73	-0.441	-8.640	3.171	2.680	1.287	-1.103
2PYcw	0.0010	13.70	7.08	298.38	312.07	203.27	3.16	10.12	-6.866	7.422	-0.317	85.04	39.74	-0.445	-8.627	3.020	2.599	1.011	-1.158
2PYcx	0.0010	13.30	4.91	282.33	289.48	185.01	3.05	9.49	-7.587	5.634	-0.913	78.89	36.80	-0.674	-8.957	3.581	3.181	1.644	-0.026
2PYcy	0.0010	12.63	7.22	312.36	307.90	209.22	2.57	11.46	-8.197	7.826	-1.676	84.96	38.99	-0.619	-8.934	5.089	4.145	-2.899	0.561
2PYcz	0.0010	14.33	4.90	298.33	300.34	194.13	2.61	11.65	-10.496	4.907	-1.206	79.91	36.67	-0.438	-8.693	3.206	3.068	-0.438	-0.822
2PYdb	0.0010	11.85	7.76	290.35	277.41	189.68	3.57	8.34	6.706	4.896	0.740	85.54	41.87	-0.626	-8.423	2.415	2.109	-1.150	0.250
2PYdc	0.0010	11.60	9.37	304.38	292.51	213.64	3.61	9.26	5.039	7.051	3.261	90.31	43.62	-0.414	-8.343	0.901	-0.047	0.618	-0.654
2PYdd	0.0625	12.58	7.13	304.38	295.86	200.66	3.61	7.18	0.384	7.170	0.086	90.31	44.09	-0.454	-8.259	1.267	1.053	-0.699	0.086
2PYde	0.0010	10.63	5.76	303.18	257.51	170.13	4.11	4.46	3.274	3.022	0.051	74.99	33.58	-0.507	-8.883	1.837	-1.740	-0.588	0.016

Code	1/MIC	N-Length	Aryl Width	Mol. Mass	Mol S.A.	Mol. Vol.	Log P	Total Lipole	Lipole x	Lipole y	Lipole z	Molar Refrac.	Mean Polar.	LUMO	HOMO	Total Dipole	Dipole x	Dipole y	Dipole z
2PYdf	0.0010	10.83	5.64	258.73	252.25	166.54	3.84	3.37	2.702	2.011	0.100	72.17	33.39	-0.471	-8.823	1.910	0.407	-1.849	0.250
2PYdg	0.0160	10.68	5.63	258.73	251.91	166.11	3.37	5.82	5.532	1.773	0.377	72.20	33.23	-0.529	-8.935	3.106	2.860	-1.209	-0.060
2PYdh	0.0010	11.38	4.91	258.73	258.55	165.81	3.84	4.09	3.505	2.105	0.080	72.17	33.33	-0.547	-8.923	3.536	-1.952	-2.948	-0.023
2PYdi	0.0010	11.37	5.63	293.17	268.69	181.98	3.89	6.55	6.367	1.484	0.409	77.00	33.91	-0.688	-9.027	4.317	4.260	-0.700	-0.018
2PYdk	0.0010	10.72	5.18	242.28	243.50	156.35	3.46	3.32	2.424	2.274	0.011	67.58	31.99	-0.451	-8.769	1.710	0.596	-1.602	-0.035
2PYdn	0.0625	10.66	5.93	269.29	256.67	170.30	2.81	6.33	-1.377	6.154	-0.557	74.72	33.83	-1.259	-9.153	6.953	5.544	-4.194	-0.114
2PYdp	0.0010	12.11	4.91	249.30	261.69	164.89	3.19	3.05	1.640	2.567	-0.066	73.56	35.12	-0.761	-9.018	5.682	-3.100	-4.761	-0.049
2PYdr	0.0010	13.71	4.91	281.35	297.01	186.22	2.17	11.51	-9.554	6.324	-1.135	80.45	38.07	-0.374	-8.495	3.052	0.014	-3.051	0.077
2PYds	0.0010	19.13	4.91	339.49	370.98	244.70	3.55	21.08	-20.245	5.465	-2.102	101.36	47.45	-0.348	-8.522	1.154	-0.503	0.643	-0.816
2PYdt	0.0010	10.30	4.30	213.27	228.07	139.23	2.09	4.31	-1.700	3.946	-0.377	62.00	29.15	-0.393	-8.467	2.530	-2.355	-0.925	0.029
2PYdu	0.0010	9.62	5.34	228.29	246.38	150.12	1.44	8.04	-6.210	5.045	-0.787	65.10	30.17	-0.475	-8.685	4.308	-3.819	-1.994	0.035
2PYdv	0.0010	10.60	4.85	225.28	235.47	147.57	2.41	4.01	0.252	3.995	-0.239	64.83	31.38	-0.439	-8.846	1.786	0.808	-1.593	-0.006
2PYdw	0.0010	10.68	4.85	225.28	235.94	147.35	2.47	3.00	-1.351	2.665	-0.292	65.18	31.34	-0.532	-8.947	3.113	-2.769	-1.421	0.040
2PYdx	0.1250	12.74	7.12	317.43	321.12	217.81	4.12	10.79	-6.904	8.298	-0.039	97.52	47.28	-0.513	-8.331	1.477	1.206	0.566	-0.638
2PYdy	0.0010	10.96	6.65	263.33	264.20	170.50	3.09	2.36	-2.192	0.861	-0.153	78.45	38.12	-0.273	-8.240	1.774	1.277	-1.230	0.061
2PYdz	0.0010	14.72	6.65	353.46	348.73	246.96	5.12	2.38	0.964	0.819	2.015	107.96	52.31	-0.263	-8.173	1.954	0.052	-1.941	0.218
2PYea	0.0010	10.28	4.30	214.25	226.52	138.27	2.27	3.21	-0.883	3.070	-0.279	59.75	28.09	-0.437	-8.734	1.739	-0.543	-1.652	0.001
2PYeb	0.0010	12.66	7.01	292.32	279.94	183.79	2.41	1.94	0.067	1.920	-0.252	81.91	38.79	-0.484	-8.702	1.812	-0.080	-1.806	-0.119
2PYec	0.0010	12.62	7.98	306.35	301.69	196.51	2.87	2.48	-0.722	2.357	-0.308	86.95	41.07	-0.456	-8.673	1.479	-0.499	-1.387	-0.120
2PYed	0.0625	10.35	4.31	230.31	228.85	149.25	2.15	3.66	2.174	2.942	-0.021	66.23	31.26	-0.495	-8.771	1.555	1.551	-0.115	0.001
2PYee	0.0010	12.83	4.91	270.38	275.25	183.01	2.95	4.50	-0.924	4.237	1.204	80.30	37.42	-0.539	-8.743	3.553	3.011	0.150	-1.880
2PYeh	0.0800	10.63	9.79	366.89	345.62	248.05	5.15	7.87	5.779	4.735	2.467	104.88	47.38	-0.612	-8.417	2.353	1.283	-1.922	0.443
3PYab	0.0010	13.14	4.90	238.32	259.28	166.82	3.39	3.80	1.928	3.252	0.381	72.78	34.78	-0.436	-8.886	1.789	-1.260	0.014	1.270
3PYae	0.0310	14.50	4.89	280.41	307.29	205.74	4.55	2.72	-0.090	2.718	-0.066	86.40	41.50	-0.423	-8.873	2.103	-1.677	1.104	0.626
3PYaf	0.0310	14.36	4.89	294.44	313.95	218.28	4.95	4.41	-1.357	4.012	-1.216	91.00	43.78	-0.422	-8.865	2.036	-1.633	-0.012	-1.216
3PYai	0.0010	12.19	6.81	252.35	266.30	179.76	3.79	5.30	4.021	3.443	0.174	77.38	37.10	-0.440	-8.933	1.555	-0.041	0.812	-1.326
3PYal	0.0010	12.86	7.13	274.35	271.91	188.10	3.92	7.78	7.420	2.289	0.487	84.19	41.31	-0.622	-8.667	1.422	-0.659	0.130	-1.253
3PYas	0.0010	14.05	4.90	254.32	268.47	175.19	2.67	5.54	-2.186	5.086	-0.203	74.20	34.92	-0.413	-8.720	2.092	-1.040	1.254	1.312
3PYaw	0.0010	23.26	4.90	352.53	393.01	263.65	5.46	5.85	-5.057	2.883	-0.544	106.48	50.68	-0.396	-8.677	2.575	-2.051	-0.850	1.305
3PYax	0.0010	12.15	6.10	254.32	259.08	174.16	2.67	5.65	3.158	4.640	-0.652	74.20	35.06	-0.353	-8.703	2.303	0.687	1.911	1.086
3PYaz	0.0010	12.11	7.99	282.38	291.13	204.19	3.48	5.59	3.146	4.227	1.855	83.47	39.12	-0.459	-8.916	2.847	1.106	0.196	2.616

Code	1/MIC	N-Length	Aryl Width	Mol. Mass	Mol S.A.	Mol. Vol.	Log P	Total Lipole	Lipole x	Lipole y	Lipole z	Molar Refrac.	Mean Polar.	LUMO	HOMO	Total Dipole	Dipole x	Dipole y	Dipole z
3PYba	0.0010	12.09	8.86	296.41	309.90	218.11	3.88	5.70	3.033	4.302	2.178	88.07	41.34	-0.457	-8.915	2.862	-0.836	-0.096	-2.735
3PYbb	0.0010	12.16	11.55	310.44	337.60	224.48	4.27	6.79	3.292	5.937	-0.271	92.67	43.95	-0.342	-8.680	2.437	0.163	2.067	1.281
3PYbc	0.0010	12.10	11.51	324.47	352.17	244.00	4.67	6.09	2.794	4.727	2.642	97.27	45.87	-0.456	-8.920	2.910	-0.380	0.615	2.819
3PYbe	0.0010	12.17	8.70	330.42	323.81	236.09	4.45	5.50	4.173	2.882	-2.134	98.81	46.65	-0.373	-8.761	1.831	-1.696	0.213	0.655
3PYbf	0.0010	12.04	10.77	330.42	336.01	225.20	4.45	4.70	4.551	0.794	0.840	98.81	47.71	-0.501	-8.947	1.376	0.490	0.249	1.261
3PYbg	0.0010	18.03	4.90	330.42	343.46	225.13	4.45	5.53	5.292	1.392	0.813	98.81	47.74	-0.423	-8.740	1.806	-0.712	-1.071	1.268
3PYbh	0.0010	18.21	7.02	360.45	361.05	255.87	4.19	6.25	4.315	4.446	-0.821	105.27	49.37	-0.537	-8.950	1.395	0.180	-0.123	1.378
3PYbi	0.0010	18.20	7.04	374.48	388.57	263.51	4.44	8.94	3.232	7.677	3.251	110.03	52.09	-0.448	-8.739	2.578	-0.870	-1.539	-1.876
3PYbj	0.0010	20.49	7.05	388.51	401.17	281.82	4.84	6.78	5.317	3.798	-1.818	114.63	53.68	-0.423	-8.693	2.149	-1.138	1.805	0.257
3PYbk	0.0010	19.11	7.09	374.48	384.94	265.68	4.66	7.50	3.787	6.423	-0.845	110.32	52.09	-0.506	-8.765	1.255	0.629	-1.062	-0.228
3PYbl	0.0010	20.60	7.02	416.57	423.84	307.46	5.82	5.91	0.454	5.653	-1.662	123.94	58.28	-0.533	-8.937	1.267	-0.660	-0.812	0.715
3PYbm	0.0010	19.22	7.01	405.45	385.87	279.20	4.15	10.33	-7.037	7.495	-0.963	112.60	50.30	-1.311	-9.142	6.817	6.733	-0.537	-0.924
3PYbp	0.0010	14.29	13.73	388.51	402.77	270.53	4.84	3.41	-2.317	-2.501	0.072	114.63	54.77	-0.444	-8.543	1.645	-0.919	-0.484	-1.276
3PYbs	0.0010	18.25	11.20	436.55	466.00	316.32	5.97	5.78	5.642	-0.456	1.156	129.89	61.70	-0.555	-8.963	1.382	0.371	0.440	-1.257
3PYbt	0.0010	12.17	7.52	346.42	329.99	244.85	4.16	5.89	1.705	4.892	-2.808	100.51	46.72	-0.422	-8.846	2.281	-1.889	-1.191	0.466
3PYbu	0.0010	12.84	8.55	362.42	349.55	249.31	3.88	4.19	-1.367	2.035	-3.392	102.20	46.74	-0.418	-8.554	2.964	-1.885	2.255	0.384
3PYdd	0.0010	12.90	7.83	304.38	301.04	205.91	3.67	5.98	0.693	5.926	0.335	90.65	43.77	-0.528	-8.373	1.962	-1.159	0.917	-1.291
3PYdg	0.0010	12.05	5.63	258.73	252.23	170.22	3.44	5.97	5.937	0.646	0.127	72.54	32.99	-0.598	-9.131	1.862	0.824	-1.270	1.084
3PYdh	0.0010	12.76	4.91	258.73	252.25	170.03	3.44	6.56	6.470	1.080	0.208	72.54	33.10	-0.615	-9.118	1.858	-0.852	-1.125	1.209
3PYdm	0.0010	12.06	5.70	292.29	258.96	191.80	3.80	5.95	5.921	0.362	0.499	73.71	32.35	-0.658	-9.094	3.051	2.146	-0.228	2.156
3PYdn	0.0010	12.03	5.93	269.29	261.97	174.40	2.88	5.03	-0.983	4.920	-0.351	75.06	33.58	-1.339	-9.354	5.537	2.251	-5.002	0.757
3PYdx	0.0010	12.88	8.08	317.43	318.08	226.01	3.72	7.32	-2.881	6.639	1.122	97.89	47.14	-0.574	-8.437	1.119	-0.953	0.083	0.580
3PYed	0.0010	11.62	4.31	230.31	228.52	153.95	2.21	3.15	2.648	1.695	-0.092	66.57	30.97	-0.561	-8.973	1.365	0.463	0.367	1.231
3PYeh	0.0010	12.01	9.57	366.89	336.99	254.04	5.21	7.21	5.318	4.305	2.262	105.22	47.31	-0.652	-8.649	2.838	-1.054	-1.952	1.770
4PYaa	0.0010	12.43	4.91	224.29	238.67	154.52	2.92	5.73	5.495	1.626	0.050	67.74	32.45	-0.426	-9.038	2.318	-0.313	2.198	0.666
4PYab	0.0010	13.43	4.90	238.32	253.95	168.28	3.39	2.39	2.178	0.922	-0.326	72.78	34.73	-0.409	-8.947	2.811	-2.334	1.486	0.498
4PYae	0.1250	14.66	4.89	280.41	304.03	207.48	4.55	1.84	-0.778	1.535	-0.655	86.40	41.46	-0.393	-8.936	3.142	-2.692	1.547	0.483
4PYaf	0.1250	15.46	4.90	294.44	309.55	220.09	4.95	2.46	-1.445	1.938	-0.466	91.00	43.73	-0.398	-8.939	3.174	-2.780	-1.364	-0.696
4PYeh	0.0625	12.47	10.23	366.89	335.88	252.12	5.21	7.12	6.443	-2.917	0.786	105.22	48.01	-0.486	-8.589	1.731	-1.292	1.064	-0.440
4PYai	0.0010	12.47	6.81	252.35	265.76	180.54	3.79	4.12	3.359	2.346	-0.392	77.38	37.07	-0.413	-8.992	2.717	-1.918	1.800	0.679
4PYal	0.0625	15.03	7.13	274.35	274.29	189.45	3.92	7.84	7.405	2.537	0.353	84.19	41.23	-0.637	-8.706	2.206	-1.729	1.361	-0.160

Code	1/MIC	N-Length	Aryl Width	Mol. Mass	Mol S.A.	Mol. Vol.	Log P	Total Lipole	Lipole x	Lipole y	Lipole z	Molar Refrac.	Mean Polar.	LUMO	HOMO	Total Dipole	Dipole x	Dipole y	Dipole z
4PYam	0.0625	12.90	9.47	324.41	311.00	238.96	4.93	7.40	7.394	0.319	0.154	100.64	49.70	-1.009	-8.246	2.144	-1.457	1.326	-0.845
4PYan	0.0010	13.02	9.20	324.41	305.58	232.15	4.93	8.35	8.337	0.240	0.326	100.64	49.81	-0.690	-8.663	2.247	-1.739	1.413	-0.163
4PYas	0.0010	14.51	4.90	254.32	264.29	175.91	2.67	3.36	-1.939	2.578	-0.947	74.20	34.85	-0.381	-8.768	3.469	-2.108	2.711	0.488
4PYaw	0.0010	23.51	4.90	352.53	399.40	264.76	5.46	5.95	-5.074	3.032	-0.640	106.48	50.64	-0.363	-8.731	2.840	-1.263	-2.474	0.591
4PYax	0.0010	12.42	7.09	254.32	260.91	174.73	2.67	2.51	0.346	-2.442	0.471	74.20	34.83	-0.329	-8.802	3.094	-3.006	-0.455	0.576
4PYay	0.0010	12.48	7.80	268.35	281.12	188.08	3.01	6.19	3.157	5.320	0.184	78.95	37.15	-0.308	-8.740	3.776	-0.298	3.620	1.033
4PYaz	0.0010	12.42	9.62	282.38	299.33	200.62	3.48	3.11	0.100	-3.097	0.219	83.47	39.27	-0.317	-8.770	2.817	-2.782	-0.020	0.439
4PYba	0.0010	12.47	8.81	296.41	308.76	218.21	3.88	6.03	2.892	4.656	2.507	88.07	41.56	-0.440	-8.994	2.192	-1.913	0.861	-0.635
4PYbb	0.0010	12.49	11.55	310.44	345.58	225.98	4.27	6.96	3.235	6.156	0.116	92.67	43.93	-0.310	-8.738	3.894	-0.514	3.806	-0.642
4PYbc	0.0010	12.48	11.38	324.47	347.45	245.67	4.67	6.10	2.731	4.799	2.595	97.27	45.82	-0.438	-8.985	2.867	-2.056	0.806	1.829
4PYbe	0.0010	12.48	8.78	330.42	328.63	241.49	4.45	5.59	5.490	-0.984	-0.413	98.81	46.32	-0.453	-9.013	2.324	-1.705	0.916	1.286
4PYbf	0.0010	12.42	11.20	330.42	336.28	230.02	4.45	3.71	3.270	-1.737	0.165	98.81	47.53	-0.430	-9.011	2.618	-2.443	0.765	0.548
4PYbh	0.0010	18.34	7.03	360.45	363.62	248.19	4.19	4.90	4.257	1.463	-1.924	105.27	49.96	-0.425	-8.786	2.275	-1.765	-0.097	1.432
4PYbi	0.0010	17.86	7.01	374.48	378.95	270.66	4.44	7.13	4.149	5.795	-0.224	110.03	51.26	-0.513	-9.005	1.877	-1.081	1.491	-0.364
4PYbj	0.0010	20.96	7.04	388.51	406.51	283.89	4.84	5.82	5.250	1.401	2.085	114.63	53.74	-0.397	-8.734	2.717	-2.231	0.320	1.517
4PYbk	0.0010	19.61	7.08	374.48	391.24	266.91	4.66	5.74	4.144	3.788	-1.177	110.32	52.06	-0.490	-8.810	2.589	-0.517	-2.500	0.431
4PYbl	0.0010	20.73	7.09	416.57	433.81	305.27	5.82	4.42	1.613	3.921	-1.244	123.94	58.84	-0.481	-8.797	2.492	0.414	-2.236	-1.019
4PYbn	0.2000	14.64	9.20	360.45	357.87	258.96	4.19	4.20	-3.900	0.017	1.561	105.27	49.15	-0.396	-8.761	2.206	-2.037	-0.561	0.633
4PYbo	0.0010	14.48	11.81	374.48	381.24	270.60	4.44	4.95	-4.159	-2.206	1.541	110.03	51.38	-0.478	-8.831	3.042	-0.457	2.537	-1.615
4PYbp	0.0010	14.63	13.74	388.51	409.15	270.96	4.84	5.45	-2.086	-5.007	-0.488	114.63	54.73	-0.410	-8.577	1.266	0.945	-0.552	-0.636
4PYbq	0.0010	14.64	12.25	374.48	379.91	270.93	4.66	2.94	-2.358	-1.745	-0.096	110.32	51.38	-0.408	-8.777	2.440	-2.071	0.304	1.253
4PYbr	0.0010	14.63	13.63	416.57	419.09	298.18	5.82	2.49	-2.476	0.244	0.017	123.94	59.19	-0.406	-8.590	2.096	-1.985	-0.358	-0.570
4PYbs	0.0010	18.70	11.20	436.55	466.86	317.76	5.97	6.52	5.909	-2.694	0.625	129.89	61.64	-0.547	-9.024	1.374	-0.724	-1.057	-0.496
4PYcy	0.0010	14.46	8.33	312.36	310.24	211.26	2.17	7.13	-2.413	6.697	-0.310	85.33	39.11	-0.483	-8.941	3.762	-2.793	1.529	-2.004
4PYdd	0.0010	14.48	7.13	304.38	294.51	206.63	3.67	4.96	0.139	4.866	-0.951	90.65	43.85	-0.541	-8.402	3.170	-2.226	-2.169	-0.625
4PYdg	0.0010	12.42	5.63	258.73	257.24	170.89	3.44	5.28	5.222	-0.277	0.742	72.54	33.00	-0.595	-9.206	0.742	-0.456	0.072	-0.581
4PYdh	0.0010	13.14	4.91	258.73	257.12	170.93	3.44	6.60	6.461	1.332	0.108	72.54	33.09	-0.614	-9.188	1.756	-1.541	0.601	0.589
4PYdm	0.0010	12.46	5.71	292.29	264.22	192.79	3.80	5.33	5.268	-0.548	0.572	73.71	32.14	-0.682	-9.172	2.141	-1.998	-0.639	0.430
4PYdn	0.0010	12.41	5.93	269.29	257.71	175.99	2.88	4.18	-1.702	3.685	-1.018	75.06	33.53	-1.365	-9.437	3.638	2.238	-2.862	0.194
4PYed	0.0010	11.84	4.31	230.31	232.12	154.64	2.21	2.08	1.962	0.627	-0.310	66.57	30.95	-0.561	-9.040	2.173	-1.759	1.124	0.603
PZab	0.0010	12.45	4.90	239.31	253.31	160.49	2.48	8.03	7.949	0.988	0.552	70.25	33.74	-0.705	-8.838	1.593	-0.458	1.525	-0.028

Code	1/MIC	N-Length	Aryl Width	Mol. Mass	Mol S.A.	Mol. Vol.	Log P	Total Lipole	Lipole x	Lipole y	Lipole z	Molar Refrac.	Mean Polar.	LUMO	HOMO	Total Dipole	Dipole x	Dipole y	Dipole z
PZai	0.0010	11.50	6.81	253.34	269.17	173.12	3.34	4.42	3.864	2.141	0.190	74.82	36.05	-0.715	-8.884	2.043	-1.787	0.990	-0.018
PZal	0.0010	11.96	7.13	275.34	271.13	178.83	3.48	7.47	7.253	1.702	0.489	81.63	40.48	-0.769	-8.628	1.381	0.170	1.368	0.088
PZbe	0.0010	11.50	10.19	331.41	322.76	226.64	4.00	2.67	2.331	-0.414	1.241	96.25	46.55	-0.639	-8.702	1.782	-0.667	1.652	-0.022
PZbi	0.0010	17.39	7.04	375.47	376.12	256.56	3.53	13.39	11.342	5.436	4.583	107.50	51.16	-0.704	-8.694	0.615	-0.060	-0.099	-0.604
PZbn	0.0010	13.60	11.21	361.44	355.03	249.84	3.28	6.81	5.779	-3.554	-0.643	102.75	47.86	-0.766	-8.909	1.450	0.927	-1.095	-0.213
PZbo	0.0010	13.62	11.81	375.47	382.16	263.37	3.53	4.80	2.282	-4.019	1.288	107.50	50.31	-0.752	-8.754	3.114	1.440	-2.558	1.038
PZdd	0.0010	13.64	7.82	305.37	301.15	198.27	3.22	5.07	1.161	4.940	-0.062	88.09	42.86	-0.705	-8.336	2.276	-0.312	2.254	0.057
PZdm	0.0010	11.57	5.70	293.28	257.46	185.50	3.36	5.55	5.481	-0.584	0.690	71.15	31.31	-0.816	-9.058	1.092	0.450	-0.074	0.992
PZdn	0.0010	11.52	5.93	270.28	259.07	168.29	2.43	3.23	-0.613	3.165	-0.135	72.50	32.67	-1.325	-9.315	4.865	0.586	-4.816	-0.358
PZdx	0.0010	13.67	8.08	318.42	318.89	216.34	3.27	5.99	-1.898	5.660	0.461	95.33	46.00	-0.740	-8.411	2.115	-0.207	2.058	-0.441

A.3 TSAR RESULTS TABLE FOR PYRIDINE-2-CARBOXAMIDRAZONES ACTIVE AGAINST *M.FORTUITUM*

Code	1/MIC	N-Length	Aryl Width	Mol. Mass	Mol. S.A.	Mol. Vol.	Log P	Total Lipole	Lipole x	Lipole y	Lipole z	Molar Refrac.	Mean Polar.	LUMO	HOMO	Total dipole	Dipole x	Dipole y	Dipole z
2PYaa	0.0010	10.69	4.91	224.29	237.59	149.60	3.32	3.64	2.809	2.308	0.022	67.36	32.68	-0.400	-8.771	1.498	-0.742	-1.301	-0.023
2PYab	0.0625	11.80	4.90	238.32	255.97	162.46	3.32	3.98	2.457	3.130	-0.036	72.44	34.99	-0.387	-8.697	0.892	0.891	-0.041	-0.027
2PYac	0.0625	12.75	4.90	252.35	277.45	175.99	4.18	4.32	-2.196	3.592	-0.949	77.01	37.20	-0.384	-8.707	0.902	0.869	0.077	-0.231
2PYad	0.1250	12.69	4.90	266.38	293.08	188.64	4.05	4.05	0.147	4.041	-0.264	81.59	39.45	-0.385	-8.696	0.746	0.744	0.059	-0.009
2PYae	0.1250	13.17	4.89	280.41	309.18	200.94	4.48	3.97	-0.379	3.939	-0.278	86.06	41.69	-0.374	-8.691	0.479	0.472	-0.073	0.039
2PYaf	0.2500	13.03	4.89	294.44	323.54	214.23	4.88	4.08	-0.806	3.946	-0.672	90.66	43.95	-0.371	-8.682	0.525	0.505	-0.143	-0.008
2PYah	0.0010	10.85	5.87	238.32	250.54	162.34	3.79	4.09	1.579	3.769	-0.128	72.40	35.07	-0.393	-8.740	1.632	-1.090	-1.214	-0.025
2PYai	0.0160	10.87	7.25	252.35	265.84	175.16	3.72	5.85	3.621	4.594	-0.011	77.04	37.31	-0.393	-8.736	1.518	1.406	0.573	0.016
2PYaj	0.0010	10.68	5.86	238.32	261.44	162.30	3.79	3.99	0.435	3.954	-0.254	72.40	34.96	-0.389	-8.745	1.227	-0.917	-0.815	-0.001
2PYal	0.0556	11.89	7.13	274.35	271.61	181.88	4.32	5.48	4.536	3.074	0.242	83.81	41.74	-0.548	-8.534	1.530	1.520	-0.158	-0.064
2PYam	0.0010	11.41	9.47	324.41	309.84	232.84	4.86	7.99	7.658	2.229	0.411	100.30	50.28	-0.900	-8.127	1.780	1.778	0.083	-0.012
2PYan	0.0010	12.43	9.21	324.41	307.12	225.73	4.86	8.87	8.606	2.093	0.556	100.30	50.38	-0.592	-8.510	1.566	1.561	-0.079	0.096
2PYao	0.0010	13.23	4.91	250.33	267.36	169.60	3.73	5.13	4.415	2.597	0.186	77.61	37.53	-0.479	-8.623	1.482	-0.579	-1.364	0.008
2PYaq	0.0010	10.99	4.85	228.33	253.90	167.24	2.63	4.42	-3.037	3.202	-0.290	68.75	31.82	-0.297	-8.979	1.485	-0.467	-1.395	0.206
2PYas	0.0625	12.65	4.90	254.32	265.58	169.93	2.60	5.27	-1.648	4.976	-0.494	73.86	35.13	-0.364	-8.558	1.592	1.130	1.121	0.047

Code	1/MIC	N-Length	Aryl Width	Mol. Mass	Mol. S.A.	Mol. Vol.	Log P	Total Lipole	Lipole x	Lipole y	Lipole z	Molar Refrac.	Mean Polar.	LUMO	HOMO	Total dipole	Dipole x	Dipole y	Dipole z
2PYaw	0.0010	21.91	4.90	352.53	403.21	259.76	5.86	12.17	-11.276	4.459	-1.098	106.10	50.81	-0.350	-8.529	1.511	-0.994	1.138	0.001
2PYax	0.0625	10.82	7.08	254.32	257.05	169.56	2.60	6.52	2.642	5.959	-0.224	73.86	35.22	-0.295	-8.525	0.438	0.067	0.432	0.030
2PYay	0.0625	10.81	8.29	268.35	279.34	182.77	2.95	6.89	2.736	6.322	0.202	78.61	37.44	-0.289	-8.506	0.814	-0.751	0.103	0.296
2PYaz	0.0625	10.82	9.60	282.38	295.62	195.30	3.41	7.03	2.767	6.455	-0.302	83.13	39.66	-0.291	-8.505	0.881	0.172	0.864	0.024
2PYbe	0.0400	10.85	11.15	330.42	325.76	228.35	4.84	2.52	-0.306	2.460	0.455	98.44	47.84	-0.322	-8.570	0.339	-0.016	-0.338	0.014
2PYbh	0.2500	15.59	7.02	360.45	359.15	251.12	4.59	5.19	-1.199	4.121	2.924	104.90	49.70	-0.456	-8.719	2.673	2.257	-1.360	-0.449
2PYbj	0.0010	19.06	7.05	388.51	408.92	277.83	4.78	7.06	5.951	3.609	-1.180	114.29	53.78	-0.373	-8.545	2.364	1.084	1.855	-0.987
2PYbk	0.0010	17.78	7.09	374.48	385.50	264.98	4.59	7.76	4.398	6.331	0.878	109.98	52.05	-0.455	-8.642	3.189	2.878	-0.868	-1.066
2PYbl	0.0010	19.10	7.08	416.57	430.84	303.53	5.75	6.65	2.078	6.295	0.507	123.60	58.84	-0.455	-8.634	2.870	2.291	-1.032	-1.386
2PYbm	0.0010	17.85	7.01	405.45	385.28	274.70	4.08	9.67	-6.249	7.311	-1.037	112.26	50.23	-1.276	-8.960	8.957	8.940	-0.475	0.286
2PYbn	0.2500	12.62	11.21	360.45	361.44	251.93	4.13	1.30	-0.644	0.047	-1.126	104.93	49.17	-0.471	-8.773	2.357	2.288	-0.518	0.232
2PYbo	0.1250	12.67	11.79	374.48	390.01	265.43	4.38	3.95	-3.881	0.085	0.719	109.69	51.54	-0.440	-8.648	3.182	2.807	0.949	-1.159
2PYbp	0.0010	12.92	13.73	388.51	403.99	266.18	4.78	3.26	-1.894	-2.635	0.306	114.29	54.92	-0.395	-8.421	2.537	-2.153	1.342	-0.015
2PYbq	0.0625	12.93	12.26	374.48	386.21	264.66	4.59	2.00	-1.920	0.434	-0.347	109.98	51.56	-0.384	-8.578	2.408	1.259	1.859	0.869
2PYbr	0.0010	12.94	13.61	416.57	428.59	291.69	5.75	3.21	-2.024	2.434	-0.520	123.60	59.48	-0.393	-8.434	1.650	1.566	0.417	-0.310
2PYbu	0.0010	12.79	10.71	390.48	378.35	275.16	3.87	6.04	-3.555	-0.708	-4.826	111.40	51.50	-0.400	-8.546	1.301	-0.207	-1.284	0.014
2PYbw	0.0010	10.75	5.65	240.29	232.63	156.72	2.57	5.61	4.286	3.606	0.236	69.09	32.86	-0.516	-8.751	2.831	2.680	-0.795	0.448
2PYbx	0.0010	10.66	5.69	240.29	248.37	156.32	3.04	4.31	0.533	4.278	-0.108	69.06	32.66	-0.458	-8.819	2.938	-1.505	-2.523	-0.041
2PYby	0.0010	11.61	4.90	240.29	249.99	156.36	3.04	3.16	-1.260	2.883	-0.322	69.06	32.75	-0.393	-8.633	2.262	0.007	-2.259	-0.114
2PYbz	0.0010	10.73	5.70	256.29	251.54	162.74	2.75	5.75	-1.547	5.516	-0.473	70.75	32.82	-0.330	-8.569	1.144	1.128	-0.189	0.003
2PYca	0.0010	11.08	5.72	256.29	253.58	163.02	2.75	5.96	-2.583	5.339	-0.633	70.75	32.77	-0.453	-8.621	3.471	-2.612	-2.285	-0.045
2PYcb	0.0010	11.20	6.62	272.29	260.87	170.50	2.47	7.52	-3.959	6.327	-0.901	72.45	32.74	-0.382	-8.561	1.381	-0.786	-0.906	-0.685
2PYcc	0.0010	11.31	6.32	272.29	260.80	168.99	2.47	5.19	-3.914	3.356	-0.578	72.45	33.19	-0.551	-8.440	4.203	-2.382	-3.455	-0.235
2PYcd	0.0010	11.35	6.28	272.29	260.73	169.83	2.47	5.49	-3.932	3.798	-0.538	72.45	32.85	-0.226	-8.395	1.274	0.035	1.272	0.057
2PYch	0.0010	11.09	7.09	270.32	270.44	177.47	2.78	8.34	-4.178	7.110	-1.254	75.52	35.15	-0.428	-8.556	3.483	3.099	1.589	0.041
2PYcj	0.0010	11.73	6.78	285.29	269.81	175.93	2.99	6.73	-6.345	2.100	-0.767	76.38	34.12	-1.181	-9.318	7.843	-7.338	-2.760	0.205
2PYck	0.0010	11.72	7.41	315.32	294.23	196.16	2.74	9.00	-7.653	4.655	-0.856	82.85	36.77	-1.179	-9.231	6.591	5.279	3.946	0.094
2PYcl	0.0010	11.05	6.47	364.18	281.51	196.89	3.78	8.94	-2.586	8.562	0.051	84.01	35.30	-1.378	-9.384	9.041	-1.368	-8.879	-1.015
2PYcm	0.0010	11.72	6.96	330.29	292.58	197.06	2.94	8.65	-7.386	4.437	-0.790	83.71	35.65	-1.780	-9.708	10.710	10.698	0.505	0.088
2PYcq	0.0010	12.60	9.06	352.53	364.69	258.99	6.29	5.38	-3.424	4.126	-0.453	106.39	51.00	-0.475	-8.588	2.208	2.062	0.533	-0.582
2PYcr	0.0010	12.59	9.26	352.53	381.48	259.29	6.29	7.21	-5.702	4.387	-0.446	106.39	50.77	-0.384	-8.636	1.811	-0.051	-0.195	-1.800

Code	1/MIC	N-Length	Aryl Width	Mol. Mass	Mol. S.A.	Mol. Vol.	Log P	Total Lipole	Lipole x	Lipole y	Lipole z	Molar Refrac.	Mean Polar.	LUMO	HOMO	Total dipole	Dipole x	Dipole y	Dipole z
2PYcs	0.0010	11.77	9.19	284.35	284.44	193.36	2.82	5.25	-4.417	2.835	-0.026	80.29	37.43	-0.423	-8.681	3.112	2.541	-1.235	-1.304
2PYcv	0.0010	12.67	8.29	298.38	313.06	203.68	3.16	10.13	-6.793	7.487	-0.646	85.04	39.73	-0.441	-8.640	3.171	2.680	1.287	-1.103
2PYcx	0.0010	13.30	4.91	282.33	289.48	185.01	3.05	9.49	-7.587	5.634	-0.913	78.89	36.80	-0.674	-8.957	3.581	3.181	1.644	-0.026
2PYcy	0.0010	12.63	7.22	312.36	307.90	209.22	2.57	11.46	-8.197	7.826	-1.676	84.96	38.99	-0.619	-8.934	5.089	4.145	-2.899	0.561
2PYcz	0.0010	14.33	4.90	298.33	300.34	194.13	2.61	11.65	-10.496	4.907	-1.206	79.91	36.67	-0.438	-8.693	3.206	3.068	-0.438	-0.822
2PYdb	0.0010	11.85	7.76	290.35	277.41	189.68	3.57	8.34	6.706	4.896	0.740	85.54	41.87	-0.626	-8.423	2.415	2.109	-1.150	0.250
2PYdc	0.0010	11.60	9.37	304.38	292.51	213.64	3.61	9.26	5.039	7.051	3.261	90.31	43.62	-0.414	-8.343	0.901	-0.047	0.618	-0.654
2PYdd	0.0625	12.58	7.13	304.38	295.86	200.66	3.61	7.18	0.384	7.170	0.086	90.31	44.09	-0.454	-8.259	1.267	1.053	-0.699	0.086
2PYde	0.0010	10.63	5.76	303.18	257.51	170.13	4.11	4.46	3.274	3.022	0.051	74.99	33.58	-0.507	-8.883	1.837	-1.740	-0.588	0.016
2Pydf	0.0010	10.83	5.64	258.73	252.25	166.54	3.84	3.37	2.702	2.011	0.100	72.17	33.39	-0.471	-8.823	1.910	0.407	-1.849	0.250
2PYdg	0.0160	10.68	5.63	258.73	251.91	166.11	3.37	5.82	5.532	1.773	0.377	72.20	33.23	-0.529	-8.935	3.106	2.860	-1.209	-0.060
2PYdh	0.0010	11.38	4.91	258.73	258.55	165.81	3.84	4.09	3.505	2.105	0.080	72.17	33.33	-0.547	-8.923	3.536	-1.952	-2.948	-0.023
2PYdi	0.0010	11.37	5.63	293.17	268.69	181.98	3.89	6.55	6.367	1.484	0.409	77.00	33.91	-0.688	-9.027	4.317	4.260	-0.700	-0.018
2PYdk	0.0010	10.72	5.18	242.28	243.50	156.35	3.46	3.32	2.424	2.274	0.011	67.58	31.99	-0.451	-8.769	1.710	0.596	-1.602	-0.035
2PYdo	0.0010	11.98	4.91	269.29	265.69	169.91	3.27	9.08	-7.712	4.721	-0.841	74.69	33.89	-1.442	-9.264	8.247	-4.657	-6.806	-0.066
2PYdp	0.0010	12.11	4.91	249.30	261.69	164.89	3.19	3.05	1.640	2.567	-0.066	73.56	35.12	-0.761	-9.018	5.682	-3.100	-4.761	-0.049
2PYdr	0.0010	13.71	4.91	281.35	297.01	186.22	2.17	11.51	-9.554	6.324	-1.135	80.45	38.07	-0.374	-8.495	3.052	0.014	-3.051	0.077
2PYds	0.0010	19.13	4.91	339.49	370.98	244.70	3.55	21.08	-20.245	5.465	-2.102	101.36	47.45	-0.348	-8.522	1.154	-0.503	0.643	-0.816
2PYdt	0.0010	10.30	4.30	213.27	228.07	139.23	2.09	4.31	-1.700	3.946	-0.377	62.00	29.15	-0.393	-8.467	2.530	-2.355	-0.925	0.029
2PYdu	0.0010	9.62	5.34	228.29	246.38	150.12	1.44	8.04	-6.210	5.045	-0.787	65.10	30.17	-0.475	-8.685	4.308	-3.819	-1.994	0.035
2PYdv	0.0010	10.60	4.85	225.28	235.47	147.57	2.41	4.01	0.252	3.995	-0.239	64.83	31.38	-0.439	-8.846	1.786	0.808	-1.593	-0.006
2PYdw	0.0010	10.68	4.85	225.28	235.94	147.35	2.47	3.00	-1.351	2.665	-0.292	65.18	31.34	-0.532	-8.947	3.113	-2.769	-1.421	0.040
2PYdx	0.1250	12.74	7.12	317.43	321.12	217.81	4.12	10.79	-6.904	8.298	-0.039	97.52	47.28	-0.513	-8.331	1.477	1.206	0.566	-0.638
2PYdy	0.0010	10.96	6.65	263.33	264.20	170.50	3.09	2.36	-2.192	0.861	-0.153	78.45	38.12	-0.273	-8.240	1.774	1.277	-1.230	0.061
2PYdz	0.0010	14.72	6.65	353.46	348.73	246.96	5.12	2.38	0.964	0.819	2.015	107.96	52.31	-0.263	-8.173	1.954	0.052	-1.941	0.218
2PYea	0.0010	10.28	4.30	214.25	226.52	138.27	2.27	3.21	-0.883	3.070	-0.279	59.75	28.09	-0.437	-8.734	1.739	-0.543	-1.652	0.001
2PYeb	0.0010	12.66	7.01	292.32	279.94	183.79	2.41	1.94	0.067	1.920	-0.252	81.91	38.79	-0.484	-8.702	1.812	-0.080	-1.806	-0.119
2PYec	0.0010	12.62	7.98	306.35	301.69	196.51	2.87	2.48	-0.722	2.357	-0.308	86.95	41.07	-0.456	-8.673	1.479	-0.499	-1.387	-0.120
2PYed	0.0625	10.35	4.31	230.31	228.85	149.25	2.15	3.66	2.174	2.942	-0.021	66.23	31.26	-0.495	-8.771	1.555	1.551	-0.115	0.001

A.4 TSAR RESULTS TABLE FOR HETEROARYLCARBOXAMIDRAZONES ACTIVE AGAINST *M.TUBERCULOSIS*

Code	%Inh.	N-Length	Aryl Width	Mol. Mass	Mol. S.A.	Mol. Vol.	Log P	Total Lipole	Lipole x	Lipole y	Lipole z	Molar Refrac.	Mean Polar.	LUMO	HOMO	Total Dipole	Dipole X	Dipole Y	Dipole Z
2Pyaa	24	10.69	4.91	224.29	237.59	149.60	3.32	3.64	2.809	2.308	0.022	67.36	32.68	-0.400	-8.771	1.498	-0.742	-1.301	-0.023
2PYab	40	11.80	4.90	238.32	255.97	162.46	3.32	3.98	2.457	3.130	-0.036	72.44	34.99	-0.387	-8.697	0.892	0.891	-0.041	-0.027
2PYad	69	12.69	4.90	266.38	293.08	188.64	4.05	4.05	0.147	4.041	-0.264	81.59	39.45	-0.385	-8.696	0.746	0.744	0.059	-0.009
2PYae	80	13.17	4.89	280.41	309.18	200.94	4.48	3.97	-0.379	3.939	-0.278	86.06	41.69	-0.374	-8.691	0.479	0.472	-0.073	0.039
2PYaf	94	13.03	4.89	294.44	323.54	214.23	4.88	4.08	-0.806	3.946	-0.672	90.66	43.95	-0.371	-8.682	0.525	0.505	-0.143	-0.008
2PYag	66	14.87	4.91	300.39	306.90	209.45	4.54	9.67	9.577	1.207	0.606	92.53	45.20	-0.456	-8.692	1.487	1.487	0.030	0.011
2PYai	53	10.87	7.25	252.35	265.84	175.16	3.72	5.85	3.621	4.594	-0.011	77.04	37.31	-0.393	-8.736	1.518	1.406	0.573	0.016
2PYam	90	11.41	9.47	324.41	309.84	232.84	4.86	7.99	7.658	2.229	0.411	100.30	50.28	-0.900	-8.127	1.780	1.778	0.083	-0.012
2PYan	82	12.43	9.21	324.41	307.12	225.73	4.86	8.87	8.606	2.093	0.556	100.30	50.38	-0.592	-8.510	1.566	1.561	-0.079	0.096
2PYay	10	10.81	8.29	268.35	279.34	182.77	2.95	6.89	2.736	6.322	0.202	78.61	37.44	-0.289	-8.506	0.814	-0.751	0.103	0.296
2PYbe	59	10.85	11.15	330.42	325.76	228.35	4.84	2.52	-0.306	2.460	0.455	98.44	47.84	-0.322	-8.570	0.339	-0.016	-0.338	0.014
2PYbg	60	16.91	4.90	330.42	338.37	219.81	4.38	6.86	6.374	2.511	0.287	98.47	47.95	-0.379	-8.584	1.704	1.439	-0.912	0.045
2PYbh	42	15.59	7.02	360.45	359.15	251.12	4.59	5.19	-1.199	4.121	2.924	104.90	49.70	-0.456	-8.719	2.673	2.257	-1.360	-0.449
2PYbn	72	12.62	11.21	360.45	361.44	251.93	4.13	1.30	-0.644	0.047	-1.126	104.93	49.17	-0.471	-8.773	2.357	2.288	-0.518	0.232
2PYca	1	11.08	5.72	256.29	253.58	163.02	2.75	5.96	-2.583	5.339	-0.633	70.75	32.77	-0.453	-8.621	3.471	-2.612	-2.285	-0.045
2PYcc	7	11.31	6.32	272.29	260.80	168.99	2.47	5.19	-3.914	3.356	-0.578	72.45	33.19	-0.551	-8.440	4.203	-2.382	-3.455	-0.235
2PYcg	2	12.66	6.00	270.32	277.71	177.04	2.78	8.47	-5.825	5.992	-1.389	75.52	35.08	-0.478	-8.717	3.467	3.192	0.458	1.273
2PYcj	16	11.73	6.78	285.29	269.81	175.93	2.99	6.73	-6.345	2.100	-0.767	76.38	34.12	-1.181	-9.318	7.843	-7.338	-2.760	0.205
2PYcl	10	11.05	6.47	364.18	281.51	196.89	3.78	8.94	-2.586	8.562	0.051	84.01	35.30	-1.378	-9.384	9.041	-1.368	-8.879	-1.015
2PYcm	14	11.72	6.96	330.29	292.58	197.06	2.94	8.65	-7.386	4.437	-0.790	83.71	35.65	-1.780	-9.708	10.710	10.698	0.505	0.088
2PYcs	18	11.77	9.19	284.35	284.44	193.36	2.82	5.25	-4.417	2.835	-0.026	80.29	37.43	-0.423	-8.681	3.112	2.541	-1.235	-1.304
2PYct	3	12.58	6.00	254.32	266.53	169.08	2.60	5.23	-1.684	4.929	-0.493	73.86	35.17	-0.401	-8.448	1.698	1.288	1.106	0.030
2PYcv	10	12.67	8.29	298.38	313.06	203.68	3.16	10.13	-6.793	7.487	-0.646	85.04	39.73	-0.441	-8.640	3.171	2.680	1.287	-1.103
2PYcy	1	12.63	7.22	312.36	307.90	209.22	2.57	11.46	-8.197	7.826	-1.676	84.96	38.99	-0.619	-8.934	5.089	4.145	-2.899	0.561
2PYdb	35	11.85	7.76	290.35	277.41	189.68	3.57	8.34	6.706	4.896	0.740	85.54	41.87	-0.626	-8.423	2.415	2.109	-1.150	0.250
2PYdg	51	10.68	5.63	258.73	252.52	166.07	3.37	5.82	5.532	1.773	0.378	72.20	33.23	-0.532	-8.936	3.103	2.855	-1.213	-0.059
2PYdi	60	11.37	5.63	293.17	268.92	181.97	3.89	6.55	6.368	1.484	0.409	77.00	33.91	-0.689	-9.026	4.321	4.265	-0.695	-0.016
2PYdk	11	10.72	5.18	242.28	243.50	156.35	3.46	3.32	2.424	2.274	0.011	67.58	31.99	-0.451	-8.769	1.710	0.596	-1.602	-0.035
2PYdm	46	10.67	6.09	292.29	255.50	187.71	3.74	5.72	5.514	1.421	0.550	73.37	32.42	-0.580	-8.892	2.530	1.336	-1.914	-0.977

Code	%Inh.	N-Length	Aryl Width	Mol. Mass	Mol. S.A.	Mol. Vol.	Log P	Total Lipole	Lipole x	Lipole y	Lipole z	Molar Refrac.	Mean Polar.	LUMO	HOMO	Total Dipole	Dipole X	Dipole Y	Dipole Z
2PYdn	19	10.66	5.93	269.29	256.67	170.30	2.81	6.33	-1.377	6.154	-0.557	74.72	33.83	-1.259	-9.153	6.953	5.544	-4.194	-0.114
2PYdo	16	11.89	4.91	269.29	265.69	169.91	3.27	9.08	-7.712	4.721	-0.841	74.69	33.89	-1.442	-9.264	8.247	-4.657	-6.806	-0.066
2PYdq	2	12.99	4.89	267.37	284.38	185.76	3.11	10.35	-8.798	5.402	-0.738	81.07	38.66	-0.292	-8.070	0.631	-0.266	-0.118	-0.560
2PYef	72	10.63	8.55	312.47	312.36	223.07	3.78	2.85	0.242	-0.221	2.827	94.11	44.26	-0.440	-8.587	2.488	-1.855	-1.134	-1.209
2PYeh	51	10.63	9.79	366.89	343.92	249.48	5.15	7.89	5.821	4.675	2.556	104.88	47.42	-0.583	-8.576	2.222	1.058	-1.859	0.601
4PYae	79	14.66	4.89	280.41	304.25	207.49	4.55	1.84	-0.779	1.535	-0.655	86.40	41.45	-0.391	-8.935	3.138	-2.687	1.548	0.481
4PYaf	73	15.46	4.89	294.44	309.53	220.06	4.95	2.46	-1.445	1.939	-0.466	91.00	43.72	-0.398	-8.940	3.172	-2.777	-1.365	-0.697
4PYeh	64	12.47	10.22	366.89	335.65	252.12	5.21	7.12	6.443	-2.917	0.786	105.22	48.01	-0.485	-8.589	1.730	-1.296	1.059	-0.436
PZae	48	12.99	4.90	281.40	298.07	199.31	3.64	6.89	6.758	1.267	0.416	83.87	40.44	-0.699	-8.828	1.691	-0.810	1.484	-0.033
PZag	74	14.87	4.90	301.38	304.73	207.81	3.69	14.79	14.723	-0.802	1.175	90.34	43.90	-0.747	-8.821	1.560	0.096	-1.556	-0.052
PZbg	48	16.92	4.90	331.41	333.72	221.89	3.53	12.91	12.886	-0.116	0.748	96.28	46.63	-0.704	-8.696	2.520	0.060	2.519	-0.042
PZbt	14	11.49	8.02	361.44	345.41	251.25	3.28	7.35	5.413	2.622	-4.218	102.75	48.02	-0.649	-8.756	1.862	-1.571	0.884	-0.465
PZbu	6	11.46	8.73	363.41	336.13	243.75	2.96	5.63	4.236	-1.418	-3.419	99.67	45.60	-0.662	-8.528	4.060	-0.986	3.823	-0.948
PZcc	19	11.08	4.88	273.28	262.74	166.65	1.62	1.34	-0.445	1.260	-0.136	70.26	32.08	-0.858	-8.521	3.328	2.921	1.588	0.141
PZcl	25	11.05	6.38	365.17	286.27	194.44	2.93	5.84	2.164	5.422	0.153	81.82	34.19	-1.462	-9.518	7.190	-2.008	-6.887	-0.479
PZcx	2	13.31	4.91	283.32	280.36	183.71	2.20	4.16	-3.094	2.741	-0.441	76.70	35.60	-0.884	-9.116	3.651	1.768	3.193	-0.104
PZdb	42	11.82	7.13	291.34	273.30	186.63	2.73	12.00	11.411	3.542	1.138	83.35	40.64	-0.843	-8.514	1.046	0.831	0.410	0.486
PZdd	29	12.57	7.13	305.37	301.15	198.27	3.22	5.07	1.161	4.940	-0.062	88.09	42.86	-0.705	-8.336	2.276	-0.312	2.254	0.057
PZdf	6	10.82	4.95	259.72	249.81	163.86	2.99	5.05	5.040	0.004	0.347	69.98	32.21	-0.755	-8.978	0.254	-0.221	0.122	0.031
PZdx	17	12.76	7.13	318.42	318.89	216.34	3.27	5.99	-1.898	5.660	0.461	95.33	46.00	-0.740	-8.411	2.115	-0.207	2.058	-0.441
QNaf	79	12.99	4.89	344.50	364.35	245.56	6.28	12.36	-11.138	5.010	-1.894	106.74	53.10	-0.713	-8.697	0.799	0.793	-0.018	0.092
QNaq	6	10.97	4.29	278.39	295.92	198.40	3.57	9.42	-8.712	3.528	-0.638	84.86	40.89	-0.686	-8.987	1.754	-0.784	-1.558	0.184
QNbu	12	12.78	10.78	440.54	424.39	306.95	5.28	14.82	-13.821	0.537	-5.311	127.48	60.43	-0.717	-8.564	1.568	1.164	-1.048	-0.082
QNdw	12	10.66	4.85	275.34	275.83	178.51	3.41	5.18	-4.238	2.925	-0.525	81.28	40.51	-0.808	-8.963	3.505	-3.117	-1.602	0.012
QNdy	27	10.93	6.65	313.39	306.43	203.18	4.03	6.23	-5.984	1.392	-1.023	94.56	47.26	-0.645	-8.256	1.686	0.964	-1.325	-0.399
QNeb	2	12.64	7.01	342.38	321.58	215.30	3.34	5.42	-4.720	2.615	-0.517	98.02	47.91	-0.704	-8.721	1.599	1.293	-0.941	0.011

A.5 TSAR RESULTS TABLE FOR PYRIDINE-2-CARBOXAMIDRAZONES ACTIVE AGAINST *M.TUBERCULOSIS*

Code	%Inh.	N-Length	Aryl Width	Mol. Mass	Mol. S.A.	Mol. Vol.	Log P	Total Lipole	Lipole x	Lipole y	Lipole z	Molar Refrac.	Mean Polar.	LUMO	HOMO	Total Dipole	Dipole X	Dipole Y	Dipole Z
2PYaa	24	10.69	4.91	224.29	237.59	149.60	3.32	3.64	2.809	2.308	0.022	67.36	32.68	-0.400	-8.771	1.498	-0.742	-1.301	-0.023
2PYab	40	11.80	4.90	238.32	255.97	162.46	3.32	3.98	2.457	3.130	-0.036	72.44	34.99	-0.387	-8.697	0.892	0.891	-0.041	-0.027
2PYad	69	12.69	4.90	266.38	293.08	188.64	4.05	4.05	0.147	4.041	-0.264	81.59	39.45	-0.385	-8.696	0.746	0.744	0.059	-0.009
2PYae	80	13.17	4.89	280.41	309.18	200.94	4.48	3.97	-0.379	3.939	-0.278	86.06	41.69	-0.374	-8.691	0.479	0.472	-0.073	0.039
2PYaf	94	13.03	4.89	294.44	323.54	214.23	4.88	4.08	-0.806	3.946	-0.672	90.66	43.95	-0.371	-8.682	0.525	0.505	-0.143	-0.008
2PYag	66	14.87	4.91	300.39	306.90	209.45	4.54	9.67	9.577	1.207	0.606	92.53	45.20	-0.456	-8.692	1.487	1.487	0.030	0.011
2PYai	53	10.87	7.25	252.35	265.84	175.16	3.72	5.85	3.621	4.594	-0.011	77.04	37.31	-0.393	-8.736	1.518	1.406	0.573	0.016
2PYam	90	11.41	9.47	324.41	309.84	232.84	4.86	7.99	7.658	2.229	0.411	100.30	50.28	-0.900	-8.127	1.780	1.778	0.083	-0.012
2PYan	82	12.43	9.21	324.41	307.12	225.73	4.86	8.87	8.606	2.093	0.556	100.30	50.38	-0.592	-8.510	1.566	1.561	-0.079	0.096
2PYay	10	10.81	8.29	268.35	279.34	182.77	2.95	6.89	2.736	6.322	0.202	78.61	37.44	-0.289	-8.506	0.814	-0.751	0.103	0.296
2Pybn	72	12.62	11.21	360.45	361.44	251.93	4.13	1.30	-0.644	0.047	-1.126	104.93	49.17	-0.471	-8.773	2.357	2.288	-0.518	0.232
2PYbu	68	12.79	10.71	390.48	378.35	275.16	3.87	6.04	-3.555	-0.708	-4.826	111.40	51.50	-0.400	-8.546	1.301	-0.207	-1.284	0.014
2PYca	1	11.08	5.72	256.29	253.58	163.02	2.75	5.96	-2.583	5.339	-0.633	70.75	32.77	-0.453	-8.621	3.471	-2.612	-2.285	-0.045
2PYcc	7	11.31	6.32	272.29	260.80	168.99	2.47	5.19	-3.914	3.356	-0.578	72.45	33.19	-0.551	-8.440	4.203	-2.382	-3.455	-0.235
2PYcg	2	12.66	6.00	270.32	277.71	177.04	2.78	8.47	-5.825	5.992	-1.389	75.52	35.08	-0.478	-8.717	3.467	3.192	0.458	1.273
2PYcj	16	11.73	6.78	285.29	269.81	175.93	2.99	6.73	-6.345	2.100	-0.767	76.38	34.12	-1.181	-9.318	7.843	-7.338	-2.760	0.205
2PYck	19	11.72	7.41	315.32	294.23	196.16	2.74	9.00	-7.653	4.655	-0.856	82.85	36.77	-1.179	-9.231	6.591	5.279	3.946	0.094
2PYcl	10	11.05	6.47	364.18	281.51	196.89	3.78	8.94	-2.586	8.562	0.051	84.01	35.30	-1.378	-9.384	9.041	-1.368	-8.879	-1.015
2PYcm	14	11.72	6.96	330.29	292.58	197.06	2.94	8.65	-7.386	4.437	-0.790	83.71	35.65	-1.780	-9.708	10.710	10.698	0.505	0.088
2PYcs	18	11.77	9.19	284.35	284.44	193.36	2.82	5.25	-4.417	2.835	-0.026	80.29	37.43	-0.423	-8.681	3.112	2.541	-1.235	-1.304
2PYct	3	12.58	6.00	254.32	266.53	169.08	2.60	5.23	-1.684	4.929	-0.493	73.86	35.17	-0.401	-8.448	1.698	1.288	1.106	0.030
2PYcv	10	12.67	8.29	298.38	313.06	203.68	3.16	10.13	-6.793	7.487	-0.646	85.04	39.73	-0.441	-8.640	3.171	2.680	1.287	-1.103
2PYdb	35	11.85	7.76	290.35	277.41	189.68	3.57	8.34	6.706	4.896	0.740	85.54	41.87	-0.626	-8.423	2.415	2.109	-1.150	0.250
2PYdg	51	10.68	5.63	258.73	252.52	166.07	3.37	5.82	5.532	1.773	0.378	72.20	33.23	-0.532	-8.936	3.103	2.855	-1.213	-0.059
2PYdi	60	11.37	5.63	293.17	268.92	181.97	3.89	6.55	6.368	1.484	0.409	77.00	33.91	-0.689	-9.026	4.321	4.265	-0.695	-0.016
2PYdk	11	10.72	5.18	242.28	243.50	156.35	3.46	3.32	2.424	2.274	0.011	67.58	31.99	-0.451	-8.769	1.710	0.596	-1.602	-0.035
2PYdm	46	10.67	6.09	292.29	255.50	187.71	3.74	5.72	5.514	1.421	0.550	73.37	32.42	-0.580	-8.892	2.530	1.336	-1.914	-0.977
2PYdn	19	10.66	5.93	269.29	256.67	170.30	2.81	6.33	-1.377	6.154	-0.557	74.72	33.83	-1.259	-9.153	6.953	5.544	-4.194	-0.114
2PYdo	16	11.89	4.91	269.29	265.69	169.91	3.27	9.08	-7.712	4.721	-0.841	74.69	33.89	-1.442	-9.264	8.247	-4.657	-6.806	-0.066

Code	%Inh.	N-Length	Aryl Width	Mol. Mass	Mol. S.A.	Mol. Vol.	Log P	Total Lipole	Lipole x	Lipole y	Lipole z	Molar Refrac.	Mean Polar.	LUMO	HOMO	Total Dipole	Dipole X	Dipole Y	Dipole Z
2PYdq	2	12.99	4.89	267.37	284.38	185.76	3.11	10.35	-8.798	5.402	-0.738	81.07	38.66	-0.292	-8.070	0.631	-0.266	-0.118	-0.560
2PYef	72	10.63	8.55	312.47	312.36	223.07	3.78	2.85	0.242	-0.221	2.827	94.11	44.26	-0.440	-8.587	2.488	-1.855	-1.134	-1.209

A.6 BROAD SPECTRUM RESULTS FOR THE COMPOUNDS ACTIVE AGAINST MRSA

Fluclox.= Flucloxacillin, Amp.= Ampicillin, Vanc.= Vancomycin hydrochloride. Upper values of the MIC readings are given.

Reference	NCTC 6571	NCTC 10788	Cowan 1	NH 123	96-5665	96-7475	96-7778	NH 278	Moore	Cooper	Morgan	Barnhill	Mickiewicz	ACTCC 10541	NCTC 7171	NCTC 5957	EBH1	Docker	Phillips	24455	Bastrup	Laugesen	NCTC 11047	Woods	O'Neil	W3110 R-	W3110 R+	327	4444	NCTC 6749	NCTC 6017	NCTC 10257	NCTC 11582	NCTC 8344	NCTC 5887
Strain	*S.aureus*	*S.aureus*	*S.aureus*	*MRSA*	*MRSA*	*MRSA*	*MRSA*	*MRSA*	*MRSA*	*MRSA*	*MRSA*	*MRSA*	*MRSA*	*E.faecium*	*E.faecium*	*E.faecalis*	*E.faecalis*	*E.faecalis*	*E.faecalis*	*E.faecalis*	*E.faecalis*	*E.faecalis*	*S.epidemisis*	*S.epidemisis*	*S.haemolyticus*	*E.coli*	*E.coli*	*K.pneumoniae*	*S.marcesens*	*P.auriginosa*	*S. aboni*	*S.maltophilia*	*E.cloacae*	*B.bronchiseptica*	*P.mirbilis*
Code																																			
Fluclox.	0.05	0.05	0.05	0.05	8	8	16	0.05	0.25	0.25	8	8	0.25	1	1	1	0.5	1	0.5	-	1	1	0.05	>16	0.5	>16	>16	>16	>16	8	0.05	16	>16	>16	16
Amp.	0.05	0.05	0.05	0.12	8	8	8	8	8	8	8	8	8	2	1	2	0.05	0.05	0.05	0.05	2	2	4	8	1	1	>16	>16	8	16	0.05	16	16	1	4
Vanc.	0.05	0.12	0.25	0.12	0.12	0.12	0.12	0.12	0.12	0.12	0.12	0.12	0.12	0.12	0.12	0.25	0.12	0.25	0.25	0.12	16	2	8	8	8	>16	>16	>16	>16	>16	0.05	>16	>16	>16	>16
3PYaf	64	64	64	64	64	64	64	64	64	64	64	64	64	64	64	64	128	64	64	-	128	128	32	128	64	64	64	X	256	64	-	64	X	X	64
4PYaf	64	64	64	64	64	64	64	64	64	64	64	64	64	64	64	64	64	64	64	64	128	128	64	64	64	X	X	X	X	X	X	X	X	X	X
4PYam	32	64	32	32	64	64	32	32	32	64	64	32	32	X	256	X	X	256	256	-	256	256	256	128	256	X	X	X	X	X	32	X	X	X	X
3PYay	>256	X	X	256	128	128	128	128	X	X	X	X	256	X	X	128	128	128	128	-	X	X	128	X	256	256	256	256	256	128	-	256	X	X	128
QNca	128	128	128	128	128	128	128	128	128	128	128	128	128	256	256	256	256	256	256	256	256	256	64	64	128	256	256	256	256	256	256	256	32	-	X
2PYcb	X	X	256	X	X	X	X	256	X	X	X	X	X	X	256	X	X	X	X	X	X	X	X	256	X	X	X	X	X	X	X	X	X	256	X
PZcb	256	256	256	256	256	256	256	256	256	256	256	256	256	X	X	X	X	X	256	256	X	X	256	X	256	X	X	X	X	X	X	X	X	-	X
3PYcc	256	256	256	256	256	256	256	256	256	256	256	256	256	X	256	256	X	256	256	-	256	128	32	X	X	X	X	X	X	X	256	X	X	X	X
QNcc	256	256	256	256	X	X	X	X	X	X	X	X	X	X	X	X	X	X	256	256	X	X	X	X	X	X	X	X	X	X	X	X	X	256	X
HDcd	256	256	256	256	256	256	256	256	256	256	256	256	256	256	256	256	256	128	128	128	256	128	128	128	128	256	256	256	256	256	128	128	256	256	256
cj	4	2	16	2	4	2	2	2	4	4	4	4	4	X	X	X	X	256	X	-	X	256	2	2	X	256	256	256	X	256	1	256	256	256	128
2PYcj	16	16	32	16	16	4	8	16	16	8	4-8	8	8	X	X	X	X	X	X	256	X	256	256	256	256	X	X	X	X	X	X	X	X	-	X
3PYcj	8	8	16	4	4	4	4	4	8	8	8	8	8	X	X	256	X	128	128	-	X	X	64	128	X	X	X	X	X	X	256	X	X	X	X
PZcj	16	16	256	8	8	4	4	16	16	16	16	16	16	X	X	X	X	X	X	256	X	X	X	256	X	X	X	X	X	X	X	X	X	-	X
HDcj	32	32	32	64	64	64	32	32	64	64	64	64	64	128	128	128	128	128	128	-	64	128	64	64	128	128	128	128	256	256	128	128	256	128	128
cl	16	16	32	16	16	32	16	16	32	32	32	32	X	X	X	X	X	X	X	X	X	X	X	X	X	X	X	X	X	X	X	X	X	X	X
2PYcl	32	32	64	64	64	64	32	32	64	64	64	64	64	128	256	256	256	X	X	X	X	X	X	X	X	X	X	X	X	X	256	X	X	X	X
3PYcl	32	32	64	64	64	64	32	32	64	64	64	64	64	128	256	128	256	128	128	-	256	128	256	256	128	X	X	X	X	X	X	X	X	-	X
QNcl	>256	X	X	X	64	64	64	X	X	X	X	X	X	X	X	X	X	X	256	256	X	X	256	X	256	X	X	X	X	X	X	X	X	-	X
HDcl	128	128	128	128	128	128	128	128	128	128	128	128	128	128	128	128	128	128	32	16	128	128	64	128	128	128	128	128	256	128	128	128	256	128	128
4PYcq	4	4	4	4	4	4	4	4	4	4	4	4	4	4	4	4	4	4	4	-	4	4	4	4	4	X	X	X	X	X	-	X	X	X	X
4PYcr	>256	X	X	X	X	>256	X	X	X	X	X	X	X	X	X	X	X	X	X	X	X	X	X	X	X	X	X	X	X	X	-	X	X	X	X
2PYdb	>256	X	X	X	X	>256	X	X	X	X	X	X	X	X	X	X	X	X	X	X	X	X	X	X	X	X	X	X	X	X	X	X	X	-	X
3PYdb	256	256	256	256	256	256	256	256	256	256	256	256	256	X	X	X	X	X	256	-	X	256	256	256	256	256	256	256	X	256	32	256	256	256	256
4PYdb	>256	X	128	128	X	256	256	X	X	X	X	X	X	X	X	X	X	X	256	256	X	X	128	128	128	X	X	X	X	X	X	128	X	X	X
HDdb	8	8	8	8	8	8	8	8	8	8	16	8	8	4	4	4	4	4	4	4	8	8	4	4	4	X	X	X	X	X	X	X	X	X	X
QNds	128	128	128	64	64	64	64	64	64	64	64	64	64	128	64	64	128	128	128	128	128	64	256	256	256	X	X	X	X	X	X	256	X	-	X
4PYdx	128	128	128	128	128	128	128	128	128	128	128	128	128	256	256	256	256	256	256	-	256	256	64	128	256	256	128	256	256	32	32	128	256	256	128
4PYeh	128	16	8	16	16	16	16	16	16	64	32	16	16	X	X	X	X	X	X	X	X	X	256	256	256	X	X	X	X	X	X	X	X	X	X